

VOLUME 11

NUMBER 2

2018

ISSN 2218-7979
eISSN 2409-370X

International Journal of
Biology
and **Chemistry**



Al-Farabi Kazakh National University

International Journal of Biology and Chemistry is published twice a year by al-Farabi Kazakh National University, al-Farabi ave., 71, 050040, Almaty, Republic of Kazakhstan
website: <http://ijbch.kaznu.kz/>

Any inquiry for subscriptions should be sent to:
Prof. Mukhambetkali Burkitbayev, al-Farabi Kazakh National University
al-Farabi ave., 71, 050040, Almaty, Republic of Kazakhstan
e-mail: [Mukhambetkali Burkitbayev@kaznu.kz](mailto:Mukhambetkali.Burkitbayev@kaznu.kz)

EDITORIAL

The most significant achievements in the field of natural sciences are reached in joint collaboration, where important roles are taken by biology and chemistry. Therefore publication of a Journal, displaying results of current studies in the field of biology and chemistry, facilitates highlighting of theoretical and practical issues and distribution of scientific discoveries.

One of the basic goals of the Journal is to promote the extensive exchange of information between the scientists from all over the world. We welcome publishing original papers and materials of biological and chemical conferences, held in different countries (after the process of their subsequent selection).

Creation of special International Journal of Biology and Chemistry is of great importance, because a great amount of scientists might publish their articles and it will help to widen the geography of future collaboration. We will be glad to publish also the papers of the scientists from the other continents.

The Journal aims to publish the results of the experimental and theoretical studies in the field of biology, biotechnology, chemistry and chemical technology. Among the emphasized subjects are: modern issues of technologies for organic synthesis; scientific basis of the production of physiologically active preparations; modern issues of technologies for processing of raw materials; production of new materials and technologies; study on chemical and physical properties and structure of oil and coal; theoretical and practical issues in processing of hydrocarbons; modern achievements in the field of nanotechnology; results of studies in the fields of biology, biotechnology, genetics, nanotechnology, etc.

We hope to receive papers from a number of scientific centers, which are involved in the application of the scientific principles of biological and chemical sciences on practice and carrying out research on the subject, whether it relates to the production of new materials, technologies and ecological issues.

IRSTI 615.01

¹*R.T. Kenzhebekova, ²A.O. Abekova, ¹K.D. Raziyeva,
¹Zh.S. Abramova, ¹R.A. Islamov, ³A.K. Nersesyan, ¹A.I. Ilin

¹JSC «Scientific Center for Anti-Infectious Drugs», Almaty, Kazakhstan

²al-Farabi Kazakh National University, Almaty, Kazakhstan

³Institute of Cancer Research, Medical University of Vienna, Austria

*e-mail: nurrosenur@inbox.ru

Investigation of the impact of iodine coordination compound on production of interleukin-4 and interferon- γ *in vitro* and primary evaluation of local irritation *in vivo*

Abstract: It is known that some iodine-containing drugs have pleiotropic effects on the body's immune response. The immune system can both inhibit and activate the production of pro-inflammatory and anti-inflammatory cytokines in response to stimuli. Those properties can be valuable when developing drugs for various purposes as well as for evaluating their safety. Key regulatory cytokines that can be involved in the response to iodine are IL-4 and IFN- γ . Therefore, relation of those cytokines is often regarded as a marker when evaluating cellular and humoral immunity, including allergies. Studies of an allergic response to iodine give conflicting results. Difficulties in interpreting results are usually associated with the fact that molecular iodine is not able to cause an allergic reaction on its own. However, by acting as a hapten, iodine is capable of forming bounds with the body's proteins and consequently can induce immune response to iodinated proteins. Thus, by studying production of IL-4 and IFN- γ we can characterize effects of new iodine coordination compound on some components of the immunity. This paper presents the results of our study, where we evaluated cytotoxicity and the ability to induce production of IL-4 and IFN- γ cytokines by MDCK (Madin-Darby canine kidney cells) and PBMN (mononuclear cells from peripheral blood) after treatment with a new coordinated compound (KC). KC is a drug that contains a multiple polymer complex comprising of molecular iodine coordinated by lithium and potassium halides, di- and tri-peptides and α -dextrin. An induction of IFN- γ was only detected in PBMN cells treated at concentrations close to 50% cytotoxic concentration (CC_{50}), which can be interpreted as a cytotoxic effect. *In vivo* study showed the absence of irritating effect on the skin of tested animals. Treatment had no impact on the body weight of rabbits. Results of this study add new knowledge to the influence of iodine complexes on immunity.

Key words: iodine coordination compound, molecular iodine, toxicity, cytokine, local irritation effect.

Introduction

Iodine is a micronutrient that is vital at all stages of life and is of a crucial importance for the proper function of all organ systems [1]. Iodine complex compounds are applied to a broad spectrum of procedures in medicine in form of biocides [2]. Molecular iodine and its complexes also show properties of antineoplastic agents, by inhibiting proliferation of cancer cells [3]. However, practical use of iodine complexes shows negative side effects in some cases. Some of the published work describes various harmful effects of iodine, such as thyroid toxicity, local irritating effect on mucosa and so-called iodine allergy [4-6].

In clinical practice, the term "allergy" is used to refer to a broad variety of immune responses. Iodine does not have antigenic properties, which means that it is not recognized by the immune system and is not able to trigger an allergic reaction by itself. However, iodine may cause immune responses as a hapten molecule when attached to larger proteins [7; 8]. Povidone iodine, which is widely used in medicine, may cause adverse skin reactions from a simple skin irritation to a serious rash resembling chemical burn. Iodinated contrast dye, which is administered intravenously as an X-ray radiocontrast agent can cause an allergic reaction, in some cases leading to anaphylaxis [9-11].

In addition, iodine solutions produce diverse effects on the production of certain cytokines. An in-

duction of TNF- α is effectively inhibited by iodine solution in case of rabbit skin inflammation after treatment with mustard gas [12]. Similar effect is observed when iodine solutions are administered to rats with testosterone-induced oxidative stress [13].

Contrariwise, an excess of iodine intake in form of iodides leads to increased level of IL-6 and TNF- α in serum [14]. Treatment of lymphocytes with Lugol's solution *in vitro* results in the production of TNF- α , but not IL-6 or IL-8 cytokines. Simultaneously, interaction of KI₃ with keratinocytes does not induce cytokine response [15]. An oral rinse with iodine solutions in chronic gingivitis reduces clinical manifestations of inflammation as well as the level of IL-2 and IFN- γ production in biopsy material [16]. It is well known that a high level of iodine intake can activate autoimmune mechanisms [17]. This pathological process underlies the autoimmune diseases of the thyroid gland [18]. It should be noted that an effect is dependent on the chemical form of iodine entering the body.

Thus, for the proper evaluation of immune responses 2 types of cytokines have to be studied, which are proinflammatory (type 1 cytokines, including interleukin-2 (IL-2) and interferon- γ (IFN γ), that promote cell-mediated immune responses; and anti-inflammatory (type 2 cytokines, including IL-4 and IL-10), that promote antibody production and allergy.

Therefore, the purpose of this work was to study an effect of a new iodine coordinating compound (KC) on the production of IL-4 and IFN- γ . Cell lines that were used as models are human peripheral blood mononuclear cells (PBMN) and Madin-Darby canine kidney cells (MDCK) that are able to form multilayer culture and produce some cytokines [19]. Rabbits were used as *in vivo* models for primary evaluation of local irritation.

Materials and methods

Test substance. KC is a multiple polymer complex consisting of molecular iodine coordinated by lithium and potassium halides, di- and tri-peptides and α -dextrin [20].

Cells. MDCK cell line was purchased from Russian Cell Biotechnology Laboratory and PBMN cells - from RSE on REU "Republican Blood Center" of the Ministry of Healthcare of the Republic of Kazakhstan, donor denotation code 1410104939, contract No. 49, from March 1, 2018.

Isolation of mononuclear cell fraction. Human peripheral blood was pre-mixed with 6% dextran solution in a 50 mL polypropylene centrifuge tube to

precipitate erythrocytes. Then, the supernatant was washed, resuspended and fractionated by density gradient centrifugation on Ficoll-Paque (Sigma, USA), corresponding to the floating density of human mononuclear cells (density = 1.078) at 4 °C, 3000 rpm for 20 minutes (Centrifuge 5810R; Eppendorf, Germany). The mononuclear cell fraction was washed by centrifugation and resuspended in RPMI-1640 culture medium (Sigma, USA). The percentage of viable cells was assessed using trypan blue incorporation. In all the experiments, suspensions with a percentage of viable cells greater than 90 % were used.

Cell culturing. Cells were cultured in RPMI-1640 medium supplemented with 10 % heat inactivated FBS, 100 U/ml penicillin and 100 μ g/ml streptomycin at 37 °C in humidified environment of 5 % CO₂ for 24 hours before treatment. Cell viability was assessed by trypan blue (Sigma, USA). Cell culture with the percentage of viable cells greater than 90 % was used in the experiment.

Cytotoxic effects of KC. The cytotoxicity of KC determined by cell uptake of 3-[4,5-dimethylthiazol-2-yl]-2,5-diphenyl-tetrazolium bromide (MTT; Sigma, USA) colorimetric assay. Estimation of cell viability by MTT method is based on the measurement of cellular mitochondrial dehydrogenase activity [21]. Cells were cultured in 96-well plates (BRAND plates, Germany) at a concentration of 3 \times 10⁴ cells/well, including 200 μ l fresh medium. After 24 hours of incubation, growth medium was removed from wells and 200 μ l of KC diluent containing seven different concentrations, namely: 0.01, 0.06, 0.31, 0.78, 1.56, 3.91 and 7.82 mM, were added. Wells with negative control samples contained 200 μ l of nutrient medium without any substance. Photometric measurement of the optical density of dissolved formazan was performed on a Sunrise RC.4 microplate reader (Tecan, Austria) at the wavelength of the main filter of 540 nm and a reference wave of 620 nm. To calculate 50 % cytotoxic concentration (CC₅₀) GraphPad Prism V6 (GraphPad Software; La Jolla California USA) was used for each tested compound.

Study of IFN- γ and IL-4 cytokines production after KC treatment. IFN- γ was evaluated by enzyme-linked immunosorbent assay using a commercial kit Gamma-Interferon (JSC Vector-Best, Russia). IL-4 was evaluated by enzyme-linked immunosorbent assay using a commercial kit IL-4 (R&D Systems, USA). To determine the production of IFN- γ and IL-4, mononuclear and epithelial cells suspensions were dispersed into 96-well plates (BD Falcon, USA) at a concentration of 10⁵ cells/well and incubated in a CO₂ incubator for 24 hours in complete culture me-

dium containing various concentrations of KC. 10% RPMI-1640 culture medium was used. Sterile deionized water was used as a negative control in all experiments. ConA was used as a positive control. It is widely used as a potential agent able to induce production of a wide range of cytokines *in vitro* [22]. For ELISA assay cell culture supernatant was used. Measurement of optical density was performed on a Sunrise RC.4 microplate reader (Tecan, Austria) using Magelan 2.0 software (Tecan, Austria) at a wavelength of 450 nm with a reference filter at 650 nm. Concentration of released cytokines and standards was calculated using GraphPad Prism V6 (GraphPad Software; La Jolla California, USA).

Skin irritation test on animals. Three male rabbits were obtained from the Scientific and Practical Center of Sanitary and Epidemiological Expertise and Monitoring (Almaty, Kazakhstan). The animal studies were conducted in accordance with the procedures and principles outlined in the Guide for the Care and Use of Laboratory Animals by the National Institutes of Health (NIH, USA). The rabbits were individually housed in environmentally monitored and ventilated rabbit experimental room I, maintained at 15-21°C temperature and a relative air humidity of 30-70%. Feed and water containers were changed and sanitized once a week at least. Before the study, rabbits were acclimated for 24 days. The study was approved by the Ethics Committee of the Scientific Center (Protocol No. 25/13).

The study was started with administration of one animal. No signs of irritation were observed within 72 hours, thus next two animals were administered in the same manner. Approximately 24 hours before the study, fur was removed by closely clipping the dorsal area of animal trunks, approximately 10 x 15 cm in size. The operation was performed carefully to prevent abrading of the skin, which could alter its permeability. Only animals with healthy intact skin were used. The KC in the amount of 0.5 ml was administered on application site of 2.5 x 2.5 cm in size. After the administration the corresponding skin surface was covered with a patch and non-irritating tape. Control sites were administered with 0.5 ml of water for injection only and the corresponding skin surface was covered with non-irritating patch and tape (2.5 x 2.5 cm in size). The exposure period was 4 hours. At the end of the exposure period residual application form was removed with a small quantity of water for injection. All the rabbits were individually weighed at delivery before administration and at the end of the study. The animals were euthanized

by injecting the overdose of pentobarbital at the end of the study.

Statistical data analysis. Results are presented as the means \pm SD of three independent experiments. The method of dispersion analysis with nonparametric procedures was used in this study according to the abnormal distribution of data. Statistical significance of experimental values when comparing with control was assessed by the GraphPad Prism version 6 for Windows (GraphPad Software; La Jolla California, USA), using Mann-Whitney test, Kruskal-Wallis one-way analysis and nonlinear standard curves for ELISA test. Values of $P > 0.05$ were considered as insignificant.

Results and discussion

Cytotoxicity of KC. CC_{50} was calculated after treatment of MDCK and PBMN cells with KC using Hill equation in GraphPad Prism (Table 1). The difference between concentrations of two cell lines was non-significant ($P > 0.05$). No selectivity was found. The results also indicate that iodine had a direct effect as an oxidizing agent on membranes of MDCK and PBMN cells.

Table 1 – Comparative CC_{50} values of KC in monolayer and suspension cells

Cell lines	CC_{50} (Mean \pm SD), mM
MDCK	1.45 \pm 0.22
PBMN	0.74 \pm 0.04

In dose-response analysis for KC on a logarithmic scale after 24 hours of exposure (Figure 1) KC “dose – response” log-curves were characterized by a classical sigmoidal shape.

According to the chart, MDCK line is steeper than that of PBMN. This can be explained by the difference in the type of cultured cells, monolayer and suspension.

The level of the production of IFN- γ and IL-4 cytokines. ELISA assay was done to determine the levels of cytokines in MDCK and PBMN cell supernatants pre-treated with KC. MDCK culture did not produce IFN- γ and IL-4 after 24 hours of exposure with KC (Table 2).

However, KC induced production of IFN- γ by human mononuclear cells at high concentrations (Table 3).

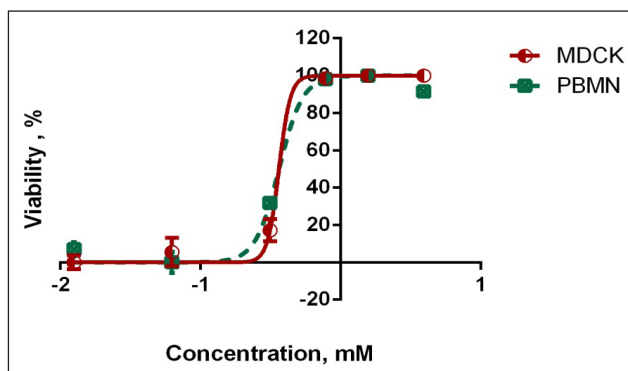


Figure 1 – Log-curves “dose – response” for KC
Note: MDCK – MDCK cell,
PBMN – mononuclear cells from peripheral blood

Table 2 – Production of cytokines by MDCK after 24 hours of treatment

KC concentrations, mM	Cytokine concentrations, pg/ml	
	IFN- γ	IL-4
NC	1.56 \pm 0.67	1.76 \pm 0.71
PC	13.71 \pm 1.05*	29.05 \pm 1.10*
7.82	1.15 \pm 0.06	1.12 \pm 0.32
3.91	1.78 \pm 0.13	2.00 \pm 0.67
1.56	0.00	1.50 \pm 0.56
0.78	1.77 \pm 0.51	0.00
0.31	0.00	1.48 \pm 0.54
0.06	1.82 \pm 0.54	1.82 \pm 0.80
0.01	0.00	1.28 \pm 1.47

Note: NC – negative control,
PC – positive control; * P<0.05 vs NC

Iodine complexes and solutions (KI₃ and PVP-iodine), when exposing locally to both damaged and healthy epithelial tissue *in vivo* or *in vitro* can either suppress the production of TNF- α and IL-2 proinflammatory cytokines or not act at all [23-25]. Due to such features it is often concluded that iodine solutions have anti-inflammatory properties [26]. However, we observed that an effect on cytokines production depends on the type of cells used. For example, treatment with high concentrations of KC showed that only PBMN cells are able to respond with the production of solely IFN- γ cytokines. We did not observe a response from MDCK cells. It should be noted that the studied cytokine IL-4 plays an essen-

tial role by promoting Th2 cell differentiation while inhibiting Th1 cell differentiation. The pleiotropic effect of IL-4 reveals the important role that this cytokine plays during a normal immune response [27]. Presence of IL-4 during *in vitro* priming determines the lymphokine-producing potential of CD4⁺ T cells from T cell receptor transgenic mice. An association of IL-4 with allergic reactions is also significant. IL-4 increases production of IgE [28]. Nevertheless, the lack of IL-4 production and increase of IFN- γ expression when administering KC at high-doses (3.9–7.8 mM) can only be interpreted as cytotoxic effect of KC on PBMN cells. Correlation of IL-4 and IFN- γ and their imbalance are often considered as indicators of certain pathological processes. Therefore, the absence of PBMN cells reaction to KC at concentrations lower than 1.5 mM can indicate lack of disregulating properties on the studied components of the immune system [29-31].

Table 3 – Production of cytokines by PBMN after 24 hours of treatment

KC concentrations, mM	Cytokine concentrations, pg/ml	
	IFN- γ	IL-4
NC	1.56 \pm 0.67	0.00
PC	39.13 \pm 1.05*	6.07 \pm 1.31*
7.82	791.02 \pm 1.56*	0.00
3.91	900.73 \pm 0.95*	0.00
1.56	0.00	0.00
0.78	0.00	0.00
0.31	0.00	0.00
0.06	0.00	0.00
0.01	0.00	0.00

Note: NC – negative control,
PC – positive control; * P<0.05 vs NC

Skin irritation test on rabbit. All rabbits were observed daily for clinical signs, morbidity or mortality during the study. Changes in the skin, gait, somatic activity and behavior pattern were also observed. The visual aspect of each application site was evaluated in 1 hour after treatment. After removing the patch, time intervals of 24, 48, and 72 hours were investigated and the skin reaction for erythema and oedema was graded according to the following table classification system for skin reaction (ISO 10993-10). The

daily clinical observation of the general health status of all tested animals revealed no pathological abnormalities.

The erythema and oedema on rabbits were not observed. The irritation index was 0. Therefore the irritation response has been defined as negligible. The body weight (Table 4) of the animals was not negatively affected by the KC application. The body weight increases of all the rabbits were normal and corresponded with their age.

Table 4 – Body weight of rabbits, kg

Animal No.	At delivery	Before administration	48 hours after administration	72 hours after administration
M 1	2.90	3.18	-	3.38
M 2	3.00	-	3.38	3.58
M 3	2.68	-	3.20	3.29

Evaluation of local irritating effect of iodine-containing drugs (primarily PVP-iodine) remains relevant since there are clinical incidences of contact dermatitis in some patients in the postoperative period [32]. Moreover, a degree of irritation with PVP-iodine is dose-dependent [32; 33]. Despite the development of alternative test methods *in vitro*, clinical manifestation of the irritation effect to test substance is a valuable prognostic marker [34]. The results, obtained from evaluating KC irritating effect on rabbits' skin, showed the absence of damaging properties. Some researchers believe that the complexation of iodine with polymers can reduce the irritating effect of iodine [35]. Molecular iodine, which is contained in KC, is localized inside of the dextrin helix in form of a polyiodide. Peptides create a competitive environment with body proteins, which ensures high stability of the complex [36]. These features may possibly explain the absence of disregulating properties on some components of immunity and local irritation.

Conclusion

Madin-Darby canine kidney cells (MDCK) and mononuclear cells from peripheral blood (PBMN) were treated with a new iodine coordination compound (KC). Close to 50% cytotoxic concentration (CC_{50}) is estimated as 1.45 mM for MDCK and

0.74 mM for PBMN. We detected an induction of IFN- γ in PBMN cells treated with KC at concentrations close to CC_{50} (from 7.82 to 3.91 mM), which can be interpreted as a cytotoxic effect. KC also does not irritate rabbits' skin. The results, obtained from evaluation of KC irritating effect on rabbits' skin, showed the absence of deteriorative properties. Results of this study add new knowledge to the influence of iodine complexes on immunity. Obviously, future experiments aim to analyze immune response, through other key cytokines production.

Acknowledgment

The research was funded by the program "Development of new anti-infectious drugs", for 2018-2020 yy., provided by the Ministry of Industry and Infrastructural Development of the Republic of Kazakhstan, with scientific and technical program included in the State Register of scientific and technical progress, register number – 0.0777.

References

- Zimmermann M.B. (2011) The role of iodine in human growth and development. *Semin Cell Dev Biol*, vol. 22, no. 6, pp. 645-652.
- McDonnell G., Russell A.D. (1999) Antiseptics and Disinfectants: Activity, Action, and Resistance. *Clin Microbiol Rev.*, vol. 12, no. 1, pp. 147-179.
- Rösner H., Möller W., Groebner S., Torremante P. (2016) Antiproliferative/cytotoxic effects of molecular iodine, povidone-iodine and Lugol's solution in different human carcinoma cell lines. *Oncol Lett.*, vol. 12, pp. 2159-2162.
- Leung A.M. (2014) Consequences of excess iodine. *Nat Rev Endocrinol.*, vol. 10, no. 3, pp. 136-142.
- Tsurumaru D., Utsunomiya T., Matsuura Sh., Komori M., Kawanami S., Ishibashi T., Honda H. (2010) Gastric Mucosal Changes Caused by Lugol's Iodine Solution Spray: Endoscopic Features of 64 Cases on Screening Esophagogastroduodenoscopy. *Gastroenterol Res Pract*, pp. 1-4.
- Iijima S., Kuramochi M. (2002) Investigation of irritant skin reaction by 10% povidone-iodine solution after surgery. *Dermatology*, vol. 204, no. 1, pp.103-108.
- Katellaris C.H., Smith W.B. (2009) 'Iodine allergy' label is misleading. *Aust Prescr.*, vol. 32, pp. 125-128.

8. Coakley F.V., Panicek D.M. (1997) Iodine Allergy: An Oyster Without a Pearl? *AJR*, vol. 169, pp. 951-952.
9. Dewachter P., Mouton-Faivre C., Felden F. (2001) Allergy and contrast media. *Allergy*, vol. 56, pp. 250-251.
10. Dewachter P., Trechot P., Mouton-Faivre C. (2005) "Allergie a l'iode": le point sur la question. *Ann Fr Anesth Reanim.*, vol. 24, no. 1, pp. 40-52.
11. Nadolski G. J, Stavropoulos S. W. (2013) Contrast alternatives for iodinated contrast allergy and renal dysfunction: Options and limitations. *J Vasc Surg.*, vol. 2013, no. 57, pp. 593-598.
12. Wormser U., Brodsky B., Proscura E., Foley J.F., Jones T., Nyska A. (2005) Involvement of tumor necrosis factor-alpha in sulfur mustard-induced skin lesion; effect of topical iodine. *Arch Toxicol.*, vol. 79, no. 11, pp. 660-670.
13. Quintero-García M., Delgado-González E., Sánchez-Tusie A., Vázquez M., Aceves C., Anguiano B. (2018) Iodine prevents the increase of testosterone-induced oxidative stress in a model of rat prostatic hyperplasia. *Free Radic Biol Med.*, vol. 115, pp. 298-308.
14. Saha A., Mukherjee S., Bhattacharjee A., Sarkar D., Chakraborty A., Banerjee A., Chandra A.K. (2018) Excess iodine-induced lymphocytic impairment in adult rats. *Toxicol Mech Methods*, vol. 28, pp. 1-9.
15. Frankova J., Kubala L., Velebny V., Ciz M., Lojek A. (2006) The effect of hyaluronan combined with KI₃ complex (Hyiodine wound dressing) on keratinocytes and immune cells. *J Mater Sci Mater Med.*, vol. 17, no. 10, pp. 891-898.
16. Sharma S., Saimbi C.S., Koirala B., Shukla R. (2008) Effect of various mouthwashes on the levels of interleukin-2 and interferon-gamma in chronic gingivitis. *J Clin Pediatr Dent.*, vol. 32, no. 2, pp. 111-114.
17. Yang X., Gao T., Shi R., Zhou X., Qu J., Xu J., Shan Z., Teng W. (2014) Effect of iodine excess on Th1, Th2, Th17, and Treg cell subpopulations in the thyroid of NOD.H-2h4 mice. *Biol Trace Elem Res.*, vol. 159, pp. 288-296.
18. Shi Y.N., Liu F.H., Yu X.J., Liu Z.B., Li Q.X., Yuan J.H., Zang X.Y., Li L.Y. (2013) Poly-inosine-polycytidylic acid promotes excessive iodine intake induced thyroiditis in non-obese diabetic mice via Toll-like receptor 3 mediated inflammations. *Chin Med J.*, vol. 126, no. 4, pp. 703-710.
19. Park W.J., Park B.J., Song Y.J., Lee D.H., Yuk S.S., Lee J.B., Park S.Y., Song C.S., Lee S.W., Choi I.S. (2015) Analysis of cytokine production in a newly developed canine tracheal epithelial cell line infected with H₃N₂ canine influenza virus. *Arch Virol.*, vol. 160, no. 6, pp. 1397-1405.
20. Ilin A.I., Kulmanov M.E. (2014) Antibacterial agent for treating infectious diseases of bacterial origin. Patent 389 US 2014/0010782 A1
21. Mosmann T. (1983) Rapid colorimetric assay for cellular growth and survival: application to proliferation and cytotoxicity assays. *J Immunol Methods*, vol. 65, no 1-2, pp. 55-63.
22. Kelso A, Gough N. (1987) Expression of hemopoietic growth factor genes in murine T lymphocytes. In: *Lymphokines*, vol. 13, pp. 209-238.
23. Wormser U., Brodsky B., Proscura E., Foley J.F., Jones T., Nyska A. (2005) Involvement of tumor necrosis factor-alpha in sulfur mustard-induced skin lesion; effect of topical iodine. *Arch Toxicol.*, vol. 79, no. 11, pp. 660-670.
24. Sharma S., Saimbi C.S., Koirala B., Shukla R. (2008) Effect of various mouthwashes on the levels of interleukin-2 and interferon-gamma in chronic gingivitis. *J Clin Pediatr Dent.*, vol. 32, no. 2, pp. 111-114.
25. Frankova J., Kubala L., Velebny V., Ciz M., Lojek A. (2006) The effect of hyaluronan combined with KI₃ complex (Hyiodine wound dressing) on keratinocytes and immune cells. *J Mater Sci Mater Med.*, vol. 17, no. 10, pp. 891-898.
26. Bigliardi P.L., Alsagoff S.A.L., El-Kafrawi H.Y., Pyon J.K., Wa C.T.C., Villa M.A. (2017) Povidone iodine in wound healing: A review of current concepts and practices. *Int J Surg.*, vol. 44, pp. 260-268.
27. Seder R.A., Paul W.E., Davis M.M., Fazekas de St. Groth B. (1992) The presence of interleukin 4 during *in vitro* priming determines the lymphokine-producing potential of CD4⁺ T cells from T cell receptor transgenic mice. *J Exp Med.*, vol. 176, no. 4, pp. 1091-1098.
28. Deo S. S., Mistry K. J., Niphadkar P.V. (2010) Role played by Th2 type cytokines in IgE mediated allergy and asthma. *Lung India*, vol. 27, no. 2, pp. 66-71.
29. Halminen M., Juhela S., Vaarala O, Simell O, Ilonen J. (2001) Induction of interferon-gamma and IL-4 production by mitogen and specific antigens in peripheral blood lymphocytes of Type 1 diabetes patients. *Autoimmunity*, vol. 34, no. 1, pp. 1-8.
30. Byron K.A., Varigos G.A., Wootton A.M. (1994) IL-4 production is increased in cigarette smokers. *Clin Exp Immunol.*, vol. 95, no. 2, pp. 333-336.

31. Akpınarlı A., Güc D., Kalaycı O., Yigitbaş E., Ozon A. (2002) Increased interleukin-4 and decreased interferon gamma production in children with asthma: function of atopy or asthma? *J Asthma*, vol. 39, no 2, pp. 159-165.
32. Kozuka T. (2002) Patch testing to exclude allergic contact dermatitis caused by povidone-iodine. *Dermatology*, vol. 204, no. 1, pp. 96-98.
33. Naor J., Savion N., Blumenthal M., Assia E.I. (2001) Corneal endothelial cytotoxicity of diluted povidone-iodine. *J Cataract Refract Surg.*, vol.27, no. 6, pp. 941-947.
34. Robinson M.K., Perkins M.A. (2002) A strategy for skin irritation testing. *Am J Contact Dermat.*, vol. 13, no. 1, pp. 21-29.
35. Lee S.K., Zhai H., Maibach H.I. (2005) Allergic contact dermatitis from iodine preparations: a conundrum. *Contact Dermat.*, vol. 52, no. 4, pp. 184-187.
36. Yuldasheva G., Zhidomirov G., Leszczynski J., Ilin A. (2018) Iodine containing drugs: complexes of molecular iodine and tri-iodide with bioorganic ligands and lithium halogenides in aqueous solutions. *Pract Asp Comput Chem.*, vol. IV, ch. 17, pp. 637-685.

IRSTI 34.15.23; 34.15.25; 31.27.31; 76.03.31; 76.29.49

^{1*}A.N. Akimniyazova, ²M. Régnier, ¹Sh.A. Atambayeva,
¹R.E. Niyazova, ¹A.T. Ivashchenko

¹al-Farabi Kazakh National University, Almaty, Kazakhstan

²Ecole Polytechnique, Paris, France

*e-mail: akimniyazova@gmail.com

Characteristics of miRNA interaction with mRNA of candidate genes of small intestinal cancer

Abstract: miRNAs is a class of small non-coding RNAs that regulate the expression of genes, and associated with approximately all known physiological and pathological processes, especially cancer. Expression of many genes is regulated by binding of miRNA with mRNA, therefore it is required to identify candidate genes, associated with small intestinal cancer and the extent of their interaction with miRNA. To determine the important miRNAs binding sites in genes, involved in the development of small intestinal cancer, MirTarget program was used. The article presents the results of studying the characteristics of the interaction of miRNAs with mRNAs of 40 candidate genes involved in the development of small intestinal cancer, out of which only 27 genes were targets for miRNAs. 135 miRNAs have binding sites at 5'UTR, CDS, and 3'UTR; the average free energy of binding (ΔG) of miRNAs with mRNAs was - 126 kJ/mole, - 119 kJ/mole and - 109 kJ/mole, respectively. 79 associations of miRNAs and mRNAs of genes with a free energy of interaction more than - 125 kJ/mole are recommended for the diagnosis of small intestinal cancer. *ARID1A*, *ASXL1*, *KRAS*, *NF1*, *PDXP*, *PTEN* and *SMAD4* genes are characterized as a candidate target genes for miRNAs having binding sites in 5'UTR of mRNA, while *ARID1A*, *CDKN2B*, *EGFR*, *GNAS*, *MLL2*, *MSH6* and *PDXP* are characterized as a candidate genes, having miRNAs binding sites in CDS, and *CDKN2B*, *SMAD4* as a candidate genes, having miRNAs binding sites in 3'UTR. Based on the results obtained, groups of miRNA and mRNA associations of candidate genes are recommended for developing methods for early diagnosis of small intestinal cancer.

Key words: miRNA, mRNA, genes, small intestinal cancer, clusters.

Introduction

Gastrointestinal (GI) tract cancer is one of the three most common oncological diseases in the world with a high mortality rate [1; 2]. Contrary to common belief, an overall and cancer-specific survival of patients with small intestinal tumors are not different from those of patients with stomach cancer, and takes the second place among the leading causes of death from oncology diseases all over the world [3-5]. Understanding of genetic events driving the pathogenesis of small intestinal cancer is of critical importance for devising of new strategies aimed to treat this disease. miRNAs play an important role in carcinogenesis. In recent years, the interaction of miRNA with mRNA of genes, responsible for the development of small intestinal cancer, was actively studied. Recently, a change in the expression of miRNA became an important feature of cancer. Various miR-

NAs can function as tumor suppressors or oncogenes in cancer cells, while dysregulation of some miRNAs can contribute to human cancer [6; 7]. An individual miRNA could potentially alter complex cellular processes, such as cell growth, cell cycle, apoptosis and invasion. Identification of specific miRNAs and their target genes, participating in carcinogenesis allows better understanding the mechanism of regulation of genes expression [8].

Berillo O.A. et al. have previously studied the characteristics of intronic miRNAs and features of their interaction with mRNA [9]. The present study is aimed to identify previously undefined miRNAs binding sites in mRNA of genes involved in the development of small intestinal cancer and the clusters of miRNA binding sites and their properties. Studying miRNA binding sites clusters in mRNA of human genes is valuable for identification of the role of these genes and miRNAs in oncogenesis.

Materials and methods

The information about the role and function of genes participating in the development of small intestinal cancer was taken from the GenBank databases and publications. mRNA nucleotide sequences of the human genes were derived from GenBank (<http://www.ncbi.nlm.nih.gov>). 40 mRNAs of genes associated with the development of small intestinal cancer were used in the study. The nucleotide sequences of 3,707 miRNAs were taken from Londin et al. [10].

Search for miRNA's target genes was performed by the MirTarget program, created in our laboratory [11]. This program defines the start of miRNA binding sites in mRNA; localization of binding sites in 5'-untranslated region (5'UTR), protein coding region (CDS), and 3'-untranslated region (3'UTR); free energy of interaction (ΔG , kJ/mole) and scheme of miRNA-mRNA nucleotides (nt) interaction. The $\Delta G/\Delta G_m$ (%) ratio was calculated for each binding site, where ΔG_m is equal to the free energy of miRNA interaction with fully complementary nucleotide sequence. miRNA-mRNA binding sites with $\Delta G/\Delta G_m$ ratio higher than 86% were selected. However, this criterion does not include the length of miRNA, on which ΔG energy also varies, depending on the miRNA lengths. Thus, in miRNAs with the same $\Delta G/\Delta G_m$ value, but varying lengths of 17 nt

and 25 nt, correspondingly, the energy of binding of mRNA for miRNA with the length of 25 nt was 1.47 times higher than for miRNA with the length of 17 nt. $\Delta G/\Delta G_m$ value leads to the reduction in the number of false-positive miRNAs with a length of less than 20 nt. The position of binding sites is indicated from the first nucleotide of the 5'UTR in mRNA. The unique property of MirTarget program include consideration of nucleotide interaction in miRNA with mRNA of target genes not only between adenine (A) and uracil (U), guanine (G) and cytosine (C), but also between A and C, G and U via single hydrogen bond [12; 13]. The distance between A-C and G-U is equal to distance value between G-C and A-U.

Results and discussion

The search of genes responsible for the development of small intestinal cancer was performed by the fragmented data because there is no available unified database of genes. To create the database of genes, we took as a basis the information available in the NCBI (National Center for Biotechnology Information) and through a search of PubMed. Table 1 presents the information about the candidate genes involved in the development of small intestinal cancer. The list of candidate genes was formed from publications based on laboratory research.

Table 1 – Candidate genes of small intestinal cancer

Gene	PMID	Gene	PMID	Gene	PMID	Gene	PMID
<i>APC*</i>	29575536	<i>EGFR</i>	26892442	<i>MME*</i>	25759539	<i>PIK3CA</i>	28617917
<i>ARID1A</i>	28617917	<i>ERBB2</i>	24797764	<i>MRC1</i>	26530135	<i>PMS2*</i>	25029614
<i>ARID2*</i>	28617917	<i>FBXW7</i>	28617917	<i>MSH2*</i>	25759539	<i>PROM1</i>	21064103
<i>ASXL1</i>	28617917	<i>GNAS</i>	28617917	<i>MSH6</i>	25029614	<i>PTEN</i>	28617917
<i>ATM</i>	28617917	<i>KIT*</i>	18246046	<i>MUC2*</i>	25759539	<i>SMAD4</i>	28617917
<i>BRAF*</i>	26892442	<i>KRAS</i>	26892442	<i>MUC5AC</i>	25759539	<i>SOAT1</i>	25987131
<i>CD34*</i>	25264210	<i>LRP1B</i>	28617917	<i>MUC6</i>	25759539	<i>SOX9</i>	28617917
<i>CDKN2A*</i>	28617917	<i>MDM2</i>	28617917	<i>NF1</i>	28617917	<i>TP53</i>	27546842
<i>CDKN2B</i>	28617917	<i>MLH1*</i>	25029614	<i>PDGFRA*</i>	25264210	<i>UGT1A1*</i>	24114122
<i>CTNNB1</i>	27546842	<i>MLL2</i>	28617917	<i>PDXP</i>	21297586	<i>VEGFA</i>	27546842

Note: * – indicates mRNAs, which are not targets for miRNA with chosen criteria

Genes that are not targets of miRNAs with $\Delta G/\Delta G_m$ value higher than 86%, show that their expression level is independent of miRNAs. It was found that 33% of 40 candidate genes are not regulated by miRNA, and therefore their expression could not be suppressed.

As a result of the analysis of the binding schemes of miRNA with mRNA of the genes *ASXL1*, *GNAS* and *LRP1B* complete complementarity of binding sites was revealed (Table 2).

The binding sites TJU_CMC_MD2.ID00061.3p-miR and TJU_CMC_MD2.ID03064.3p-miR in

The free energy (ΔG) of miRNAs binding sites in different mRNAs varied from -108 to -132 kJ/mole. These changes occurred in connection with several nucleotide substitutions of G-C to G-U pairs.

The results show the study of miRNAs interaction with mRNA of 11 genes in 5'UTR, each of which binds from one to several miRNAs (Table 4). Some of these mRNAs bind six or more miRNAs. mRNA of *ASXL1* gene in a region from 172 nt to 197 nt and form the cluster of this binding site with whole length of 26 nt and average $\Delta G = -129$ kJ/mole. TJU_CMC_MD2.ID00021.5p-miR and TJU_CMC_MD2.ID01895.5p-miR have binding sites from 400 nt, but most likely TJU_CMC_MD2.ID01895.5p-miR will occupy this site cause of the energy of interaction of this miRNA due to the higher concentration of GC-pairs.

mRNAs of most genes containing two or more miRNA binding sites with overlapping of their nucleotide sequences form clusters. mRNA of *ARID1A* gene contain 2 clusters of binding sites located in 5'UTR. TJU_CMC_MD2.ID01257.3p-miR, TJU_CMC_MD2.ID00414.3p-miR and TJU_CMC_MD2.ID02428.3p-miR form a cluster from 295 to 332 nt with a length of 38 nt. The free energy of interaction of these miRNAs average ΔG value is equal to -111 kJ/mole. TJU_CMC_MD2.ID02106.3p-miR, TJU_CMC_MD2.ID01778.3p-miR, TJU_CMC_MD2.ID00296.3p-miR, TJU_CMC_MD2.ID01804.3p-miR, TJU_CMC_MD2.ID01702.3p-miR, TJU_CMC_MD2.ID02592.5p-miR and TJU_CMC_MD2.ID03065.3p-miR form a cluster with a length equal to 58 nt and average $\Delta G = -142$ kJ/mole. TJU_CMC_MD2.ID02751.3p-miR has a binding site from 206 nt and $\Delta G/\Delta G_m$ equal to 92%.

19 miRNAs form a cluster of binding sites in 5'UTR mRNA of *LRP1B* gene with a whole length equal to 36 nt and average free energy of interaction equal to -131 kJ/mole. The full length of this 19 miRNAs 553 nt. The formation of such cluster of binding sites indicates the great ability of this gene to compaction, which serves the formation of competition for this binding site.

mRNA of *GNAS* gene contain the cluster of binding sites from 31 nt to 70 nt with an average free energy of interaction equal to -104 kJ/mole. Three miRNAs formed a cluster of binding sites in mRNA of *PDXP* gene in position from 17 nt to 53 nt with an average free energy of interaction equal to

-127 kJ/mole. *KRAS* gene had four binding sites, of which three sites formed a cluster with overlapped nucleotide sequences. mRNA of *CTNNB1*, *SOAT1* and *SOX9* genes have binding sites for single miRNAs.

PTEN is onco-suppressor gene. Byun et al. [15] observed that *PTEN* inactivation by deletion alone is sufficient to initiate developing intestinal tumors, including adenocarcinomas. mRNA of *PTEN* gene contain the cluster of binding sites from 531 to 558 nt with a total length of 28 nt and average $\Delta G = -120$ kJ/mole. The binding sites for TJU_CMC_MD2.ID01315.3p-miR and TJU_CMC_MD2.ID01377.3p-miR in position from 705 to 726 nt form the cluster of binding sites with a whole length of 22 nt. That is why suppression of translation of this mRNA provides the development of this disease.

The average free energy of binding of all miRNAs with mRNAs in the 5'UTR region equals -126 kJ/mole. 27 miRNAs bound with mRNAs of corresponding target genes, and the number of miRNA associations with mRNA having free energy of interaction greater than -125 kJ/mole is 57. These associations are recommended as markers for early diagnosis of small intestinal cancer.

Some binding sites are located in overlapping mRNA nucleotide sequences in protein-coding regions (Table 5). Presence of multiple binding sites for one and/or several miRNAs in one mRNA increases the probability of their interaction, and as a consequence, translation of such mRNAs is reduced [16].

When the binding energy of one miRNA site decreases, this can be compensated by other sites. Several binding sites with mRNA can enhance the inhibitory effect.

mRNA of *CDKN2B* ($\Delta G = -132$ kJ/mole), *EGFR* ($\Delta G = -127$ kJ/mole), *ERBB2* ($\Delta G = -113$ kJ/mole), *FBXW7* ($\Delta G = -108$ kJ/mole), *MSH6* ($\Delta G = -134$ kJ/mole), *PIK3CA* ($\Delta G = -100$ kJ/mole) and *SOX9* ($\Delta G = -119$ kJ/mole) genes are bound by one miRNAs.

Nine miRNAs have binding sites in mRNA of *MLL2* gene. Kantidakis et al. [17] identified that *MLL2* knockdown affects adhesion-related processes and suppresses cell growth. These binding sites are located without overlapping on protein-coding region of mRNA of *MLL2* gene, and we could say that the expression of this gene will be suppressed. The average free energy of interaction of these miRNAs is equal to -114 kJ/mole.

Table 4 – Characteristics of the binding sites of miRNA and mRNA in 5'UTR of genes involved in the development of SIC

Gene	miRNA	Start of binding site, nt	ΔG , kJ/mole	$\Delta G/\Delta G_m$, %	Length, nt
<i>ARID1A</i>	TJU_CMC_MD2.ID02751.3p-miR	206	-125	92	23
	TJU_CMC_MD2.ID01257.3p-miR	295	-113	93	20
	TJU_CMC_MD2.ID00414.3p-miR	303	-108	93	20
	TJU_CMC_MD2.ID02428.3p-miR	310	-113	91	22
<i>ASXL1</i>	TJU_CMC_MD2.ID00522.5p-miR	172	-125	89	23
	TJU_CMC_MD2.ID01804.3p-miR	173	-138	87	25
	TJU_CMC_MD2.ID02187.5p-miR	174	-123	89	23
	TJU_CMC_MD2.ID00021.5p-miR	400	-117	92	20
	TJU_CMC_MD2.ID01895.5p-miR	400	-132	89	24
<i>CTNNB1</i>	TJU_CMC_MD2.ID00477.5p-miR	77	-113	95	20
<i>GNAS</i>	TJU_CMC_MD2.ID02111.3p-miR	31	-108	91	21
	TJU_CMC_MD2.ID00724.5p-miR	49	-100	92	21
<i>KRAS</i>	TJU_CMC_MD2.ID01310.3p-miR	17÷29 (2)	-121÷-123	92÷94	22
	TJU_CMC_MD2.ID03332.3p-miR	37	-132	89	24
	TJU_CMC_MD2.ID00805.3p-miR	96	-113	91	21
<i>NF1</i>	TJU_CMC_MD2.ID02352.5p-miR	157	-123	91	24
	TJU_CMC_MD2.ID01787.3p-miR	297	-115	89	23
	TJU_CMC_MD2.ID01491.3p-miR	349	-125	91	23
<i>PDXP</i>	TJU_CMC_MD2.ID01018.3p-miR	17	-125	89	24
	TJU_CMC_MD2.ID01622.3p-miR	23	-132	91	23
	TJU_CMC_MD2.ID00714.3p-miR	29	-123	88	24
<i>PTEN</i>	TJU_CMC_MD2.ID02079.5p-miR	75	-115	92	20
	TJU_CMC_MD2.ID02611.3p-miR	486	-125	91	22
	TJU_CMC_MD2.ID01310.3p-miR	531	-119	90	22
	TJU_CMC_MD2.ID02430.3p-miR	533	-108	96	18
	TJU_CMC_MD2.ID02761.3p-miR	533	-132	89	24
	TJU_CMC_MD2.ID03037.3p-miR	536	-121	90	22
	TJU_CMC_MD2.ID01315.3p-miR	705	-115	92	20
	TJU_CMC_MD2.ID01377.3p-miR	708	-110	96	18
<i>SMAD4</i>	TJU_CMC_MD2.ID00577.3p-miR	160÷161 (2)	-104÷-106	92÷94	20
	TJU_CMC_MD2.ID00961.3p-miR	248	-127	90	23
<i>SOAT1</i>	TJU_CMC_MD2.ID03036.3p-miR	46	-115	89	23
<i>SOX9</i>	TJU_CMC_MD2.ID01969.3p-miR	294	-113	96	20

Note: Here and in the tables below the number of miRNAs binding sites is indicated in parentheses

Table 5 – Characteristics of the binding sites of miRNA and mRNA in CDS of genes involved in the development of SIC

Gene	miRNA	Start of binding site, nt	ΔG , kJ/mole	$\Delta G/\Delta G_m$, %	Length, nt
<i>ARID1A</i>	TJU_CMC_MD2.ID02057.3p-MIR	385	-110	95	19
	TJU_CMC_MD2.ID01753.3p-miR	749	-104	91	21
	TJU_CMC_MD2.ID02294.5p-miR	851	-129	88	24
	TJU_CMC_MD2.ID00061.3p-miR	852	-125	91	22
	TJU_CMC_MD2.ID01473.3p-miR	1093	-125	89	23
	TJU_CMC_MD2.ID02986.5p-miR	1387	-117	92	21
	TJU_CMC_MD2.ID03167.3p-miR	1399	-123	91	23
	TJU_CMC_MD2.ID01610.5p-miR	1404	-110	91	21
	TJU_CMC_MD2.ID01508.5p-miR	1459	-129	90	23
	TJU_CMC_MD2.ID01388.5p-miR	4587	-119	89	23
TJU_CMC_MD2.ID01565.5p-miR	4916	-115	93	21	
<i>CDKN2B</i>	TJU_CMC_MD2.ID02899.3p-miR	412	-132	89	24
<i>EGFR</i>	TJU_CMC_MD2.ID02344.3p-miR	1779	-127	88	24
<i>ERBB2</i>	TJU_CMC_MD2.ID00692.3p-miR	3815	-113	90	22
<i>FBXW7</i>	TJU_CMC_MD2.ID02514.3p-miR	1243	-108	93	22
<i>GNAS</i>	TJU_CMC_MD2.ID02093.5p-miR	1589÷1590 (2)	-117÷ -123	92÷97	22
	TJU_CMC_MD2.ID00377.3p-miR	1617	-119	90	22
	TJU_CMC_MD2.ID02093.5p-miR	1625÷1626 (2)	-117÷ -127	92÷100	22
	TJU_CMC_MD2.ID00377.3p-miR	1653	-119	90	22
	TJU_CMC_MD2.ID02093.5p-miR	1662	-117	92	22
	TJU_CMC_MD2.ID03100.3p-miR	1830	-110	91	22
<i>LRP1B</i>	TJU_CMC_MD2.ID02669.5p-miR	14051	-96	92	20
<i>MLL2</i>	TJU_CMC_MD2.ID01491.3p-miR	3300	-125	91	23
	TJU_CMC_MD2.ID01753.3p-miR	5258	-104	91	21
	TJU_CMC_MD2.ID02409.3p-miR	5878	-102	91	21
	TJU_CMC_MD2.ID02562.3p-miR	5967	-115	90	22
	TJU_CMC_MD2.ID02664.5p-miR	7226	-104	92	20
	TJU_CMC_MD2.ID01013.3p-miR	7483	-123	88	24
	TJU_CMC_MD2.ID03483.3p-miR	11514	-115	90	22
	TJU_CMC_MD2.ID01562.3p-miR	12237	-117	90	22
	TJU_CMC_MD2.ID02045.3p-miR	13623	-123	89	23
<i>MSH6</i>	TJU_CMC_MD2.ID00156.5p-miR	246	-134	90	24
<i>PDXP</i>	TJU_CMC_MD2.ID01242.3p-miR	172÷173 (2)	-121÷ -125	88÷91	24
	TJU_CMC_MD2.ID01877.3p-miR	386	-123	88	24
	TJU_CMC_MD2.ID01610.5p-miR	646	-110	91	21
<i>PIK3CA</i>	TJU_CMC_MD2.ID00724.5p-miR	3043	-100	92	21

Continuation of Table 5

Gene	miRNA	Start of binding site, nt	ΔG , kJ/mole	$\Delta G/\Delta G_m$, %	Length, nt
<i>SOX9</i>	TJU_CMC_MD2.ID00978.5p-miR	1065	-119	90	22
<i>VEGFA</i>	TJU_CMC_MD2.ID03238.3p-miR	775	-113	91	22
	TJU_CMC_MD2.ID03097.3p-miR	887	-123	88	24
<i>MUC5AC</i>	TJU_CMC_MD2.ID00481.5p-miR	668	-113	90	22
	TJU_CMC_MD2.ID02341.3p-miR	2037	-113	90	23
	TJU_CMC_MD2.ID02620.5p-miR	3277	-110	90	22
	TJU_CMC_MD2.ID00967.5p-miR	4672	-115	90	22
	TJU_CMC_MD2.ID00967.5p-miR	5791	-115	90	22
<i>MUC6</i>	TJU_CMC_MD2.ID02841.5p-miR	1226	-108	93	20
	TJU_CMC_MD2.ID00611.5p-miR	1574	-115	89	23
	TJU_CMC_MD2.ID02888.5p-miR	2918	-121	89	23
	TJU_CMC_MD2.ID00564.5p-miR	6488	-110	90	22
	TJU_CMC_MD2.ID02507.3p-miR	7353	-115	89	24

TJU_CMC_MD2.ID00522.5p-miR, TJU_CMC_MD2.ID01804.3p-miR, TJU_CMC_MD2.ID02052.5p-miR, TJU_CMC_MD2.ID02187.5p-miR, TJU_CMC_MD2.ID02692.5p-miR, TJU_CMC_MD2.ID01323.3p-miR, TJU_CMC_MD2.ID00457.3p-miR, TJU_CMC_MD2.ID02084.3p-miR, TJU_CMC_MD2.ID02064.5p-miR and TJU_CMC_MD2.ID02538.3p-miR formed a cluster of binding sites with a whole length equals 33 nt and average $\Delta G = -128$ kJ/mole. The full length of this 10 miRNAs equals 249 nt; TJU_CMC_MD2.ID01704.5p-miR, TJU_CMC_MD2.ID01810.3p-miR, TJU_CMC_MD2.ID02430.3p-miR and TJU_CMC_MD2.ID02761.3p-miR formed cluster in segment with a whole length of 47 nt and average $\Delta G = -124$ kJ/mole; TJU_CMC_MD2.ID02986.5p-miR, TJU_CMC_MD2.ID03167.3p-miR and TJU_CMC_MD2.ID01610.5p-miR form a cluster of binding sites with a whole length of 39 nt and average free energy of interaction equal to -117 kJ/mole. The formation of cluster of binding sites in this mRNA notes the ability of this gene to compaction, and thereby causes the competition of these miRNAs for binding site. Also, mRNA of *ARID1A* gene has the binding sites for single miRNAs. TJU_CMC_MD2.ID02057.3p-miR have a binding site in position from 385 nt. Kim et al. [18] established that the expression level of *ARID1A* could be used as a prognostic marker in small intestinal cancer, because the low or loss of expression of this gene is

correlated considerably with a high-grade tumors. Suppression of expression of this gene by miRNA promotes the development of this disease.

mRNA of *GNAS* gene has multiple binding sites of TJU_CMC_MD2.ID02093.5p-miR in position from 1589 nt to 1612 nt with an average $\Delta G = -120$ kJ/mole, and from 1625 nt to 1648 nt with an average $\Delta G = 122$ kJ/mole. Also this mRNA have a cluster of binding sites from 1653 to 1684 nt with a whole length of 32 nt and average $\Delta G = -118$ kJ/mole.

Kumagai et al. [19] indicate that mucin core proteins (*MUC5AC*, *MUC6* and *MUC2*) expressed in the cytoplasm of the tumor cells. 4 miRNAs have binding sites in mRNA of *MUC5AC* gene. All binding sites have the same $\Delta G/\Delta G_m$ value, equal to 90% and relatively equal ΔG value. It is important to mention the significance of free energy of interaction. TJU_CMC_MD2.ID00967.5p-miR with a length of 22 nt has multiple binding sites in *MUC5AC* gene with $\Delta G = -115$ kJ/mole. mRNA of *MUC6* gene have 5 binding sites in CDS. The higher ΔG is observed in association with TJU_CMC_MD2.ID02888.5p-miR ($\Delta G = -121$ kJ/mole).

The average free energy of binding of all miRNAs with mRNAs in the CDS equals -119 kJ/mole. The number of miRNA associations with mRNA having free energy of interaction greater than -125 kJ/mole is 22. All of them can serve as markers in the development of methods for early diagnosis of small intestinal cancer.

Table 6 shows the binding sites of some miRNAs with mRNA genes involved in the development of small intestinal cancer in 3'UTR region.

From 12 target genes in 3'UTR, binding sites for 26 miRNAs were identified (Table 6). mRNA of *SMAD4* gene contained multiple binding sites for TJU_

CMC_MD2.ID00470.5p-miR and TJU_CMC_MD2.ID02299.5p-miR in the same region. Moreover, TJU_CMC_MD2.ID00470.5p-miR, which binds to mRNA with free energy of -108 kJ/mole, can have the highest efficiency of regulation of *SMAD4* gene expression. *SMAD4* plays the role of tumor growth suppressor.

Table 6 – Characteristics of the binding sites of miRNA and mRNA in 3'UTR of genes involved in the development of SIC

Gene	miRNA	The beginning of binding site, nt	ΔG , kJ/mole	$\Delta G/\Delta G_m$, %	Length, nt
<i>ATM</i>	TJU_CMC_MD2.ID03006.5p-miR	9778	-121	89	24
	TJU_CMC_MD2.ID00367.5p-miR	11069	-110	90	22
<i>CDKN2B</i>	TJU_CMC_MD2.ID00470.5p-miR	1746÷1752 (4)	-108	89	23
	TJU_CMC_MD2.ID02299.5p-miR	1746÷1752 (4)	-100	90	22
<i>KRAS</i>	TJU_CMC_MD2.ID03224.5p-miR	3163	-121	92	23
<i>MDM2</i>	TJU_CMC_MD2.ID01404.5p-miR	2154	-110	90	23
	TJU_CMC_MD2.ID01815.5p-miR	2257	-106	89	23
	TJU_CMC_MD2.ID01360.3p-miR	2476	-104	91	21
	TJU_CMC_MD2.ID01838.5p-miR	3214	-110	88	24
<i>MLL2</i>	TJU_CMC_MD2.ID02459.5p-miR	16748	-110	91	21
	TJU_CMC_MD2.ID03342.3p-miR	16931	-119	92	23
	TJU_CMC_MD2.ID00670.3p-miR	16971	-102	91	21
	TJU_CMC_MD2.ID03270.3p-miR	17062	-123	88	25
	TJU_CMC_MD2.ID02547.5p-miR	17065	-113	91	21
	TJU_CMC_MD2.ID01254.5p-miR	17780	-110	91	21
	TJU_CMC_MD2.ID00564.5p-miR	17894	-113	91	22
<i>NF1</i>	TJU_CMC_MD2.ID02733.5p-miR	10571	-89	91	21
<i>PROM1</i>	TJU_CMC_MD2.ID02076.5p-miR	3221	-104	94	19
<i>SMAD4</i>	TJU_CMC_MD2.ID01838.5p-miR	4291	-113	90	24
	TJU_CMC_MD2.ID01404.5p-miR	4349	-115	93	23
	TJU_CMC_MD2.ID02732.3p-miR	7721	-123	91	23
	TJU_CMC_MD2.ID00470.5p-miR	7744÷7752 (5)	-108	89	23
	TJU_CMC_MD2.ID02299.5p-miR	7744÷7752 (5)	-100	90	22
	TJU_CMC_MD2.ID00106.5p-miR	7825	-106	91	22
	TJU_CMC_MD2.ID01592.3p-miR	8227	-117	89	23
<i>SOAT1</i>	TJU_CMC_MD2.ID00868.5p-miR	4885	-123	88	25
	TJU_CMC_MD2.ID01815.5p-miR	4953	-106	89	23
	TJU_CMC_MD2.ID01404.5p-miR	5523	-110	90	23
<i>SOX9</i>	TJU_CMC_MD2.ID00509.3p-miR	2153	-98	92	21
<i>TP53</i>	TJU_CMC_MD2.ID02379.3p-miR	1397	-119	89	24
	TJU_CMC_MD2.ID01838.5p-miR	2459÷2460 (2)	-110÷-115	88÷92	24
	TJU_CMC_MD2.ID00785.5p-miR	2520	-113	90	23
<i>MUC6</i>	TJU_CMC_MD2.ID01401.3p-miR	7883	-108	91	21

Interestingly, TJU_CMC_MD2.ID00470.5p-miR and TJU_CMC_MD2.ID02299.5p-miR have multiple binding sites in mRNA of *CDKN2B* gene in the same region with ΔG value equal to -108 kJ/mole and -100 kJ/mole, respectively. TJU_CMC_MD2.ID00470.5p-miR will have the advantage of binding for this site. miRNA with higher ΔG value is more prevalent takes this binding site and therefore inhibit the expression of this gene.

TP53 is a transcription factor that regulates the cell cycle and performs the function of onco-suppressor. Binding sites in mRNA of this gene were identified. TJU_CMC_MD2.ID01838.5p-miR has multiple consistently located binding sites with an average ΔG value equals -113 kJ/mole.

The results obtained show that interactions of the examined miRNA and mRNA can serve as the basis for the choice of miRNA and mRNA associations for the diagnosis of small intestinal cancer.

Seven miRNAs have binding sites in mRNA of *MLL2* gene. These binding sites are scattered throughout all 3'UTR of mRNA, and we could say that the expression of this gene will be suppressed. Free energy of interaction of these miRNAs equals -113 kJ/mole.

mRNAs of *KRAS*, *NF1*, *PROM1*, *SOX9*, *MUC6* genes have binding sites for single miRNAs. This evidence have the positive phenomena, since typically each miRNA has one or several target genes, and conversely, one gene can be a target for one or more miRNA. That is why, these associations can possibly serve as a marker for early diagnosis of this disease.

The average free energy of binding of miRNAs with mRNAs in 3'UTR equals -109 kJ/mole. Two miRNAs (TJU_CMC_MD2.ID00470.5p-miR and TJU_CMC_MD2.ID02299.5p-miR) have multiple binding sites in mRNA of *CDKN2B* and *SMAD4* genes and therefore are also suggested as associations for the diagnosis of small intestinal cancer.

Thus, miRNAs that participate in the formation of fully complementary binding sites have been identified. With this binding, mRNA degradation may occur to a greater extent than its inhibition. There were revealed slightly different binding sites with the same miRNA located in different mRNA target genes. This shows the effect of resistance to point mutations (single nucleotide polymorphism) in miRNA binding site. Revealed closely related miRNAs having simi-

lar sequences and capable of binding to the same site with different hybridization energy.

Conclusion

In this paper, we studied the characteristics of the interaction of miRNA with mRNA of genes involved in the development of small intestinal cancer. 79 key associations of miRNAs and mRNAs were identified that have had a free energy of interaction of -125 kJ/mole or more that can be recommended both for the diagnostic markers of violations of the expression of these genes, and for the development of methods for the treatment of these disease at the molecular level.

The average free energy of miRNA binding in mRNA of genes involved in small intestinal cancer development is greater in 5'UTR and CDS compared to 3'UTR, which suggests preferential binding of miRNA to 5'UTR and CDS of the studied genes. *ARID1A*, *ASXL1*, *KRAS*, *NF1*, *PDXP*, *PTEN* and *SMAD4* genes was selected as candidate target genes for miRNAs having binding sites in 5'UTR of mRNA. *ARID1A*, *CDKN2B*, *EGFR*, *GNAS*, *MLL2*, *MSH6* and *PDXP* are candidate genes, having miRNAs binding sites in CDS, *CDKN2B* and *SMAD4* are candidate genes, having miRNAs binding sites in 3'UTR.

In summary, mRNA of these genes binds with miRNA with high affinity and, therefore, if the concentrations of the corresponding miRNAs are the same or exceed the concentrations of mRNAs, the effect of mRNA translation inhibition will be significant. Given that miRNAs are endogenous regulators of gene expression, these methods are quite feasible. The results obtained may be able to provide insights into the pathogenesis mechanism and pave the way for the development of new diagnostic markers and therapeutic targets for patients with small intestinal cancer.

Acknowledgments

The work was performed within the framework of the grant project AP05132460 "Development of test systems for early diagnosis of cardiovascular, oncological and neurodegenerative diseases based on miRNA associations and their target genes", financed by the Ministry of Education and Science of the Republic of Kazakhstan.

References

1. Syngal S., Brand R.E., Church J.M., Giardiello F. M., Hampel H. L., Burt R.W. (2015) ACG Clinical guideline, genetic testing and management of hereditary gastrointestinal cancer syndromes. *Am J Gastroenterol.*, vol. 110, no. 2, pp. 223-262.
2. Torre L.A., Bray F., Siegel R.L., Ferlay J., Lortet-Tieulent J., Jemal A. (2015) Global cancer statistics, 2012. *CA Cancer J Clin.*, vol. 65, pp. 87-108.
3. Guller U., Tarantino I., Cerny T., Ulrich A., Schmieid B.M., Warschkow R. (2017) Revisiting a dogma: similar survival of patients with small bowel and gastric GIST. A population-based propensity score SEER analysis. *Gastric Cancer.* vol. 20, no. 1, pp. 49-60.
4. Giuliano K., Nagarajan N., Canner J., Najafian A., Wolfgang C., Schneider E., Meyer C., Lennon AM., Johnston F.M., Ahuja N. (2017) Gastric and small intestine gastrointestinal stromal tumors: Do outcomes differ? *J Surg Oncol.*, vol. 115, no. 3, pp. 351-357.
5. Ye H., Xin H., Zheng Q., Shen Q., Dai W., Wu F., Zheng C., Chen P. (2018) Prognostic role of the primary tumour site in patients with operable small intestine and gastrointestinal stromal tumours: a large population-based analysis. *Oncotarget*, vol. 9, no. 8, pp. 8147-8154.
6. Lee Y. S., Dutta A. (2009) MicroRNAs in cancer. *Annu Rev Pathol.*, vol. 4, pp. 199-227.
7. Grammatikakis I., Gorospe M., Abdelmohsen K. (2013) Modulation of cancer traits by tumor suppressor microRNAs. *Int J Mol Sci.*, vol. 14, no. 1, pp. 1822-1842.
8. Rath S.N., Das D., Konkimalla V.B., Pradhan S.K. (2016) In silico study of miRNA based gene regulation, involved in solid cancer, by the assistance of Argonaute protein. *Genomics Inform.*, vol. 14, no. 3, pp. 112-124.
9. Berillo O., Régnier M., Ivashchenko A. (2013) Binding of intronic miRNAs with mRNAs of genes coding intronic microRNAs and proteins participating in tumorigenesis. *Comput Biol Med.*, vol. 43, no 10, pp. 1374-1381.
10. Londin E., Lohera P., Telonisa A.G., Quanna K., et al. (2015) Analysis of 13 cell types reveals evidence for the expression of numerous novel pri-mate- and tissue-specific microRNAs. *PNAS USA*, vol. 112, no. 10., pp. 1106-1115.
11. Ivashchenko A., Berillo O., Pyrkova A., Niyazova R., Atambayeva S. (2014) The properties of binding sites of miR-619-5p, miR-5095, miR-5096 and miR-5585-3p in the mRNAs of human genes. *Biomed Res Int.*, vol. 2014, pp. 1-8.
12. Kool E.T. (2001) Hydrogen bonding, base stacking, and steric effects in DNA replication. *Annu Rev Biophys Biomol Struct.*, vol. 30, pp. 1-22.
13. Leontis N.B., Stombaugh J., Westhof E. (2002) The non-Watson-Crick base pairs and their associated isosteric matrices. *Nucleic Acids Res.*, vol. 30, no. 16, pp. 3497-3531.
14. Ivashchenko A. T., Niyazova R. Ye., Atambayeva Sh. A., Pyrkova A. Yu., Aisina D. E., Yurikova O. Yu., Kondybayeva A., Akimniyazova A., Bayzhitova D., Bolshoy A.A. (2018) miRNA: achievements, misconceptions, perspectives. *News of NAS RK*, vol 4, no. 328, pp. 36-46.
15. Byun D., Ahmed N., Nasser S., Shin J., Al-Obaidi S., Goel S., Corner G., Wilson A., Flanagan D., Williams D., Augenlicht L., Vincan E, Mariadason J. (2011) Intestinal epithelial-specific PTEN inactivation results in tumor formation. *Am J Physiol Gastrointest Liver Physiol.*, vol. 301, no.5, pp. 856-864.
16. Niyazova R., Atambayeva Sh., Akimniyazova A., Pinsky I., Alybaeva A., Faye B., Ivashchenko A. (2015) Features of mir-466-3p binding sites in mRNA genes with different functions. *Int J Biol Chem.*, vol. 8, no. 2, pp. 44-51.
17. Kantidakis T., Saponaro M., Mitter R., Horswell S., Kranz A., Boeing S., Aygün O., Kelly G.P., Matthews N., Stewart A., Stewart A.F., Svejstrup J.Q. (2016) Mutation of cancer driver MLL2 results in transcription stress and genome instability. *Genes Dev.*, vol.30, no. 4, pp. 408-420.
18. Kim M.J., Gu M.J., Chang H.K., Yu E. (2015) Loss of ARID1A expression is associated with poor prognosis in small intestinal carcinoma. *Histopathology*, vol. 66, no. 4, pp. 508-516.
19. Kumagai R., Kohashi K., Takahashi S., Yamamoto H., Hirahashi M., Taguchi K., Nishiyama K., Oda Y. (2015) Mucinous phenotype and CD10 expression of primary adenocarcinoma of the small intestine. *World J Gastroenterol.*, vol. 21, no. 9, pp. 2700-2710.

IRSTI 616-092; 634.23.53

¹A. Akparova, ²M. Abishev, ¹B. Abdrakhmanova, ^{1*}R. Bersimbaev

¹Department of General Biology and Genomics, L.N. Gumilyov Eurasian National University

²Pulmonary Department of the City Hospital № 2, Astana, Kazakhstan

*e-mail: ribers@mail.ru

Identification of the unique and common genes for asthma and chronic obstructive pulmonary disease: a case-control study in Kazakhstan

Abstract: Asthma and chronic obstructive pulmonary disease (COPD) are lung inflammatory diseases characterized by bronchial obstruction, which is often the cause of difficulties in conducting differential diagnosis between them. They belong to the polygenic diseases, which arise in a result of the gene-environment interactions. Identification of the unique and common genes for these diseases facilitates understanding of their complicated pathogenesis, and provides possible markers for their diagnosis and treatment. The aim of this study was to investigate the association of two single-nucleotide polymorphisms (-1082 A/G *IL-10* and His161Arg *IL17F*) with asthma and COPD in Kazakh population. The study groups consisted of 72 COPD patients, 71 asthmatics and 70 control individuals. Genotyping was performed on purified DNA using real-time polymerase chain reaction with specific primers and probes. Results revealed that the G allele and GG genotype frequencies of -1082 A/G *IL-10* polymorphism were significantly different between the COPD patients and the controls. Furthermore, the G allele and GG genotype of His161Arg *IL-17F* were significantly more common in the COPD patients than among the control individuals ($p < 0.05$). No significant associations were observed for any of these examined SNPs with asthma. These data suggest that the -1082 A/G *IL-10* and the His161Arg *IL-17F* polymorphisms are associated with COPD susceptibility in the Kazakh population, and may be considered as potential biomarkers of this disease.

Key words: chronic obstructive pulmonary disease, asthma, IL-10, IL-17F, genetic polymorphism, Kazakhstan.

Introduction

Asthma and COPD are widespread diseases, leading to significant and constantly increasing economic and social damage [1-3]. Globally, about 300 million people suffer from asthma with 250,000 deaths per year [1]. According to rough estimates, from 0.2% to 37% of the population in different countries live with a diagnosis of COPD. Mortality from this disease varies from 3 to 111 deaths per 100,000 population, and unlike coronary heart disease and stroke this leading cause of death is still increasing [2; 3].

Asthma and COPD are characterized by airflow limitation, but the bronchial obstruction of COPD is irreversible and progressive. With a long-term presence of asthma, difficulties arise in the differential diagnosis of asthma and COPD due to the similarity of their clinical and functional parameters [4]. Various approaches are used for the diagnosis of asthma and COPD, with the definition of standard indicators,

which do not always allow separation of these diseases. Unlike the vast number of proposed biomarkers, genetic polymorphisms have several advantages, including lack of variability in one individual, availability of material and relative ease of detection.

In addition to the genes unique to asthma and COPD, there is a large number of common genes involved in both diseases [5]. The interleukin 10 (IL-10) gene encodes an anti-inflammatory cytokine expressed by many cell populations, including monocytes, Th-2 cells, mast cells, B cells, activated and regulatory T cells [6]. According to the studies [6; 7], -1082 A/G *IL-10* is the most important functional promoter polymorphism, which is localized in the binding site of the transcription factor, and can alter the production and secretion of IL-10. There are only a few studies [8-10] of association between the -1082A/G SNP in IL-10 gene and COPD and their results are conflicting. Seifart et al. [8] found that the G allele of this polymorphism is significantly more

common in COPD patients than in healthy controls. As well a correlation between this polymorphism and higher lung function was obtained in COPD patients with severe α 1-antitrypsin deficiency [9]. However, He et al. [10] did not reveal any association for this SNP with lung function in COPD. To assess the contribution of IL-10-1082A/G polymorphism to asthma the three meta-analysis were conducted in 2012, 2013, and 2014 years, showing its involvement in atopic asthma, asthma in Asians and adults [6; 11; 12].

Interleukin 17F (IL-17F) is an important cytokine engaged in airway remodeling and steroid resistance in asthma and COPD [13-15]. Kawaguchi et al. conducted the functional study of the His161Arg IL-17F polymorph variant *in vitro* for the first time [16]. They demonstrated that the wild type His161Arg is unable to activate the signaling pathway in which one of the MAP kinases (ERK1/2) is phosphorylated, resulting in suppression of cytokines and chemokines expression in bronchial epithelial cells. Hizawa et al. were first to identify the participation of His161Arg IL-17F polymorphism in predisposition to asthma and COPD in 1125 unrelated Japanese individuals [17]. It should be noted that the study of this polymorphism in COPD alone has not been conducted. Currently the three meta-analyses of the His161Arg polymorphism in *IL-17F* gene with asthma were performed [18-20], but only one of them has shown the association with asthma susceptibility in Asian population.

The purpose of this work is to examine the association of -1082 A/G polymorphism in *IL-10* gene and His161Arg polymorphisms in *IL-17F* gene in patients with asthma and COPD in Kazakh population.

Materials and methods

Blood samples and questionnaires were obtained from patients with asthma and COPD, residing in Astana and Akmola region of Kazakhstan for not less than 5 years. Sampling was carried out in the Pulmonary Department of the City Hospital № 2, Astana, Kazakhstan. 71 patients with asthma, 72 patients with COPD and 70 healthy individuals were enrolled in the study. Each subject gave written informed consent. The study was conducted in accordance with the WMA declaration of Helsinki. Demographical data and smoking status were assessed through a questionnaire.

The clinical diagnosis of asthma was made by the expert doctors according to the Global Strategy for Asthma (GINA) recommendations, based on clinical, laboratory and instrumental workup ([\[ma.org\]\(https://ginasthma.org\)\). 36 men \(50.7%\) and 35 women \(49.3%\) with the age range from 31 to 68 years were examined among patients with asthma. COPD diagnosis was established in accordance with the Global Strategy for the treatment and prevention of COPD \(GOLD\) \(<https://goldcopd.org>\) using validated questionnaires for assessment of breathlessness and symptoms: the modified British Medical Research Council \(mBMRC\) scale and the COPD Assessment Test \(CAT\). The COPD group consisted of 72 patients \(37 men \(51.4%\) and 35 women \(48.6%\) aged 43-75 years. Patients with severe respiratory diseases, such as lung cancer, tuberculosis and cystic fibrosis were excluded from the study.](https://ginasth-</p></div><div data-bbox=)

70 healthy volunteers (controls) living in Astana were recruited for the study. Individuals of the control group had no signs of airway obstruction (FEV_1 and $FVC \geq 80\%$, $FEV_1/FVC \geq 70\%$). The criteria for the selection of healthy subjects were the absence of neurological, autoimmune, allergic, endocrine and metabolic diseases, and the lack of family history of atopic and respiratory symptoms. All participants, including asthma and COPD patients, healthy individuals were ethnic Kazakhs. All three groups matched each other with respect to age and gender status.

Isolation of DNA. Genomic DNA was extracted from EDTA treated peripheral blood samples using the standard phenol-chloroform method [21]. Quantitative and qualitative assessment of the DNA was performed by gel electrophoresis and spectrophotometry.

IL-10-1082A/G and IL-17F His161Arg genotyping. The -1082A/G polymorphism in the *IL-10* gene (rs 1800896) and the His161Arg polymorphism in the *IL-17F* gene (rs763780) were detected using the TaqMan Allelic Discrimination assay with proprietary TaqMan probes and primers, produced in the National Center for Biotechnology of the Republic of Kazakhstan.

All polymerase chain reactions were carried out with a reaction mixture, consisting of 16 μ l of Master Mix and 3 μ l of Primer Mix. To perform RT-PCR FAM and ROX dyes were used. 45 cycles of amplification were conducted. At first, denaturation step was carried out at 95°C for 3 minutes, followed by two step denaturation performed at 95°C for 10 seconds, annealing and elongation performed at 60°C for 40 seconds. FAM dye corresponds to the T allele, and the dye ROX matched to the C allele. The discrimination of genotypes was carried out using BioRad CFX manager 3.1 software. To validate the results of genotyping approximately 5% of the samples were

randomly selected and re-genotyped. A 100% double coincidence of genotyping was achieved.

Statistical data analysis. All statistical tests were carried out using GraphPad InStat 7 Software (Graphpad Software Inc., San Diego, CA). Differences in basic characteristics of the participants were determined using the Students' unpaired T-test and the Chi-square test. Hardy-Weinberg equilibrium was assessed using the χ^2 test comparing genotype frequencies among cases and controls. Odds ratio (OR), 95% confidence intervals, and two-tailed p values were calculated for assessing the risk of the variant genotype towards the development of asthma and COPD. Statistical significance was set at $p < 0.05$.

Results and discussion

In recent decades, a lot of information has been produced on asthma and COPD, but there are still a lot of unclear questions about the inheritance mecha-

nisms of these complex diseases. The formation of COPD is most often associated with smoking and the presence of bronchial obstruction in childhood, but only 10-20% of the lifetime incidence of COPD occurs in people with a long history of smoking [22]. The accumulation of asthma cases in families is observed, and the coefficient of its heritability can reach up to 60% [23]. This data demonstrates that heredity plays an important role in the development of asthma and COPD.

A large number of common genes are implicated in formation of asthma and COPD [24], but their involvement to asthma and COPD varies in different populations. We investigated the association between -1082A/G polymorphism in *IL-10* gene and His161Arg polymorphism in *IL-17F* gene with asthma and COPD in Kazakh population.

In total, 213 participants were enrolled in this study. Demographic data and clinical characteristics of the study participants are shown in Table 1.

Table 1 – Characteristics of the study population

Parameters	Asthmatics	COPD patients	Controls
Number of study participants (N)	71	72	70
% male	36 (50.7%)	37 (51.4%)	35 (50%)
Age, M±m	52.3±10.6	54.5±14.3	53.7±11.3
Work experience at harmful work place, M±m	5.4±1.6	17±4.2	0
Index of smoking (PY), M±m	1.3±0.5	**39.6±14.3	1.8±0.3
Smokers/former smokers, n (%)	9 (12.7%)	****48 (66.7%)	12 (17.1%)
Baseline FEV1% predicted (SD)	89.4 ±17.3	****52.3±4.05	95.1 (±7.3)
FEV ₁ /FVC (SD)	0.76 (±0.13)	**0.54 (±0.09)	0.82 (±0.03)
Family history of asthma, n (%)	32 (45.1%)	-	-
Age at onset of diseases (y; median, range)	31; 0-64	57.3; 39-75	-
Note: *, **, ***, ****p value <0.05, 0.01, 0.001, 0.0001 when compared to the control group; <i>Genotyping of the polymorphisms in IL-10 and IL17F among the asthma patients</i>			

No significant differences were observed between the cases and controls in the age and gender. The forced expiratory volume in the first second of expiration (FEV1, % predicted) and FEV1/FVC (FVC – forced vital capacity) showed significant differences in the COPD patients compared with the control group. The COPD patients and controls differed significantly with regards to the smoking status, index of smoking and work experience at harmful work place. The controls in our study matched to Hardy-Weinberg equilibrium (*IL-10* rs1800896, $\chi^2=0.09$, $p=0.76$; *IL-17F* rs763780, $\chi^2=0.33$, $p=0.57$).

Association of polymorphisms in IL-10 and IL17F genes with COPD. Tables 2 and 3 show the allele and genotype distributions of -1082 A/G *IL-10* and His161Arg *IL17F* in COPD patients and controls. We observed that the G allele and GG genotype of -1082 A/G *IL-10* polymorphism have a significantly more frequencies in the COPD patients compared to the controls ($p=0.005$ and $p=0.009$, respectively). A significant difference in frequencies of G allele (OR=2.77; CI=1.23–6.21) and GG genotype (OR=9.26; CI=0.49–175.33) was found between COPD patients and control subjects for *IL-17F* gene His161Arg SNP.

Table 2 – Allele frequency of His161Arg *IL-17F* polymorphism among COPD patients and normal Kazakh population

Cytokine polymorphism	Allele	COPD		Control		Fisher exact p-value	Odds ratio	Wald's 95% CI
		N	F	N	F			
IL-10	A	95	0.660	113	0.807	0.005	2.16	1.25 – 3.72
	G	49	0.340	27	0.193			
IL-17F	A	121	0.840	131	0.936	0.01	2.77	1.23 – 6.21
	G	23	0.160	9	0.064			

Table 3 – Genotype distributions of His161Arg *IL-17F* polymorphism among COPD patients and normal Kazakh population

Cytokine polymorphism	Genotype	COPD		Control		Fisher exact p-value	Odds ratio	Wald's 95% CI
		N	F	N	F			
IL-10	AA	34	0.472	46	0.657	0.009	0.47	0.24 – 0.92
	AG	27	0.375	21	0.300		1.40	0.70 – 2.82
	GG	11	0.153	3	0.043		4.03	1.07 – 15.12
IL-17F	AA	53	0.736	61	0.871	0.02	0.41	0.17 – 0.99
	AG	15	0.208	9	0.129		1.78	0.72 – 4.40
	GG	4	0.056	0	0.000		9.26	0.49 – 175.33

The main biological functions of IL-10 as expected are the limit and termination of inflammatory responses and the regulation of differentiation and proliferation of immune cells, such as T cells, B cells, natural killer cells, antigen-presenting, mast cells and granulocytes. It was demonstrated that IL-10 participates in Tregs mediated suppression of allergic reactions, and also promotes immune homeostasis in the lung tissue [25]. Low levels of IL-10 are associated with the pathogenesis of asthma and COPD [26]. Our results showed that the GG genotype and G allele of -1082A/G polymorphism in IL-10 gene are more common in patients with COPD and patients with the presence of this genotype have a higher risk of developing a disease. As mentioned above, only a few studies have been devoted to the finding of association between -1082A/G polymorphism in IL-10 and COPD, and our data matches them. Study of Seifart C. et al. involved 469 unrelated Caucasian German individuals, including 113 COPD patients; the statistical significance was achieved, when COPD-smokers were compared with the population control [8]. Besides, DeMeo et al. found the association of IL-10 -1082A/G polymorphism with higher lung function in COPD patients with ZZ genotype of α 1-antitrypsin gene [9].

Association of Th17-lymphocytes with a number of neutrophils, macrophages and proinflammatory cytokines is seen in the airways of COPD patients. It is known that the effects of Th17-lymphocytes are mediated by appropriate cytokines, including IL-17F [27]. Increasing the IL-17F level in the blood serum of COPD patients with acute exacerbation compared with stable COPD or control was obtained [28], as well as enhance of the IL-17F expression in local lung cells after cigarette smoke exposure in COPD patients [15]. We observed an association between His161Arg IL-17 polymorphism and COPD.

Genotyping of the polymorphisms in IL-10 and IL17F among the asthma patients. The genotypes and allele frequencies of the -1082A/G polymorphism in IL-10 gene and His161Arg polymorphism in IL17F gene are presented in Tables 4 and 5. None of the SNPs showed any association with asthma ($p > 0.05$).

The alveolar macrophages of asthma patients produce significantly less of IL-10 [29]. Asthma severity is clearly dependent on IL-10 levels, which in return leads to the production of some pro-inflammatory cytokines, contributing to the formation of chronic inflammation in the lower respiratory tract [29]. Large number of associative studies of -1082A/G *IL-10* polymorphism with asthma and its phenotypes were performed. The results of most of these studies were

summarized and evaluated in the three meta-analyses reported above, demonstrating the effect of this polymorphism on the development of asthma in adults,

Asians and atopic asthma. However, we observed no significant associations between -1082A/G *IL-10* polymorphism and asthma in Kazakh population.

Table 4 – Allele frequency of -1082A/G *L-10* polymorphism among asthma patients and normal Kazakh population

Cytokine Polymorphism	Allele	Asthma		Control		Fisher exact p-value	Odds ratio	Wald's 95% CI
		N	F	N	F			
IL-10	A	109	0.768	113	0.807	0.42	0.79	0.45– 1.40
	G	33	0.232	27	0.193			
IL-17F	A	133	0.937	131	0.936	0.98	1.02	0.39 – 2.64
	G	9	0.063	9	0.064			

Table 5 – Genotype distributions of -1082A/G *L-10* polymorphism among asthma patients and normal Kazakh population

Cytokine Polymorphism	Geno-type	Asthma		Control		Fisher exact p-value	Odds ratio	Wald's 95% CI
		N	F	N	F			
IL-10	AA	43	0.606	46	0.657	0,43	0.80	0.40– 1.59
	AG	23	0.324	21	0.300		1.12	0.55– 2.28
	GG	5	0.070	3	0.043		1.69	0.39– 7.37
IL-17F	AA	62	0.873	61	0.871	0.97	1.02	0.38 – 2.73
	AG	9	0.127	9	0.129		0.98	0.37 – 2.65
	GG	0	0.000	0	0.000		0.99	0.02 – 50.39

Numerous studies demonstrating the important role of IL-17F in the pathogenesis of asthma is increased. The expression of *IL-17F* is observed in a wide range of asthmatics cells, such as activated CD4+ T lymphocytes, basophils, mast cells, Th17 lymphocytes, bronchial epithelial cells, etc. [13]. IL-17F can increase the allergic inflammation in airways and contributes the formation of severe asthma due to the induction of the chemokine ligand 20 (CCL20) by Th17 lymphocytes [13]. Moreover, the role of IL-17F in exacerbations frequent of neutrophilic asthma was shown [30]. In our study, we did not identify an association between His161Arg *IL-17* polymorphism and asthma.

Kawaguchi et al. [16] first showed that His161Arg SNP is a protective variant of the *IL-17F* gene against asthma in Japan. Du et al. [18] investigated the His161Arg polymorphism of the *IL-17F* gene in Han ethnicity individuals living in China. This study showed no significant differences between patients with asthma and control in additive models with significant differences in allele models. Also in this study, a meta-analysis of His161Arg *IL-17F* SNP in Asian populations was conducted and this polymor-

phism indicated association with asthma susceptibility. In another meta-analysis, Ke et al. reported no association between the His161Arg polymorphism in the *IL-17F* gene and the predisposition to asthma [19]. Further, a meta-analysis of 11 single nucleotide polymorphisms of *IL-17F* showed no significant connection between this SNP and asthma susceptibility in a study, implemented by Yan Jin et al. [20].

Recent achievements of asthma and COPD genetics suggest that one gene does not play the significant role in the total amount of etiologic factors in these diseases, and, as it can be seen from our study, smoking is also an important factor in the development of COPD. In addition, summation of pathological agents may lead to an increase in susceptibility to diseases, and the necessary condition for its finding is the establishment of a group of involved genes, as well as a detailed description of patients with indication of ethnicity.

Conclusion

This study examined the involvement of the *IL-10* and *IL17F* genes in development of asthma

and COPD in Kazakh population. We concluded that His161Arg polymorphism in *IL-17F* gene and -1082A/G polymorphism in *IL-10* are associated with COPD and may serve as the differential markers for this disease in population of ethnic Kazakhs.

Acknowledgements

This work has been supported by the program "Grant funding for research" № 0112RK02125 from the Ministry of Education and Science of the Republic of Kazakhstan. Principal Investigators: R. Ber-simbaev, A. Akparova. We would like to gratefully acknowledge Dr. I. Ahmetollaev from the National Centre for Biotechnology of the Republic of Kazakhstan for kindly supplying the RT-PCR reagents in this project.

References

1. Brasier A.R. (2014). Heterogeneity in Asthma. *Springer*, pp. 17-18.
2. Rycroft C., Heyes A., Lanza L., Becker K. (2012) Epidemiology of chronic obstructive pulmonary disease: a literature review. *Int J Chron Obstruct Pulmon Dis.*, vol. 7, pp. 457-494.
3. May S., Li J. (2015) Burden of chronic obstructive pulmonary disease: Healthcare costs and beyond. *Allergy Asthma Proc.*, vol. 36, no. 1, pp. 4-10.
4. Athanazio R. (2012) Airway disease: similarities and differences between asthma, COPD and bronchiectasis. *Clinics.*, vol. 67, no. 11, pp. 1335-1343.
5. Postma D., Kerkhof M., Boezen H., Koppelman G.H. (2011) Asthma and Chronic Obstructive Pulmonary Disease. Common Genes, Common Environments? *Am J Respir Crit Care Med.*, vol. 183, pp. 1588-1594.
6. Hyun M.H., Lee Ch.H., Kang M.H., Park B.K., Lee Y.H. (2013) Interleukin-10 Promoter Gene Polymorphisms and Susceptibility to Asthma: A Meta-Analysis. *Plos one*, vol. 8, pp. 1-8.
7. Bocşan I., Muntean A., Buzoianu A. (2015) The association between the interleukin-10 gene polymorphism (-1082 G/A) and allergic diseases. *Hum Vet Med.*, vol. 7, pp. 237-243.
8. Seifart C., Dempfle A., Plagens A., Seifart U., Clostermann U., Müller B., Vogelmeier C., Von Wichert P. (2005) TNF-a-, TNF-b-, IL-6-, and IL-10-promoter polymorphisms in patients with chronic obstructive pulmonary disease. *Tissue Antigens*, vol. 65, pp. 93-100.
9. DeMeo D., Campbell E., Barker A. (2008) IL10 polymorphisms are associated with airflow obstruction in severe α 1-antitrypsin deficiency. *Am J Respir Cell Mol Biol.*, vol. 38, pp. 114-120.
10. He J.-Q., Shumansky K., Zhang X., Connett J. E., Anthonisen N. R., Sandford A. J. (2007) Polymorphisms of interleukin-10 and its receptor and lung function in COPD. *Eur Respir J.*, vol. 29, pp. 1120-1126.
11. Zheng X., Guan W., Mao C., Chen H.F., Ding H., Zheng J.P., Hu T.T., Luo M.H., Huang Y.H., Chen Q. (2014) Interleukin-10 promoter 1082/-819/-592 polymorphisms are associated with asthma susceptibility in Asians and atopic asthma: a meta-analysis. *Lung*, vol. 192, pp. 65-73.
12. Nie W., Fang Z., Li B., Xiu Q. (2012) Interleukin-10 promoter polymorphisms and asthma risk: a meta-analysis. *Cytokine*, vol. 60, pp. 849-855.
13. Ota K., Kawaguchi M., Matsukura S., Kurokawa M., Kokubu F., Fujita J., Morishima Y., Huang Sh.K., Ishii Y., Satoh H., Hizawa N. (2014) Potential involvement of IL-17F in asthma. *J Immun Res.*, pp. 1-8.
14. Akimzhanov A., Yang X., Dong C. (2007) Chromatin remodeling of interleukin-17 (IL-17)-IL-17F cytokine gene locus during inflammatory helper T cell differentiation. *J Biol Chem.*, vol. 282, pp. 5969-5972.
15. Chang Y., Al-Alwan L., Alshakfa S., Audusseau S., Mogas A. K., Chouiali F., Nair P., Baglolle C. J., Hamid Q., Eidelman D. H. (2014) Upregulation of IL-17A/F from human lung tissue explants with cigarette smoke exposure: implications for COPD. *Changet al. Respiratory Research*, vol. 15, pp. 1-10.
16. Kawaguchi M., Takahashi D., Hizawa N., Suzuki S., Matsukura S., Kokubu F., Maeda Y., Fukui Y., Konno S., Huang S.K., Nishimura M., Adachi M. (2006) IL-17F sequence variant (His161Arg) is associated with protection against asthma and antagonizes wild-type IL-17F activity. *J Allergy Clin Immunol.*, vol. 117, pp. 795-801.
17. Hizawa N. (2009) Genetic backgrounds of asthma and COPD. *Allergol Int.*, vol. 58, pp. 315-322.
18. Du J., Han J.C., Zhang Y.J., Qi G.B., Li H.B., Zhang Y.J., Cai S. (2016) Single-nucleotide polymorphisms of IL-17 gene are associated with asthma susceptibility in an Asian population. *Med Sci Monit.*, vol. 22, pp. 780-787.
19. Ke R., Xie X., Su X., Song Y., Yang L., and Li M. (2015) Association between IL-17Fr5763780 polymorphism and susceptibility of asthma: a me-

ta-analysis. *Int J Clin Exp Med.*, vol. 8, no. 8, pp. 12928-12934.

20. Jin Y., Deng Z., Cao C., Li L. (2015) IL-17 polymorphisms and asthma risk: a meta-analysis of 11 single nucleotide polymorphisms. *J Asthma*, Early Online, pp. 1-8.

21. Sambrook J., Fritsch E., Maniatis T. (1989) Molecular Cloning, *Cold Spring Harbor Laboratory Press, NY*. 545 p.

22. Yuan C., Chang D., Lu G., Deng X. (2017) Genetic polymorphism and chronic obstructive pulmonary disease. *Int J of COPD*, vol. 16(4), pp. 1385-1393.

23. Hizawa N. (2015) Genetics of Asthma. *J Gen Fam Med.*, vol. 16(4), pp. 252-259.

24. Smolonska J., Koppelman G., Wijmenga C., Vonk J.M., Zanen P., Bruinenberg M., Curjurić I., Imboden M., Thun G.-A., Franke L., Probst-Hensch N.M., Nürnberg P., Riemersma R.A., van Schayck O., Loth D.W., Bruselle G.G., Stricker B.H., Hofman A., Uitterlinden A.G., Lahousse L., London S. J., Loehr L.R., Manichaiku A., Barr R.G., Donohue K.M., Rich S.S., Pare P., Bossé Y., Hao K., van den Berge M., Groen H.J.M., Lammers J.-W.J., Mali W., Boezen H.M., and Postma D.S. (2014) Common genes underlying asthma and COPD? Genome-wide analysis on the Dutch hypothesis. *Eur Respir J.*, vol. 44, no. 4, pp. 860-872.

25. Martín-Orozco E., Norte-Muñoz M. and Martínez-García J. (2017) Regulatory T cells in allergy and asthma. *Front Pediatr.*, vol. 5, 117, pp. 1-18.

26. Tarzi M., Klunker S., Texier C., et al. (2006) Induction of interleukin-10 and suppressor of cytokine signalling-3 gene expression following peptide immunotherapy. *Clin Exp Allergy*, vol. 36, pp. 465-474.

27. Ponce-Gallegos M., Ramirez-Venegas A., Falfan-Valencia R. (2017) Th17 profile in COPD exacerbations. *Int J of COPD*, vol. 12, pp. 1857-1865.

28. Zou Y., Chen X., Liu J., et al. (2017) Serum IL-1 β and IL-17 levels in patients with COPD: associations with clinical parameters. *Int J Chron Obstruct Pulmon Dis.*, vol. 12, pp. 1247-1254.

29. Trifunović J., Miller L., Debeljak Ž., Horvat V. (2015) Pathologic patterns of interleukin 10 expression – a review. *Biochem Med (Zagreb)*, vol. 25, no. 1, pp. 36-48.

30. Ricciardolo F., Sorbello V., Folino A., Gallo F., Massaglia G.M., Favatà G., Conticello S., Vallese D., Gani F., Malerba M., Folkerts G., Rolla G., Profita M., Mauad T., Di Stefano A., Ciprandi G. (2017) Identification of IL-17F/frequent exacerbator endotype in asthma. *J Allergy Clin Immunol.*, vol. 140, no. 2, pp. 395-406.

IRSTI 34.27.39

^{1*}A. Baubekova, ²Sh. Akhmetsadykova, ^{1,2}A. Kondybayev,
³B. Faye, ¹G. Konuspayeva

¹Al-Farabi Kazakh National University, Almaty, Kazakhstan

²Research and Production Enterprise “Antigen” Co. Ltd, Almaty region, Kazakhstan

³UMR Selmet, Cirad, Montpellier, France

*e-mail: Almagul.Baubekova@kaznu.kz

Volatile organic compounds profile of *Lactobacillus casei* and *Streptococcus thermophilus* in fermented mare milk of Kazakhstan

Abstract: Fermented milk is a common beverage in many countries, but its flavor is highly variable from one region to another. The fermented mare milk, common beverage in Central Asia, has a typical flavor of *koumiss*, but those flavors were never described using aroma compound determination. In the present study, six lactic acid bacteria were identified in local *koumiss*. Due to the apparent technological advantage of *Lactobacillus casei* and *Streptococcus thermophilus* (notably their acidification speed), the main objective of this study was to compare their volatile compound profiles. 35 aromatic compounds were detected. To compare the aroma profiles of each strain, the ratio proportion strain/control was calculated for each strain and for each aroma showing significantly different profiles with predominance of 2-methyl-1-propanol and 2-undecanol in milk fermented with *L. casei*, and of 2,3-pentanedione in milk fermented with *S. thermophilus*. *L. casei* strain produced more aroma and its profile was significantly ($P>0.03$) different from *S. thermophilus* profile.

Key words: mare milk, *koumiss*, *Lactobacillus casei*, *Streptococcus thermophilus*, aromatic compounds.

Introduction

Fermented milk is a common beverage in many countries, but their taste is highly variable from one region to another [1]. Flavor development mainly depends on the microflora, composed of lactic bacteria and yeasts [2]. The main biodiversity of taste in fermented products as wine is due to “terroir”, which depends on different factors: local microflora, traditional tools and dishes used, climatic conditions (temperatures, humidity), etc. The characterization of microflora from fermented dairy products originated from non-cattle milk are few investigated especially, there is few data regarding the microflora biodiversity in fermented mare milk [3]. Traditionally, mare milk is produced and consumed in Central Asian countries, such as Kazakhstan, Mongolia, Kyrgyzstan, Uzbekistan, Russia, China (western provinces) [4].

In other countries, mare milk is consumed under milk form, essentially for newborn babies in France, in Germany etc. The main strains isolated in fermented mare milk (in international data called *koumiss*, and phonetically in Kazakh – *koumiss*), are lactic

bacteria such as *Lactobacillus (L.) casei*, *L. helveticus*, *L. plantarum*, *L. fermentum*, *L. acidophilus*, *Leuconostoc mesenteroides*, *Lactococcus lactis*, *Streptococcus (S.) thermophilus*, *Enterococcus faecalis*, *Enterococcus durans*, *Enterococcus casseliflavus*; and yeasts, such as *Kazachstania unispora*, *Saccharomyces cerevisiae*, *Torulopsis koumiss* [3; 5-11].

The characterization of aroma production by microflora was mainly achieved in cheese, notably after ripening [12-15]. The fermented mare milk has a typical flavor of *koumiss* [16]. However, those flavors are generally described as organoleptic properties, only with words, such as acid, milky, creamy, sweet and some other. Traditionally produced on-farm by mixing fresh milk with already fermented milk; the organoleptic qualities of *koumiss* are highly variable. Face to industrialization of the process, there is necessity to standardize the production. For that, the characterization of aroma by selected microflora is a way to propose standardized *koumiss* to the consumers. At our knowledge, the aroma description of fermented mare milk was never achieved.

As the target of our strain selection was to prepare starters for fermentation process at industrial

level [17]. Lactic acid bacteria (LAB) strains were tested for their acidification speed and their survival capacity in selective milieu for industrial use, especially acid-resistance and growth speed in bioreactor [18]. Finally, the main objective of the present study was to compare the volatile compound profile of mare milk fermented separately by the selected strains among the natural lactic bacteria.

Materials and methods

Analyzed samples and microflora isolation. One sample of *koumiss* with typical pleasant taste was collected in Almaty region, Saryzhailau dairy plant for isolation of natural microflora. The LABs were isolated on MRS and M17 media at the conditions described *infra* in Table 1.

Table 1 – Lactic acid bacteria strains isolated from koumiss in Almaty region

No.	Microorganism code	Growth medium	Growth conditions in broth	Growth conditions on agar
1	<i>K5</i>	<i>MRS</i>	37°C/AE, 24 h	37°C/AE, 24 h
2	<i>K7</i>	<i>MRS</i>	37°C/AE, 24 h	37°C/AE, 24 h
3	<i>K5.C</i>	<i>MRS</i>	37°C/AE, 24 h	37°C/AE, 24 h
4	<i>K14</i>	<i>MRS</i>	37°C/AE, 24 h	37°C/AE, 24 h
5	<i>K12</i>	M17	42°C/AE, 24 h	42°C/AE, 48 h
6	<i>K17</i>	M17	42°C/AE, 48 h	42°C/AE, 48 h

Identification of strains. To identify the strains, polymorphism in the DNA fragment of ribosomal 16S was used according to the methods of Ampe and Leasing [19; 20]. The purity and quantity of extracted DNA was verified by measuring the absorbance (Biospec-Nano, Japan), and by electrophoresis and loaded into 0.8% agarose gel in 1x TAE buffer (40 mM Tris-HCl, pH 7.4, 20 mM sodium acetate, 1.0 mM Na₂-EDTA, Eppendorff, Hamburg, Germany) with a molecular weight ladder 1kb (Supercoiled DNA Ladder, Invitrogen, USA). After running at 100 V for 40 min, the gels were stained for 30 min in an ethidium bromide solution (50 µg/mL/1; Promega), rinsed for 10 min in distilled water, then observed and photographed on a UV transilluminator.

PCR amplification of extracted DNA. The V3 variable region of bacterial 16S rDNA was amplified using Seqfor1 (5'-GGA AAC AGA TGC TAA TAC CG-3', Sigma) and seqrev 1 (5'-GCT GCT GGC ACG TAG TTA-3', Sigma) primers.

PCR amplifying procedure was as follows: 3 min at 94°C, 30 cycles of 1 min at 94°C, 1 min at 46°C, 1 min at 72°C and then 5 min at 72°C. It was carried out on the automatic thermal cycler (PTC-100 Peltier Thermal Cycler). Isolation and purification of PCR products was carried out using the Wizard PCR Preps (Promega, USA) kit, as recommended by the manufacturer. The sequencing of purified products was performed by GATC Biotech (Germany). Raw sequences data were edited using Sequence Scanner software and compared to the GenBank database us-

ing the BLAST program (<http://www.ncbi.nlm.nih.gov/BLAST/>) and the Ribosomal Database Project (<http://rdp.cme.msu.edu/index.jsp>). Sequences having a percentage of identity of 97% or greater were considered to belong to the same species [21; 22].

Acidification tests and growth kinetic of the identified LABs. The process of lactic acid bacteria fermentation was evaluated using Cinac. The Cinac system (INRA, France), allows continuous monitoring of the activity of acid-enzymatic fermentation by simultaneously observing changes in pH and temperature in several samples. LAB was inoculated into ultra-sterilized cow milk (2.5% fat, UHT, bio, Casino, France) in an amount of 2% and cultured at optimal temperature conditions: 42±1°C for thermophilic *Streptococci*, 37±1°C for *Lactobacilli*.

All tests were carried out in duplicate. After 24h of incubation, 2.5 mL aliquots of the samples were placed in vials (PerkinElmer, 22 mL) with polytetrafluoroethylene (PTFE)/silicone septa. Samples were stored at -80°C until analysis of volatile compounds.

Analyses of volatile compounds (VOC). Samples were analyzed by the team from UMR 1253 STLO (INRA-Rennes, France). Aliquots (2.5 g) of cultures were placed in 22 mL PerkinElmer vials with polytetrafluoroethylene/silicone septa. Vials were stored at -80°C until analysis of volatile compounds. Samples were randomized in the sample list.

Extraction of volatile compounds. A Perkin Elmer Turbomatrix HS-40 trap automatic headspace sampler with trap enrichment was used to extract

volatiles according to Pogacic et al, 2015 [15]. The principle of the HS-trap method has been previously described in detail [23; 24]. It includes several steps: equilibration, pressurization, trap load, trap dry-purge, trap desorption and trap hold. Conditions were as follows. Samples were warmed for 15 min at 65°C (equilibration). The vials were then pressurized for 1 min at 207 kPa with the carrier gas (helium), by introducing a needle through the septum. A Tenax™ trap at 35°C was then loaded for 2.3 min by allowing the pressure to fall through the trap, permitting the adsorption and the concentration of the analytes of the headspace on the trap. The trap load was repeated twice for each vial trap. The adsorbed water was then removed by purging helium through the trap (dry purge: 3 min). The trap was heated at 250°C for 0.1 min and back flushed at 89 kPa, leading to desorption of the analytes, which were then transferred to the GC through a transfer line maintained at 150°C, with an injection time of 0.6 min. The trap was held at 250°C for 5 min.

Analysis of volatile compounds. Volatiles were analyzed using a Clarus 680 gas chromatograph coupled to a Clarus 600T quadrupole mass spectrometer (Perkin Elmer, Courtaboeuf, France). They were separated on a Stabilwax-MS capillary column (30 m x 0.25 mm x 0.25 µm; Restek, France), with helium as the mobile phase. The initial temperature of the oven, 30°C, was maintained for 10 min. The increase of temperature was performed at a rate of 5°C/min up to 230°C. The mass spectrometer was operated in the scan mode (scan time 0.3 s, interscan delay 0.03 s) within a mass range of m/z 29 to 206. Ionization was done by electronic impact at 70 eV. Standards were regularly injected to verify the absence of instrumental drift of the GC-MS system. Blank samples (boiled deionized water) were also injected to check the absence of carry-over. Volatile compounds were identified by comparison of mass spectra and retention times with those of authentic standards purchased from Sigma-Aldrich (St-Quentin-Fallavier, France), on the basis of their retention index and mass spectral data from the NIST 2008 Mass Spectral Library (Scientific Instrument Services, Ringoes, NJ, USA). Some compounds were tentatively identified on the basis of mass spectral data only when data on retention indices were not available.

Data processing. Data pre-processing was performed using PerkinElmer Turbomass software, version 5.4.2.1617. The GC-MS raw data files were converted to netCDF format with Data Bridge (Perkin Elmer, Waltham, Massachusetts, USA) for further analysis. GC-MS data were processed by converting

the raw data to time- and mass-aligned chromatographic peaks areas using the open source XCMS package implemented with the R statistical language [25]. The full width at half maximum was set to 5, the group band-width to 3, and the other parameters were those by default.

Statistical data analysis. Each strain was analyzed in triplicate and the mean was retained as convenient value after verification of a low variation coefficient. This coefficient for triplicates was all the times below 1%. It was on average 0.011% (range 0.001-0.058% according to compound) for control sample, 0.026% (0.001-0.107) for *L. casei* sample, and 0.018% (0.002-0.063) for *S. thermophilus* sample. The aroma profiles were compared graphically. To facilitate the comparison, the quantitative values were presented as percentage of total aroma in the results table, and transformed in log10 values for giving a better reading of the profiles' graphic. Due to the lack of homogeneity of the variance, a non-parametric test (Mann-Whitney test) was applied to compare the two entire profiles by using the software XLstat (Addinsoft®).

Results and discussion

LABs were identified by NCBI and RDP data bases with 100% confidence with Seqfor1 and Seqrev1 system of primers. Finally, six LAB strains were isolated and identified belonging to genus *Lactococcus*, *Leuconostoc*, *Lactobacillus* and *Streptococcus* (Table 2).

Table 2 – Identification of lactic acid bacteria strains isolated from koumiss

No.	Microorganism code	Identified microorganism
1	K5	<i>Lactococcus lactis</i>
2	K7	<i>Leuconostoc lactis</i>
3	K5.C	<i>Leuconostoc lactis</i>
4	K14	<i>Lactobacillus casei</i>
5	K12	<i>Streptococcus thermophilus</i>
6	K17	<i>Streptococcus thermophilus</i>

After 18 hours of incubation during acidification tests, pH of fermented milk with specific strains decreased from 6.5 to 4.14 for *Lactobacillus casei* K14 (*L. casei*) and to 5.22 for *Streptococcus thermophilus* K12 (*S. thermophilus*). The acidification speed of the

other strains was slower. Moreover, one of the most common points regarding *koumiss* microflora in the literature is the common presence of *L. casei* and *S. thermophilus*. Those species have high technological interest and could play also therapeutic effect on liv-

er damages [26]. So, finally, those two LAB strains were selected for the VOC analysis.

As the whole, 35 volatile aroma compounds produced by studied strains and control sample of milk were identified (Figure 1).

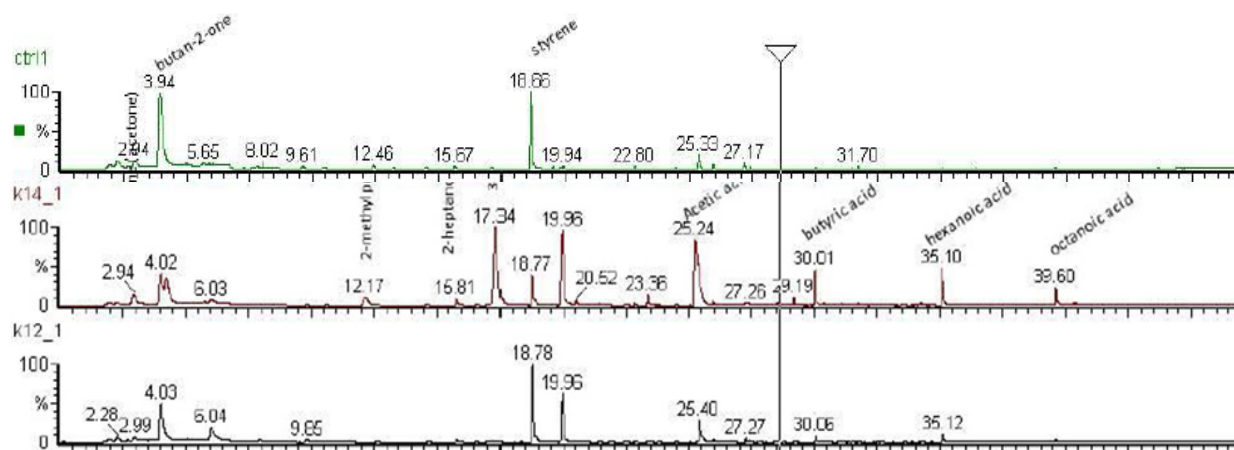


Figure 1 – Chromatographic profile of each samples of strains

The main aroma compounds among the 35 detected ones (representing more than 3.5% in percentage, i.e. above the mean of percentage of 100/35) found in control sample were styrene and 2-butanone. In sample of fermented milk inoculated with *L. casei*, the main compounds were meth-

ylbenzene, 2,3-butanedione, styrene, 2 butanone, 3-hydroxy, and 2-butanone. In milk fermented with *S. thermophilus*, they were hexanoic acid, 3-methylbutanal, butanoic acid, 2-butanone, 1-butanol, 3-methyl, 2 butanone, 3-hydroxy and acetic acid (Table 2).

Table 2 – Volatile aroma proportion (the total of column is 100%) of milk fermented by each strain and control (without fermentation, milk only)

Name	Ion	TR	CAS number	Identification database	Control	<i>L. casei</i>	<i>S. thermophilus</i>
2-undecanol	97	32.33	1653-30-1	RI, DB	0.0002	0.0006	0.0152
2-methyl-1-propanol	74	12	78-83-1	S, RI, DB	0.0007	0.0005	0.2108
2,3-pentanedione	100	9.78	600-14-6	RI, DB	0.0014	0.3684	0.0004
propionic acid, 2-methyl	73	28.5	79-31-2	S, RI, DB	0.0033	0.0067	0.1613
2-tridecanone	71	34.33	593-08-8	RI, DB	0.0050	0.0187	0.0515
2-propanone, 1-hydroxy	74	20.5	116-09-6	RI, DB	0.0061	0.0099	0.1230
propionic acid	74	27.76	79-09-4	S, RI, DB	0.0103	0.0350	0.1043
2-buten-1-ol, 3-methyl-, acetate	67	21.43	1191-16-8	RI, DB	0.0128	0.0308	0.1222
2-undecanone	58	29.18	112-12-9	RI, DB	0.0182	0.1264	0.6356
2-butenal-3-methyl	84	16.55	107-86-8	RI, DB	0.0246	0.0226	0.1718

Continuation of Table 3

Name	Ion	TR	CAS number	Identification database	Control	<i>L. casei</i>	<i>S. thermophilus</i>
hexanol	56	22.47	111-27-3	RI, DB	0.0280	0.1299	0.0764
butanoic acid, 3-methyl	60	31.02	503-74-2	S, RI, DB	0.0357	0.0584	0.2868
1-butanol, 3-methyl	55	17.3	123-51-3	S, RI, DB	0.0415	0.1065	15.7518
hexanal	82	10.65	66-25-1	RI, DB	0.0663	0.0022	0.0005
p-xylene	106	13.07	106-42-3	S, RI, DB	0.0886	0.0091	0.0022
octanoic acid	60	39.58	124-07-2	S, DB	0.0889	0.7855	0.9837
2-nonanone	58	23.33	821-55-6	S, RI, DB	0.1814	0.2485	1.2712
2-pentanone	86	5.75	107-87-9	RI, DB	0.1985	0.1197	0.1913
hexanoic acid	60	35.08	142-62-1	S, DB	0.2136	1.6628	4.1169
acetic acid	60	25.4	64-19-7	S, RI, DB	0.2965	2.6020	22.7597
dimethyl sulfone	79	36.42	67-71-0	DB	0.3180	0.1723	0.1991
2 butanone, 3-hydroxy	45	19.93	513-86-0	S, RI, DB	0.3460	25.3227	18.8271
3-methylbutanal	58	4.2	590-88-3	S, RI, DB	0.3549	0.1514	4.4287
2,3-butanedione	86	6	431-03-8	S, RI, DB	0.3618	9.4461	1.1770
butanoic acid	60	30	107-92-6	S, RI, DB	0.4051	1.8169	7.8582
methylbenzene	92	7.33	108-88-3	RI, DB	0.5098	3.5170	0.1331
1-butanol	56	14.6	71-36-3	RI, DB	0.5405	0.0566	0.0386
2-heptanone	58	15.78	110-43-0	S, RI, DB	0.7164	0.4933	0.7284
benzaldehyde	105	27.23	100-52-7	S, RI, DB	0.7377	0.4935	0.1209
ethylbenzene	91	12.63	100-41-4	RI, DB	1.4873	0.5172	0.1002
acetone	58	2.98	67-64-1	RI, DB	2.5985	1.4827	0.5605
styrene	104	18.75	100-42-5	RI, DB	15.1948	19.8396	3.4508
2-butanone	43	4	78-93-3	S, RI, DB	75.1078	30.3467	15.3409
Total					100%	100%	100%

Note: S – Retention time and mass spectrum from standard, RI – Retention index, DB – Mass spectral data

To compare the aroma profiles of each strain, the ratio proportion strain/control was calculated for each strain and for each aroma (Figure 2).

L. casei strain from *koumiss* produced more aroma compounds and its profile was significantly ($P > 0.03$) different of *S. thermophilus* profile. 3-methylbutanal, 2-pentanone and dimethyl sulfone were produced mainly by *L. casei* and not by *S. thermophilus*. At reverse, methylbenzene, styrene, benzaldehyde and 2,3-pentanedione were mainly produced by *S. thermophilus* and few by *L. casei*. Capacity of lactic acid bacteria to produce aroma in *koumiss* was similar to that described by Helinck et al. [27].

As the production of volatiles is highly strain-dependent (both qualitatively and quantitatively) and is depending also on the conditions, it is dif-

ficult to compare our results with those of the literature. The comparison to the data obtained using other strains, on other dairy products such as cheese, and extracted with other GC-MS methods is quite debatable. Moreover, no data regarding VOCs in mare milk was available in the literature. In one reference regarding Cheddar cheese where *L. casei* is dominating LAB, the main aromas were nonanoic, undecanoic, heptanoic and myristoleic acid and their ethers [14]. Branched aldehydes, such as 3-methyl butanal are important flavor compounds in many food products, fermented and non-fermented (heat-treated) and are products of *S. thermophilus* strains [27; 28]. Such aroma pattern appeared close to that isolated from our *koumiss* samples.

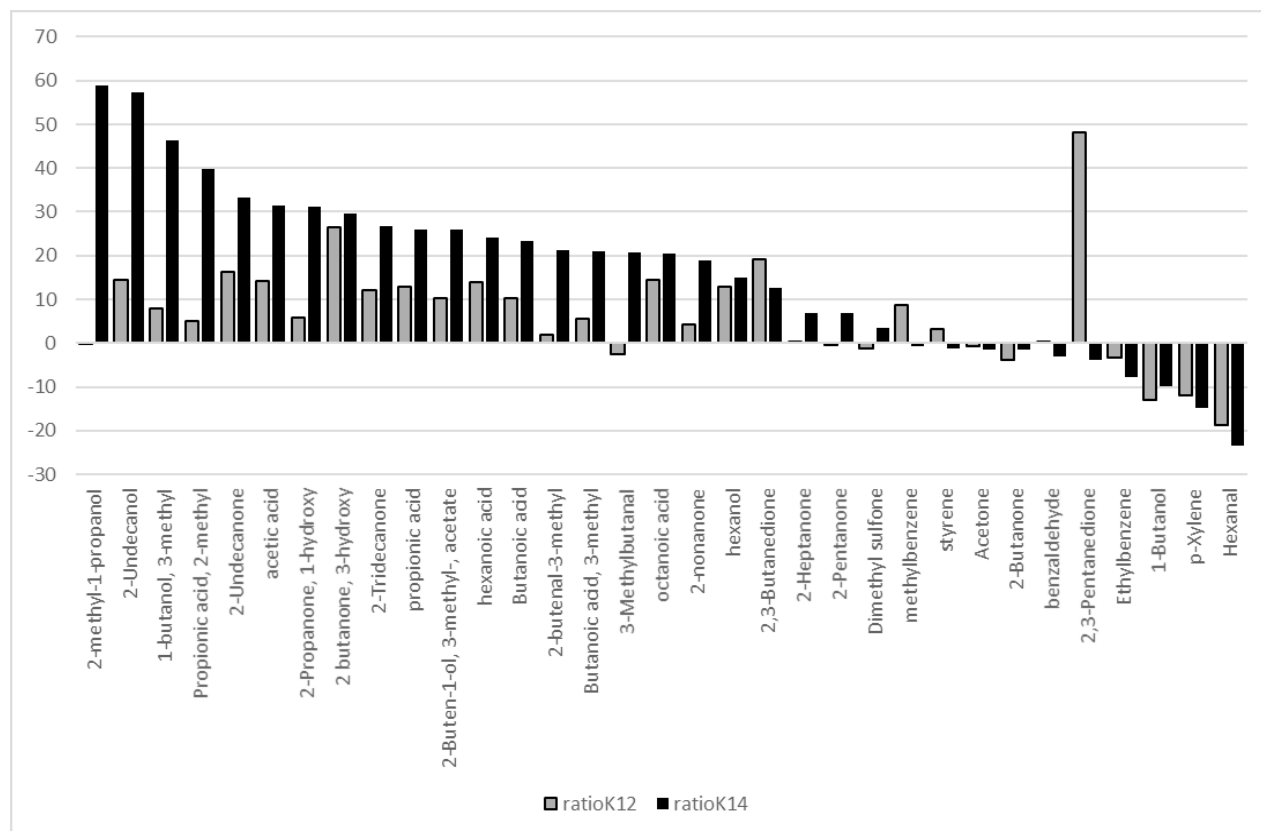


Figure 2 –Ratio of strain aroma compounds /control aroma compounds for *L. casei* (in black) and *S. thermophilus* (in grey). The aroma compounds are in decreasing order for *L. casei*

Obviously, the proportion of each aroma can be lower even if the absolute amount increases, and the total was the sum of the abundance of one selected fragment for each compound and not the sum of total current intensity (TIC) value. Moreover, the flavour-impacting compounds are rarely the dominant ones, and that the method of extraction markedly influence the nature and ratio of the compounds extracted. The present results aimed only to describe the global “aroma profile” of two strains expected to be used in specific starters. Further investigations regarding the sensory analysis should be necessary to assess potential relationship between felt flavor and aroma profile.

Conclusion

The present characterization of *L. casei* and *S. thermophilus* from *koumiss* samples was new and until now no data was available. 35 aroma compounds were detected in fermented and control samples. *L. casei* showed greater aroma producing capacity. Due to the place of traditional fermented dairy products in Central Asia, the description of aroma profiles of

koumiss could be an important step in the modernization of this specific sector. It is a good potential for improving the technology of production at industrial level. However, it would be necessary to complete such analysis by using several strains of the same species grown under the same conditions and using the same method.

Acknowledgements

Study was conducted within the framework of the project “Investigation of functional properties of lactic acid bacteria and yeasts from fermented milks of Kazakhstan”, supported by the Ministry of Education and Science of the Republic of Kazakhstan for 2015-2017 yy.

References

1. Dugan F.M. (2009). Dregs of our forgotten ancestors. *Fungi*, vol. 2, no.4, pp. 16-39.
2. Holland R., Liu S.Q., Crow V. L., Delabre M.L., Lubbers M., Bennett M., Norris G. (2005) Esterases of lactic acid bacteria and cheese flavour: Milk

fat hydrolysis, alcoholysis and esterification. *Int. Dairy J.*, vol.15, no. 6-9, pp.711-718.

3. Baubekova A., Akhmetsadykova S., Konuspayeva G., Akhmetsadykov N., Faye B., Loiseau G. (2015) Biodiversity study of the yeast in fresh and fermented camel and mare milk by denaturing gradient gel electrophoresis. *J. Camel Pract Res.*, vol. 22, no. 1, pp. 91-95.

4. Faye B., Konuspayeva G. (2012) The sustainability challenge to the dairy sector – The growing importance of non-cattle milk production worldwide. *Int Dairy J.*, vol. 24, no. 2, pp. 50-56.

5. Hao Y., Zhao L., Zhang H., Zhai Z., Huang Y., Liu X., Zhang L. (2010) Identification of the bacterial biodiversity in koumiss by denaturing gradient gel electrophoresis and species-specific polymerase chain reaction. *J Dairy Sci.*, vol. 93, no. 5, pp. 1926-1933.

6. Sun Z., Liu W., Zhang J., Yu J., Zhang W., Cai C., Menghe B., Sun T., Zhang H. (2010) Identification and characterization of the dominant lactobacilli isolated from koumiss in China. *The J Gen Appl Microb.*, vol. 56, no. 3, pp. 257-265.

7. Yu J., Wang W. H., Menghe B. L. G., Jiri M. T., Wang H. M., Liu W. J., Bao Q. H. (2011) Diversity of lactic acid bacteria associated with traditional fermented dairy products in Mongolia. *J Dairy Sci.*, vol. 94, no. 7, pp. 3229-3241.

8. Mu Z., Yang X., Yuan H. (2012) Detection and identification of wild yeast in Koumiss. *Food Microb.*, vol. 31, no. 2, pp. 301-308.

9. Kozhakhmetov S., Tynybayeva I., Baikhanova D., Saduakhasova S., Shakhbayeva G., Kushugulova A., Nurgozhin T., Zhumadilov Zh. (2014) Metagenomic Analysis of Koumiss in Kazakhstan. *Cent Asian J Glob Health*, vol. 3, suppl., p.163.

10. Yu J., Wang H. M., Zha M. S., Qing Y. T., Bai N., Ren Y., Xi X., Liu W. J., Menghe B. L. G., Zhang H. P. (2015) Molecular identification and quantification of lactic acid bacteria in traditional fermented dairy foods of Russia. *J Dairy Sci.*, vol. 98, no. 8, pp. 5143-5154.

11. Gesudu Q., Zheng Y., Xi X., Hou Q.C., Xu H., Huang W., Zhang H., Menghe B., Liu W. (2016) Investigating bacterial population structure and dynamics in traditional koumiss from Inner Mongolia using single molecule real-time sequencing. *J Dairy Sci.*, vol. 99, no. 10, pp. 7852-7863.

12. Deetae P., Bonnarme P., Spinnler H. E., Helinck S. (2007) Production of volatile aroma compounds by bacterial strains isolated from different surface-ripened French cheeses. *Appl Microb Biot.*, vol.76, no. 5, pp. 1161-1171.

13. Martin N., Berger C., Le Du C., Spinnler H. E. (2001) Aroma compound production in cheese curd by coculturing with selected yeast and bacteria. *J Dairy Sci.*, vol. 84, no. 10, pp. 2125-2135.

14. Hong-Xin J., Mi-Ya S., Guang-Yu G. (2015) Influence of *Lactobacillus casei* LC2W on the proteolysis and aroma compounds of Cheddar cheese during ripening period. *CyTA-J of Food*, vol. 13, no. 3, pp. 464-471.

15. Pogačić T., Maillard M-B., Leclerc A., Hervé C., Chuat V., Yee A. L., Valence F., Thierry A. (2015) A methodological approach to screen diverse cheese-related bacteria for their ability to produce aroma compounds. *Food microb.*, vol. 46, pp. 145-153.

16. Niamsiri N., Batt C.A. (2009) Kefir and Kumiss. *Encyclopedia of Microbiology*, Academic Press, pp. 34-44.

17. Akhmetsadykova S., Baubekova A., Konuspayeva G., Akhmetsadykov N., Faye B., Loiseau G. (2014) Industrial production starters for traditional fermented milk products. *Le lait, vecteur de développement*. pp. 1-2.

18. Baubekova A. (2017) Study of technological properties of starter lactic acid bacteria and yeast for the production of national lactic acid products. Final research report, number 3751GF/4, Ministry of Education and Science of Republic of Kazakhstan, p.40

19. Ampe F., Omar N.B., Moizan C., Wachter C., Guyot J.P. (1999) Polyphasic study of the spatial distribution of microorganisms in Mexican pozol, a fermented maize dough, demonstrates the need for cultivation-independent methods to investigate traditional fermentations. *Appl Env Microb.*, vol. 65, no. 12, pp. 5464-5473.

20. Leesing R. (2005) Identification and validation of specific markers for traceability of aquaculture fish for import/export. *PhD thesis*. University of Montpellier, p.183.

21. Stackebrandt E., Goebel B.M. (1994) Taxonomic note: a place for DNA-DNA reassociation and 16S rRNA sequence analysis in the present species definition in bacteriology. *Int J Syst Evol Microb.*, vol. 44, no. 4, pp. 846-849.

22. Palys T., Nakamura L. K., Cohan F. M. (1997) Discovery and classification of ecological diversity in the bacterial world: the role of DNA sequence data. *Int J Syst Evol Microb.*, vol. 47, no. 4, pp.1145-1156.

23. Barani F., Dell'Amico N., Griffone L., Santoro M., Tarabella C. (2006) Determination of volatile organic compounds by headspace trap. *J Chrom Sci.*, vol. 44, no. 10, pp. 625-630.

24. Schulz K., Dreßler J., Sohnius E.-M., Lachenmeier D.W. (2007) Determination of volatile constituents in spirits using headspace trap technology. *J Chrom A*, vol. 1145, no. 1-2, pp. 204-209.
25. Smith C. A., Want E. J., O'Maille G., Abagyan R., Siuzdak G. (2006) XCMS: processing mass spectrometry data for metabolite profiling using non-linear peak alignment, matching, and identification. *Analyt chem.*, vol.78, no. 3, pp. 779-787.
26. Zhao Z.W., Pan D.D., Wu Z., Sun Y.Y., Guo Y.X., Zeng X.Q. (2014) Antialcoholic liver activity of whey fermented by *Lactobacillus casei* isolated from koumiss. *J Dairy Sci.*, vol. 97, no. 7, pp. 4062-4071.
27. Helinck S., Le Bars D., Moreau D., Yvon M. (2004) Ability of thermophilic lactic acid bacteria to produce aroma compounds from amino acids. *Appl env microb.*, vol. 70, no. 7, pp. 3855-3861.
28. Smit B.A., Engels W.J.M., Smit G. (2009) Branched chain aldehydes: production and breakdown pathways and relevance for flavour in foods. *Appl microb biotech.*, vol. 81, no. 6, pp. 987-999.

IRSTI 34.23.41; 34.23.02

^{1*}R. Islamov, ^{1,2}A. Aitynova, ²A. Zhussupova

¹Scientific Center of Anti-Infective Drugs, Almaty, Kazakhstan

²Al-Farabi Kazakh National University, Almaty, Kazakhstan

*e-mail: renat-biochem@mail.ru

Genetic toxicology and genetically active environmental factors

Abstract: Anthropogenic impact on the environment, including, but not limited to water and soil contamination with oil and xenobiotics, causes cytotoxic, mutagenic and carcinogenic effects, and nowadays is considered the main negative factor of genetic alterations in living populations. In examinations of mutation processes in populations, inhabiting at ecologically unfavorable areas, high frequency of dominant mutations that alter normal growth inside uterus, causes development glitches in newborns, or even stillbirth. Such data is conditioned by direct dependence between the intensity of environmental pollution and impairment of ecologically effected genetic situation. Assessment of genotoxicity can be provided through specific tests, indicating degree of mutagenic effect and probability of its manifestation. Nevertheless, even living organisms, such as plants, suffering from environmental pollution, can produce chemical compounds that induce genotoxicity. Medicinal substances isolated from these plants are not exception as well. An attempt to provide analysis of genotoxicity implementation and importance of investigations performed in this field is presented in this paper.

Key words: genotoxicity, mutagenic effect, carcinogenicity, chemical compounds, negative factors, regulatory documents.

Introduction

Genetic toxicology is the scientific discipline dealing with mutagenic effects of chemical, physical and biological agents, resulting in DNA damage. Progress in this field of science comes in close connection with the development of various techniques for visualization of genetic material impairment (eg. the Ames assay, Comet assay, or single cell gel electrophoresis, and micronucleus assay), mechanisms laying in the basis of those (eg. chromosome aberrations and single nucleotide polymorphisms) and means for repair of such lesions (eg. photoreactivation, base and nucleotide excision repair) in cells of eukaryotic and prokaryotic organisms.

From the ecological point of view, one should pay close attention to the previous studies, related to the influence of toxicological agents on physiology and life span of ecosystem participants, such as animals and plants. For instance, when analyzing the data from the study of oil pollution on plant morphology and cytogenetic characteristics we can detect the accumulation of strong mutagens and carcinogens in plants as clear indicator of the negative impact of oil. A genotoxic agent may cause DNA and chromosome

damage. Such alteration in a germ cell may further lead to an inheritable mutated trait, affecting genotype of all individuals in a given population. On the other hand, DNA damage in somatic cells is one of the main factors that trigger malignance and cancer. Some carcinogens and mutagens go through metabolic pathway for activation until reactive species that can interact with DNA forming DNA adducts are detected in cells and tissues by different techniques. Such methods include micronucleus tests, Ames test, biotransformation, dominant lethal tests, reverse mutation assay, sister chromatid exchange test, specific locus test and others. These assays play an important role in predicting potential of compounds to cause genotoxicity and carcinogenicity, as well as revealing the nature and effect of damage. Cytogenetic methods, such as anaphase-telophase chromosome aberration assay, were developed for rapid screening of chemicals and environmental samples (water, soil, air, and waste). Conventional cytogenetics using regular chromosome analysis remains a simple and popular technique for visualization of the human karyotype. Implementation of cytogenetic analyses, at least at diagnosis, is mandatory for analyzing the outcomes of many clinical trials, and it can also be

used to stratify patients for different types of therapy. However, we have molecular methods of damaged DNA recovery as well; to include: direct repair, base excision repair, nucleotide excision repair, mismatch repair, single/double strand break repair. If talking about other related areas, we may take as an example nuclear medicine using ionizing radiation as an important clinical tool for both medical diagnosis and therapy. The use of radiopharmaceuticals in diagnostic imaging has brought a significant contribution to the field of health sciences [1].

Development of genetic toxicology as science

Even before the biochemical bases of heredity were understood, the field of genetic toxicology began its development with the early investigators observing the possibility of heritable mutations due to the action of physical and chemical agents. Muller was the first to report the role of radiation in producing heritable changes in a living organism, while Auerbach was the first to report the ability of chemicals to cause mutations. Based on these early investigations of induced alterations in genetically heritable traits the field of science was created nowadays known as genetic toxicology. Genetic toxicology testing is required for all classes of chemicals and drugs in order to reveal their pharmacodynamics and pharmacokinetic effect, negative side effects, analyzing the probability of positive result during treatment. Since the 1980s, there has been an increase in our knowledge of the mechanisms leading to genetic toxicity as well as in our experience with the use of the tests on genetic toxicity. Our interpretation of test results has evolved, comprising our identification of the critical steps, strengths and weaknesses of the different tests. Moreover, it has become clear that tests detecting the types of genetic damage, which can be transmitted (gene mutations, structural chromosome damage and numerical chromosomal abnormalities) in mammalian cells, should be considered as the most relevant for the evaluation of the mutation inducing potential of certain chemicals.

Genetic toxicology for many years has explored the mechanisms of heredity with tools applied to study the nucleic acids structure, DNA repair and recombination, the role of mutation at the individual level. The study of mutagenesis has proved significantly important in many areas including environmental monitoring with notable ecological aspects. This field involves studies of air, water, soil and sediments pollution as result of industry development leading to accumulation of mutagenic and carcinogenic substances in cells of living organisms. In the

final stage, we have substantially altered genotype, manifesting mutation in phenotypical characteristics. Different test systems include high diversity of both eukaryotes and prokaryotes, as well as bacteriophages, viruses and mammalian cells in culture. Endpoints that have been used to measure genotoxicity comprise DNA adducts, DNA strand breakage, changes in chromosome number or structure, DNA repair, and cell transformation to malignant phenotypes. The rapidly increasing number of researchers and amount of published material in genetic toxicology through the 1960s led to the formation of professional societies (to name a few Genetic Toxicology Association, US Environmental Protection Agency, Organization for Economic Cooperation and Development, European Environmental Mutagen Society, Mutagenicity and Experimental Pathology Society of Australasia, Genotoxicity and Environmental Mutagen Association as well as several European organizations for the development of alternative genetic toxicology methods) and information resources focused on genetic toxicology.

Application of computational toxicology to safety testing within a regulatory setting and *in silico* genotoxicity screening approaches are some of the current means for reducing the need for animal testing and human clinical trials. Computer modeling, molecular biology systems and/or adverse outcome pathway approaches can provide more accurate toxicity predictions, whether high-content study data, pluripotent stem cells or new scientific disciplines, such as epigenetics and adductomics, could be integrated into the risk assessment process. With close collaboration between industry, academia and regulators next generation predictive models and high-content screening have the potential to transform genetic toxicology testing in the 21st century [2].

One of the recent major events with more than 160 sessions took place in San Antonio, TX, USA in March 2018 with the topics ranging from ecotoxicology and exposure assessment to epidemiology and human population evaluation, and from immunotoxicity to pesticide neurotoxicology (<http://www.toxicology.org/events/am/AM2018>).

High spectrum of the negative factors

International agency for research on cancer estimated that more than 90% of classified chemical compounds may nowadays be considered as carcinogenic as they simultaneously induce tumors at multiple sites in rodent species. Modern genotoxicity studies allow simple, rapid, and inexpensive risk identification via assessing genetic lesion caused by

chemical induction. Important step that must be followed include reliable and accurate measuring of previously existed and newly appeared chemicals for toxicological and mutagenic properties, genetic potential more efficiently, cost-effectively, and with lesser reliance on animal models. Computational prediction of genotoxicity and carcinogenicity on the base of physicochemical nature, biological aspects has proven of value, while using in the framework of research, also may be applied to chemicals that are not currently synthesized. The Ames bacterial mutagenicity assay has stood the test of time and has gained strong consensus as the assay of choice for prediction of mutagenicity and carcinogenicity. The assay detects 90% of known human carcinogens, most of which are trans-species rodent carcinogens [3]. Among other well-known human carcinogens are benzene and its principal metabolites, phenol, catechol and hydroquinone. Chromosomal aberrations in cultured cells are triggered by catechol, lesser by hydroquinone, and to a marginal extent by phenol at concentration of only 100 μ M. Aneuploidy in the near diploid range of cells is significantly induced by benzene and catechol [4].

Risk factors affecting background rates of micronuclei and chromosomal aberration formation include both endogenous factors and those due to methodological variation were evaluated. A number of host risk factors, namely age, gender, smoking habit, folate, vitamin B and hormonal status need to be identified for assessing probability of their impact on background levels of genotoxicity biomarkers. Evaluation of these factors has to be considered in genotoxicity biomonitoring studies, as well as weak or insufficient evidence including alcohol consumption, disease conditions and infections, physical exercise, body mass index and genotype [5]. Some negative factors may influence the authenticity of data resulted in research. Negative factors, as reactive oxygen species, ultraviolet and ionizing radiation, nucleoside analogues, topoisomerase inhibitors, protein synthesis inhibitors and others may contribute to the false or skewed results, even with different defense mechanisms present in animals, and are one of the biggest issues in animal testing.

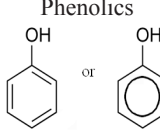
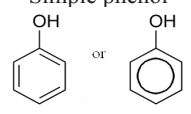
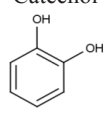
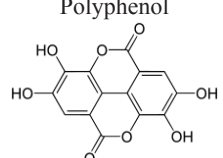
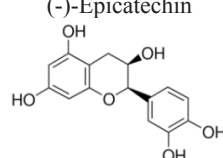
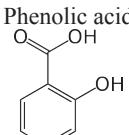
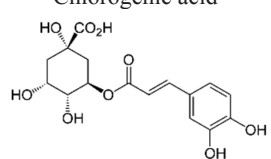
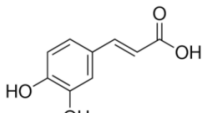
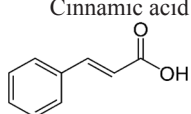
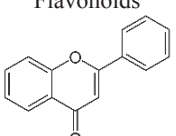
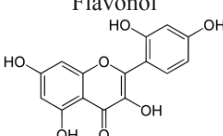
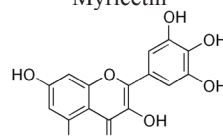
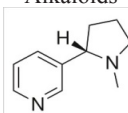
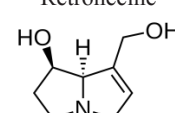
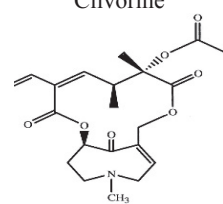
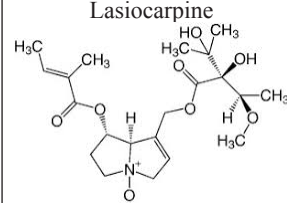
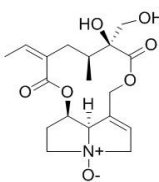
There is a vast variety of phytochemicals, known as secondary plant metabolites, which possess different biological activities, such as antioxidant, antimicrobial effects, modulation of hormone metabolism and detoxification enzymes, stimulation of the immune system, decrease in platelet aggregation and anticancer properties. Phytochemicals are non-essential nutrients; nevertheless, they have ability to prevent or fight against some common diseases.

Many of these benefits suggest a possible role of phytochemicals in prevention and treatment of diseases. Secondary constituents are the remaining plant chemicals, such as alkaloids, terpenes, flavonoids, lignans, plant steroids, curcumines, saponins, phenolics, flavonoids and glucosides. Phytochemicals may reduce the risk of coronary heart disease by preventing the oxidation of low density lipoprotein, cholesterol, reducing its synthesis and absorption, normalizing blood pressure and clotting, and improving arterial elasticity [6]. They may detoxify substances that cause cancer. They appear to neutralize free radicals, inhibit enzymes that activate carcinogens, and activate enzymes that detoxify carcinogens. Among other physiological activities of such biologically active compounds are alkylation, used for construction of carbon skeleton as well as for protection of functional groups, and intercalation, insertion between flatness of DNA nitrogen bases, alternating its structure.

As can be seen from the Table 1 most of the mentioned phytochemicals, such as chlorogenic acid, isatin, caffeic acid have genotoxic effects and cause DNA damage.

When providing examination of genotoxicity, various specific screening methods must be applied, such for instance as electrochemiluminescent arrays aimed at sensing DNA damage to identify genotoxic chemistry related to reactive metabolites [16]. These arrays feature DNA/enzyme films that form reactive metabolites of test chemicals that can subsequently react with DNA, thus enabling prediction of genotoxic chemical reactions. They are used for determining chemical toxicity of new drug that is why good in preclinical researches. Yeast DNA repair reporter, also GreenScreen assay is cost-effective method, developed to perform pre-regulatory screening. It provides a higher throughput and a lower compound consumption than existing eukaryotic genotoxicity assays and is sensitive to a broad spectrum of mutagens and, importantly, clastogens. One more technique, named ToxTracker assay is a mechanism based on mouse embryonic stem cells that uses GFP-tagged biomarkers for detection of DNA damage, oxidative stress and general cellular stress upon exposure. It identifies dangerous properties and mechanisms of elements, such as metal oxides, silver nanoparticles, and non-metallic materials (diesel, carbon nanotubes and quartz). BlueScreen™ HC is a precise and rapid *in vitro* human cell-based assay, estimating genotoxicity and cytotoxicity of compounds and mixtures. This method detects substances that can cause damage in genetic material, especially DNA [17].

Table 1 – Classification of biologically active substances and their mutagenic activity *in vitro*

Class	Subclass	Name	Genotoxicity
Phenolics 	Simple phenol 	Catechol 	Not mutagenic in the Ames test, but is co-mutagen with benzopyrene. Mutagenic in comet assay on human lymphocytes [7].
	Polyphenol 	(-)-Epicatechin 	(-)-Epicatechin significantly diminished the oxidative DNA damage induced by etoposide, in comparison to etoposide alone. It effectively protected bone marrow cells of rats against oxidative DNA damage induced by etoposide [8].
	Phenolic acid 	Chlorogenic acid 	Both chlorogenic acid and caffeic acid induced single strand breaks in DNA in acellular test systems that favored formation of oxygen radicals, particularly in the presence of transition metals (co-mutagens). Not mutagenic in standard bacterial mutagenicity assays [9].
		Caffeic acid 	
		Cinnamic acid 	
	Flavonoids 	Flavonol 	Myricetin 
Alkaloids  Alkaloid: Nicotine	Retronecine 	Clivorine 	Mutagenic, (±)-6, 7-dihydro-7-hydroxy-1-hydroxymethyl-5H-pyrrolizine (DHP)-derived DNA adducts were formed <i>in vitro</i> [13].
		Lasiocarpine 	DHP-derived DNA adducts were formed [14].
		Isatidin 	<i>In vitro</i> comet assay detected DNA strand break [15].

Genetic toxicology, old and new: *in vivo* vs. *in vitro*

Many *in vitro* and *in vivo* tests for genotoxicity have been developed that, with a range of endpoints, detect DNA damage or its biological consequences in prokaryotic (e.g. bacterial) or eukaryotic (e.g. mammalian, avian or yeast) cells.

During the process of using *in vitro* genotoxicity testing it is necessary to include tests in both bacterial and mammalian cells, and be able to detect gene mutations, chromosome damage and aneuploidy. This method may be conducted via combination of the Ames test and the *in vitro* micronucleus test, consequently in the result observing both chromosomal aberrations and aneuploidy [18]. There have been a number of recent advances in the area of genetic toxicity testing that would reduce animal usage and still provide the necessary information for an assessment of the genotoxic potential of substances. Certain genotoxicity studies, including the micronucleus and comet assays, can be effectively incorporated into routine toxicology

studies. The integration of the cytogenetic tests into repeated dose toxicity studies can be used to satisfy the *in vivo* cytogenetic data requirement. The evaluation of micronuclei in peripheral blood or bone marrow cells covers the evaluation of structural and numerical chromosomal aberrations. The integration of the mammalian bone marrow and the rodent erythrocyte micronucleus assays is technically feasible and is a scientifically acceptable alternative to conducting independent *in vivo* cytogenetic assays. The assessment of genotoxicity represents an essential component of the safety assessment of all types of substances. Several *in vitro* tests are available at different stages of development and acceptance, yet they are not considered at present sufficient to fully replace animal tests needed to evaluate the safety of substances. For an overall improvement of the traditional genotoxicity testing paradigm, several recent activities have taken place. These include the improvement of existing tests, the development of novel tests, as well as the establishment and exploration of approaches to optimize *in vitro* testing accuracy.

Table 2 – *In vitro* assays with *in vivo* follow-up studies measuring comparable endpoints [19]

Basic Test	<i>In vitro</i>	<i>In vivo</i>
Gene mutation endpoint	Ames (or other bacterial) Mouse lymphoma Chinese hamster ovary (hypoxanthine-guanine phosphoribosyltransferase test) Yeast forward or reverse mutation Direct chemical/DNA interaction	Mouse somatic cell coat color (spot) assay <i>Drosophila melanogaster</i> sex-linked recessive lethal test Mouse specific-locus assay or suitable dominant mutation assay (germ cell) Clastogenicity
Chromosome aberration endpoint	<i>In vitro</i> cytogenetic analysis in various cell lines Chromosomal aberrations Micronucleus test Sister chromatid exchange test	Rodent micronucleus Rodent bone marrow metaphase analysis Dominant lethal assay (germ cell) Heritable translocation (germ cell) Germ cell chromosome aberrations
Techniques for identifying genotoxic chemicals	Bromodeoxyuridine (or other) is injected prior to metaphase arrest; sister chromatids exchange is evaluated in M2 cells Cell culture treated with ³ H-thymidine (or other radioisotope) is evaluated by auto radiographic method Cell culture is placed into selective and non-selective (or other medium); further stimulation by growth factors is provided	Natural metaphase stop and assessing of chromosomal lesions Exposing of animals <i>in vivo</i> , perfusing target organs (liver) and collecting cells (hepatocytes) Collecting material by surgical methods; fixing and staining for microscopic examination For each substance tested in <i>in vivo</i> studies it is recommended performing homogeneity and stability testing including analytical method validation/evaluation in the vehicle used
Mammalian cell assay	Lymphoma assay Chinese hamster ovary mutation assay Unscheduled DNA synthesis assay Chromosome aberrations Sister chromosome exchange Cell transformation	Dominant lethal assay Cytogenetic analysis Micronucleus assay Heritable translocation assay Specific locus assay DNA adduct formation

Continuation of table 2

Basic Test	<i>In vitro</i>	<i>In vivo</i>
Most frequently used systems	Metabolically proficient mammalian cell systems	Mammalian models (eg. rats, mice, zebra fish, Chinese hamster)
Most frequently used methods	<i>In vitro</i> : cytogenetic evaluation of chromosomal damage with mammalian cells or mouse lymphoma assay <i>In vitro</i> adduct formation <i>In vitro</i> cell transformation	<i>In vivo</i> test for chromosomal damage using rodent hematopoietic cells DNA binding in selected target organs using radiolabeled chemical or ³² P-postlabeling Liver focus assay in rats

As can be seen from the Table 2 differences between *in vivo* and *in vitro* assays mostly include objects of investigations, scheme of experiment and screening methods. Dose-response modeling to relate the concentrations at which effects can be seen in the *in vitro* assays to anticipated human exposures requires the development of computational systems that model the molecular signals underlying genotoxicity pathways. In order to choose the most effective toxicity prediction model it is necessary to understand its strengths, limitations, scope of application and interpretation and customize these methods for each problem if necessary. It is however possible to follow those factors only if the data and processes to develop the model are transparent, applicability domains are well defined, the outputs

of the models are clearly explained, and models are simplified. One of the promising examples is the Tox-21c stresses replacing animal testing with human-relevant testing methods, either *in vitro* or *in silico*. With the increasing number and variety of alternative testing methods, it is necessary to apply strategies to intelligently combine and use this information for toxicity assessment and decision-making.

In perspective, computational methods are likely to expand to include models for special and new types of toxicity endpoints and chemicals, provide insight into toxicological pathways, combine and compare results from different models, customize models to meet users' expectations, and refine models as new data becomes available [20].

Table 3 – Genotoxicity testings *in vivo* in OECD Principles on Good Laboratory Practice*

Assay	End point	Guidelines OECD
Mammalian erythrocyte micronucleus test	Determination of chromosomal damages induced by testing chemicals, or erythroblasts mitotic apparatus due to formation of micronuclei in erythrocytes of bone marrow and peripheral vessels.	Test No. 474
Mammalian bone marrow chromosomal aberration test	Determination of chromosomal aberrations, induced by testing chemicals in cells of animal bone marrow	Test No. 475
Rodent dominant lethal test	Detecting of chromosomal aberrations in sexual cells due to number of implants and mortality of embryos in pregnant females	Test No. 478
Mammalian spermatogonial chromosomal aberration test	Determination of structural chromosomal aberrations in dividing spermatogonial epithelia of mammals	Test No. 483
Genetic toxicology: mouse spot test	Detecting of chemical impact on target cells in developing embryo, precisely melanoblasts by using mice special lines. Measuring is provided due to frequency of colored spots formation in wool.	Test No. 484
Genetic toxicology, mouse heritable translocation assay	Determination of translocation activity due to embryonic mortality and cytological aberration analysis in the stage of diakinesis (metaphase I) in primary spermatocytes.	Test No. 485
Unscheduled DNA synthesis test with mammalian liver cells <i>in vivo</i>	Measuring of labelled thymidine introducing during DNA synthesis (S phase).	Test No. 486
<i>In vivo</i> mammalian alkaline comet assay	Identification of DNA damage using electrophoresis in alkaline pH and recording of migrating DNA "tails" length.	Test No. 489
*Based on: OECD Guidelines for the Testing of Chemicals, Section 4: Health Effects, 2014-2016 (http://www.oecd-ilibrary.org/environment/oecd-guidelines-for-the-testing-of-chemicals-section-4-health-effects_20745788)		

As can be seen from the Table 3, laboratory animals are widely used in study of chemicals genotoxicity using different methods. However, not all of given tests are used in assessment of medicinal phytochemicals. According to recommendations of ICH Topic S2B “Genotoxicity: a standard battery for genotoxicity testing of pharmaceutical” guide, standards battery from three tests, including the Ames assay, *in vitro* test assessing chromosomal aberrations and *in vivo* test of bone marrow cells and erythrocytes of mammals is used. If the results from these three methods are reliable and negative, then chemical is considered as non-mutagenic. In the cases, when even one test gives positive result, then wide researches will be provided, for example dominant lethal mutation test on rodents [21]. Often there is a difficulty in assessment of the genotoxicity of many natural compounds. Some flavonoids become mutagens after metabolic transformations or depending on concentration or dose like when testing *Quercus sideroxylla* plant extract containing polyphenols [22]. Controversial data were obtained when testing catechins from green tea, when positive results were obtained in the test of chromosomal aberrations *in vitro* and negative – *in vivo* [23].

Such differences in genotoxicity testing of some flavonoids and polyphenols related with molecular structure, as well as influence of biological system features. Flavonoids and polyphenols are double- and triple-bounded compounds. They easily interact with various reactive oxygen forms and with radicals. At the same time, they are converted into more stable and less active form than the radical, what trigger their transformation into pro-oxidants [24]. As a result, they exhibit antimicrobial activity – inhibit the electron transport chain, synthesis of nucleic acids or damage bacterial DNA; consequently, it explains the genotoxicity of many flavonoids and polyphenols. With positive results of testing for genotoxicity, it is necessary to include additional research on animals. From our opinion, this may be *in vivo* test of mammalian alkaline comet assay, rather than a rodent dominant lethal test. This choice is explained by cell genetic apparatus damage mechanism and by the method of detecting DNA strands disruption, which is observed under the flavonoids activity [25].

Regulatory issues

Genotoxicity investigations are controlled by regulatory documents. Those include: Interstate standard (2013), Rules of Registration and Examination of drug plants for medical application (Module 4,

section 4.2.3.3 Genotoxicity), Uniform Requirements for general characteristics of drugs for medical applications (2015), Organization for Economic Cooperation and Development Principles on Good Laboratory Practice and others (1998) and others. Interstate standard is valid in countries: Belarus, Kazakhstan, Kyrgyzstan, Russia, Tajikistan, and Uzbekistan since 2013, comprising standards on genotoxicity, carcinogenicity studies and toxic effects on reproductive system (Part 3). Most of such documents reveal potential dangerous, taking into account influence of such factors, like degree of impact, mechanical and physical aspects.

The Organization for Economic Cooperation and Development is an intergovernmental organization in which representatives from 29 industrialized countries in North America, Europe and the Pacific, as well as the European Commission meet to coordinate and harmonize policies, discuss issues of mutual concern, and work together to respond to international problems. Regulatory papers issued by them contain principles of the Good Laboratory Practice (GLP) that should be applied to the non-clinical safety testing of test items contained in pharmaceutical products, pesticide products, cosmetic products, veterinary drugs as well as food additives, feed additives, and industrial chemicals in the laboratory, greenhouses and in the field. These test items are frequently synthetic chemicals, but may be of natural or biological origin and, in some circumstances, may be living organisms. The purpose of testing these items is to obtain data on their properties and/or their safety with respect to human health and/or the environment. GLP is a quality system concerned with the organizational process and the conditions under which non-clinical health and environmental safety studies are planned, performed, monitored, recorded, archived and reported, in Kazakhstan basic rules were adopted in 2006 (Standard 1613-2006, approved by the Order No. 392 of the Ministry of Healthcare and Social Development of the Republic of Kazakhstan from May 27, 2015).

Education and innovations

International in scope, with contributions from over 30 countries Information Resources in Toxicology (Academic Press, 2009) with Philip Wexler as Chief-Editor mentions MEDLINE/PubMed® (Entrez) and the NLM Gateway with eChemPortal and TOXNET among the most widely used Internet-based resources on genotoxicology. Initiatives such as the “Human Toxome Project” (humantoxome.

com) which aims to map the “Pathways of Toxicity” in man illustrate a trend that moves away from our current reliance on high-dose animal toxicity studies to a wide range of new tools such as functional genomics, proteomics, metabolomics, high data content screening, pharmacokinetic modeling, and systems biology to study the effects of chemicals on cells, tissues, and organisms in a rapid and cost-efficient manner. These technologies are also paving the way to improve the evaluation of health risks posed by chemicals found at low levels in the environment. These advances have led to a new sub-discipline of toxicology: “toxicogenomics”, which may be defined as “the study of the relationship between the structure and activity of the genome (the cellular complement of genes) and the adverse biological effects of exogenous agents”. This broad definition encompasses most of the variations in the current usage of this term, and in its broadest sense includes studies of the cellular products controlled by the genome (messenger RNAs, proteins, metabolites, etc.).

The new “global” methods of measuring families of cellular molecules, such as RNA, proteins, and intermediary metabolites have been termed “-omic” technologies, based on their ability to characterize all, or most, members of a family of molecules in a single analysis. With these new tools, we can now obtain complete assessments of the functional activity of biochemical pathways, and of the structural genetic (sequence) differences among individuals and species, that were previously unattainable. These powerful new methods of high-throughput and multi-endpoint analysis include gene expression arrays that will soon permit the simultaneous measurement of the expression of all human genes on a single “chip”.

Although nucleic acid microarray technologies have received much attention recently, other powerful new tools for global analysis of cellular constituents are already available and will also have a major impact on the field of toxicology. These include technologies for global analysis of proteins and peptides (proteomics), and of cellular metabolites (metabonomics). Among these advances are improvements in classical 2-dimensional gel electrophoresis, the introduction of multidimensional liquid chromatography, tandem mass spectrometry, and database searching technologies, and improved mass spectroscopic identification of protein sequences.

Many companies that employ toxicologists (such as pharmaceutical, chemical, food and automotive companies) provide postdoctoral training opportunities for individuals with doctoral degrees in toxicology or related disciplines. For instance, Col-

gate-Palmolive Postdoctoral Fellowship is directed specifically toward innovations in toxicology methodology involving alternatives to whole animal use in testing (<https://researchfunding.duke.edu/colgate-palmolive-postdoctoral-fellowship-award-vitro-toxicology>).

Fields of genotoxicity in Kazakhstan

Most of investigations concerning genotoxicity in Kazakhstan are related to either ecological issues or medical aspect, including, but not limited to the health effects of radon and uranium on the population of Kazakhstan [26], apoptotic and genotoxic effects of low-intensity ultrasound on healthy and leukemic human peripheral mononuclear blood cells [27], genotoxicity evaluation of drinking water and rates of population morbidity in the Northern Kazakhstan region [28], mutagenic effect of the rocket fuel component asymmetric dimethylhydrazine on rats of various ages [29], Glycophorin A somatic cell mutations in a population living in the proximity of the Semipalatinsk nuclear testing site [30].

One of the major factors affecting the environment and human health is the problem of contamination by radioactive elements. The World Health Organization has identified the chronic residential exposure to radon and its decay products as the second cause of lung cancer in healthy non-smokers. Enhanced levels of radon are observed in the Northern and Eastern regions of Kazakhstan due to the natural radiation sources and the long-term and large-scale mining of uranium that is why this direction is still important [26].

The Semipalatinsk nuclear testing site was the primary nuclear testing site for the Soviet Union. The prize for successful development of nuclear bomb was its terrible impact on local population, suffering in the result from numerous types of genetic anomalies and mutagenic sicknesses. The work published by the Radiation Research Society on somatic cell mutations in a population living in the proximity of the Semipalatinsk nuclear testing site and other related to this event investigations are considered as one of the most important of genotoxicity related studies in the history of Kazakhstan. Here Glycophorin A somatic mutation assay was performed to evaluate the magnitude of exposure to ionizing radiation among the human population living in the nearest areas to the nuclear testing site [30].

In the case of genotoxicity evaluation of drinking water and rates of population morbidity in Northern Kazakhstan region, assay of the drinking water in

the regional centers was carried out by a cytogenetic anaphase-telophase method using barley root tips, resulting on the water's compatibility to cause toxic and mutagenic effects. These effects are mostly congenital abnormalities (because of lesions of intrauterine development), including malignant neoplasms and further developing cancer, gastric and duodenal ulcers [31].

One more mentioned research on apoptotic and genotoxic effects of low-intensity ultrasound on healthy and leukemic human peripheral mononuclear blood cells is more related to medicine. It has been shown that ultrasound has a great potential for therapeutic applications, specifically for induction of apoptosis and cell death in malignant cells and also for drug delivery [32]. Positive for the use of the low-intensity ultrasound for damaging cancerous cells were obtained, but only when healthy cells do not largely undergo to this process. However, considering the long-term effects of ultrasound on DNA in healthy cells, therapeutic application of low-intensity ultrasound requires further experiments and analysis for exploring various ultrasound parameters and experimental conditions, including *in vivo* studies.

One more investigation that will be reviewed here is associated with therapeutics. Chemo-resistance is the main obstacle to the effectiveness of cancer therapies as it allows the cancer cells to survive the treatment and proliferate uncontrollably. Currently, no therapy has an efficacy of 100% since drug resistance limits the potency of both conventional chemotherapeutic and novel biological agents. Chemotherapy kills drug-sensitive cells, but resistant cells survive and become more aggressive and prone to metastasis due to the hypoxic conditions established by the therapy in the neoplastic mass [33]. This research reveals that microRNAs can represent an effective therapeutic strategy for overcoming the obstacle of chemo-resistance to anti-cancer drugs. However, there are still many challenges, such as their stability in body fluids and tissues, and ability to reach the target tissue that is why these problems require further study before microRNAs can be effectively used in humans.

The rapid development of nanotechnology, obtaining of nanomaterials with new, unique properties actualized the problem of their investigation. This problem is topical and is on the agenda of OECD. A special Testing Program of Manufactured Nanomaterials was developed in which the interaction of nanomaterials with DNA was noted as a separate item (<http://www.oecd.org/chemicalsafety/nanosafety/overview-testing-programme-manufactured-nano->

[materials.htm](#)). For instance, sulfur nanoparticles display broad activity against bacteria, fungi as well as insects, parasitizing on skin integuments, intensity of which depends on polymorphism, size and form of sulfur. At the same time, the relatively low toxicity of elemental sulfur for mammalian cells makes sulfur nanoparticles very promising for antimicrobial preparations based on them. There is also data on the antitumor activity of elemental sulfur. However, if the toxicity of precipitated microcrystalline sulfur is well studied, then its nanoform requires in-depth studies. It is known that the structure and arrangement of atoms or molecules in a crystal affect the biological activity of pharmaceutical substances. In addition to the polymorphism of the crystals, the particle sizes also affect the properties of the substance. It is shown that the size of the particles of sulfur, selenium, zinc, copper, and titanium depends on their bioavailability, activity and toxicity, and not. In all cases this dependence is linear. Acute oral toxicity of nanosulfur size of about 75 nm was studied in female's mice. LD₅₀ values were between 300–2000 mg/kg for females in mice. Toxic signs were manifested in the form of depression locomotor activity. The thoracic and abdominal cavities were meticulously examined. At necropsy and histology we revealed flatulence colon, dystrophic changes in the liver and kidneys. Hepatocytes are filled with small and medium-sized lipid droplets. These results indicate that nanosulfur more toxic than powdered sulfur. The micronuclear test showed no mutagenic properties of sulfur nanoparticles. The metabolic activation of sulfur nanoparticles with a microsomal rat liver fraction does not affect toxicity. It is assumed that the mechanism of cytotoxic action might be associated with the interaction of elemental sulfur with sulfhydryl groups of molecules inside the cell previously mentioned in several publications. This investigation was performed within the framework of the program-oriented financing from the Ministry of Education and Science Republic of Kazakhstan for 2015-2017 on the priority direction "Rational use of natural resources, processing of raw materials and products": "Development of new methods for the preparation of sulfur nanoparticles to create different functional appointment technologies" [34-36].

Conclusion

Even before the biochemical bases of heredity were understood, the field of genetic toxicology began its development with early investigators observing the possibility of heritable mutations as con-

sequence of physical and chemical agents' action. Nowadays we know a number of agents, which may result in genomic instabilities and/or epigenetic alterations translated into a variety of diseases. Therefore, finding new effective testing methods to identify and measure the genotoxicity of given agents is quite important. An attempt to provide analysis of genotoxicity studies implementation and importance of investigations performed in this field, as well as diversity of genotoxic agents and testing of their mutagenic and carcinogenic properties in various conditions is presented in this paper.

References

1. Aerts A., Impens N., Gijs M., D'Huyvetter M., Vanmarcke H., Ponsard B., Lahoutte T., Luxen A., Baatout S. (2014) Biological carrier molecules of radiopharmaceuticals for molecular cancer imaging and targeted cancer therapy. *Curr Pharm Des.*, vol. 20, pp. 5218-5244.
2. Turkez H., Arslan M.E., Ozdemir O. (2017) Genotoxicity testing: progress and prospects for the next decade. *Expert Opin Drug Met.*, vol. 13, no. 10, pp. 1089-1098.
3. Kirkland D., Aardema M., Henderson L., Muller L. (2006) Evaluation of the ability of a battery of three *in vitro* genotoxicity tests to discriminate rodent carcinogens and non-carcinogens I. Sensitivity, specificity and relative predictivity. *Mutat Res.*, vol. 608, no. 1, pp. 29-42.
4. Takeki T., Nobuko H., Heiji M., James H., J. Carl B. (1997) Benzene-, catechol-, hydroquinone- and phenol-induced cell transformation, gene mutations, chromosome aberrations, aneuploidy, sister chromatid exchanges and unscheduled DNA synthesis in Syrian hamster embryo cells. *Mutat Res.*, vol. 373, no. 1, pp.113-123.
5. Battershill J.M., Burnett K., Bull S. (2008) Factors affecting the incidence of genotoxicity biomarkers in peripheral blood lymphocytes: impact on design of biomonitoring studies. *Mutagen.*, vol. 6, pp. 423-437.
6. Meagher E., Thomson C. (1999) Vitamin and mineral therapy in medical nutrition and disease, 2nd ed., *Massachusetts: Blackwell Science Inc.*, pp. 33-58.
7. Andersson M.A., Hellman B.E. (2007) Evaluation of catechol-induced DNA damage in human lymphocytes: a comparison between freshly isolated lymphocytes and T-lymphocytes from extended-term cultures. *Toxicol in vitro*, vol. 21, no. 4, pp. 716-722.
8. Papież M.A. (2013) The influence of curcumin and (-)-epicatechin on the genotoxicity and myelosuppression induced by etoposide in bone marrow cells of male rats. *Mutat Res.*, vol. 36, no. 1. pp 93-101.
9. Tice R. (1998) Toxicological summary for chlorogenic acid and caffeic acid. *Integrated Laboratory Systems*, pp. 120.
10. Brendler-Schwaab S., Hartmann A., Pfuhrer S., Speit G. (2005) The *in vivo* comet assay: use and status in genotoxicity testing. *Mutagen.*, vol. 4, pp. 245-254.
11. Salamone M., Heddle J., Stuart E., Katz M. (1980) Towards an improved micronucleus test. *Mutat Res.*, vol. 74, pp. 347-356.
12. Hobbs C.A., Swartz C., Maronpot R., Davis J., Recio L., Koyanagi M., Hayashi S.M. (2015) Genotoxicity evaluation of the flavonoid, myricitrin, and its aglycone, myricetin. *Food Chem Toxicol.*, vol. 83, pp. 283-292.
13. Xia Q., Chou M.W., Lin G., Fu P.P. (2004) Metabolic formation of DHP-derived DNA adducts from a representative otonecine type pyrrolizidine alkaloid clivorine and the extract of *Ligularia hodgsonii* hook. *Chem Res Toxicol.*, vol. 17, pp. 702-708.
14. Xia Q., Chou M.W., Edgar J.A., Doerge D.R., Fu P.P. (2006) Formation of DHP derived DNA adducts from metabolic activation of the prototype heliotridine-type pyrrolizidine alkaloid, lasiocarpine. *Cancer Lett.*, vol. 231, pp. 138-145.
15. Uhl M., Helma C., Knasmuller S. (2004) Evaluation of the single cell gel electrophoresis assay with human hepatoma (Hep G2) cells. *Mutat Res.*, vol. 6, pp. 213-225.
16. Itti B., Kiran B., James F.R. (2017) Screening genotoxicity chemistry with microfluidic electrochemiluminescent arrays. *Sensors*, vol.17, no. 5, p. 1008.
17. Etter S., Birrell L., Cahill P., Scott H., Billinton N., Walmsley R.M. (2015) Smith B. The 'Blue-Screen HC' assay as a decision making test in the genotoxicity assessment of flavour and fragrance materials. *Toxicol in vitro.*, vol. 29, no. 7, pp. 1425-1435.
18. Kirkland D., Reeve L., Gatehouse D., Vanparys P. (2011) A core *in vitro* genotoxicity battery comprising the Ames test plus the *in vitro* micronucleus test is sufficient to detect rodent carcinogens and *in vivo* genotoxins. *Mutat Res.*, vol. 721, no. 1, pp. 27-73.
19. Brusick D (1987) Principles of Genetic Toxicology, 2nd ed., *NY: Plenum Press*, p. 284.
20. Richardson R.J., Johnson D.J. (2017) Computational Systems Pharmacology and Toxicology, 1st ed., *UK: Royal Society of Chemistry*, p. 332.
21. Abilev S.K., Glazer V.M. (2015) Mutagenesis osnovami genotoksikologii: uchebnoe posobie

[Mutagenesis with the basics of genotoxicology: manual]. SPb.: Nestor-Istoriya, p. 304.

22. Moreno-Jimenez M.R., Trujillo-Esquivel F., Gallegos-Corona M.A., Reynoso-Camacho R., González-Laredo R.F., Gallegos-Infante J.A., Rocha-Guzmán N.E., Ramos-Gomez M. (2015) Antioxidant, anti-inflammatory and anticarcinogenic activities of edible red oak (*Quercus* spp.) infusions in rat colon carcinogenesis induced by 1,2-dimethylhydrazine. *Food Chem Toxicol.*, vol. 80, pp. 144-153.

23. Ogura R., Ikeda N., Yuki K., Morita O., Saigo K., Blackstock C., Nishiyama N., Kasamatsu T. (2008) Genotoxicity studies on green tea catechin. *Food Chem Toxicol.*, vol. 46, no.6, pp. 2190-2200.

24. Procházková D., Boušová I., Wilhelmová N. (2011) Antioxidant and prooxidant properties of flavonoids. *Fitoterapia*, vol. 2, no. 4, pp. 513-523.

25. Cemeli E., Baumgartner A., Anderson D. (2009) Antioxidants and the comet assay. *Mutat Res.*, vol. 681, no.1, pp. 51-67.

26. Bersimbaev R.I., Bulgakova O. (2015) The health effects of radon and uranium on the population of Kazakhstan. *Genes Environ.*, vol. 37, p. 18.

27. Saliev T., Begimbetova D., Baiskhanova D., Abetov D., Kairov U., Gilman C.P., Matkarimov B., Tachibana K. (2018) Apoptotic and genotoxic effects of low-intensity ultrasound on healthy and leukemic human peripheral mononuclear blood cells. *J Med Ultrason.* vol. 45, no. 1, pp. 31-39.

28. Larikova N.V., Baboshkina S.V., Likhodumova I.N., Beletskaya N.P., Puzanov A.V., Kirillov V.V., Gorbachev I.V. (2012) Genotoxicity evaluation of drinking water and rates of population morbidity in North Kazakhstan oblast. *Ecol genet.*, vol. 4, pp. 40-49.

29. Kolumbaeva S.Z., Shalakhmetova T.M., Begimbetova D.A., Bersimbaev R.I., Kalimagambe-

tov A.M. (2007) Mutagenic effect of the rocket fuel component asymmetric dimethylhydrazine on rats of various ages. *Genetika*, vol. 43, no. 6, pp. 726-742.

30. Lindholm C., Murphy B.P., Bigbee W.L., Bersimbaev R.I., Hultén M.A., Dubrova Y.E., Salomaa S. (2004) Glycophorin A somatic cell mutations in a population living in the proximity of the Semipalatinsk nuclear test site. *Radiat Res.*, vol. 162, no. 2, pp. 164-170.

31. Buschini A., Carboni P., Frigerio S., Furlini M., Marabini L., Monarca S., Poli P., Radice S., Rossi C. (2004) Genotoxicity and cytotoxicity assessment in lake drinking water produced in a treatment plant. *Mutagen.*, vol. 19, no. 5, pp. 341-347.

32. Burgess A., Shah K., Hough O. (2015) Focused ultrasound-mediated drug delivery through the blood-brain barrier. *Expert Rev Neurother.*, vol. 15, pp. 477-491.

33. Gilkes D.M., Semenza G.L. (2013) Role of hypoxia-inducible factors in breast cancer metastasis. *Future Oncol.*, vol. 9, pp. 1623-1636.

34. Il'in A.I., Islamov R.A., Burkitbaev M.M., Sabitov A.N., Kurmanbekov A.S. (2016) Biologicheskaja aktivnost' nanosery [Biological activity of nanosulfur]. *Vestnik NAN RK*, vol. 362, no. 4. pp. 36-43.

35. Burkitbaev M.M., Islamov R.A., Kustova T.S., Kon G.A., Sabitov A.N., Il'in A.I. (2016) Izuchenie ostroj toksichnosti nanosery [The study of acute toxicity of nanosulfur]. *Izvestija NAN RK: Serija Biologicheskaja i Medicinskaja*, vol. 6, no. 318, pp. 53-59.

36. Islamov R.A., Bishimova I., Sabitov A.N., Ilin A.I., Burkitbaev M.M (2018). Lack of mutagenic activity of sulfur nanoparticles in micronucleus test on L5178Y cell culture. *Cell and Tissue Biol.*, vol. 12, no. 1, pp. 27-32.

IRSTI 34.23.19, 34.15.23

¹S.S. Kenzhebeyeva, ²A. Abekova, ¹A. Alnurova, ¹S.A. Shoinbekova,
³G. Zhang, ¹S.Sh. Asrandina, ¹D.K. Tashenev, ⁴F. Sarsu

¹Institute of Biology and Biotechnology, Almaty, Kazakhstan,

²Kazakh Institute of Agriculture and Breeding, v. Almalybak, Kazakhstan

³Agronomy Department, Zhejiang University, Hangzhou, China

⁴Plant Breeding and Genetics Section, Joint FAO/IAEA Division, IAEA, Vienna, Austria

*e-mail: kenzhebss@gmail.com

Variation in grain proteins content and nutritionally important protein fractions concentration in spring wheat mutant lines

Abstract: Wheat is a major cereal crop for both human and animal nutrition, providing 28 % of the world's edible dry matter and up to 60 % of the daily calorie intake in developing countries. Across years, wheat breeding reduced its genetic diversity by replacing traditional cultivars with modern higher yielding varieties and this has resulted in decreased nutritional quality. Spring wheat genetically stable mutant lines (M_7 generation) produced on genetic background of cv. Eritrospermum-35 after 100 and 200 Gy gamma treatments to broaden genetic variation and search for new resources were analyzed for grain protein content and nutritionally important protein fractions (albumins, globulins and prolamins). A significant positive correlation between grain protein content and yield-associated traits, such as grain number and weight per spike, were observed in the 100- and 200 Gy-dosed mutant lines with different means, $r^2 = 0.141$, ($p < 0.05$) and $r^2 = 0.068$, ($p < 0.05$), respectively. Albumins ranged from 139.5 to 890.4 μ g/g, globulins – from 130.1 to 344.04 μ g/g. The 200 Gy-dosed M_7 mutant lines showed the highest globulins concentration by 1.84 fold higher, compared to cv. Eritrospermum-35. Prolamins level varied from 65.1 to 398.2 μ g/g in mutant lines. High dose of irradiation (200 Gy) generated higher level of variation, when compared to 100 Gy. ANOVA analysis revealed significant variation ($p < 0.05$) in globulins and prolamins. In order to improve both quantity and quality of wheat proteins and influence selection of improved raw materials for the flour and bread-making industry a more detailed knowledge of the variability of grain proteins and protein fractions accumulation among new spring wheat mutant lines varieties could be useful. In addition, to improve whole-wheat flour application in production of functional food, rich in health-beneficial components, the study of the whole grain proteins content, their structure and quality is significant.

Key words: bread wheat, correlations, gamma irradiation, concentrations, grain protein fractions, mutation.

Introduction

Wheat (*Triticum aestivum* L.) is a major cereal crop for both human and animal nutrition. It is a major source of energy, protein, and dietary fiber in human nutrition and animal feeding. It provides 28% of the world's edible dry matter and up to 60% of the daily calorie intake of the world's population [1; 2]. Currently, about 95% of the wheat grown worldwide is hexaploid bread wheat, with most of the remaining 5% being tetraploid durum wheat. Nutritionally, wheat is important sources of dietary protein, carbohydrates, the B complex of vitamins, vitamin E, iron, trace minerals, and fiber [3].

The ability of wheat flour to be processed into different foods is largely determined by the proteins. Mature wheat grains contain 8% to 20% proteins [4]. Wheat proteins show high complexity and different interactions with each other, thus making them difficult to characterize. Usually, wheat proteins are either divided into four solubility classes, called Osborne fractions, or extracted in a series: albumins, which are water-soluble; globulins, which are soluble in salt solutions, but insoluble in water; gliadins, which are soluble in 70-90 % alcohol; and glutenins, which are insoluble in neutral aqueous solutions, saline solutions, or alcohol. The respective wheat protein fractions are also applicable to other cereals and are gen-

erally known as albumins, globulins, prolamins, and glutenins, soluble in diluted acid or sodium hydroxide, which make up to 10-22 % of total flour protein [5; 6]. Wheat prolamins are the major component of gluten, the properties of which determine quality of wheat flour for various technological processes, including bread making [7]. An alternative classification to that described above has been proposed based on composition and structure rather than solubility described by Shewry and Halford [8], indicating that wheat proteins consist of two classes based on storage property seed, storage proteins (gliadins/glutenins) and nonseed storage proteins (albumins/globulins) [9].

Albumins and globulins of wheat endosperm represent 20% to 25% of total grain proteins [10; 11]. Albumin is biologically active protein, which is responsible for breakdown of starch and other enzymatic reactions, e.g. amylase and proteases, and is the first to be stored in significant amounts [12]. Nutritionally, albumins and globulins (non-glutens) have a very good amino acid balance. Some proteins, which mostly belong to a family of trypsin and α -amylase inhibitors, participate in plant defense [13]. The role of α -amylase and trypsin inhibitors as wheat allergens in baker's asthma has been shown [14]. Prevailing number of the physiologically active proteins influence the processing and rheological properties of wheat flour. The benefits of the use of amylases, xylanases, lipoxygenase, pentosanase, glucoseoxidase stimulated further interest in the bread-making industry [15; 16].

The objectives of this study were: (1) to evaluate the variability in grain protein content (GPC) and protein fractions (albumins, globulins and prolamins) concentrations, in grains of spring wheat, parental cv. Eritrospermum-35, advanced mutant lines (M_7), produced after 100- and 200 Gy-gamma dose treatments; (2) to evaluate the correlations between grain number and weight per spike, thousand grain weight (TGW) and GPC; (3) to estimate the significant variation ($p < 0.05$) in albumin, globulin and prolamins storage proteins by ANOVA analysis.

Materials and methods

Plant material. Seeds of the spring bread wheat awn variety Eritrospermum-35 were irradiated with 100 Gy and 200 Gy doses from a ^{60}Co source at the Kazakh Nuclear Centre. After irradiation seeds were planted to raise M_1 plants [17]. The M_1 generation was grown in the experimental field of the Kazakh Institute of Agricultural and Breeding in near Almaty

(43°15'N, 76°54'E, elevation 550 m above mean sea level). Single spikes from each plant for the M_2 generation were harvested, and selection of the best lines based on the yield of individual plants continued to M_7 generation. Seed was gathered from the main spike; although tiller number and size varied each plant produced only a single main spike. Seeds from the best yielding mutant lines were selected individually in each generation. The selection criteria for these lines was grain weight per main spike (GWS) and per plant (GWP) and it was applied in the M_3 and M_4 generations (2011 and 2012) and based on the values for the parent cv. Eritrospermum-35 grown in the same trial conditions. In 2011, the parent had mean GWS of 0.79 ± 0.24 g and GWP of 2.02 ± 0.6 g yield values. The threshold criteria for selection in the M_4 generation were GWS > 1.1 g and GWP > 2.2 g for mutant lines. The initial number of lines in the M_1 generation was 300 each for the 100 Gy and 200 Gy radiation doses. In the M_3 generation, 61 lines (20%) were selected from the 100 Gy radiation dose population and 48 lines (16%) were selected from the 200 Gy dose. The same numbers of lines for each radiation dose were selected for the M_4 - M_6 generation. After harvesting the M_7 plants, 14 lines and 24 lines from the original 100 and 200 Gy-treated germplasm were selected. The 100 Gy lines were numbered as follows: 145(12), 147(25), 148(1), 149(2), 151(2), 153(4), 155(2), 159(2), 161(7), 165(2), 166(10), 167(2), 169(14) and 171(1) and 200 Gy lines were numbered: 5(43), 6(4), 7(4), 8(26), 11(5), 11(14), 13(3), 14(3), 16(12), 20(4), 22(46), 26(2), 29(15), 30(4), 31(3), 32(3), 33(1), 34(12), 35(1), 36(5), 37(4), 38(1), 41(1) and 172(1). These mutated populations, selected from the two different levels of radiation, were then used for further analysis. Grain samples from each mutant line and parent Eritrospermum-35 were planted together in a field trial and were grown in three replicates of three row plots, 2 m long, 1.20 m width and 20 cm between rows with planting 30 seeds per row for further evaluation. The trial was managed according to locally recommended agronomic practices. Applied fertilizers, time of their use and soil were described [17]. Ten randomly selected spikes from each line were taken for analysis (5 samples per row).

To record yield associated traits, the following plant parameters were measured: grain number and weight per spike (GNS and GWS), and thousand grain weight (TGW) which was calculated as the mean weight of three sets of 100 grains per line multiplied by 10.

Determination of grain protein content. Grain protein content was determined with near-infra red

reflectance (NIR) spectroscopy on whole grains (ZX50 Portable Grain Analyzer, USA) using proprietary calibration software provided (Zeltex Hagerstown, Ma USA). **Three repetitions were done using 25 grains per line.** The sequential extraction of protein fractions of grain from storage proteins of grain, albumins, globulins and prolamins was carried out using the Osborne method [5]. Extraction of albumins fraction of storage proteins was performed from 0.5 g crushed grains (flour), with a 2-step extraction of 0.05 M Tris-HCl (pH 7.0) for 2 hours with constant stirring, at room temperature.

The precipitate obtained after centrifugation at 4000 g for 10 min was used to isolate the globulin fraction by 2-fold extraction with 1 M NaCl with constant stirring, at room temperature. The fraction of prolamins was obtained by 2-step procedure extraction of the precipitate obtained after centrifuging the globulin fraction using of 55% propanol with constant stirring, at room temperature.

Protein concentration in the obtained fractions was measured by the Bradford method using a Coomassie Blue G-250 solution an Eppendorf BioPhotometer plus spectrophotometer at 595 nm.

Statistical data analysis. The data was analyzed by one-way ANOVA (single factor) using Excel 2007 for significant F-statistics, If overall F-test was significant ($p < 0.05$), a Fachers T-test was performed to discern difference between the varieties.

Results and discussion

Wheat genetic improvement requires the identification of key traits in high performing cultivars to deploy in breeding programs. To generate new sources of variation in the genetic background of modern varieties by introducing more major re-organizations within the genome. Genetic changes produced by irradiation are much larger than the subtle single-base changes introduced by chemical mutagens [18]. Mutated lines generated by irradiation can be used as potential donors for genes/alleles beneficial for wheat-breeding programs to increase yield and improve grain quality [17].

In the present study, spring wheat genetically stable M₇ mutant lines were generated from parent seed (cv. Eritrospermum-35) given two doses of radiation (100 and 200 Gy). These wheat mutant resources were evaluated on grain protein content (GPC) and protein fractions (albumins, globulins and prolamins (glutenins) and determination of correlations between GPC and grain number and weight per spike and thousands grain weight.

We have plotted the pooled GPC data to show the range of values generated by the irradiation treatments. The GPC for the pooled data showed considerable variation, from 12.5 to 16.0%, with a mean of 14.7 ± 0.4 % ($n=106$). Thirty genotypes (78.9%), mainly in the 200-Gy-dosed treatment, had 7.3–12.5 % higher GPC than that of the parent (cv. Eritrospermum-35). The highest GPC measured in the irradiated mutants was 16.0%, which was 12.5% increase over that of the parent cv. Eritrospermum-35, shown in Figure 1.

Analysis of variance (ANOVA) with differences in GPC among cv. Eritrospermum-35 and spring wheat mutant lines is shown in Table 1.

These results revealed significant differences between the cv. Eritrospermum-35 and derived 100 Gy- and 200 Gy-mutant lines for this grain quality character. The radiation effect of 200 Gy was highest in GPC, indicating its increased efficiency to generate mutations in the genome associated with this grain quality trait. There is also significant difference between low (100 Gy) and high (200 Gy) level of radiation to generate variation in GPC. The association between grain nutrients characteristics and yield components is important. Our results showed that no significant correlations between the parent GPC with yield-associated traits such as grain number per spike (GNS), grain weight per spike (GWS) and thousand-grain weight (TGW). A significant positive correlation between GPC and GNS and GWS were observed in the 100- and 200 Gy-dosed mutant lines with different means, $r^2 = 0.141$ ($p < 0.05$) and $r^2 = 0.068$ ($p < 0.05$), respectively (Table 2). These results may suggest that higher grain number and weight per spike improve the capacity to accumulate higher grain protein content.

Albumins are water-soluble proteins in wheat, which are accounted for about 10% of total grain proteins. They perform the metabolic functions in plant growth and development. The albumins are mostly monomeric physiologically active or structural proteins and include α -amylase, β -amylase/ protease inhibitors (13 and 16 kDa) as well as enzymes with different physiological functions (62 kDa serine carboxypeptidase) [19; 20]. It has been reported that three wheat albumin fractions (60, 24, and 12.5 kDa) inhibited amylases activity [21]. Gao *et al.* analyzed non-prolamin expression profiles during grain development of bread wheat and found that most of the proteins had masses of 14-97 kDa, which were mostly distributed in the pH 4-7 range [22]. Out of 400 protein spots, 230 proteins were identified and more than 85% of the identified pro-

teins were enzymes possessing different physiological functions. It was revealed that among the identified 89 non-prolamins more than 80% were various enzymes classified into eight functional categories including carbohydrate metabolism (27%), protein metabolism (27%), stress/defense/detoxifi-

cation (11%), cell metabolism (6%), transcription/translation (4%), nitrogen metabolism (4%), photosynthesis (4%) and signal transduction (1%) [23]. Some high molecular weight albumins and certain globulins are considered to have a storage function [22; 23].

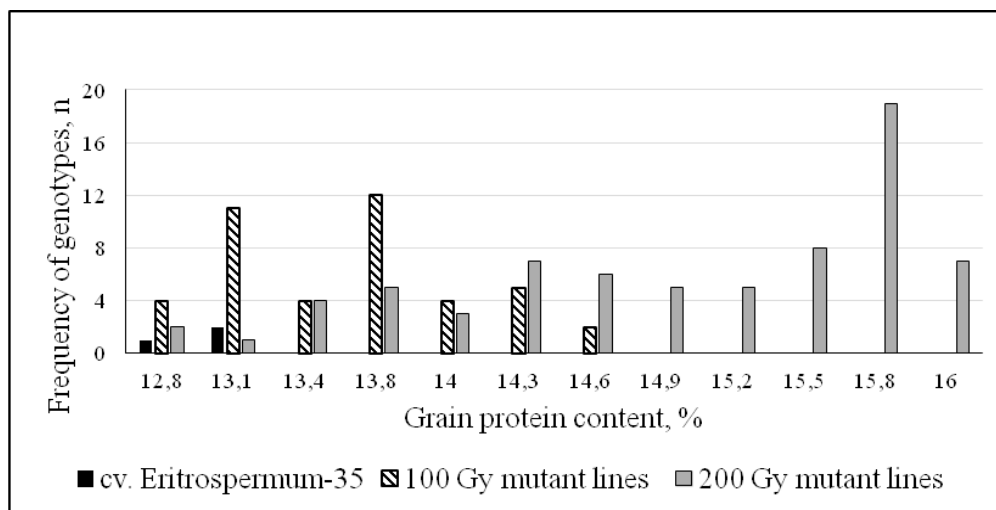


Figure 1 – Frequency of genotypes on grain protein content in the parent (cv. Eritrospermum-35), 100- and 200 Gy-dosed M₁ spring wheat mutant lines

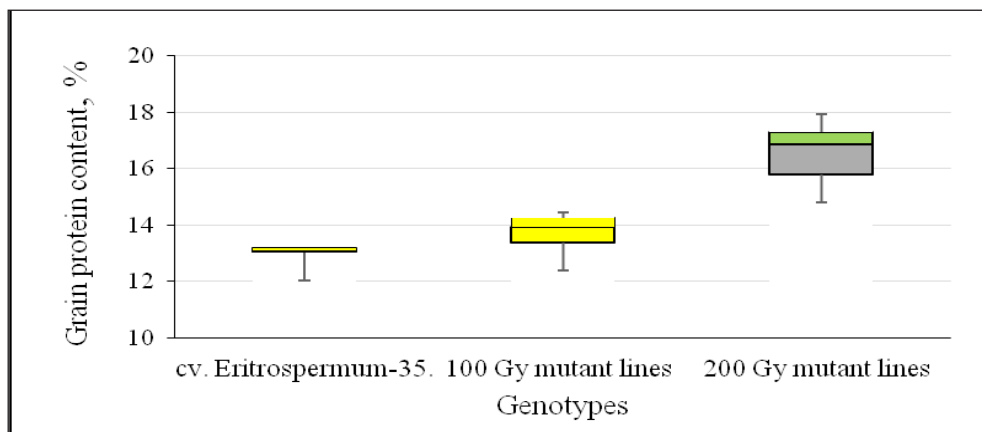


Figure 2 – Box plots showing the statistical testing for the relationships between grain protein content for the parent.
Note: indicated are cv. Eritrospermum-35, 100 (low) and 200 (high) Gy irradiated wheat

Table 1 – Comparing grain protein content of advanced M₁ mutant lines of spring wheat developed using 100 Gy and 200 Gy and the parent cv. Eritrospermum-35 expressed as percentage of the total sum of squares from ANOVA analysis

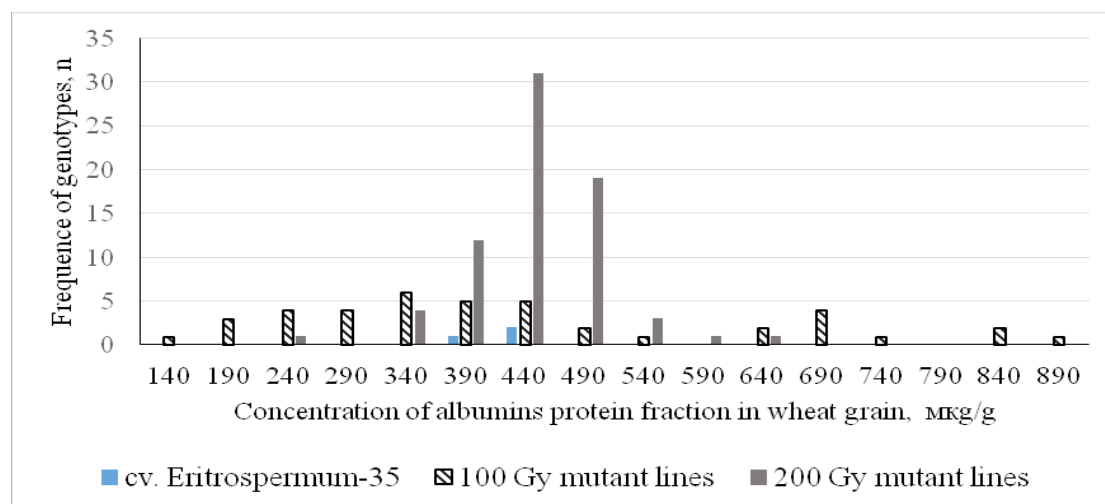
Source of variation	Df	Grain protein content, %
cv. Eritrospermum-35 x 100 Gy- dosed mutant lines	60	37.47***
cv. Eritrospermum-35 x 200 Gy- dosed mutant lines	90	86.26***
100 Gy- x 200 Gy-dosed mutant lines	114	68.53***

Table 2 – The square R correlations correlation coefficients with p values between yield-associated traits (TWG, GNS and GWS) and grain protein content in parent (cv. Eritrospermum-35) and spring wheat M₇ 100- and 200 Gy-dosed mutant lines

	GWS [g]	TGW [g]	GPC [%]
cv. Eritrospermum-35			
Grain number per spike (GNS)	0.566**	0.261	0.000
Grain weight per spike (GWS), [g]		0.118	0.250
Thousand grain weight (TGW), [g]			0.008
100 Gy-dosed M ₇ mutant lines			
Grain number per spike (GNS)	0.087	0.047	0.141*
Grain weight per spike (GWS), [g]		0.087*	0.013
Thousand grain weight (TGW), [g]			0.001
200 Gy –dosed M ₇ mutant lines			
Grain number per spike (GNS)	0.304***	0.001	0.014
Grain weight per spike (GWS), [g]		0.201***	0.068*
Thousand grain weight (TGW), [g]			0.030
Note: *, ** and *** denote significance at $p < 0.05$, <0.01 and <0.001 probability level, respectively			

Evaluation of new spring wheat mutant lines for grain water-soluble albumins protein has been quantified as depicted in Figure 3. Enormous variation on

this grain protein fraction, ranged from 139.5 to 890.4 μ g/g is noted. It is revealed that 100-Gy-dosed M₇ mutant lines contain the highest albumins concentration.

**Figure 3** – Frequency of genotypes on concentration of albumins protein fraction in spring wheat grain in the parent (cv. Eritrospermum-35) and 100- and 200 Gy-dosed M₇ mutant lines

The embryo and outer aleurone layer of the endosperm contain globulins storage proteins, and those from maize embryos have been characterized in some detail [24]. These proteins are readily soluble in dilute salt solution and have sedimentation coefficients of about 7. Related proteins have been found

in embryos and/or aleurone layers of wheat [25]. The 7S globulins are stored in protein bodies and appear to function solely as storage proteins. The high content of globulin storage proteins in oat grain may contribute to high nutritional value when compared with other cereals, such as barley and wheat, an important

factor in view of the widespread use of oats for livestock feed [26].

In our study, comparing the 100- and 200-Gy M_7 -mutated lines of spring wheat showed that consider-

able variation was generated by irradiation doses for globulins storage protein fraction (Figure 4). Globulins storage protein ranged from 130.1 to 344.04 μ g/g (Figure 4).

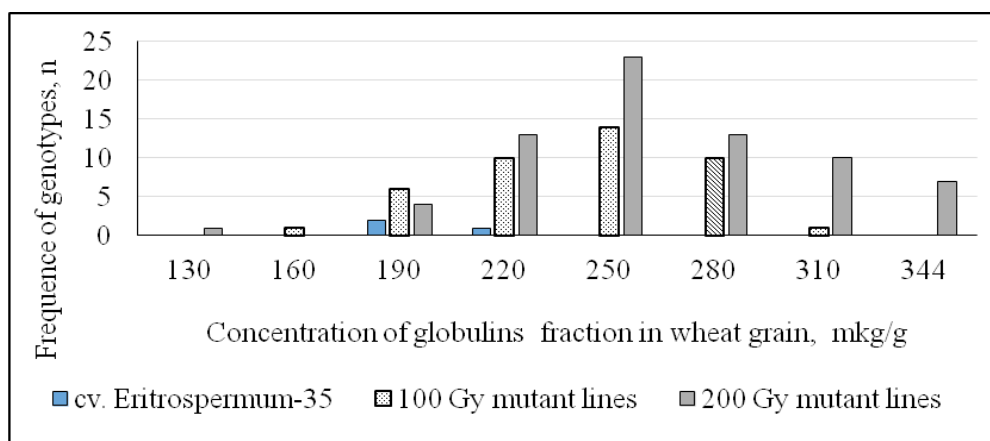


Figure 4 – Frequency of genotypes on concentration of globulins storage protein fraction in spring wheat grain in the parent (cv. Eritrospermum-35) and 100- and 200 Gy-dosed M_7 mutant lines

It was revealed that 200 Gy-dosed M_7 mutant lines showed the highest globulins storage concentration by 1.84 fold higher than that of cv. Eritrospermum-35. Similar to observed for GPC (Table 1), the radiation effect of 200 Gy was highest, indicating its increased efficiency to generate mutations in the genes associated with this grain protein fraction. It was reported the identification of three unique wheat globulin genes, *Glo-3A*, *Glo-3B* and *Glo-3C*, the genomic structure of these genes and their expression pattern in wheat seeds [27]. The *Glo-3A* gene shared 99% identity with the cDNA of WP5212 at the nucleotide and deduced amino acid level, indicating that the identified the gene(s) encoding wheat protein WP5212. In addition, southern analysis carried out in this research revealed the presence of multiple copies of *Glo-3*-like sequences in all wheat samples, including hexaploid, tetraploid and diploid species wheat seed. Importantly, the results reported indicate that a diverse group of globulins exists in wheat, some of which could be associated with the pathogenesis of type 1 diabetes (T1D) in some susceptible individuals. The identification of spring wheat mutant lines, characterized by the lowest globulins concentration offers promising donors for improving immune response in some genetically susceptible individuals, wheat proteins induce an acute mucosal inflammatory response known as celiac disease [28] or Baker's asthma [29].

Prolamins form the major endosperm storage protein fraction in all the major cereals except oats and rice [30]. The name of prolamins was originally based on fact that they are generally rich in proline and amide nitrogen derived from glutamine [30]. The combined proportions of these amino acids actually vary from about 30–70% of the total among different cereals and protein groups [30]. There also is new system of classification all of the prolamins of the Triticeae (wheat, barley and rye) which separate them to three broad groups: sulphur-rich (S-rich), sulphur-poor (S-poor) and high molecular weight (HMW) prolamins, with several subgroups within the S-rich group [30]. These groups do not correspond directly to the polymeric and monomeric fractions in wheat (glutenins and gliadins, respectively) recognized by cereal chemists, as both. The prolamins storage proteins vary greatly, from about 10 000 to almost 100 000, in their molecular masses and they are much more variable in structure than the 7S and 11u12S globulins. In wheat, the prolamins form the major components of the gluten protein fraction and commonly known as “gluten”. Structurally, wheat prolamins are a complex mixture of 71–78 proteins, which constitute ~80% of the proteins in the wheat grains and form the unique viscoelastic network in doughs and is largely responsible for the ability to process wheat to form bread, pasta and many other food products.

This study quantified the concentration of prolamins storage protein fraction in spring wheat grain in the parent (cv. Eritrospermum-35) and 100- and 200 Gy-dosed M_7 mutant lines (Figure 5).

Prolamins concentration considerably varied from 65.1 to 398.2 μ g/g in mutant lines. This range of variation (6.1 times) is much higher comparing to that of globulins (Figure 4), but not albumins (Figure 3) protein fractions. Similar to globulins storage protein fraction, high dose of irradiation (200 Gy) was generated higher level

of variation than 100 Gy. The lowest mean of prolamins level was revealed in 200 Gy-dosed M_7 mutant lines. This observation is seeming, importance of since prolamins are also responsible for numerous gluten-induced health disorders, such as celiac disease, gluten sensitivity and food allergies [31; 32].

Analysis of variance with differences in albumins, globulins and prolamins storage protein among cv. Eritrospermum-35 and mutant lines is presented in Table 3.

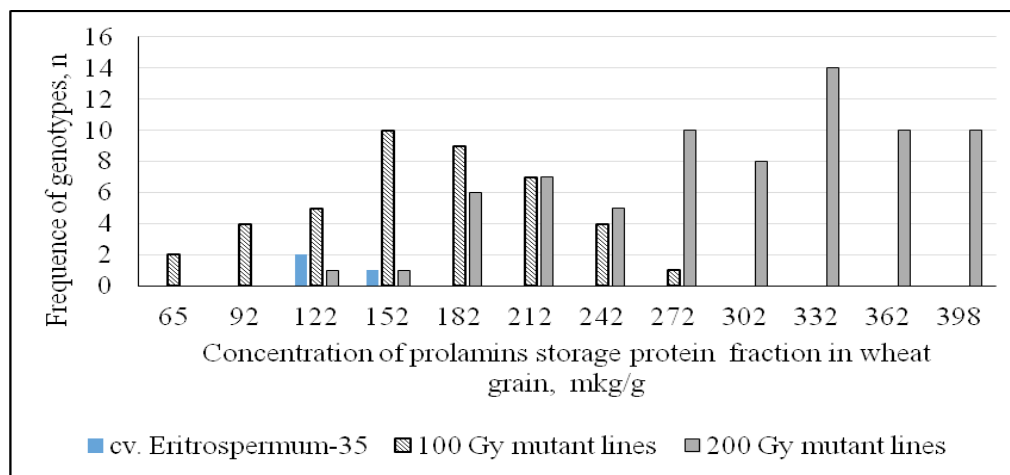


Figure 5 – Frequence of genotypes on concentration of prolamin storage protein fraction in spring wheat grain in the parent (cv. Eritrospermum-35) and 100- and 200 Gy-dosed M_7 mutant lines

Table 3 – Comparing albumin, globulin and prolamin storage proteins in the parent cv. Eritrospermum-35 and M_7 mutant lines of spring wheat developed using 100 Gy and 200 Gy and expressed as % of the total sum of squares from ANOVA analysis

Source of variation	Df	Albumins	Globulins storage proteins	Prolamins storage proteins
cv. Eritrospermum-35 x 100 Gy- dosed lines	56	0.25	36.76***	13.21**
cv. Eritrospermum-35 x 200 Gy- dosed lines	86	0.01	31.38***	101.21***
100 Gy- x 200 Gy-dosed lines	113	1.72	6.13*	94.20***

No significant differences between parent cv. Eritrospermum-35, derived 100 Gy- and 200 Gy-mutant lines for albumins protein fraction are noted, which could possibly indicate that applied doses gamma radiation were not generated mutations in genes associated with wheat predominant albumins (for instance, alpha- amylase/trypsin, serpins and purothionins) [33]. These prevailing albumins members and as well globulins serve as nutrient reserves for the germinating embryo and they also help in protecting embryo from insects and pathogens before germination [34].

Although significant differences between parent, cv. Eritrospermum-35 and derived 100 Gy- and 200 Gy-mutant lines were found for globulins protein fraction, there was not considerable residual for 100 Gy- and 200 Gy-mutant lines (Table 3).

The radiation effect of 100 Gy and of 200 Gy were lowest and highest in prolamins storage proteins, respectively, indicating its efficiency to generate mutations in the genome associated with this trait. There is also significant difference between low and high level of radiation to generate variation in

genome associated with prolamins storage proteins (Table 2). Wheat prolamins are encoded by several loci on the group one and six chromosomes [8] and study has described the relationships between allelic variability at these loci and the functional properties of dough [35].

Conclusion

Successful breeding for yield-associated traits and grain quality traits including protein composition in spring wheat grains requires genetic variation, which has to be distinguishable from environmental effects and permits breeding for genotypes based on end-use product quality and marketing parameters. Mutagenesis, a powerful tool for wheat broaden genetic variation and improvement, has been used for yield improvement, but this technique has not been as widely applied for improving nutritional quality of the grain, including the quality protein fractions to achieve desired end-use product quality. The present study reveals that some new spring wheat genetically stable mutant lines (M₇ generation) generated on genetic background of cv. Eritrospermum-35 and after 100 and 200 Gy gamma treatments have higher grain protein content by 7.3–12.5%, mainly in the 200-Gy-dosed lines, than that of parent. A significant positive correlation between grain protein content and grain number and weight per spike were observed in the 100- and 200 Gy-dosed mutant lines. These mutant lines have great nutritional potential in term of grain important proteins fractions (albumins, globulins and prolamins) characterizing by their enormous variation. High dose of irradiation (200 Gy) was generated higher level of variation in prolamins storage protein fraction as compared to 100 Gy. These new mutant resources of spring wheat can be explored for baking products and for breeding of new cultivars with high nutritional benefits for consumers. To facilitate ongoing efforts to improve both quantity and quality of wheat proteins and influence the selection of better raw materials for the flour and bread-making industry a more detailed knowledge of the variability of grain proteins and protein fractions accumulation among new spring wheat mutant lines varieties could be useful. In addition, be able to use whole wheat flour in production of functional food, rich in health-beneficial components, the study of the whole grain proteins content, their structure and quality are important.

Acknowledgments

This research was funded by the Ministry of Education and Science of the Republic of Kazakhstan for funding the project 074/GF “The creation and study of mutant genotypes of wheat for identifying valuable breeding forms and new alleles of genes controlling key adaptive properties” and AP05131881 “Development of integrated approaches for biofortification, high bioavailability of the most important micronutrients of spring wheat and health”. The authors are thankful to the International Atomic Energy Agency (IAEA, Austria) for providing technical and financial assistance under National TC project KAZ/5003, “Increasing Micronutrient Content and Bioavailability in Wheat Germplasm by Means of an Integrated Approach”.

References

1. Food and Agriculture Organization database. Available online: <http://www.faostat.fao.org>
2. Godfray H. C., Beddington J, J, R., Crute, I.R., Haddad L., Lawrence D., Muir J.F., Pretty J., Robinson S., Thomas S.M., Toulmin C. (2010) Food security: the challenge of feeding 9 billion people. *Science*, vol. 327, pp. 812-818.
3. Shewry P.R. (2009) Heterosis and Combining Ability in F1 Population of Hexaploid Wheat (*Triticum aestivum* L.). *J Exp Bot*, vol. 60, no. 6, pp. 1537-53.
4. Krupnov V.A., Krupnova O.V. Genetic architecture of the protein content in wheat grain. *Genetics*, 2012, vol. 48, no. 2, pp. 149-159.
5. Osborne T.B. 1907. The Proteins of the wheat kernel. Carnegie Inst., Washington, DC. 1924
6. Singh H., MacRitchie F. Application of polymer science to properties of gluten. *J Cereal Science*, 2001, vol. 33, pp. 231-243.
7. Kaushik R., Kumar N., Manvesh Kumar Sihag M. K., Ray A. (2015) Isolation, characterization of wheat gluten and its regeneration properties. *J Food Sci Technol.*, 2015, vol. 52, no. 9, pp. 5930-5937.
8. Shewry P.R., Halford N.G. (2002) Cereal seed storage proteins: structures, properties and role in grain utilization. *J Exp Bot.*, vol. 53, no. 370, pp. 947-958.
9. Shewry P.R., Tatham A.S., Forde J., Kreis M., Mifflin B.J. (1986) The classification and nomenclature of wheat gluten proteins: a reassessment. *J Cereal Sci.*, vol. 4, pp. 97-106.

10. Belderok B., Mesdag J., Donner D.A. (2000) Bread-making quality of wheat: a century of breeding in Europe. Kluwer Academic Publisher: Dordrecht, The Netherlands, pp. 30-31.
11. Merlino M., Leroy P., Chambon C., Branlard G. (2009) Mapping and proteomic analysis of albumin and globulin proteins in hexaploid wheat kernels (*Triticum aestivum* L.). *Theor Appl Gen.*, vol. 18, pp. 1321-1337.
12. Waga J. (2004) Structure and allergenicity of wheat gluten proteins - a review. *Polish J Food Nutr Sci.*, vol. 13, pp. 327-338.
13. Carbonero P., Salcedo G., Sánchez-Monge R., Garcia-Maroto F., Royo J., Gomez L., Mena M., Diaz L. (1993) A multigene family from cereals which encodes inhibitors of trypsin and heterologous-amylases. In: *Innovations of Proteases and Their Inhibitors*; Aviles F.X., Ed.; Walter de Gruyter: Berlin, Germany, pp. 333-348.
14. Posch A., Weiss W., Wheeler C., Dunn M.J., Görg A. (1995) Sequence analysis of wheat grain allergens separated by two-dimensional electrophoresis with immobilized gradients. *Electroph.*, vol. 18, pp. 1115-1119.
15. Jiménez T., Martínez-Anaya M.A. (2001) Amylases and hemicellulases in breadmaking. Degradation by-products and potential relationship with functionality. *Food Sci Tech Int.*, vol. 7, pp. 5-14.
16. Toyosaki T. (2007) Effect of hydroperoxide in lipid peroxidation on dough fermentation. *Food Chem.*, vol. 104, pp. 680-685.
17. Kenzhebayeva S.S., Doktyrbay G., Capstaff N.M., Sarsu, F., Omirbekova N., Eilam Zh., T., Tashenev D.K., Miller A.J. (2017) Searching a spring wheat mutation resource for correlations between yield, grain size, and quality parameters. *Crop Impr.*, vol. 31, pp. 208-228.
18. Morita R., Kusaba S., Iida H., Yamaguchi T., Nishio M. (2009) Molecular characterization of mutations induced by gamma irradiation in rice. *Genes & Gen Syst.*, vol. 84, pp. 361-370.
19. Goesaert H., Brijs K., Veraverbeke W.S., Courtin C.M., Gebruers K., Delcour J. (2005) Wheat flour constituents: How they impact bread quality, and how to impact their functionality. *Trends Food Sci Tech.*, vol. 16, pp. 12-30.
20. Singh J., Blundell M., Tanner G. and Skerrett J. (2001) Albumin and globulin proteins of wheat flour: immunological and N-terminal sequence characterization. *J Cereal Sci.*, vol. 34, pp. 85-103.
21. Silano V., Furia M., Gianpreda L., Macri A., Palescandolo R., Scardi V., Stella E., Valfre F. (1975) Inhibition of amylases from different origins by albumins from the wheat kernel. *Biochim Biophys Acta*, vol. 391, pp. 170-178.
22. Gao L., Wang A., Li, X., Dong K., Wang K., Appels R., Ma W., Yan Y. (2009) Wheat quality related differential expressions of albumins and globulins revealed by two-dimensional difference gel electrophoresis (2-D DIGE). *J Proteom.*, vol. 73, pp. 279-296.
23. Dong K., Ge P., Ma C., Wang K., Yan X., Gao L., Li X., Liu J., Ma W., Yan Y. (2012). Albumin and globulin dynamics during grain development of elite chinese wheat cultivar Xiaoyan 6. *J Cereal Sci.*, vol. 56, pp. 615-622.
24. Wallace NH, Kriz Al. (1991) Nucleotide sequence of a cDNA clone corresponding to the maize globulin-2 gene. *Plant Physiol.*, vol. 95, pp. 973-975.
25. Burgess S.R., Shewry P.R. (1986) Identification of homologous globulins from embryos of wheat, barley, rye and oats. *J Exp Bot.*, vol. 37, pp.1863-1871.
26. Cuddeford D. (1995) Oats for animal feed. In: Welch RW, ed. The oat crop: production and utilization. London: Chapman & Hall, pp. 321-368.
27. Loit E., Melnyk Ch.W., MacFarlane A.J., Scott F.W., Altosaar I. (2009) Identification of three wheat globulin genes by screening a *Triticum aestivum* BAC genomic library with cDNA from a diabetes-associated globulin. *BMC Plant Biology*, vol. 9, no. 93, pp. 1-11.
28. Berti C., Roncoroni L., Falini M.L., Carmanico R., Dolfini E., Bardella M.T., Elli L., Terrani C., Forlani F. (2007) Celiac-related properties of chemically and enzymatically modified gluten proteins. *J Agric Food Chem.*, vol. 55, no. 6, pp. 2482-2488.
29. Bittner C., Grassau B., Frenzel K., Baur X. (2008) Identification of wheat gliadins as an allergen family related to baker's asthma. *J Allergy Clin Immunol.*, vol. 121, no. 3, pp.744-749.
30. Shewry P.R., Halford N.G. (2002) Cereal seed storage proteins: structures, properties and role in grain utilization. *J Exp Bot.*, vol. 53, no. 370, pp. 947-958.
31. Mejías J.H., Lu X., Osorio C., Ullman J.L., von Wettstein D., Rustgi S. (2014) Analysis of wheat prolamins, the causative agents of celiac sprue, using reversed phase high performance liquid chromatography (RP-HPLC) and matrix-assisted laser desorption ionization time of flight mass spectrometry (MALDI-TOF-MS). *Nutrients*, vol. 6, pp. 1578-1597.

32. Hadjivassiliou M., Sanders D.S., Grünewald, R.A., Woodroffe N., Boscolo S. Aeschlimann D. (2010) Gluten sensitivity: From gut to brain. *Lancet Neurol.*, vol. 9, pp. 318-330.

33. Malik A.H. (2009) Nutrient uptake, transport and translocation in cereals; influents of environment and farming conditions. Introductory Paper at the Faculty of Landscape Planning, Horticulture and Agricultural Science. *Swedish Uni Agric Sci Alnarp.*, pp. 4-28.

34. Dupon F.M., Altenbach S.B. (2003) Molecular and biochemical impacts of environmental factors on wheat grain development and protein synthesis. *J Cereal Sci.*, vol. 38, pp. 133-146.

35. Miwako Ito M., Fushie S., Maruyama-Funatsuki W., Ikeda T.M, Nishio Z., Nagasawa K., Tabiki T., Yamauchi H. (2011) Effect of allelic variation in three glutenin loci on dough properties and bread-making qualities of winter wheat. *Breeding Sci.*, vol. 61, pp. 281-287.

IRSTI 34.27.39

^{1*}A. Kondybayev, A. ¹Zhakupbekova, ¹F. Amutova, ¹A. Omarova,
¹M. Nurseitova, ¹Sh. Akhmetsadykova,
^{1,2}N. Akhmetsadykov, ¹G. Konuspayeva, ⁴B. Faye

¹ANTIGEN Co. LTD, Almaty region, Azerbayev Str., 4, Abay v., 040905 Kazakhstan

³Kazakh National Agrarian University, Abai str., 8, 050010, Almaty, Kazakhstan

⁴UMR Selmet, Cirad, Montpellier, France

*e-mail: askond@gmail.com

Volatile organic compounds profiles in milk fermented by lactic bacteria

Abstract: The organoleptic properties of traditional dairy beverages done with non-conventional dairy species (horse, camel), popular in Central Asia, were rarely described in the literature. To characterize the Volatile Organic Compounds (VOC) profile of fermented mare milk, 12 samples of cow milk, used as matrix were inoculated by different strains from two types of bacteria (bacilli and cocci) isolated from natural fermented mare milk. The analysis performed by Gas Chromatography coupled with Solid-Phase Micro-Extraction allowed identification of 160 different compounds from the 12 strains, and 90 from natural fermented mare milk. After cluster analysis, 3 types of profiles were observed. Those profiles were distinct by the amount of acid compounds (low, medium, high), negatively related to aromatic and aliphatic hydrocarbons. The analysis of the mean volatile compound profile of each type of bacteria (bacilli and cocci) by factorial discriminant analysis showed that 3 molecules (oxime-methoxy-phenyl, propanedioic acid propyl and 2-propanamine) allowed to well class 100% of the samples. Further researches on bacterial identification and experiments with different fermentation matrices from other dairy species will be conducted.

Key words: volatile organic compounds, mare milk, discriminant analysis, lactic acid bacteria, fermented milk.

Introduction

Volatile organic compounds (VOC) are used to characterize the organoleptic properties of dairy products [1; 2]. However, their routine determination is relatively new due to the improvement of the equipment for their detection. Consequently, the characterization of dairy products by VOCs is also new and provides a better knowledge of the molecules responsible for aroma production in those products. VOCs composition in dairy products depends on several factors: types of feeds of the dairy animal, microflora naturally present in the raw milk, and also on the processing procedure. The taste and smell of dairy products largely depend on the degree of accumulation of volatile carbonyl compounds, carboxylic acids and other aromatic substances. These compounds determine not only the taste and quality of products, but also have great physiological importance, since they contribute to the secretion of digestive juices and provide good digestibility of the product by human.

In Central Asia, the consumption of fermented milk from different dairy species (cow, horse, camel) is an important element of the local culture [3]. Data for describing those local products by their physico-chemical, biochemical and microbiological composition is widely available [4], but the organoleptic properties were defined only by qualitative description. At our knowledge, the characterization of organoleptic properties of fermented mare milk (*koumiss*), one of the typical products produced in Kazakhstan, by the analysis of VOCs was never achieved. Microorganisms responsible of fermentation process are involved in the production of a large number of different volatile compounds, including, alcohols, esters, hydrocarbons, terpenes, ketones, sulfur-containing compounds and carboxylic acids.

Thus, the objective of the present paper was to determine the VOC profile of milk fermented by different microorganisms isolated from mare milk.

Materials and methods

Samples used. Five samples of fermented mare milk (*koumis*) and one sample of raw mare milk from 6 different locations of Kazakhstan (Merke, Almaty, Semey, Taraz, Shymkent and Urzhar) were collected directly on farm in sterile tubes of 10 ml. They were carried at 4°C to ANTIGEN laboratory for further analysis. The strains of lactic acid bacteria used as starter cultures were isolated from mare's milk and *koumiss* obtained by spontaneous fermentation and identified as the predominant species during the production process. LAB strains were isolated from sample by using wire loops on the M17 and MRS agar (Biokar Diagnostics, France). After the incubation period (48 h, 37°C), single colonies that had different morphological traits were sub-cultured. Microorganisms were maintained at -4°C in the tubes on the correspondent nutritive medium and at -20°C in the culture broth supplemented with 30% glycerol. 12 strains of lactic acid bacteria were obtained, including, seven strains of bacilli and five strains of cocci were identified morphologically. The strains were characterized by using Gram's staining (reagent kit "Color Gram2-E" BioMérieux, France), catalase tests (ID color catalase ID-ASE Biomérieux, France) and oxidase tests (Oxidase reagent Biomérieux, France).

Experiment design. One unique matrix (commercial UHT cow milk Lactel®, 2.5% fat matter) was used for inoculation of each specific strain for fermentation process. Normalized cow milk was heated to 65°C, homogenized at 20 MPa, pasteurized at 95°C for 5 min and cooled to inoculation temperature. Milk was inoculated (5% of the mother culture) and incubated at 37°C. Samples of this matrix without inoculation were used as control.

After inoculation, samples were stored at 37°C for 48 hours to start the fermentation process. Then, each sample was analyzed for VOCs profiles determination using Gas Chromatography with Mass spectrometry detection (GC-MS). For VOCs profile determination, one control was tested for each day of analysis (3 controls). One sample of naturally fermented *koumis* from Taraz was also analyzed for comparison.

Analytical procedure. Solid-phase microextraction (SPME) technique with 50/50µm DVB/CAR/PDMS extraction fiber was used for sample preparation according to method of Xu et al. [5]. The extraction temperature was 60°C, extraction time 30 minutes, the depth of fiber immersion in the vial 22 mm. The desorption time was 3 min.

After the extraction, the fiber was placed in the injector of gas chromatograph, heated to 260°C in splitless mode. Separation of VOC was carried out using a 30m long capillary column HP-5MS (Agilent, USA), inner diameter - 0.25 mm and a film thickness of 0.25 µm at a constant gas carrier (helium) rate of 1.0 ml/min.

The chromatography temperature was programmed from 40°C (5 min) to 200°C at a heating rate of 5°C/min (5 min), followed by heating to 260°C (1 min) at 5°C/min. The total chromatographic time was 55 minutes. The temperatures of the interface, ion source and quadrupole of the mass spectrometric detector were 260, 230 and 150°C, respectively.

Mass spectrometric detection was performed in the SCAN mode in the range of mass numbers (m/z) from 34 to 550 amu (atomic mass unit).

The analysis was carried out on a gas chromatograph with mass spectrometer detector 7890B/5977B quadrupole, with electron impact ionization (Agilent, USA, 2017). The device is annually tested. The chromatograph is equipped with an autosampler MultiPurpose Sampler MPS (Gerstel, Germany, 2017), which allows to automate the analysis of samples. The MassHunter GC/MS Acquisitions B.07.05.2479 and Agilent MSD ChemStation software (version F.01.03.2357) were used to control the gas chromatographic system, record and process the chromatographic data. Data processing included determining retention times, peak heights and areas, and processing of spectral information obtained with the mass spectrometric detector. To investigate the obtained mass spectra, the library Wiley 10th edition was used (the total number of spectra in the library is more than 550,000).

The content of the components was determined by the method of rationing peak areas (reduction to 100%), i.e. finding the percentage of each component in the mixture being analyzed.

Statistical analyses. The software used was XLstat, 2017 (Addinsoft®). The objective of the statistical analysis was to identify VOC profiles according to the different strains used. For that, a multivariate analysis was applied. The raw data table (specific fermented milk samples * percentage of different volatiles compounds) was submitted to Principal Components Analysis (PCA) in order to identify the dissimilarity between the profiles [6].

The type of lactic bacteria was used as supplementary variables to identify the proximity with specific VOCs profiles. In a second step, to simplify

the reading of the results, all the volatile compounds were grouped into nine organic chemical classes: aliphatic hydrocarbons, aromatic hydrocarbons, alcohols, ketones, aldehydes, acids, esters, nitrogen compounds and others. Such classification was similar to that proposed in the literature [7]. The PCA of the group of compounds was followed by a cluster analysis (Ascending Hierarchical Classification – AHC) on Ward method to identify groups of profiles [8].

To assess the difference between the two types of lactic acid bacteria (bacilli and cocci), a multivariate discriminant analysis (MDA) with forward stepwise model was applied [9]. Then, due to non-normalized data, non-parametric Mann-Whitney test was achieved to assess the significant level of difference between the VOCs profiles of these two lactic acid bacteria. Discriminant analysis was applied both on VOCs group and on VOCs profiles.

Results and discussion

As the whole, 160 volatile compounds were identified. The list of the molecules reported in Table 1 was grouped by class of organic compounds. The group “hydrocarbons” included aliphatic hydrocarbons (n=31) and aromatic hydrocarbons represented by only one compound (benzene, 1,3-bis(1,1-dimethylethyl)). The number of molecules differed between samples: 14 molecules in sample 2; 16 in sample 3; 28 in sample 4; 17 in sample 5; 17 in sample 6; 29 in sample 7; 12 in sample 8; 25 in sample 9; 27 in sample 10; 47 in sample 11; 29 in sample 12 and 49 in sample 13. The controls contained 13 molecules only.

In comparison, the natural *koumis* contained 90 different molecules and only 5 were common to the specific fermented milk (Table 2): decanoic acid, ethyl ester (25.7%), ethanol (5.8%), octanoic acid (2.07%), dodecanoic acid (1.57%), 2-methyl-5H-dibenz[b,f]azepine (0.12%) and nonanoic acid (0.02%).

In order to facilitate the analysis, a table including our 13 samples (including the 3 controls) described by the sum of percentage for each class of molecules (9 groups) was created and submitted to Principal Components Analysis.

Analysis of the groups of VOCs. The main factors of the PCA explained almost 60% of the variance and are marked by the opposition between profiles rich in hydrocarbons at the right side of the factorial plan, and profiles rich in acids and nitrogen-compounds at

the left side. On the second factor, the variable “others” was the main contributive variables with aldehydes in opposition to profiles rich in alcohols (Figure 1).

The cluster analysis showed 3 main groups of VOCs profiles (Figure 2) with high difference in their main composition (Figure 3).

The type 1 (samples 2, 7, 12, controls C1, C2 and C3) were composed mainly by aliphatic, aromatic and ketone compounds. The second type which contained 6 samples (numbers 3, 4, 8, 9, 10, 11, and 13) was characterized by its richness in ketones and acids. The last type (samples 5 and 6) contained mostly acid compounds (90%).

Description of the samples by their full profile (Figure 4a, b and c). Each sample was described by the proportion of each group of VOCs sorted, in the order, in acids (AC), aldehydes (AD), alcohols (AH), nitrogen-compounds (AM), esters (ES), aliphatic hydrocarbons (HCF), aromatic hydrocarbons (HCR), ketones (KE) and others (OT). In addition to the main components described above by groups, the analysis by molecule showed that the type 1 contained a small part of alcohol compounds (5% on average) and the type 2 a highest quantity of N-compounds, esters and others compounds while in type 3, only VOCs from acid groups were predominant.

The analysis of the table (13 samples*160 VOCs) by PCA showed that 3 samples had specific profiles quite different than the others. The sample 13 was the most original product with 49 compounds and was the only sample containing ethylene oxide, 3,5-dichloro-2-hydroxybenzaldehyde, 5,5-d₂-trans-3,4-dihydroxy-cyclohexane, 2-pentanamine, 3-amino-2-methylbutanoic acid, 12-methylaminolauric acid, ethanol, 2-(ethenyl)oxy, butanoic acid and methyl ester. After discarding sample 13, the most original sample was n°11 which is the only sample containing many molecules, especially ethanamine N-methyl-, cyclobutanol, 2,3-butanedione, acetic formic anhydride, 5-trideuteromethyltetrazole, benzeneethanamine, 2-fluoro-β,5-dihydroxy-N-methyl-, butanoic acid, butane, 1,2,4-trimethoxy-, 2,4-Pentandiol, and 2-methyl- representing as the whole 34% of the molecules in the sample. The sample n°7 was alone to contain hexane, 2,3,5-trimethyl-, 1,3-dimethylthioindole, 1H-Imidazole, 2-nitro-, methyltetradecan-2-ol 2-, alpha-D-Glucopyranoside, beta.-, nonanal, 1,3-dioxolane, 2-ethyl-2-methyl-, and heptanoic acid.

Table 1 - List of the volatile organic compounds by class of molecules identified in fermented milk samples

Acids	Aldehydes	Alcohol	N Compounds	Esters	Hydrocarbones	Ketones	Others
12-Methylaminolauric Acid; 2-Amino-6-Methylbenzoic Acid; Acetic Acid; Acetic Acid, Sodium Salt; Acetic Formic Anhydride; Benzoic Acid; Butanoic Acid; Butanoic Acid, 2-Methyl-;	2-Butenal, 3-Methyl-; 3,5-Dichloro-2-Hydroxybenzaldehyde; Acetaldehyde; Benzaldehyde, 2-Methyl-; Benzaldehyde, 3-Methyl-; Benzaldehyde, 4-Methyl-; Butanal; Dodecanal; Hexanal; Nonanal;	(S)-(+)-6-Methyl-1-Octanol; 1-(Benzylsulfonyl)Pentan-2-Ol; 1H-Imidazole, 2-Nitro-; 2,4-Pentanediol, 2-Methyl-; 2-Butanol, 3-Methyl-;	1,3-Dimethylthioindole; 1,4-Dinitrotetrahydroimidazo [4, 5-D]; 1-Amido-1-Cyano-3-Methylbut-1-Ene; 1-Butanamine, N-Methyl-; 2-Butanamine; 2-Butanamine, 3-Methyl-;	Butane, 1,2,4-Trimethoxy-; Butanoic Acid, Methyl Ester; Carbamic Acid, Methyl Ester; Decanoic Acid, Ethyl Ester; Formic Acid, 3-Methylbut-2-Yl Este;	(2e)-3-Methyl-2-Pentene; (3e)-2-Methyl-3-Heptene; (4e)-4-Methyl-4-Decene; 1,1'-Bicyclohexyl, 2-Ethyl-, Trans; 1-Dodecene; 1-Undecene; 2,4-Dimethyl-1-Heptene; 2-Pinene; 5-Dodecene, (E)-;	2,3-Butanedione; 2-Butanone, 3-Hydroxy-; 2-Heptanone; 2-Heptanone, 4,6-Dimethyl-; 2-Heptanone, 4-Methyl-; 2-Hexanone, 5-Methyl-;	(1s)-2,6,6-Trimethylbicyclo[3.1.1]; 1,3-Dioxolane, 2-Ethyl-2-Methyl-; 1- [2,5 - Dime-thoxy-4 - (Methylsulfonyl); 2-Mercapto - 4 - Phenylthiazole; 5,5-D2-Trans- 3, 4-Dihydroxy-Cyclope;
Butanoic Acid, 3-Methyl-; Carbonic Acid, Hexyl Prop-1-En-2-Yl Ester; Decanoic Acid; Diglycolic Acid, Isohexyl 2-Methyl; Dodecanoic Acid; Heptanoic Acid; Hexanoic Acid; Hexanoic Acid, 2-Methyl-; L) 3-Amino-2-Methylbutanoic Acid; N-Decanoic Acid; Nonanoic Acid; Octanoic Acid; Pentanoic Acid; Pentanoic Acid, 3-Methyl-; Propanedioic Acid, Propyl-; Propanoic Acid, 2-Methyl-, Anhydri;		2-Heptanol; 2-Methyl-2-Decanol; 2-Methyltetradecan-2-Ol; 2-Nonanol; 3-Buten-2-Ol, 2-Methyl-; 3-Heptanol; 3-Heptanol, 4-Methyl-; 4-Heptanol, 2,6-Dimethyl-; Cyclobutanol; D-Gala-L-Ido-Octitol; Ethanol; Ethanol, 2-(Ethenyloxy)-; Methyltetradecan-2-Ol 2-; Nonanol, Trimethyl-;	2-Furanmethanamine, Tetrahydro-; 2-Heptanamine; 2-Hexanamine, 4-Methyl-; 2-Methyl-5H-Dibenz[B,F]Azepine; 2-Octanamine; 2-Pentanamine; 2-Propanamine; 2-Propenamide; 3-Methoxyamphet-amine; 3-Methyl-3,5--(Cyanoethyl)Tetrahy d; 4-(P-Methylphenyl)- 2-Mercaptothiaz; 6 Methyl-2 Phenylindole; Acetamide; Acetamide, 2-Fluoro-; Acetamide, N-Acetyl-N-(1-Methylpropyl)-; Benzene-ethanamine, 2-Fluoro- B,5-Dihydroxy-N-Methyl-; Dimethylamine; DL-Alanine; Ethanamine, N-Methyl-; Guanidine, N,N-Dimethyl-; Heptanediamide, N,N'-Di-Benzoyloxy-; Hydrazine, Ethyl-; L-Alanine; N-Formyl-3-(2,4,6-Trimethoxyphenyl ; N-Hexylmethylamine;	Hydrazine, Methyl-, Oxalate (1:1); L-Alanine, Ethyl Ester; Oxalic Acid, Hexyl Neopentyl Ester; Propane, 2-Ethoxy-2-Methyl-;	Cyclohexane, 1,3,5-Trimethyl-; Cyclohexane, 3-Ethyl-5-Methyl-1-Pr; Cyclopentane, 1,3-Dimethyl-, Cis-; Cyclopropane, 1,2-Dibutyl-; Cyclopropane, 1-Butyl-2-(2-Methylp; Decane; Decane, 4-Methyl-; Dodecane; Dodecane, 2-Methyl-; Heptane, 2,2,4-Trimethyl-; Heptane, 2,4-Dimethyl-; Heptane, 4-Methyl-; Hexane, 2,2,5-Trimethyl-; Hexane, 2,3,5-Trimethyl-; N-Hexane; Nonane, 2,6-Dimethyl- ; Nonane, 4-Methyl-; Octane, 3,3-Dimethyl-; Pentane, 2,3,3-Trimethyl-; Pentane, 2-Methyl-; Propene 3,3,3-D3; R(-)-3,7-Dimethyl-1,6-Octadiene; Benzene, 1,3-Bis(1,1-Dimethylethyl);	2-Hexanone, 5-Methyl-5-Nitro-; 2-Nonanone; 2-Pentanone; 2-Pentanone, 4-Hydroxy-4-Methyl-; 2-Propanone; 2-Undecanone; Acetone; Acetophenone; Ethanone, 1-Cyclopentyl-;	5-Trideuteromethyltetrazole; 6-Chloro-2-(2,6-Dimethylphenyl) Qui; Alpha.-D-Glucopyranoside, Beta.-; Beta.-D-Glucopyranose, 4-O- Beta.; Bicyclo[3.1.1] Hept-2-Ene, 2,6,6-Trimethyl-; Cyclohex-1,4,5-Triol-3-One-1-Carbo; Dimethyl Trisulfide; Ethylene Oxide; Furan, Tetrahydro-2,2,5,5-Tetramet; Methane, Sulfonylbis-; Oxime-, Methoxy-Phenyl-; Oxirane, 2,3-Dimethyl-, Cis-; TATP; Thiazole, 2,5-Dimethyl

Table 2 - List of the volatile organic compounds identified in koumiss

Compounds	CAS#	Area%	Compounds	CAS#	Area%
Indene	000095-13-6	0.04	1-methyl-1H-indene	000767-59-9	0.01
Toluene	000108-88-3	0.02	9-Hexadecenoic acid, methyl ester,	001120-25-8 64	0.10
Ethanol	000064-17-5	5.80	Ethyl 3-phenylpropionate	002021-28-5	0.36
L-Lactic acid	000079-33-4	1.38	Octanoic acid, 3-methylbutyl ester	002035-99-6	0.07
Phenol, 2-methoxy-	000090-05-1	0.10	Pentadecanoic acid, 3-methylbutyl	002306-91-4	0.04
Naphthalene	000091-20-3	0.33	2-methoxy-4-(n-propyl)phenol	002785-87-7	0.15
Naphthalene, 2-methyl-	000091-57-6	0.02	Guaiacol, 4-ethyl-	002785-89-9	0.24
Benzoic acid, ethyl ester	000093-89-0	0.01	Dodecanoic acid, propyl ester	003681-78-5	0.09
o-Cresol	000095-48-7	0.01	Benzofuran, 2-methyl-	004265-25-2	0.05
Propanoic acid, 2-hydroxy-, ethyl ester	000097-64-3	0.20	D-Limonene	005989-27-5	0.45
1,4-Cyclohexadiene, 1-methyl-4-(1-	000099-85-4	0.10	(E)-9-Octadecenoic acid ethyl este	006114-18-7	0.05
Benzene, 1-methyl-4-(1-methylethyl	000099-87-6	0.04	Isoamyl laurate	006309-51-9	0.01
Benzene, ethenyl-	000100-42-5	0.04	Benzenebutanoic acid, ethyl ester	010031-93-3	0.03
Benzonitrile	000100-47-0	0.02	2,6-Bis(1,1-dimethylethyl)-4-(1-ox	014035-34-8	0.03
Benzenemethanol	000100-51-6	0.10	Tetradecanoic acid, propyl ester	014303-70-9	0.01
Benzaldehyde	000100-52-7	0.01	9-Decenoic acid	014436-32-9	0.04
Acetic acid, phenyl-, ethyl ester	000101-97-3	0.02	Benzofuran, 7-methyl-	017059-52-8	0.03
Butanoic acid, ethyl ester	000105-54-4	0.21	Ethyl tridecanoate	028267-29-0	0.03
Heptanoic acid, ethyl ester	000106-30-9	0.02	n-capric acid isobutyl ester	030673-38-2	0.03
Octanoic acid, ethyl ester	000106-32-1	12.57	Decanoic acid, propyl ester	030673-60-0	0.22
Dodecanoic acid, ethyl ester	000106-33-2	0.03	1H-Isoindole-1,3(2H)-dithione, 2-ethyl-	035373-06-9	0.55
Dodecanoic acid, ethyl ester	000106-33-2	17.25	Pentadecanoic acid, ethyl ester	041114-00-5	0.13
Phenol	000108-95-2	0.07	Methyl(methyl 2,3,4-tri-O-methyl-	052729-97-2	0.03
Decanoic acid, ethyl ester	000110-38-3	25.68	Ethyl 9-hexadecenoate	054546-22-4	0.65
Decanoic acid, methyl ester	000110-42-9	0.02	Ethyl 9-hexadecenoate	054546-22-4	0.01
Dodecanoic acid, methyl ester	000111-82-0	0.03	Ethyl 9-hexadecenoate	054546-22-4	1.37
Nonanoic acid	000112-05-0	0.02	Butanal, 2,3,4-tris[(trimethylsily	056196-36-2	0.04
Phenol, 4-ethyl-	000123-07-9	0.03	L-Phenylalanine, N-(trifluoroacety	058072-44-9	0.01
Nonanoic acid, ethyl ester	000123-29-5	0.07	Ethyl 9-decenoate	067233-91-4	12.33
Hexanoic acid, ethyl ester	000123-66-0	0.03	Ethyl (2-hydroxyphenyl)acetate, TM	067903-47-3	0.08
Hexanoic acid, ethyl ester	000123-66-0	0.97	2-Pentanol, 3-chloro-4-methyl-, (R	074685-48-6	0.04
Tetradecanoic acid, ethyl ester	000124-06-1	0.18	Decanoic acid, 5-chloro-, chlorome	080418-82-2	0.11
Tetradecanoic acid, ethyl ester	000124-06-1	6.71	Octadecanoic acid, ethyl ester	111-61-5	0.08
Tetradecanoic acid, ethyl ester	000124-06-1	2.70	Ethyl (S)-(-)-lactate	2000025-88-4	0.54
Octanoic acid	000124-07-2	2.07	2-Methyl-5H-dibenz[b,f]azepine	2000224-69-5	0.12
Isopropyl palmitate	000142-91-6	0.03	Glycolic acid-D2-O-(trimethylsilyl	2000264-93-4	0.02
Dodecanoic acid	000143-07-7	1.57	1,4-diphenylbut-3-ene-2-ol	2000280-70-5	0.10

Continuation of table 2

Compounds	CAS#	Area%	Compounds	CAS#	Area%
Phenol, 4-methoxy-	000150-76-5	0.02	Ethyl 9-tetradecenoate	2000381-02-2	0.77
Benzofuran	000271-89-6	0.15	Ethyl 13-methyl-tetradecanoate	2000434-94-9	0.06
Tetradecanoic acid	000544-63-8	0.04	Ethyl 4,8,12-trimethyl-tridecanoat	2000480-94-9	0.01
Octadecane	000593-45-3	0.02	Oleic Acid	52355-42-7	0.07
Propyl octanoate	000624-13-5	0.12	Octanoic acid, 2-butyl ester	5458-61-7	1.45
Undecanoic acid, ethyl ester	000627-90-7	0.02	[1,1'-Bicyclopropyl]-2-octanoic acid, 2'-hexyl-, methyl ester	56687-68-4	0.02
Undecanoic acid, ethyl ester	000627-90-7 98	0.12	2-(1-Methyl-1-silacyclobutyl)benzoic acid trimethyl-silyl ester		0.17
Hexadecanoic acid, ethyl ester	000628-97-7	0.01	3-Trifluoroacetoxypentadecane		0.05
Pentadecane	000629-62-9	0.05	E-11-Hexadecenoic acid, ethyl ester		0.04
Heptadecane	000629-78-7	0.04			

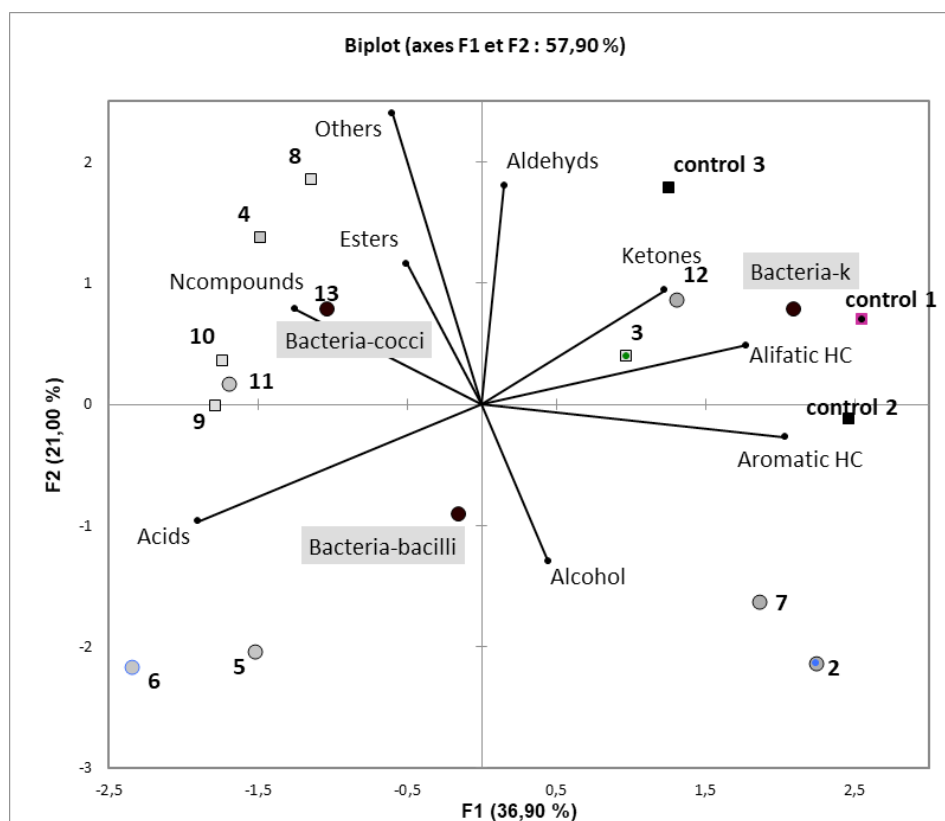


Figure 1 – Factorial plan (f1, f2) of the Principal Components Analysis (biplot projection) showing the projection of active variables (volatile compounds), supplementary variables (bacteria strains) and fermented milk samples inoculated with bacilli (○) or cocci (□)

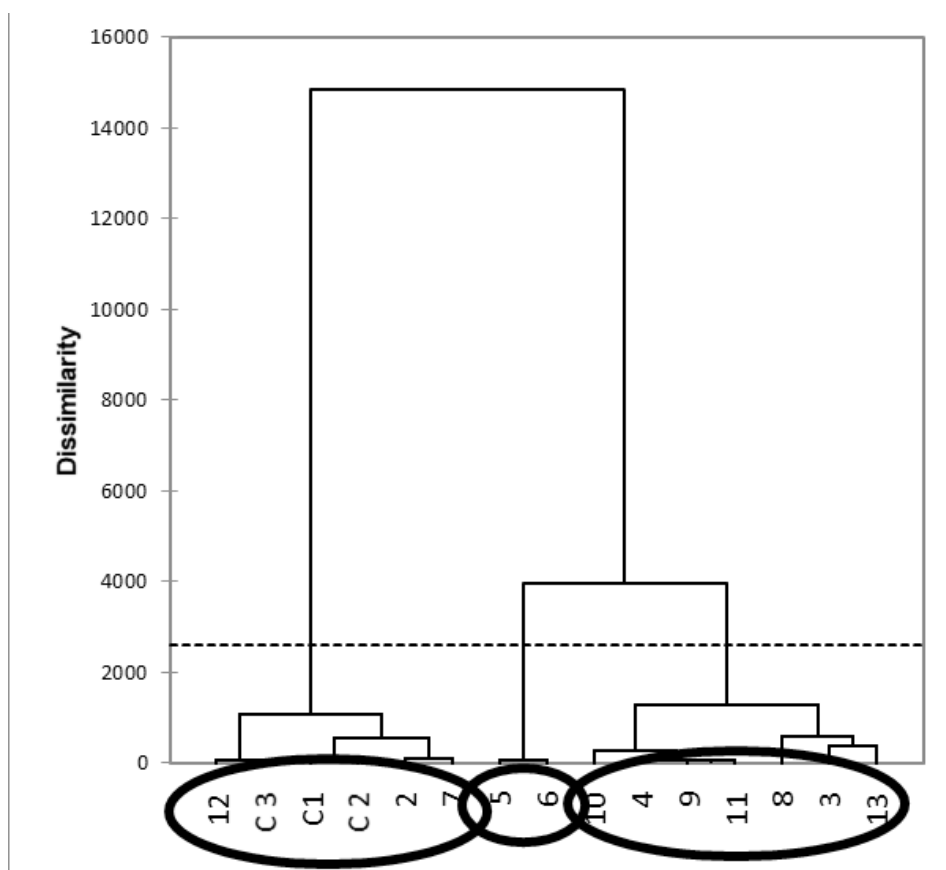


Figure 2 – Dissimilarity based classification tree of the 13 fermented milk samples and control samples (C1, C2 and C3) according to their VOCs composition

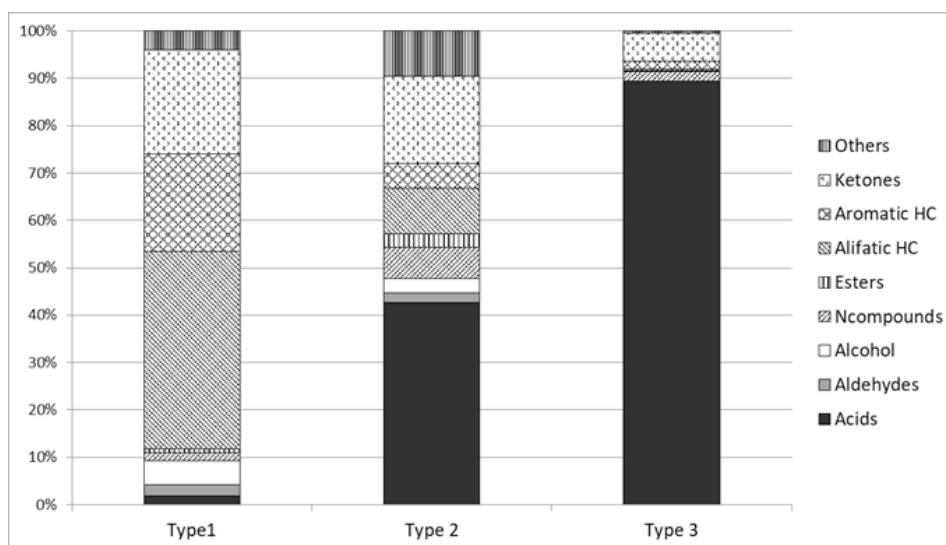
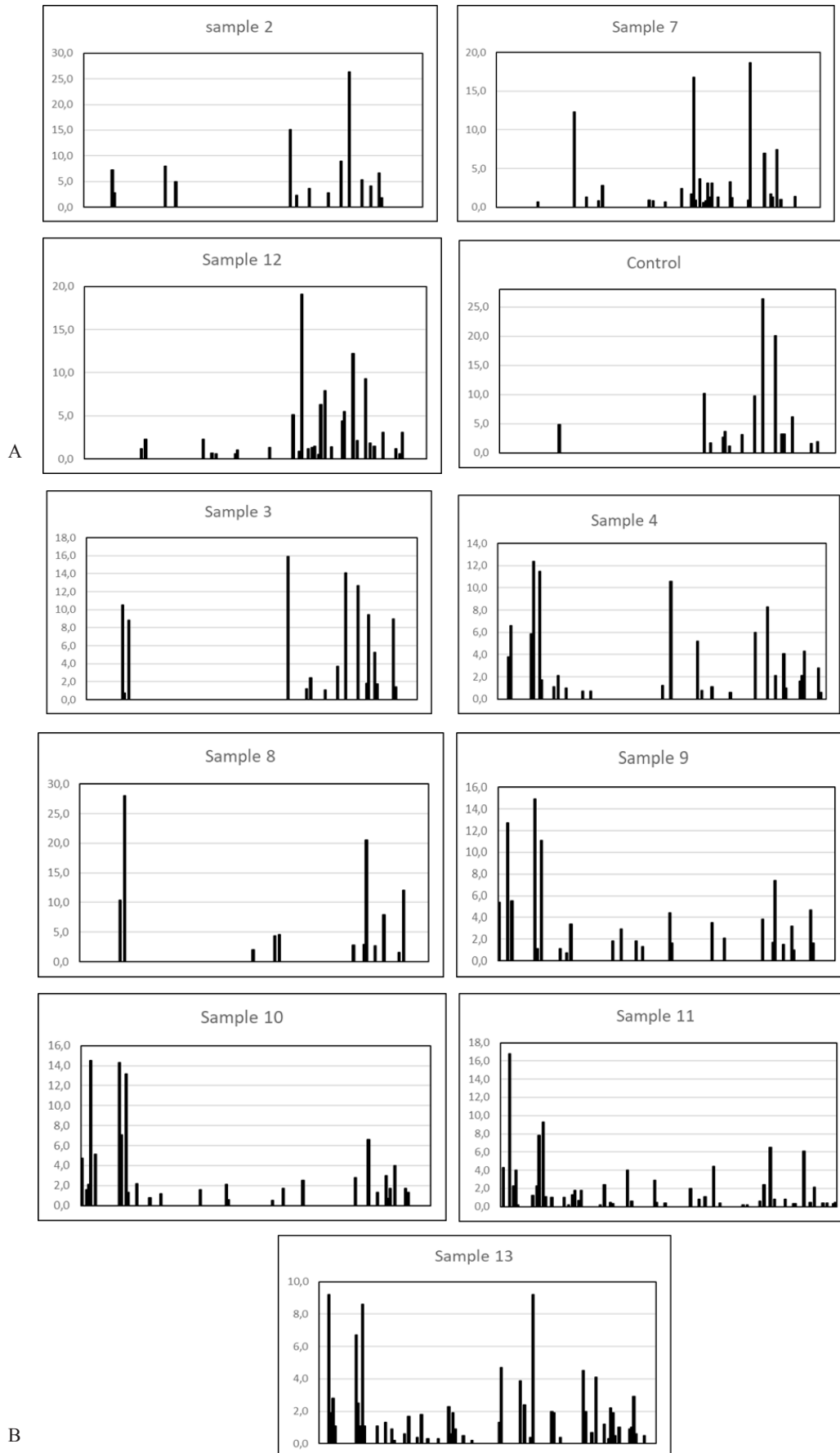


Figure 3 – Mean composition of VOCs classes in each type of samples obtained from classification tree



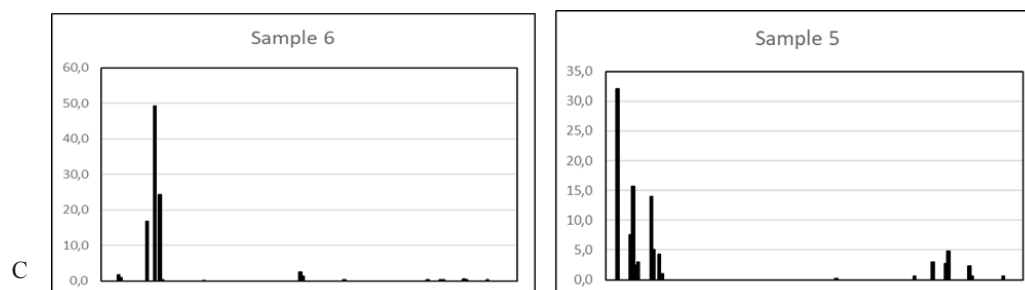


Figure 4 – Volatile organic compound profiles (A- type 1 samples: rich in hydrocarbons and ketones; B- type 2 samples: rich in ketones and acids; C- type 3 samples: rich in acids)

VOCs profile difference between bacilli and cocci starters. The PCA analysis of the VOCs groups showed an opposition between samples fermented with cocci and those fermented with bacilli starter along the second factor of the analysis (Figure 1). The discriminant analysis applied on the table (12 samples * 9 VOCs groups) showed that the mean profiles of each type of lactic acid bacteria can be discriminated with a percentage of well-classed at 83.3%. The stepwise model showed that the main discriminating group of compounds was the group “others” molecules. The integration of other groups

(the second discriminating parameter was ketones) did not improve the discriminating power. The variance analysis confirmed that only the group “other compounds” was significantly different ($P < 0.01$) between the two types of lactic acid bacteria (Table 3). Variance analysis was then applied on the “Other VOCs” group only to identify the specific molecule explaining this difference between type of bacteria. It appeared that only one molecule differed significantly: indeed, oxime-methoxy-phenyl was significantly higher ($P < 0.01$) in samples fermented with cocci bacteria (5.9 ± 4.5 %) than with bacilli (0.63 ± 1.14 %).

Table 3 – VOCs composition (in %) of the fermented milk samples using Cocci or Bacilli starters

Group of VOCs	Cocci	Bacilli	Pr > F
Acids	43.01±16.1	39.11±38.8	0.838
Aldehydes	1.8±1.8	1.15±1.5	0.520
Alcohol	1.2±1.4	6.45±6.9	0.128
N-compounds	6.4±6.1	3.78±3.9	0.357
Esters	2.24±3.9	1.74±2.1	0.779
Aliphatic HC	8.03±9.5	22.15±20.9	0.194
Aromatic HC	5.9±4.7	9.64±9.8	0.453
Ketones	21.3±10.3	12.51±6.1	0.090
Others	10.1±2.8	3.48±3.9	0.009*
Total	100	100	

The analysis of the full profiles (160 VOCs) by Mann-Whitney test showed that 77% of the molecules were significantly different between the two bacteria. However, after submission to discriminant analysis of the full table (12 samples, except control * 160 compounds), the combination of 3 molecules were sufficient to allow discriminating 100% of the samples. The main molecule was still oxime-methoxy-phenyl. The second discriminant molecule

was propanedioic acid, propyl- (group “Acids”) and the third, 2-Propanamine (group “N-compound”). The values of the second molecule were 0.99 ± 1.26 and 3.44 ± 3.18 % for bacilli and cocci, respectively. For the third one, the values were 0.17 ± 0.29 and 0 respectively.

Variability in compounds population. Natural *koumis* is known to contain a large number of lactic bacteria and yeasts strains. For example, Bai and Ji

(2016) [10] in China identified 55 LAB strains. Such microbiological biodiversity, due to spontaneous fermentation, could explain the high number of potential volatiles compounds in such typical beverages compared to our samples obtained after controlled fermentation. Compared to natural *koumis* which contained 5.8% ethanol, our samples of fermented milk had low quantity of alcohol. Indeed, the high level of ethanol usually found in natural *koumis* is usually due to yeasts [11] and not to bacteria as bacilli or cocci. However, three of our samples contained ethanol molecule (3.4% in sample 9, 1.3% in sample 11 and 0.9% in sample 13). It could be due to certain strains of bacteria (one sample was cocci and two, bacilli), but as the present study was based on preliminary data, the identification of strains was not yet achieved. Indeed, ethanol production could be possible in relatively high quantity with lactobacillus strains [12].

The use of cow milk as matrix for inoculation could also explain that only 5 compounds from natural *koumis* were common with the VOCs in our samples. Indeed, there is an important difference in lactose content between mare milk (60-80 g/L) and cow milk (30-50 g/L) and, consequently LAB strains could produce a higher compound variability.

Variability of VOCs profiles. Regarding the full VOCs profile, samples clearly divided into 3 types (issued from cluster analysis). The most apparent discriminant group of molecules was acid compounds. Control samples contained less acid compounds as they were not fermented. However, 3 samples of fermented milk presented similar pattern which attested the absence or very low level of hydrolysis of milk components. Probably, the strain of bacteria used in these samples (all bacilli) were not enough active in cow milk matrix or required more incubation time because a slow metabolic activity [13]. The second type of profile was characterized by its wide variety of compounds, with relatively higher proportion of N- and S-compounds (included in group "other"). Those molecules issued from hydrolyze of amino-acids and probably the bacteria strains (mostly cocci) in this VOCs profile type produced proteolytic enzymes. Ester compounds were also present in higher proportion which could be due mainly to fat hydrolysis [14]. The third type was milk with presence of ketones and overall high quantity of acids. Those samples were inoculated with bacilli strains probably able to have high acidification capacity. Bacilli strains are known to produce strong flavor in dairy products [14; 15].

Discriminant parameters of lactic bacteria. Despite large number of aroma distinguishing VOCs

profile of bacilli and cocci, 3 molecules only were involved in the discrimination. The most discriminating molecule (oxime-methoxy-phenyl-OMP) is a chemical product belonging to imine group which has sweetener taste used in the agro-industry [16]. OMP is normally largely present in UHT cow milk. Dursun, Güler and Şekerli (2017) [17] reported its proportion in VOCs profile of UHT milk at 46.07%.

The second molecule was propanedioic acid, propyl-, an acid component for which no information was available. Despite its role to discriminate the two types of bacteria, its effects were not described in the literature.

At reverse, more information was available for the third discriminating parameter (2-propanamine). It is an amine, building block for several pesticides and herbicides. However, its proportion in our samples was quite low, and even nil in milk inoculated with cocci. The dissimilarity between bacilli and cocci is mainly morphological, but their fermentative activity appeared also quite distinct with two VOCs profiles with only 23% of the molecules having no significant difference. However, no data is available on the VOCs profile description for these two types of bacteria and their effect on flavor of dairy products.

Conclusion

The present study focused on VOCs profile of microflora from raw and fermented milk. The description of those profiles was never done previously. Yet, there is no description of the typical flavor of these products, popular in all Central Asia. The characterization of those flavor could be an essential element to describe the wide biodiversity of those traditional dairy beverages, the flavor of which depends on their microflora. With only 3 compounds, it was possible to distinguish the products inoculated by different types of bacteria with 100% probability. This means that VOCs profiles are highly dependent on the strains used for inoculation, which could have an important impact for agro-food industry to control fermentation process and then, to obtain new dairy products. For the next step, different matrices (milk from other species) for fermentation should be tested, and the strains of bacteria will be identified for a better understanding of their effect on flavor.

Acknowledgements

The present study was conducted in the framework of the project №037-16-ГК "Modernization of

the test center for qualitative and quantitative studies of milk and dairy products” supported by “Science Fund” from the Ministry of Education and Science of the Republic of Kazakhstan.

References

1. Hansen A., Schieberle P. (2005) Generation of aroma compounds during sourdough fermentation: applied and fundamental aspects. *Trends in Food Sci & Tech.*, vol.16, no. 1-3, pp. 85-94.
2. Dragone G., Mussatto S.I., Oliveira J.M., Teixeira J.A. (2009) Characterisation of volatile compounds in an alcoholic beverage produced by whey fermentation. *Food Chem.*, vol. 112, no. 4, pp.929-935.
3. Konuspayeva G., Faye B. (2011) Identité, vertus thérapeutiques et allégations santé: les produits laitiers fermentés d'Asie Centrale. *Les cahiers de l'OCHA*, vol. 15, pp. 35-145.
4. Seitov Z.S. (2005) Koumiss. *Shubat*, Almaty, 286 p.
5. Xu C.H., Chen G.S., Xiong Z.H., Fan Y.X., Wang X.C., Liu Y. (2016) Applications of solid-phase microextraction in food analysis. *TrAC Trends in Analyt Chem.*, vol. 80, pp. 12-29.
6. Jolliffe I. (2011) Principal component analysis. In: *International encyclopedia of statistical science*. Springer, Berlin, Heidelberg, pp. 1094-1096.
7. Longo M.A., Sanromán M.A. (2006) Production of food aroma compounds: microbial and enzymatic methodologies. *Food Tech and Biotech.*, vol.44, no. 3, pp. 335-353.
8. Everitt B.S., Landau S., Leese M., Stahl D. (2011) Cluster analysis. John Wiley & Sons Ltd., Chichester, p. 346.
9. Huberty C.J. (1994) Applied discriminant analysis. Wiley, University of Michigan, p. 466.
10. Bai L., Ji S. (2017) Isolation and identification of lactic acid bacteria from koumiss in Eastern Inner Mongolia of China. In: *AIP Conference Proceedings*, vol. 1794, no. 1, pp. 050005.1-050005.4.
11. Gadaga T.H., Viljoen B.C., Narvhus J.A. (2007) Volatile organic compounds in naturally fermented milk and milk fermented using yeasts, lactic acid bacteria and their combinations as starter cultures. *Food Tech Biotech.*, vol. 45, no. 2, p. 195.
12. Pan D.D., Wu Z., Peng T., Zeng X.Q., Li H. (2014) Volatile organic compounds profile during milk fermentation by *Lactobacillus pentosus* and correlations between volatiles flavor and carbohydrate metabolism. *J Dairy Sci.*, vol. 97, no. 2, pp. 624-631.
13. Mukisa I.M., Byaruhanga Y.B., Muyanja MBK.C., Langsrud T., Narvhus J.A. (2017) Production of organic flavor compounds by dominant lactic acid bacteria and yeasts from Obushera, a traditional sorghum malt fermented beverage. *Food Sci Nutr.*, vol. 5, no. 3, pp. 702-712.
14. Chen C., Zhao S., Hao G., Yu H., Tian H., Zhao G. (2017) Role of lactic acid bacteria on the yogurt flavour: a review. *Int J Food Prop.*, vol. 20, no. sup1, pp. s316-s330.
15. Dan T., Wang D., Wu S., Jin R., Ren W., Sun T. (2017) Profiles of Volatile Flavor Compounds in Milk Fermented with Different Proportional Combinations of *Lactobacillus delbrueckii* subsp. *bulgaricus* and *Streptococcus thermophilus*. *Molecules*, vol.22, no.10, p.1633.
16. Panten J., Surburg H. (2015) Flavors and Fragrances, 2. Aliphatic Compounds. In: *Ullmann's Encyclopedia of Industrial Chemistry*, Wiley-VCH, Weinheim, p. 55.
17. Dursun A., Güler Z., Emre Şekerli Y. (2017) Characterization of volatile compounds and organic acids in ultra-high-temperature milk packaged in tetra brik cartons. *Int J Food Prop.*, vol.20, no.7, pp. 1511-1521.

IRSTI 34.21.17; 34.21.19; 34.35.51

^{1,2*} M.A. Suvorova, ² A.V. Lovinskaya, ² S.Zh. Kolumbayeva

¹Saint-Petersburg University of the humanities and social sciences, AF, Almaty, Kazakhstan

²Institute of Problems of Biology and Biotechnology, al-Farabi KazNU, Almaty, Kazakhstan

*e-mail: masyanskii@gmail.com

Application of a zebrafish embryo toxicity assay for the study of surface water toxicity in the Lower Ile river

Abstract: The quality of surface waters of Lower Ile river, Kapchagay and Kutry reservoirs was assessed in zebrafish (*Danio rerio*) embryotoxicity test. The test was performed according to OECD guideline test No. 236, the exposure period was 5-72 h post fertilization, direct mutagen methylmethanesulfonate (MMS) was used as positive control to assess test system response. The standard visual mortality criteria of the test were applied for evaluation of possible lethal or teratogenic effect of surface waters. Exposure to MMS in concentration of 3.4 mg/L resulted in coagulation of 33.3% of embryos ($p \leq 0.01$) and almost 90% ($p \leq 0.01$) of survived embryos displayed various kinds of malformations to 72 hours post fertilization, which indicates test system susceptibility to the mutagens. It was established that none of surface water samples possess significant embryo toxic effects but all induce the spectrum of malformations related to axial skeleton (scoliosis, end tail malformation), water/salt balance and chorion permeability (oedema) and growth patterns (growth retardation) in different incidences. The lowest rate of teratogenicity was observed in embryos incubated in samples from Kapchagay bay (28.2%, $p \leq 0.05$) and Ile river at Bakanas region (site 2, 27.2%, $p \leq 0.05$). The teratogenic effect of water samples from Kurty reservoir and Ile river (site 1) was commensurable – 33.3% ($p \leq 0.05$) and 36.0% ($p \leq 0.01$) respectively. Among all tested sites only the samples of surface waters form Kurty pond produced multiple phenotypic effects in zebrafish *Danio rerio* embryos congruous to MMS exposure and especially, relatively high level of growth retardation, proposing the presence of disrupting or alkylating compounds in surface water samples.

Key words: bioassay, zebrafish embryos, teratogenicity, mutagen, malformations.

Introduction

The assessment of the surface water quality is of highest importance for a great deal of potentially hazardous contaminants like heavy metals, polycyclic aromatic hydrocarbons (PAH) or polychlorinated biphenyls (PCBs) or polychlorinated dibenzodioxins and furans (PCDD/PCDF), and many other compounds unwanted in the environment may present in aqueous environment. Chemical analysis is very expensive and has the main disadvantage that exclusively the target compounds are detected thus the method is blind for unexpected chemicals or even unknown compounds. Bioassays allow analyzing unwanted effects on organisms of all contaminants present in the water sample within an integrated process, addition of toxic effects and even possible synergistic effects of multiple compounds are taken into account [1].

Current approaches for water quality assessment apply a battery of standardized bioassays using all kind of aquatic organisms such as algae (*Desmodesmus subspicatus*), bacteria (*Vibrio fischeri*, *Arthrobacter globiformis*), invertebrates (*Daphnia magna*, *Caenorhabditis elegans*, *Lumbriculus variegates*, *Diporeia* spp.; *Hyalella azteca*, *Chironomus riparius*, *Potamopyrgus antipodarum*), yeast (*Saccharomyces cerevisiae*), plants (*Myriophyllum aquaticum*) and zebrafish embryos (*Danio rerio*) [2]. In order to better address potential toxicity of aqueous contaminants, the German joint research project DanTox – Development and application of a method for the measurement of specific toxicity and molecular effect mechanisms of sediment-bound environmental pollutants using the zebrafish (*Danio rerio*) – was realized for estimation of teratogenicity, neurotoxicity, genotoxicity, mutagenicity, and subcellular mechanistic effects in embryos of the zebrafish [3]. Use of

zebrafish embryos in bioassays is beyond any doubt as this test object has numerous advantages that make it excellent alternative method to the *in vivo* embryotoxicity and teratogenicity assays: significant number of objects obtained (one female produces up to 300 eggs); transparent chorion greatly facilitates visual investigation; rapid development (hatching takes place at 27 hours post fertilization); embryos are small and easily incubated in Petri dishes or cultural plates, thus combining the advantages of cell culture and embryo culture systems; in addition, vast literature on zebrafish experiments is available [4-7].

The standard ISO 15088:2007 “Water quality – Estimation of the acute toxicity of waste water to zebrafish eggs (*Danio rerio*)” specifies a method for the determination of degrees as a measure of the acute toxic effect of waste water and industrial effluents to fish eggs within 48 h. This provide an inimitable tool for bioassay of surface waters in rivers and reservoirs of Republic of Kazakhstan. Among them Lower Ile river and two big reservoirs – Kapshagay and Kurty are of great interest for Almaty region since they support agricultural life in adjacent areas and are actually a stock for a many polluted streams. In order to investigate the potential toxic effect of surface waters on early stages of fish life the bioassay based on *Danio rerio* embryotoxicity test was performed in the Laboratory of mutagenesis, Department of molecular biology and genetics, al-Farabi Kazakh National University. The goal of this study was the assessment of embryotoxicity (acute lethal effect) and teratogenicity of surface water of Lower Ile river and adjacent reservoirs in *Danio rerio* embryo test.

Materials and methods

Water samples collection. Surface water samples collection, filtration and conservation were performed according to the GOST (State Standard) 31861-2012 “Interstate standard. Water. General Sampling Requirements” [8]. Composite samples were taken at the following sites: 1) Kapchagay bay, 43054’45.90’’ 7705’41.79’’; Kurty pond, 43051’27.11’’ 76020’9.84’’; Ile river, site 1, 43055’7.38’’ 7705’49.99’’; Ile river; 2), Bakanas, 44047’43.95’’ 76016’34.89’’.

Animal care or egg production. A breeding stock of unexposed and healthy mature zebrafish was used for the egg production. Mature fish were maintained in aquaria at 22-24°C with a loading capacity of a minimum of 1L per fish and natural light/dark cycle.

Dry flake food or live food was fed once a day. Before spawning fish were kept hungry for a day. For egg production a nest of spawners (male : female ratio 1:2) was placed for the night in a sterile spawning aquaria preliminary filled with fresh filtrated drinking water heated up to 26°C [9]. To prevent egg predation bottom was covered with neutral plastic mesh with a grid size of 2 mm. Spawning took place at the early morning and may be recognized by the decrease of female belly. Spawners and separate grid were than immediately removed and eggs were collected in sterile flask. Fertilized eggs were separated of unfertilized one using stereomicroscope Motic DM-143 (Motic, China) and used for the further assay.

Embryo exposure. Two controls were used for each experiment: 1) a positive control consisting of the aqueous solution of direct teratogen methylmethanesulfonate (3.4 mg/L MMS); 2) negative control of pure filtered water. Fish embryos were randomly transferred in sterile Petri dishes with medium volume of 25 ml. For bioassay water samples preheated up to 26°C were used as incubation media and experiments were continuous throughout all period of embryonic development. The incubation was performed at incubator Binder at 26°C for the 72 hours post fertilization (hpf). The exposure was stopped at 72 hpf when the hatching take place and it is easy to distinguish the malformations of spinal cord. Developmental parameters were monitored and documented according to OECD recommendations for acute embryotoxicity and teratogenicity assays [10].

Scoring. At different time points (24, 48 and 76 hpf) fish embryos were evaluated and scored for lethal or teratogenic effects using stereomicroscope Motic DM-143 (Motic, China). All embryos were staged according to Kimmel *et al.* [11]. Different lethal or teratogenic endpoints are summarized in Table 1.

Validity parameters and statistics. The fertilizing rate of the fish eggs should be higher than 50%. The assay is considered to be valid if the viability of the negative control eggs exceeds or is equal to 90% after 48 hpf (no lethal or teratogenic effects). The experiments were performed in triple sequence. Thus, typically 25 fish embryos per Petri dish and 75 fish embryos per group were used. Data was processed and visualized using MS Excel 2010 (Microsoft Office Professional Plus 2010 software). The standard error for each parameter is the result of three independent experiments.

Table 1 – Lethal and teratogenic effects observed in zebrafish *Danio rerio* embryos depending on the observation time, according to Busquet et al. [12]

Category	Physiological/dismorphogenic effect	24 hpf	48 hpf	72 hpf
Lethal effect	Coagulated eggs	+	+	+
Teratogenic effects	Malformation of head		+	+
	Malformation of tail		+	+
	Malformation of end tail		+	+
	Malformation of heart		+	+
	Scoliosis		+	+
	Deformity of yolk	+	+	+
	Growth retardation	+	+	+

Ethical considerations. All animal experimental procedures were conducted in accordance with the international regulations. Within the chorion, fish embryos are not subject to Directive 2010/63/EU, which regulates the use of animals in scientific experiments. As Article 1.3 of the Directive declares, independently feeding larval forms are subjected to Directive 2010/63/EU, the experiments stopped at hatching. In the current version of the test protocol the Fish embryotoxicity test is limited to two or three days and is classified as a non-animal test in legal terms.

Results and discussion

Zebrafish embryogenesis is a powerful *in vivo* model system to assess the quality of surface water and rapid developmental progression compared to mammals makes it an ideal for the embryo toxicity assay. We performed a set of experiment to assess the potential toxic and/or teratogenic profile of surface water of lower reach of Ile river and adjacent reservoirs. Experiments were started at 4-6 hpf and stopped at hatching that generally takes place at 72 hpf; by this time a larva has completed most of its morphogenesis. Actually the exposure began since early gastrula period of 50% epiboly when blastoderm remains uniform in thickness and germ ring is visible from the animal pole. The assessment for lethal and teratogenic effects took place on 24, 48 and 72 hpf. Figure 1 summarizes the lethal and teratogenic effects of controls and water samples collected at Ile river basin in *Danio rerio* embryos at 72 hpf considered to be acute embryotoxicity effect.

As shown in Figure 1 the negative control triggered no lethal effects in the fish embryos with

2.7% of eggs coagulated and only 4% of eggs displayed malformations within three experiments. The total percentage of teratogenic and/or lethal eggs in each individual control group experiment consisting of 25 eggs each was < 10% after 48 hpf and thus all experiments were considered to be valid. The ability of the test object to respond to direct teratogen was assessed in experiment with MMS, which is known to be highly toxic, teratogenic and mutagenic for vertebrates and thus was chosen as positive control. Exposure to MMS in concentration 3.4 mg/L resulted in coagulation of 33.3% of embryos ($p \leq 0.01$) and almost 90% ($p \leq 0.01$) of survived embryos displayed various kinds of malformations to 72 hpf so that test system is susceptible for the mutagens.

For the surface water samples only a very slight toxic effect (visual mortality criteria) was observed that is below required embryo toxicity level of 10% - mortality in Kurty pond was only 3.8%, 4.0% and 2.5% in Ile river (site 2 and site 1, respectively) and at Kapchagay bay was 8.9% (differences are not significant).

One may conclude that exposure of *Danio rerio* embryos to surface water of Ile river region did not lead to acute embryotoxic effect. However, when studying teratogenic effects the significant increase in number of embryos displaying various kinds of malformations has been detected (Figure 1, B). That is the lowest rate of teratogenicity was observed in embryos incubated in samples from Kapchagay bay (28.2%, $p \leq 0.05$) and Ile river at Bakanas region (site 2, 27.2%, $p \leq 0.05$). The teratogenic effect of water samples from Kurty reservoir and Ile river at bridge region (site 1) was commensurable – 33.3% ($p \leq 0.05$) and 36.0% ($p \leq 0.01$), respectively.

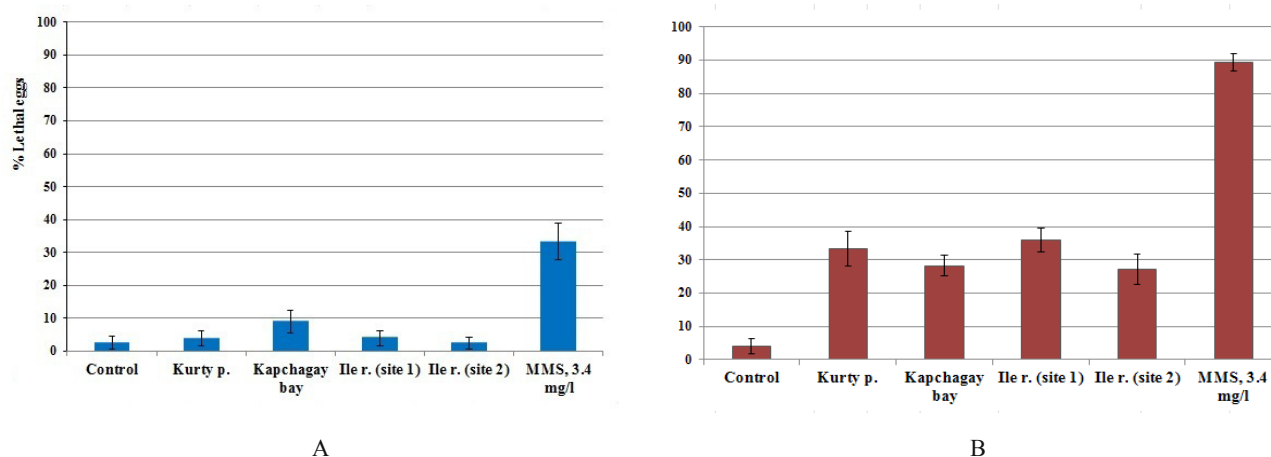


Figure 1 – Overview of the lethal (A) and teratogenic (B) effect in zebrafish embryos for 72 hours incubation in natural water samples

Note: the standard error for each parameter is the result of three independent experiments

It is very important to assess the individual morphologic malformations in zebrafish embryos exposed to surface water samples. The absolute incidences of the different induced teratogenic endpoints in zebrafish are summarized in Figure 2. The main malformations observed in fish embryos exposed to surface water were scoliosis, malformation of end-tail, growth retardation and oedemas. A clear incidences of tail curvatures and endtail absence were only observed in the group exposed to direct mutagen MMS (data not shown). Teratogenic effects are considered as fingerprint endpoints, if the endpoint is observed in $\geq 50\%$ of all teratogenic fish eggs in the test groups. Some malformations such as effects on the spinal cord, occurred more frequently than others. The scoliosis defined as S-shapes curvature of the embryo trunk occurred in all groups of tested surface water with frequency more than 50%. Despite the level of teratogenic eggs in control group is only 4.0%, the gross was of scoliosis – 66.7%, whereas other 33.3% made up by malformations of tail (data not shown) and there were observed no such alterations as growth retardation, malformations of tail tip and oedema. Scoliosis incidences were as well observed in all tested groups: 84.5% it constituted in Kurty pond samples, 85.2% and 86.4% in Ile river (sites 1 and 2 respectively) and least in Kapchagay bay – 68.2%. Scoliosis leads to the defects in somitogenesis and influence the formation of excretory system. When transition to exogenous feeding, this spinal cord malformation is actually the precondition for the excessive larvae loss.

In our study the pericardial and yolk sac oedema were summarized to facilitate scoring and observed

in three groups only: in water samples from Kurty p., Kapchagay bay and in case of embryo exposure to direct mutagen MMS, that is 53.9%, 22.7% and 20.9% of all malformation incidences, respectively. Pericardial oedema was occasionally so strong that the heart was prolonged into the narrow tube, the yolk sac oedema was accompanied by local yolk destruction and accumulation of the liquid in the cavity. The accumulation of the liquid in the pericardium and/or yolk sac is usually referred to the disruption of water and salt balance in embryo.

It is very important to mention the role of chorion in zebrafish embryos resistance and susceptibility to xenobiotics and maintenance of water balance in embryo. The chorion is the acellular, highly structured envelope enclosing a developing embryo, separating it from the external environment. The outer chorion membrane complex with a thickness of 1.5-2.5 μm consists of three layers: electron-dense outer and innermost layers with a thickness of 0.2-0.3 μm and 1.0-1.6 μm , respectively, separated by an electron-lucent middle layer (0.3-0.6 μm in thickness); the middle and inner layers are pierced by pore canals while the outermost layer is covered with projections of 2.0-3.0 μm in diameter [13]. The glycoproteins, which constitute the outer layer of the chorion, participate in creation of flexible membrane to which particles and microorganisms adhere. Chorion provides protection against microorganisms and protozoans accomplishes mechanical protection of the embryo and is assumed to offer an undefined protection against pollutants. Nevertheless, since in natural conditions the embryo is developed inside chorion and its barrier function must be considered in developmental ef-

fects of surface water the removal of chorion in case of bioassay is completely unjustified. It should also be taken into consideration that chorion permeability is not equal at all embryonic stages and for all group of substances. Although the pore canals are closed or obliterated, the chorion seems to be freely permeable to water, electrolytes and small molecules. It is suspected, that the chorion pores potentially restrict the uptake of compounds depending on their size.

This was found for fluorescent dextrans exceeding 3 kDa as well as for polymers, higher molecular weight surfactants and nanoparticles [14]. As for lipophilic substances, most of which can penetrate membranes easily, it seems rather applicable that with increasing lipophilicity the substance is accumulated in the yolk and becomes available slowly at the beginning of yolk consumption, providing delayed toxic effect [15].

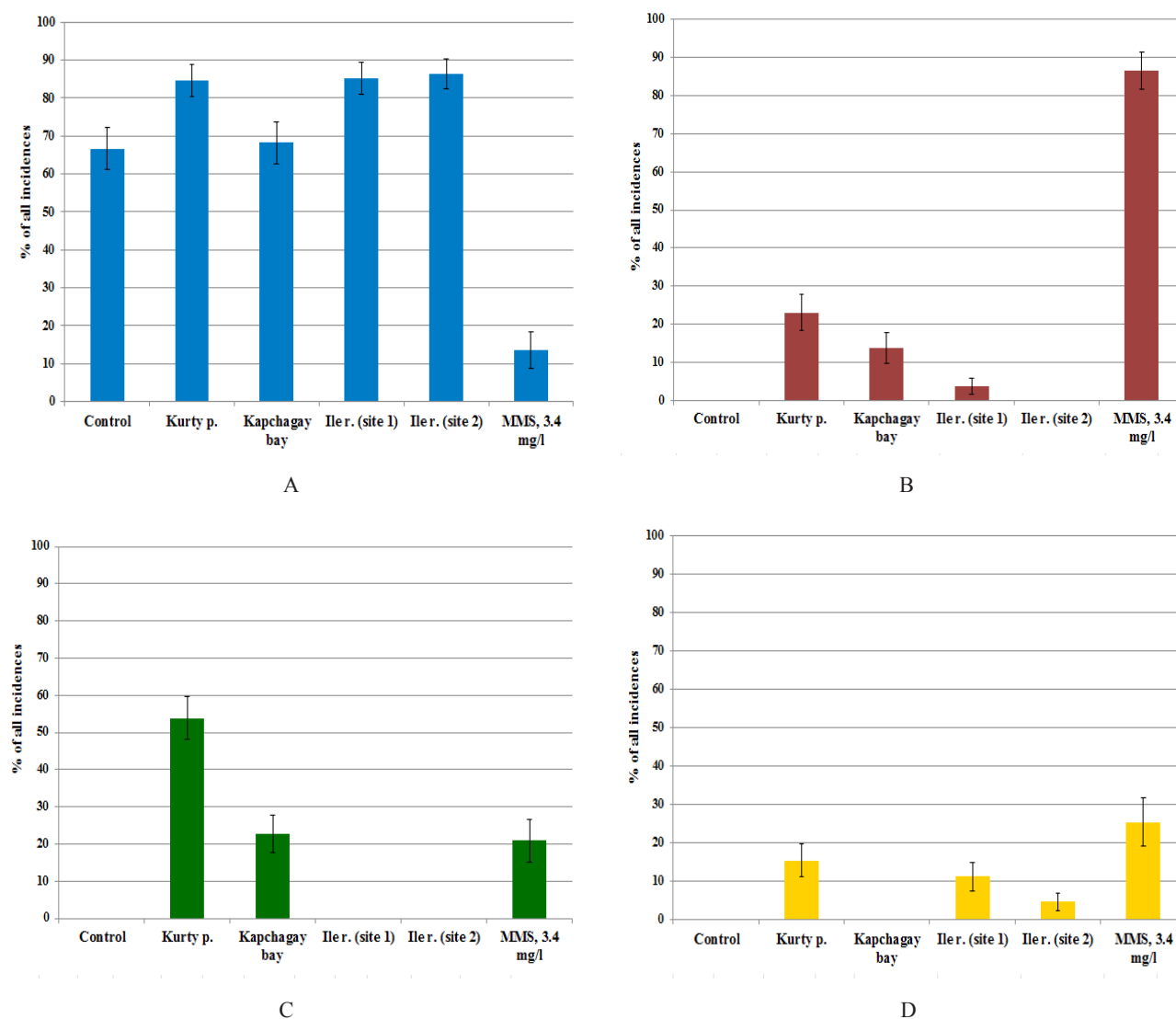


Figure 2 – Summary of individual morphologic malformations in zebrafish *Danio rerio* embryos observed for 72 hours incubation in natural water samples.

Note: A – scoliosis; B – growth retardation; C – oedema; D – endtail malformation; the standard error for each parameter is the result of three independent experiments.

On the other hand, some studies showed that dechorionated embryos were less susceptible to the toxic effect of heavy metals than embryos with in-

tact chorions, possibly because of the Donnan equilibrium: cations with negative standard electrode potentials (e.g. Zn^{2+} , Cd^{2+} , Pb^{2+}) would easily pass the

chorion (which acts as an ion exchanger) and would be accumulated in the perivitelline fluid. Thus, embryos with a chorion were more susceptible to these ions than those without. In contrast, cations with positive standard electrode potentials (e.g. Hg^{2+} , Cu^{2+} , Ag^{2+}) with high affinities to sulfhydryl groups would bind to the chorion, which thus would act as a barrier [13]. Metal accumulation in the chorion seems to be strongly pH dependant – the lower the pH is, the more metal is bound to the chorion. In our experiments MMS promoted the excessive dye (methylene blue) accumulation in perivitelline space and further capture by embryo macrophages. In normal conditions the zebrafish chorion is impermeable for the dye but the exposure leads to disruption of its permeability resulting besides in excessive water and ions influx in embryo tissues and finally oedema. The penetration of toxic substances may also be facilitated. Dye accumulation was also revealed for the samples from Kapchagay bay and Kurty pond indirectly supporting the role of chorion permeability in oedema development.

Malformations of endtail in their way did not occur in water samples from Kapchagay bay but instead were registered in Ile river samples - both point 1 and point 2 (11.1% and 4.5% of all malformations), but the share is quite beyond fingerprint endpoint. Incubation of zebrafish embryos in surface water samples from Kurty p. produced 15.4% of end tail malformations being only in 1.6 times less than exposure to MMS (25.4%). There was recorded no growth retardation in negative control and Ile r. point 2 groups, minor share of 3.4% in Ile r. point 1 group and above required 10% limit observed only in Kurty p. and Kapchagay bay samples that is 23.1% and 13.6%, respectively. Growth retardation is considered to be one of the most noticeable teratogenic effect of chemical compounds and hardly resulted from environmental changes e.g. water temperature, osmolarity or hardness being the outcome of chemical exposure whether to cytotoxic or alkylating agent. In support a clear incidence of growth retardation was only observed in the MMS group – 86.6% of all malformations. Methylmethanesulphonate was shown to significantly increase DNA damage in zebrafish embryo cells that was assessed *in vitro* and *in vivo* using the comet assay [16]. Reproductive and genotoxic effects in zebrafish after chronic exposure to methyl methanesulphonate was also determined in a multigeneration study [17]. It is also proved that MMS produces toxicity mainly by damaging cell membranes, induce cell death by activating the apoptotic pathway triggered by the activation of the mitochondrial dam-

age pathway, cause sister chromatid exchanges and chromosomal aberrations [18; 19].

In our experiments in response to MMS embryos displayed multiple effects such as growth retardation, oedema, scoliosis, malformation or absence (occasionally) of tail tip characteristic for direct mutagen/teratogen. It should be noted that MMS as direct teratogen did not induce gross incidences of spinal cord malformation – in positive control scoliosis constituted only 13.4% whereas growth retardation in opposite shares about 85% of all incidences. Among all tested sites only the samples of surface water from Kurty pond produced multiple phenotypic effects in zebrafish embryos and especially, relatively high level of growth retardation, proposing the presence of disrupting or alkylating compounds in surface water samples. Other samples did not show significant effect, nevertheless induced malformations may be due to exposure to heavy metals (oedema), surface active agents or aromatic carbohydrates (scoliosis) and others. Taken together, the surface water samples from lower rich of Ile river, Kapchagay and Kurty reservoirs did not possess significant embryo toxic effects but did induce the spectrum of malformations related to axial skeleton (scoliosis, end tail malformation), water/salt balance and chorion permeability (oedema) and growth patterns (growth retardation) in different incidences. One may predict that dwelling fish species at the early stages of their life cycle, that is considered to be the most susceptible and vulnerable stage, would be exposed to potent teratogen(s) resulting in fish population deterioration. Anyway, it could be argued that zebrafish embryos are the very susceptible, effective and informative tool for bioassay especially in terms of embryonic toxicity for vertebrates and further investigations directed towards clarification of toxic substances and their toxic effects for vertebrates in active surface water samples.

Conclusion

In the present study, we assessed the quality of surface waters of Lower Ile river, Kapchagay and Kurty reservoirs using zebrafish (*Danio rerio*) embryotoxicity test. It was established that none of surface water samples possess significant embryo toxic effects but all induce the spectrum of malformations related to axial skeleton (scoliosis, end tail malformation), water/salt balance and chorion permeability (oedema) and growth patterns (growth retardation) in different incidences. The lowest rate of teratogenicity was observed in embryos incubated in samples from Kapchagay bay (28.2%, $p \leq 0.05$) and Ile river at

Bakanas region (site 2, 27.2%, $p \leq 0.05$). The obtained knowledge of the embryotoxic effects of water will allow using them in further research on improving sanitary and hygienic standards and the developing medical and preventive measures.

Acknowledgments

The work was carried out within the framework of the grant AP05130546 "Study of mutagenic, genotoxic and toxic activity of surface waters in Almaty city and Almaty region" with the financial support of the Ministry of Education and Science of the Republic of Kazakhstan.

References

- Hafner C., Gartiser S, Garcia-Käufer M., Schiwiy S., Hercher C., Meyer W., Achten C., Larsson M., Engwall M., Keiter S., Hollert H. (2015) Investigations on sediment toxicity of German rivers applying a standardized bioassay battery. *Environ Sci Pollut Res.*, vol. 22, no 21, pp. 16358-16370.
- Di Paolo C., Ottermanns R., Keiter S., Ait-Aissa S., Bluhm K. et al. (2016) Bioassay battery interlaboratory investigation of emerging contaminants in spiked water extracts - Towards the implementation of bioanalytical monitoring tools in water quality assessment and monitoring. *Water Res.*, vol. 104, no 1, pp. 463-484.
- DanTox Symposium Methoden zur Bewertung von Sedimenttoxizität mit dem Zebraabrling *Danio rerio* vom 10-11 Juni 2013 an der RWTH Aachen im SuperC, Templergraben 55 (52062), 129 p.
- Chakraborty Ch., Sharma A.R., Sharma G., Lee S.S. (2016) Zebrafish: A complete animal model to enumerate the nanoparticle toxicity. *J Nanobiotechnology*, vol. 14, pp. 65-71.
- Haque E., Ward A.C. (2018) Zebrafish as a model to evaluate nanoparticle toxicity. *Nanomaterials*, vol. 8, no 7, pp. 561-569.
- Ali Sh., Aalders J., Richardson M.K. (2014) Teratological effects of a panel of sixty water-soluble toxicants on zebrafish development. *Zebrafish*, vol. 11, no 2, pp. 129-141.
- Gut P., Reischauer S., Stainier D.Y.R., Arnaout R. (2017) Little fish, big data: zebrafish as a model for cardiovascular and metabolic disease. *Physiol Rev.*, vol. 97, no 3, pp. 889-938.
- GOST 31861-2012. Mezhgosudarstvennyj standart. Voda. Obshhie trebovaniya k otboru prob. [Interstate standard. Water. General requirements for sampling]. M.: Standartinform, 2013, 64 p.
- Westerfield, M. (2000). The zebrafish book. A guide for the laboratory use of zebrafish (*Danio rerio*). 4th ed., Univ. of Oregon Press, Eugene. https://zfin.org/zf_info/zfbook/zfbk.html
- OECD (2013), Test No. 236: Fish embryo acute toxicity (FET) test, OECD guidelines for the testing of chemicals, Section 2, OECD Publishing, Paris, 11 p.
- Kimmel C.B., Ballard W.W., Kimmel S.R., Ullmann B., Schilling T.F. (1995) Stages of embryonic development of the zebrafish. *Dev Dyn.*, vol. 203, no. 3, pp. 253-310.
- Busquet F., Nagel R., von Landenberg F., Mueller S.O., Huebler N., Broschard T.H. (2008). Development of a new screening assay to identify proteratogenic substances using zebrafish *Danio rerio* embryo combined with an exogenous mammalian metabolic activation system (mDarT). *Toxicol. Sci.*, vol. 104, no 1, pp. 177-188.
- Henn K. (2011) Limits of the fish embryo toxicity test with *Danio rerio* as an alternative to the acute fish toxicity test. Dissertation submitted to the Combined Faculties for the Natural Sciences and Mathematics of the Ruperto-Carola, University of Heidelberg, 103 p.
- Kim K.T., Tanguay R.L. (2014) The role of chorion on toxicity of silver nanoparticles in the embryonic zebrafish assay. *Environ. Health Toxicol.*, vol. 29, e2014021.
- Braunbeck T., Lammer E. (2006) Fish embryo toxicity assays. German Federal Environment Agency, 298 p.
- Eleršek T., Plazar J., Filipič M. (2013) A method for the assessment of DNA damage in individual, one day old, zebrafish embryo (*Danio rerio*), without prior cell isolation. *Toxicol in Vitro*, vol. 27, no 8, pp. 2156-2159.
- Fassbender C., Braunbeck T. (2013) Reproductive and genotoxic effects in zebrafish after chronic exposure to methyl methanesulfonate in a multigeneration study. *Ecotoxicol.*, vol. 22, no. 5, pp. 825-837.
- Tomicic M.T., Christmann M., Fabian K., Kaina B. (2005) Apaf-1 deficient mouse fibroblasts are resistant to MNNG and MMS-induced apoptotic death without attenuation of Bcl-2 decline. *Toxicol. Appl. Pharmacol.*, vol. 207, no 1, pp.117-122.
- Pascucci B., Russo M.T., Crescenzi M., Bignami M., Dogliotti E. (2005) The accumulation of MMS-induced single strand breaks in G₁ phase is recombinogenic in DNA polymerase β defective mammalian cells. *Nucleic Acids Res.*, vol. 33, no 1, pp. 280-288.

IRSTI 34.45.05/76.31.33

¹A.N. Aralbaeva, ¹A.T. Mamataeva, ²M.V. Zamaraeva,
^{3*}M.K. Murzakhmetova

¹Almaty Technological University, Almaty, Kazakhstan

²University of Bialystok, Bialystok, Poland

³Al-Farabi Kazakh National University, Almaty, Kazakhstan
e-mail: murzakhmetova2016@gmail.com

Comparative assessment of antioxidant and membrane-protective properties of medicinal plant extracts

Abstract: Medicinal plants are a valuable raw material for obtaining phytodrugs with a wide range of pharmacological and therapeutic effects, which are acting fast, do not possess cumulative properties and are less accompanied by undesirable side effects. Modern assessment of the species diversity of the medicinal flora and its resource potential is especially important in designing an effective system that fights diseases caused by oxidative stress. Thus, the purpose of scientific research is to study and establish a list of medicinal plant extracts with strongest antioxidant and membrane-protective effect on liver cells exposed to oxidative stress. Determination of medicinal plant extracts that exhibit highest antioxidant and membrane-protective activities will allow us to use it in creating of an effective phytocomposition that would inhibit the action of lipid peroxidation (LPO) and osmotic stress, which lead to excessive damage of cell constituents and development of oxidative stress. For this purpose, LPO levels were detected by measuring malondialdehyde concentration in the liver microsomes whereas the osmotic hemolysis was measured in a hypotonic solution of 0.4% NaCl followed by optical density measurement at 540 nm. It was established that LPO levels in liver microsomes as well as osmotic fragility of erythrocyte membranes are plant extract dose-dependent. As a result, 3 out of 9 plant extracts have significant membrane-protective properties. Plants belong to the families: *Urtica dioica*, *Viola tricolor*, *Vaccinium vitis*. In addition, *Valeriana officinalis* (leaves), *Viola tricolor*, *Limonium gmelini*, *Vaccinium vitis*, *Hypericum perforatum* and *Capsella bursa-pastoris* showed the strongest antioxidant property. All plant extracts contained such biologically active compounds as polyphenols and flavonoids. Our results suggest further study of the antioxidant and membrane-protective effects of medicinal plant extracts tested here may guide phytotherapy to development of new dosage forms, and advance the development of unconventional therapeutic and preventive approaches against oxidative stress related diseases.

Key words: antioxidant, free radicals, lipid peroxidation, osmotic hemolysis, erythrocyte membranes, liver microsomes, plant extracts.

Introduction

Oxidative stress is the result of a disturbed balance in oxidant and antioxidant system, which appears from incessant rise of reactive oxygen species production [1]. That is the well-established balance between antioxidants and the pro-oxidants, reactive oxygen species, could be disturbed by exposure to physical, chemical or microbial toxic agents. Continued oxidative stress can result in many age-related diseases and altered lipid peroxidation may also be a producer of pigments and lipofuscins (oxidized insoluble parts of proteins, lipids and carbohydrates) [2]. Thus, accumulation in a large number of amphiphiles is accompanied by a massive introduction of

them into membranes, which, like an excess of lipid hydroperoxides, leads to the formation of clusters and micro-ruptures in them. Damage to membranes and cell enzymes is one of the main causes of a significant disorder in the vital activity of cells and often leads to their death [3]. Biological membranes perform many functions, a violation of any of which can lead to a change in the vital activity of the cell as a whole and even to its death. For some unfavorable factors (stress, radiation: radiation, UV, X-ray, etc., food contamination and the environment, the effects of certain medicines and medicines procedures, severe overheating or cooling, excessive physical load, etc.) the system of antioxidant protection does not cope, and the reactionary oxygen and nitrogen com-

pounds and free radicals begin to damage vital DNA molecules, proteins and lipids [4]. Biological membranes contain a large number of unsaturated fatty acids, metalloproteins, activating molecular oxygen. Therefore, it is not surprising that lipid peroxidation processes can develop in them [5]. One of the products of this reaction is lipid hydroperoxide - a relatively stable compound. In addition, a peroxide radical can form a lipid endoperoxide radical, the decomposition of which leads to the formation of a number of products, including malonic dialdehyde [5]. Polyunsaturated fatty acids, both in the free form and in the lipids, can undergo spontaneous peroxidation, which proceeds at a rather high speed in lipid films and solutions, homogeneous systems, as well as in aqueous media where lipids form liposomes and films, systems with different phases [6]. Free radicals change the permeability (and hence the barrier function) of cytoplasmic membranes in connection with the formation of channels of increased permeability, which leads to disruption of the water-ion homeostasis of the cell [7]. These radicals are particularly active in interacting with membrane lipids, containing unsaturated bonds, which leads to violation of many exchange processes. Peroxide oxidation of membrane phospholipids is one of the most common mechanisms of destruction of membrane structures, it is recorded during the development of a number of pathological conditions [8]. Nevertheless, the processes of lipid peroxidation take place in a normal cell. They are regulated by a number of enzymes: NADP(H) - dependent microsomal oxygenases, cyclooxygenases and lipoxygenases. Phospholipids in native membrane systems are effectively protected from non-enzymatic peroxidation by the presence of antioxidants in biomembranes, by the structural organization of membranes, and by special enzymatic systems regulating the concentrations in the membrane of reactive oxygen species inhibiting lipo-oxidation development [9]. Products of lipid peroxidation are precursors of the synthesis of prostaglandins, thromboxanes, prostacyclin, leukotrienes and lipoxins [10]. The most active free radicals break bonds in molecules DNA, thereby damaging the genetic apparatus of cells regulating their growth, that can lead to oncological diseases [11]. Low-density lipoproteins after oxidation by free radicals easily deposited on the walls of the vessels, leading to the accelerated development of atherosclerosis and cardiovascular diseases. At present, it is shown that hundreds of diseases are preceded by an oxidative stress [12]. Therefore, the modern assessment of the species diversity of the medicinal flora and its resource potential is especially

important in designing an effective system that fights diseases caused by oxidative stress.

Medicinal plants are a valuable raw material for obtaining phytodrugs with a wide range of pharmacological and therapeutic effects, which are acting fast, do not possess cumulative properties and are less accompanied by undesirable side effects. Also, they are the source of a variety of medicines. Currently, about 40% of all medicines are obtained from plants [13]. Medicinal plants are valuable because of they are source of bioactive compounds possessing potential biological and physiological effects [14; 15]. One group of substances is herbal polyphenols. These compounds are secondary plant metabolites, which done functions of defense in plant cells. However, it was proved various benefit influence of them on human organism cells in vitro and in vivo studies. Multisided effects of plant polyphenols make them perspective object in medicinal researches and elaborations. There was observed expressed polyphenolic compounds' antioxidative properties out of the dependence in structure and group, which cause their positive effect at disorders characterized by developing oxidative stress [16-18].

Actively developing research in the fields of biochemistry of natural compounds and phytotherapy constantly increases the number of discovered medicinal species that have high antioxidant effect on mammalian cells. However, many species as a result of haphazard collection have become rare, such as *Rhodiola rosea*, peony Maryin root, Ural licorice, marjoram, etc. The state of populations of many medicinal plants is alarming, therefore strict control over their collection is necessary [19].

For the formation of a stable raw material base of the domestic pharmaceutical industry and the creation of new phytoextracts, the study of pharmacopoeial and perspective medicinal plant species found in regions of Kazakhstan is one of the goals of this research. However, the main objective of this work is to study and establish a list of medicinal plant extracts with strongest antioxidant and membrane-protective effect on male white rats liver cells exposed to oxidative stress. The purpose of this scientific research is to determine medicinal plant extracts with strongest antioxidant and membrane-protective effect on liver microsomes and erythrocyte membranes respectively.

Materials and methods

Medicinal plant extracts collected in the Almaty region, Kazakhstan. Each plant was dried and weigh-

ing 1 g was milled and powdered and then placed in 10 ml of 50% ethanol solution. The mixture was left for 20 hours in the dark place. After, the mixture had undergone centrifugation at a speed of $20,000\times g$ for 10 min. The supernatant then was left in rotary evaporator until it is completely dry. It should be noted that all solutions with dissolved dried extracts in them (100 mg/ml) were freshly prepared in 50% ethanol prior to experiments.

For experiments was chosen healthy male white rats weight 300-350 g. Animals were kept under standard conditions that include normal light and dark cycle and free access to food and water. The blood and liver tissue were collected according to the experimental protocols approved by the Committee for the Ethical Care and Use of Animals in Experiments.

Preparation of rat liver microsomes. In the experiment rats were initially sedated by administering isoflurane anesthesia and then physically euthanized by using cervical dislocation technique. The rat livers were isolated and collected, washed, and sprayed with cold saline solution. Liver tissue was minced and homogenized (1:10 w/v) in 10mM solution of potassium phosphate buffer with pH 7.4 and containing 1mM EDTA placing a mixture on ice. After the homogenate was centrifuged at a speed of $10,000\times g$ for 20 min under a temperature of 4 °C. The obtained supernatant was further centrifuged at a speed of $100,000\times g$, for 60 min, after which we obtained the microsomal part of the liver. Microsomes were carefully isolated and suspended in a buffer containing 10mM histidine with pH 7.2, 25% (v/v) glycerol, 0.1mM EDTA and 0.2mM CaCl_2 , and were stored under a temperature of 20°C. Moreover, the protein content was determined by the Lowry assay using bovine serum albumin as a standard.

Isolation of erythrocytes. The rats were put under isoflurane anesthesia, then were euthanized and the blood through cardiac puncture was collected. Then blood was centrifuged at a speed of $1000\times g$, for 10 min, after which white blood cells were removed. Erythrocyte pellets were washed twice with 5mM Na_2HPO_4 (pH 7.4) and 150mM NaCl buffer, and immediately undergone osmotic resistance tests.

Assessment of microsomal lipid peroxidation. An assessment of LPO was held by measuring the presence of malondialdehyde in the form of thiobarbituric acid-reacting substances (TBARS) [20]. Concisely, liver microsomes were preincubated together with test agents in 50mM KH_2PO_4 (pH 7.2) and 145mM NaCl buffer at a temperature of 37 °C, for 10 min constantly stirred. 0.02mM Fe^{2+} and 0.5mM

ascorbic acid-induced microsomal LPO along with basal was then established in a reaction mixture with added 0.4% SDS, 20mM thiobarbituric acid and 0.9M sodium acetate buffer with pH 3.5, followed by incubation at a temperature of 95 °C for full 60 min [21]. After a mixture was cooled down at room temperature, the mixture was washed with n-butanol: pyridine solution with ratio of 15:1, v/v and centrifuged at a speed of $3,000\times g$, for full 5 min. After collecting organic layer of the analyzing mixture, it is absorbance was measured at 532 nm by PD-303UV spectrophotometer. The MDA concentration is represented in nmol of TBARS per mg protein.

Assessment of osmotic resistance of erythrocytes. Osmotic resistance of erythrocytes was measured as it is done in the in vitro studies. Preincubated at 37°C for 10 min isolated erythrocytes with vehicle/test agents were placed into a hypotonic 0.4% NaCl solution at 37°C, for 20 min, after which the mixture had undergone centrifugation. An absorbance of hemoglobin in the supernatant was determined by spectrophotometer at 540 nm. In the experiment with rats, a level of hemolysis of erythrocytes induced by 0.4% NaCl solution was determined and measured directly not performing preincubation. The level of hemolysis was expressed in percentage of overall hemolysis caused by 0.1% Na_2CO_3 solution.

Assessment of total phenolic and flavonoid content. The amount of total phenolics in the extracts was measured using the Folin-Ciocalteu reagent method [22]. The 0.5ml of each extract (1.0 mg/ml) was added into test tubes containing 2.5 ml of 10% Folin-Ciocalteu reagent and 2.0 ml of 2% sodium carbonate solution and the tubes were shaken thoroughly. The mixture was incubated at 45°C for 15 min with intermittent shaking. Absorbance was measured at 765 nm using a PD 303 UV-Vis spectrophotometer (Shimadzu, Japan). Gallic acid was used as a standard to obtain a calibration curve (ranging from 0 to 1 mg/ml). The results were expressed in percent per mg dry extract.

The total flavonoid contents were determined according to colorimetric assay [23], with rutin as standard. The 0.5 ml of each extract (1.0 mg/ml) were mixed with 2 ml of distilled water and 150 μl of 5% sodium nitrate. After 6 min, 150 μl of 10 % aluminum chloride and 2 ml of 1 M sodium hydroxide were added and left at room temperature for 15 min. Absorbance of the mixtures was measured at 510 nm. The calibration curve was prepared in the same manner using 0-1.0 mg/ml of rutoside solutions in methanol. The results were expressed in percent per mg dry extract.

Statistical data analysis. Results are statistically processed using the program Microsoft Excel. Given the Fisher-Student performance recorded changes were considered significant at $p \leq 0.05$.

Results and discussion

Herbal extracts were able to decrease erythrocyte hemolysis, however, their anti-hemolytic effect is observed on different levels (Table 1).

As represented in Table 1, the nettle and violet's extracts possess the best membraneprotective qualities. Plant ethanolic extracts authentically decreased erythrocyte hemolysis in concentration range from 0.005-0.1 mg/ml. In concentration 0.1 mg/ml fragility of erythrocytes accordingly lowed up to $36.9\% \pm 1.3$ and $41.0\% \pm 2.04$. Antihemolytic action of plantain comes out dose-dependent.

Phytoextracts of hypericum plant, shepherd's grass and valeriana leaves occurred insignificant influence on erythrocyte hemolysis at 0.5 mg/ml concentration – hemolysis level consists 98.6%, 95.2% and 94.1%. Nevertheless in concentration upper 0.01 mg/ml there is observed strengthening of valeriana leaves and hypericum extracts protective effect on erythrocyte membranes. Shepherd's grass extracts do not change hemolysis level in concentration 0.01 mg/ml notably, but action of extract in concentrations higher than 0.05 mg/ml there was found out significant enlarging of erythrocyte membrane resistance. Comparison of valeriana roots and leaves showed that leaves' membrane protective effect is better. Thus, there are foundations to make conclusions about more effective applying of valeriana leaves to decreasing membrane fragility than using plant roots.

Table 1 – Influence of herbal extracts on erythrocyte membrane fragility

Extract name	Extract concentration (mg dry extract/ml IM)				
	0	0.005	0.01	0.05	0.1
<i>Limonium gmelinii</i>	100	74.0±3.68	70.6±3.51	60.9±3.34	56.7±2.82
<i>Plantain – Plantago major</i>	100	73.6±3.67	66.7±3.3	66.0±3.28	61.4±3.05
<i>Valeriana officinalis</i> (leaves)	100	94.1±4.68	87.7±4.37	74.6±3.72	69.9±3.4
<i>Valeriana officinalis</i> (roots)	100	107.1±5.3	100.7±5.0	87.6±4.37	87.0±4.3
<i>Hypericum – Hypericum perforatum</i>	100	98.6± 4.9	78.6±3.91	61.4±3.06	51.1±2.5
<i>Nettle – Urtica dioica</i>	100	89.0±44.4	54.4±2.7	50.9±2.53	36.9±1.3
<i>Lingonberry – Vaccinium vitis</i>	100	65.4±3.25	61.8±3.08	58.8±2.92	46.8±2.3
<i>Violet – Viola tricolor</i>	100	59.1±2.85	58.4±2.90	49.4±2.46	41.0±2.04
<i>Shepherd's grass – Capsella bursa-pastoris</i>	100	95.2±47.5	92.7±4.6	81.2±4.03	72.1±3.59

Analysis of the results of the research showed that not all plant extracts possess a membrane-stabilizing property and reduce the hemolysis of red blood cells; moreover, roots of *Valeriana officinalis* had a damaging hemolytic effect on the membranes of red blood cells. Most of the extracts showed a great change in stability of erythrocyte membranes. However, only three extracts showed the lowest degree of hemolysis: *Urtica dioica*, *Viola tricolor*, *Vaccinium vitis* show the lowest intensity of hemolysis.

The results of the study of the influence of the 9 different plant extracts on the processes of LPO in liver microsomes showed that the extracts of these plants are strong antioxidants, which is con-

firmed by inhibition of the formation of TBA active products.

Studies of herbal extracts' influence on peroxidation processes in liver microsomes resulted that *Valeriana*, *Lingon berries* leaves, *Hypericum* and *Violet* herbs possess high-expressive antioxidative properties (Table 2), named extracts totally inhibited MDA generation in concentrations from 0.25 mg to 2.5 mg per 1 mg protein.

Nettle and *Limonium* extracts inhibited LPO product's generation in concentrations from 0.5 to 2.5 mg on 70% and 75%. Increasing of *Limonium* concentration do not lead to change in level of TBARS in incubation medium, as in case of nettle extract, enlarging

concentrations resulted to total suppressing of MDA generation. Total inhibition of LPO processes by shepherd's grass extract was occurs in concentrations upper than 1.25 mg. Data which were got at researches of valeriana roots and plantain extracts are differ from previous results. These herbal extracts showed prooxidative action increasing the intensity of lipo-

peroxidation on 23.8% and 2.3% in first researched concentrations. Nevertheless, there was observed increasing of antioxidative effect of *Valeriana* root's extract in accordance with enlarging doses upper than 0.5 mg, plantain extract came out high inhibiting action on forming of lypoperoxides in 2.5 mg concentration.

Table 2 –Influence of herbal extracts on LPO level in hepatocytes

Extract name	Extract concentration (mg dry extract/mg protein)				
	0	0.25	0.5	1.25	2.5
<i>Limonium gmelini</i>	100	24.4±1.2	18.3±0.91	18.0±0.9	16.5±0.82
<i>Plantain - Plantago major</i>	100	112.3±5.1	99.1±4.98	96.2±4.81	16.1±0.8
<i>Valeriana officinalis</i> (leaves)	100	10.8±0.54	5.2±0.26	5.3±0.27	5.1±0.25
<i>Valeriana officinalis</i> (roots)	100	123.8±6.18	80.6±4.02	59.3±2.86	22.9±1.14
<i>Hypericum- Hypericum perforatum</i>	100	8.5±0.42	6.2±0.31	6.0±0.3	5.7±0.28
<i>Nettle - Urticadioica</i>	100	31.8±1.6	5.8±0.29	4.8±0.24	2.9±0.14
<i>Lingon berry – Vaccinum vitis</i>	100	10.2±5.01	10.3±5.0	7.4±0.36	5.8±0.28
<i>Violet – Viola tricolor</i>	100	18.6±0.92	15.5±0,77	9.3±0.45	9.0±0.43
<i>Shepherd's grass - Capsella bursa-pastoris</i>	100	71.4±3.52	67.3±3.35	3.9±1.95	1.9±0.94

It can be seen that in the investigated concentration range, all these plant extracts almost completely suppress the formation of TBA-active products in liver microsomes except for *Plantago major* and *Valeriana officinalis* (roots). Extracts *Limonium gmelini*, *Valeriana officinalis* (leaves), *Vaccinum vitis* show good antioxidant properties, dose-dependent decrease in the formation of peroxide products in liver microsomes.

There was used lower concentration range to get more detail investigations of antioxidant qualities of *Limonium*, *Valeriana* leaves, *Hypericum* herb, *Lingon berry* leaves and *Violet herbs'* extracts (Figure 1). Figure 1 illustrated that all investigated plants showed dose-dependent antioxidant action in low doses. In result of studies was determined that the minimal concentration for significantly inhibition of lipid peroxidation for *Limonium* extracts was 50 µg, whereas similar action of *Violet*, *Valeriana* leaves and *Lingon berry's* extract showed in concentration 25 µg for *Hypericum* the most minimal effective dose consisted 10 µg. In concentrations upper than 200 µg *Valeriana*, *Lingon berry* and *Hypericum* extracts completely retarded LPO intensity, when violet and *Limonium* extracts conceded them in similar concentration range.

Having demonstrated that different plant extract at certain concentration can affect the processes involved in lipid peroxidation and can shift the osmotic fragility of erythrocyte membranes, it is established that all nine medicinal plant extracts collected in the Almaty region, Kazakhstan, showed dose-dependent antioxidant and membrane-protective effect on mammalian cells.

There were arranged studies of having in plants such bioactive compounds as polyphenols and flavonoids to get into probable mechanisms of antioxidant potential (Figure 2).

Content of bioactive substances is different in diverse extracts. Mass fraction of flavonoids and polyphenols were higher in *Hypericum* extract in compare with other investigated plants. Also, we should say about different level of the same bioactive compounds in different parts of one plant. So plant extracts could be placed in accordance to content of total polyphenols in next row *Hypericum perforatum* > *Limonium gmelini* > *Vaccinum vitis* > *Valeriana officinalis* (leaves) > *Capsella bursa-pastoris* > *Viola tricolor* > *Urtica dioica* > *Plantago major* > *Valeriana officinalis* (roots), whereas there are some diversities in flavonoid's content. At comparison of antioxidant potential and bioactive

substance content was brought out that there was no strong correlation between antioxidant content and antioxidative effect of extracts. Thus, content of fla-

vonoids in violet extract is lower on 42% than so one in shepherd's grass extract, but protective effect of violet was higher.

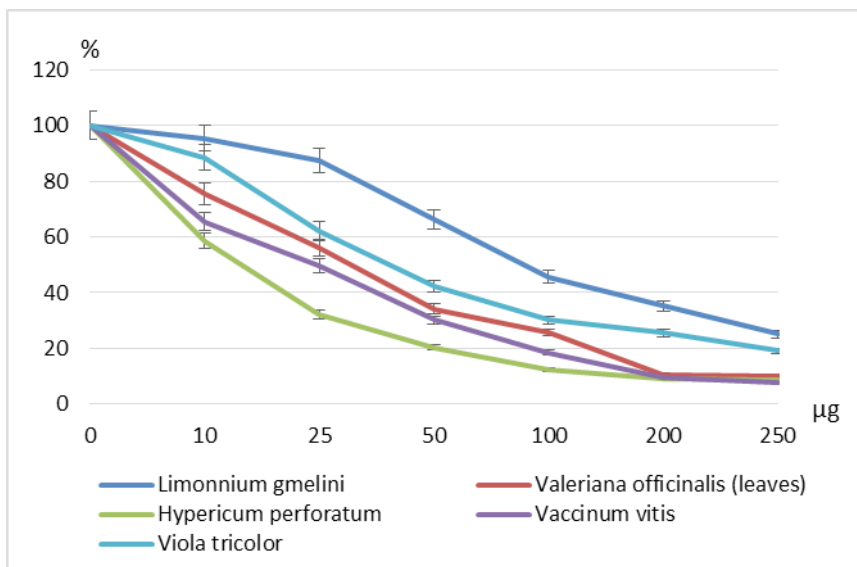


Figure 1 – Effect of selected plant extracts on the level of LPO in microsomes

Note: on the abscissa axis – plant extracts concentration µg/mg protein; on the ordinate axis – the intensity of LPO processes, % ($p \leq 0.05$)

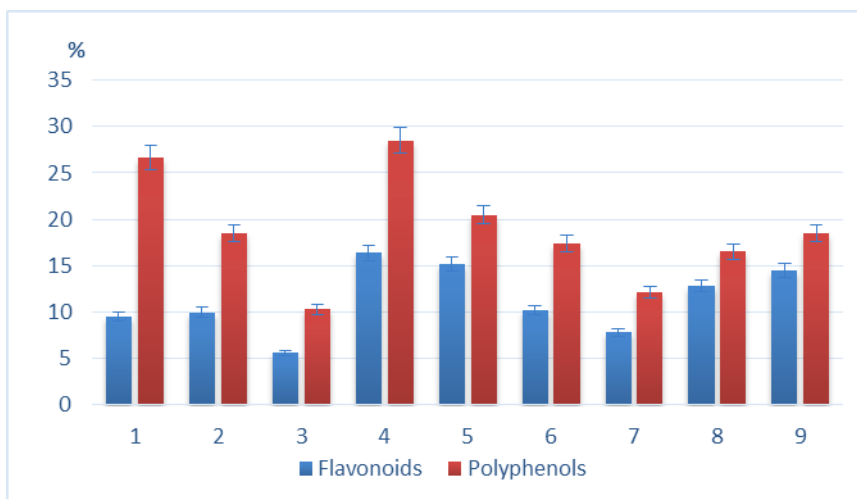


Figure 2 – Content of total polyphenols and flavonoids in extracts

Note: Mass fraction of total polyphenols and flavonoids in terms of mg of dry extract, %; on the ordinate axis - plant extracts (1 – *Limonium gmelini*, 2 – *Valeriana officinalis* (leaves), 3 – *Valeriana officinalis* (roots), 4 – *Hypericum perforatum*, 5 – *Vaccinum vitis*, 6 – *Viola tricolor*, 7 - *Plantago major*, 8 – *Urtica dioica*, 9 – *Capsella bursa-pastoris*)

Conclusion

Medicinal plant extracts, collected in the Almaty region, Kazakhstan, have antioxidant and membrane stabilizing properties, reduces the development of LPO reaction chain activation and also have a positive effect on anti-hemolytic properties of erythrocyte membranes.

Herbal plants have antioxidant and membrane-stabilizing properties that can be used to increase the resistance of the organism to the action of factors leading to excessive formation of free radicals and the development of oxidative stress.

There is observed that plant extracts' antioxidant properties based on presence of polyphenolic compounds and flavonoids. However, there was not found out clear conjunction between content of bioactive substances and protective effect. Assumingly it depends on synergetic or antagonistic interactions of different compounds in plant.

Our results suggest this research of the antioxidant and membrane-protective effects of the herbal plant extracts tested here may guide phytotherapy to development of new dosage forms, and further, to the development of unconventional therapeutic and preventive approaches against oxidative stress related diseases.

References

1. Kurutas E.B. (2016) The importance of antioxidants which play the role in cellular response against oxidative/nitrosative stress: current state. *Nutr J.*, vol. 15, no. 71, pp. 1-22.
2. Weidinger A., Kozlov A.V. (2015) Biological activities of reactive oxygen and nitrogen species: oxidative stress versus signal transduction. *Biomolecules*, vol. 5, no. 2, pp. 472-484.
3. Pamplona R. (2008) Membrane phospholipids, lipoxidative damage and molecular integrity: A causal role in aging and longevity. *Biochim. Biophys. Acta BBA - Bioenerg.*, vol. 1777, no. 10, pp. 1249-1262.
4. Rinnerthaler M., Bischof J., Streubel M.K., Trost A., Richter K. (2015) Oxidative stress in aging human skin. *Biomolecules*, vol. 5, no. 2, pp. 545-589.
5. Schneider C. (2009) An update on products and mechanisms of lipid peroxidation. *Mol Nutr Food Res.*, vol. 53, no. 3, pp. 315-321.
6. Laguerre M., Lecomte J., Villeneuve P. (2007) Evaluation of the ability of antioxidants to

counteract lipid oxidation: Existing methods, new trends and challenges. *Prog Lipid Res.*, vol. 46, no. 2, pp. 244-282.

7. Perry J.J., Shin D.S., Getzoff E.D., Tainer J.A. (2010) The structural biochemistry of the superoxide dismutases. *Biochim Biophys Acta*, vol. 1804, no. 2, pp. 245-262.

8. Ayala A, Muñoz M.F., Argüelles S. (2014) Lipid peroxidation: production, metabolism, and signaling mechanisms of malondialdehyde and 4-hydroxy-2-nonenal. *Oxid Med Cell Longev.*, vol. 2014, pp. 1-31.

9. Wambi C.O., Sanzari J.K., Sayers C.M., Nuth M., Zhou Z., Davis J., Finnberg N., Lewis-Wambi J.S., Ware J.H., El-Deiry W.S., Kennedy A.R. (2009) Protective effects of dietary antioxidants on proton total-body irradiation-mediated hematopoietic cell and animal survival. *Radiat Res.*, vol. 172, no. 2, pp. 175-186.

10. Zorov D.B., Juhaszova M., Sollott S.J. (2014) Mitochondrial reactive oxygen species (ROS) and ROS-induced ROS release. *Physiol Rev.*, vol. 94, no. 3, pp. 909-950.

11. Zhang P.Y., Xu X., Li X.C. (2014) Cardiovascular diseases: oxidative damage and antioxidant protection. *Eur Rev Med Pharmacol Sci.*, vol.18, no.20, pp. 3091-3096.

12. Tardieu F. (2013) Plant response to environmental conditions: assessing potential production, water demand, and negative effects of water deficit. *Front Physiol.*, vol. 4, no. 2, pp. 1-11.

13. Chen S.-L., Yu H., Luo H.M., Wu Q., Li C.F., Steinmetz A. (2016) Conservation and sustainable use of medicinal plants: problems, progress, and prospects. *Chin Med.*, vol. 11, no 2, pp. 281-288.

14. Gan RY, Zhang D, Wang M, Corke H. (2018) Health benefits of bioactive compounds from the genus *Ilex*, a source of traditional caffeinated beverages. *Nutrients*, vol.11, no. 10, pp. 1-17.

15. Gharbi S, Renda G, La Barbera L, Amri M, Messina CM, Santulli A. (2017) Tunisian tomato by-products, as a potential source of natural bioactive compounds. *Nat Prod Res.*, no. 6, pp.626-631.

16. Bjørklund G., Dadar M., Chirumbolo S., Ly-siuk R. (2017). Flavonoids as detoxifying and pro-survival agents: What's new? *Food Chem Toxicol.*, vol.11, pp. 240-250.

17. Mendonça R.D., Carvalho N.C., Martin-Moreno J.M., Pimenta A.M., Lopes A.C.S., Gea A., Martinez-Gonzalez M.A., Bes-Rastrollo M. (2019) Total polyphenol intake, polyphenol subtypes and incidence of cardiovascular disease: The SUN cohort

study. *Nutr Metab Cardiovasc Dis.*, vol. 29, no. 1, pp. 69-78.

18. Sen T, Samanta SK. (2015) Medicinal plants, human health and biodiversity: a broad review. *Adv Biochem Eng Biotechnol.* vol.147, pp. 59-110.

19. Kennedy D.O., Wightman E.L. (2011) Herbal extracts and phytochemicals: plant secondary metabolites and the enhancement of human brain function. *Adv. Nutr.*, vol. 2, no. 1, pp. 32-50.

20. Ohkawa H., Ohishi N., Yagi K. (1979) Assay for lipid peroxides in animal tissues by thiobarbituric acid reaction. *Anal. Biochem.*, vol. 95, no. 2, pp. 351-358.

21. Birben E. et al. (2012) Oxidative stress and antioxidant defense. *World Allergy Organ. J.*, vol. 5, no. 1, pp. 9-19.

22. Saikat Sen, Biplab De, N Devanna, Raja Chakraborty (2013) Total phenolic, total flavonoid content, and antioxidant capacity of the leaves of *Meynaspinosa Roxb.*, an Indian medicinal plant. *Chinese Journal of Natural Medicines*, vol. 11, no. 2, pp. 149-157.

23. Khodaie L., Bamdad S., Delazar A., Nazemiyeh H. (2012) Antioxidant, total phenol and flavonoid contents of two *Pedicularis L.* species from Eastern Azerbaijan, Iran. *Bioimpacts*, vol. 2, no. 1, pp. 43-57.

IRSTI 34.39.55

¹*G.A. Tussupbekova, ¹S.T. Tuleukhanov, ¹N.T. Ablaikhanova, ²Yu.A. Kim,
¹Zh.T. Abdrassulova, ¹M.S. Kulbaeva, ¹A.I. Zhussupova, ¹A. Ydyrys

¹Laboratory of Chronobiology and Ecological Physiology, Almaty, Kazakhstan

²Institute of Cell Biophysics Russian Academy of Sciences, Pushchino, Moskovskaya obl., Russia

*e-mail: gulmira.ablaikizi@gmail.com

Study of the chronic toxicity of the “Virospan” drug

Abstract: The living conditions of certain groups of Kazakhstani population, especially in regions and rural areas, where adverse factors (both environmental and anthropogenic), i.e. the quality of atmospheric air, food, and drinking water are deteriorating, might negatively affect the immune status of inhabitants and lead to the occurrence of diseases. For that reason, the restoration of immunological disorders is an urgent task, since the majority of chronic, somatic, infectious diseases are accompanied by secondary immunological failure. The algorithm of immunomodulation involves the use of pharmacological agents that can increase (immunostimulation) or reduce (immunosuppression) the level of immune response. The chronic toxicity of the immunostimulating “Virospan” drug was studied in doses of 39 mg/kg, 13 mg/kg, 4.3 mg/kg. Intranasal administration of the “Virospan” drug at a dose of 4.5 and 13 mg/kg causes a statistically significant ($P \leq 0.001$) increase in the level of white blood cells, erythrocytes, hemoglobin and hematocrit. Against the background of a statistically significant ($P \leq 0.001$) decrease in the level of polymorphonuclear neutrophils, an increase in lymphocytes was observed. “Virospan” at a concentration of 39 mg/kg leads to a decrease in the total number of leukocytes by 60 days and does not cause pronounced changes in the indicators of red blood, eosinophils and basophils.

Key words: immunostimulatory drug, chronic toxicity, hematological indicators, erythrocyte, leukocyte, body mass.

Introduction

The living conditions of certain groups of Kazakhstani population, especially in regions and rural areas, where adverse factors (both environmental and anthropogenic), i.e. the quality of atmospheric air, food, and drinking water are deteriorating, might negatively affect the immune status of inhabitants and lead to the occurrence of diseases [1-3]. For that reason, the restoration of immunological disorders is an urgent task, since the majority of chronic, somatic, infectious diseases are accompanied by secondary immunological failure [4; 5]. The algorithm of immunomodulation involves the use of pharmacological agents that can increase (immunostimulation) or reduce (immunosuppression) the level of immune response [6-9].

Therapy with drugs of natural origin is widely used in global medical practice. Herbal preparations are used for the treatment and prevention, as well as in the complex therapy of various diseases [10-13]. Often, they are used without a doctor's prescription,

while patients are at risk of exceeding the prescribed therapeutic dose until the appearance of side effects [14; 15]. Therefore, the study of the toxicity of the medicinal product of plant origin is necessary at the stage of preclinical evaluation.

Herbal preparation is a combination of different groups of biologically active compounds. Due to the complexity of herbal remedies, it is difficult to identify the component that causes its pharmacological activity. Search and study of biologically active compounds, organic drugs of natural origin are important for understanding its mechanism of action.

The aim of our work was to study the chronic toxicity of the plant-derived immunostimulating drug “Virospan”.

Materials and methods

Intra-nasal preparations were administered to rats of the experimental groups: “Virospan” in doses of 39 mg/kg, 13 mg/kg, 4.3 mg/kg, once in 5 days [6]. After the procedure, the visual observation of experi-

mental animals was carried out after 2, 4, 6 hours. The results on certain groups of rats were scored at 6, 30 and 60 days after the first injection of the substance and peripheral blood was taken.

Throughout the experiment, the animals were monitored daily: food and water consumption, condition of the hairline, mucous membranes and general condition (body weight dynamics, rectal temperature) were noted. General condition was assessed by daily inspection of animals. Weighing, measuring rectal temperature, water and feed consumption were performed once a week.

The blood of experimental animals was collected in a vacutainer with K3EDTA, mixed 10 times to eliminate the formation of microbunches and delivered to the laboratory. To assess hematological parameters, the Complete blood count was used to perform a complete blood count using the Siemens ADVIA 2120 automatic hematology analyzer (Germany) in the CBC/5-DIFF mode.

The following indicators were used: WBC – leukocytes (absolute number), RBC – erythrocytes (absolute number), HGB – hemoglobin (concentration), HCT – hematocrit (percentage), MCV – average red blood cell count, MCH – average hemoglobin content in a single erythrocyte, MCHC – average hemoglobin concentration in the erythrocyte mass, RDW – red blood cell distribution width, PLT – platelets (absolute), MPV – average platelet volume, NEUTRO% – neutrophils (relative col.), NEUTRO abs – neutrophils (absolute col.), LYMPHO% – lymphocytes (relative col.), Lympho abs – lymphocyte (absolute col.), MONO% – monocytes (relative col.), MONO abs – monocytes (absolute col.), BASO% – basophiles (relative col.), BASO abs – basophiles (absolute col.), EOS% – eosinophils (relative col.), EOS abs – eosinophils (absolute col.)

Statistical data processing was performed with the determination of the mean, standard and standard deviation, statistical error of the average and the percentage of differences. When determining the reliability of the difference between the indicators of the compared groups, the t-criterion of reliability was calculated, the value of P was determined from the table of Student values, the changes were considered significant at $P \leq 0.001$. All data were calculated in the MS Office Excel software package.

Results and discussion

To study the toxicity of the drug "Virospan" at a concentration of 4.3; 13; hemocytograms of ex-

perimental animals were analyzed for 39 mg/kg (Table 1).

As can be seen from the results of the Table 1, the following changes in hematological indices were observed on the background of the dosage of "Virospan" 4.3 mg/kg in laboratory animals – the total number of leukocytes in the dynamics of the study underwent a wave-like change; times and reached $10.54 \pm 0.23 \times 10^9/L$. in comparison with the control – $2.49 \pm 0.24 \times 10^9/L$, by the 30th day it decreased by 2 times to $5.45 \pm 0.23 \times 10^9/L$ and by the 30th day of the experiment it increased even more to 13.04 ± 0.23 while all changes were statistically significant ($P \leq 0.001$). The total number of erythrocytes practically did not change, so the average value on the 6th day in comparison with the control was 7.38 ± 0.20 , on 30 – 8.57 ± 0.20 and by the 60th day of the experimental study it was $9.61 \pm 0.20 \times 10^9/L$. The hemoglobin concentration changed insignificantly, in comparison with the control – 135.00 ± 4.82 g/L and reached 121.12 ± 2.34 g/L, by the end of the experiment increased it significantly up to 166.12 ± 2.34 g/L. The hematocrit also statistically significantly increased from 46.18 ± 1.73 % to 54.15 ± 2.32 , which indicates the thickening of the peripheral blood of experimental animals.

The erythrocyte coefficients did not change significantly throughout the whole experiment, including the average red blood cell volume, the average hemoglobin content in a single red blood cell, the average hemoglobin concentration in the red blood cell mass, the calculated width of the red blood cell distribution by volume. Despite the fact that in some cases there were statistically significant differences, the values remained within the physiological norm.

The total number of platelets significantly reduced, so in the control this indicator was $911.60 \pm 31.27 \times 10^9/L$, after 69 days of the experiment $927.80 \pm 39.82 \times 10^9/L$, and by the 30th and 60th day of the experiment it was 637.80 ± 39.82 and $741.80 \pm 39.82 \times 10^9/L$, respectively. It should be noted that the dynamics of the study showed a statistically significant ($P \leq 0.001$) decrease in the level of neutrophils from $17.50 \pm 4.98\%$ to $2.36 \pm 0.26\%$, in turn, the level of lymphocytes was statistically 0.34 ± 0.19 % to $65.94 \pm 0.50\%$ by the end of the experiment, which may indicate activation of the cellular component of the immune system, and some immunomodulating properties, and requires further detailed study of the mechanisms of the drug's action. Along with the change in the level of lymphocytes, throughout the experiment, wavy dynamics of monocytes was observed. In the control group, the level of monocytes

was $27.00 \pm 2.37\%$ and up to 30 days statistically significantly increased to $44.88 \pm 0.35\%$, but by 60 days it decreased to $14.18 \pm 0.35\%$. According to the level

of basophils and eosinophils, it is possible to judge the absence of allergenic properties of the drug "Virospan" 4.3 mg/kg.

Table 1 – Haematological parameters of rats on the background of the dosage of "Virospan" 4.3 mg/kg

Indicators	Control	6 days	30 days	60 days
WBC	2.49±0.24	10.54±0.23*	5.45±0.23*	13.04±0.23*
RBC	7.95±0.45	7.38±0.20	8.57±0.20	9.61±0.20*
HGB	135.00±4.82	121.12±2.34*	156.12±2.34*	166.12±2.34*
HCT	46.18±1.73	40.05±2.32*	47.75±2.32	54.15±2.32*
MCV	55.46±1.34	53.96±0.19*	55.56±0.19	56.16±0.19
MCH	16.18±0.27	16.09±0.18	17.99±0.18*	17.09±0.18*
MCHC	29.24±0.29	30.61±0.93	33.11±0.93*	31.11±0.93*
RDW	13.78±0.51	16.39±0.18*	10.69±0.18*	11.39±0.18*
PLT	911.60±31.27	927.80±39.82	637.80±39.82*	741.80±39.82*
MPV	6.98±0.08	6.59±0.18*	7.49±0.18*	6.99±0.18
NEUTRO %	17.50±4.98	5.16±0.26*	3.46±0.26*	2.36±0.26*
NEUTRO abs	0.42±0.17	0.62±0.18*	0.28±0.17	0.38±0.18
LYMPHO %	0.34±0.19	55.04±0.50*	26.34±0.50*	65.94±0.50*
LYMPHO abs	0.14±0.08	5.87±0.18*	1.53±0.18*	8.66±0.18*
MONO%	27.00±2.37	20.18±0.35*	44.88±0.35*	14.18±0.35*
MONO abs	4.36±1.22	2.29±0.35*	2.61±0.35*	1.46±0.35*
BASO %	0.20±0.09	0.49±0.18	0.29±0.18	0.23±0.12
BASO abs	0.10±0.06	0.19±0.11	0.17±0.11	0.17±0.11
EOS %	0.94±0.95	0.39±0.18	2.19±0.18*	1.59±0.18
EOS abs	0.08±0.05	0.19±0.11	0.26±0.12*	0.32±0.13*

Note: * statistically significant with respect to the control ($P \leq 0.001$)

An analysis of Figure 1 suggests that the tendency to an increase in the level of leukocytes by 4-6 times when taking "Virospan" 13 mg/kg is preserved. So by 6 days in this concentration, the total number of leukocytes increased to 8.17 ± 0.23 , by 30 days to 10.96 ± 0.23 and on the 60th day of the experimental study it was 12.53 ± 0.23 , in all cases the changes were statistically significant ($P \leq 0.001$).

In terms of red blood, there was a thickening, a relative increase in the level of red blood cells up to 10.46 ± 0.20 , hemoglobin – to 172.12 ± 2.34 g/L and hematocrit to $56.95 \pm 2.32\%$, the cause of this phenomenon it is necessary to evaluate together with the assessment of the behavioral activity of experimental animals, for the objectification of conclusions.

As for erythrocyte coefficients, the average red blood cell volume, the average hemoglobin content

in a single red blood cell, the average hemoglobin concentration in the red blood cell mass, the calculated width of the red blood cell distribution by volume changed insignificantly, and most likely due to blood clotting phenomena.

The total number of platelets statistically reliably changed in the direction of decrease and increase, despite significant differences remained within the physiological norm. In addition, when taking "Virospan" 13 mg/kg, the trend towards a statistically significant decrease in segmented neutrophils from $7.50 \pm 4.98\%$ to 5.96 ± 0.26 to 60 days of the experiment, at the same time, the percentage of lymphocytes was statistically maintained. significantly increased and amounted to 6 days $68.64 \pm 0.50\%$ to 60 $13.64 \pm 0.50\%$.

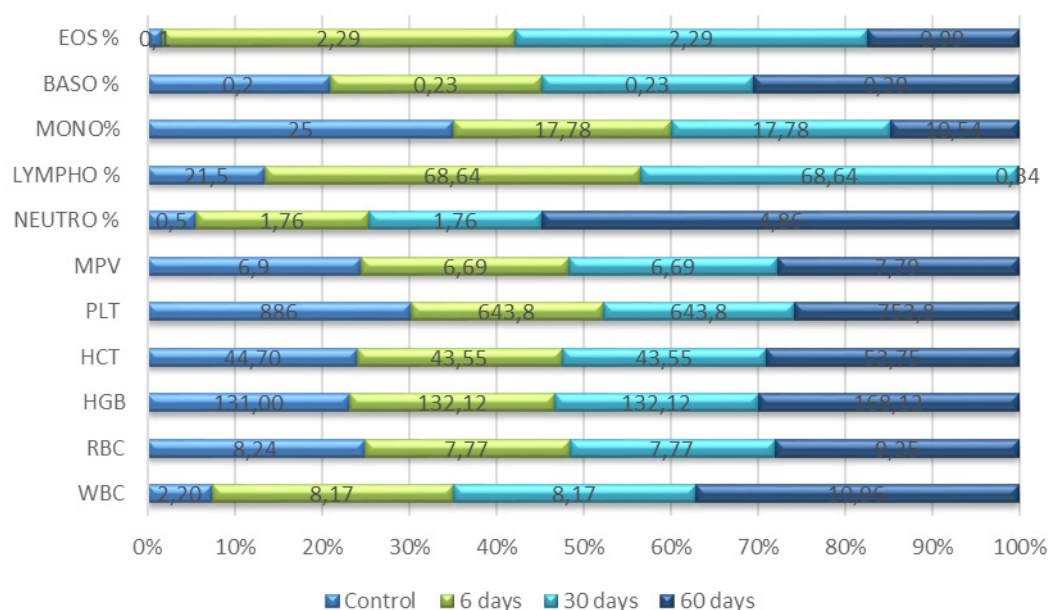


Figure 1 – Hematological parameters of rats in the background dosage of "Virospan" 13 mg/kg

Analyzing the level of monocytes in the peripheral blood of experimental animals, it should be noted that there was both a decrease and an increase in this indicator by the end of the experimental study to $77.68 \pm 0.35\%$. As in the case with the dosage of "Virospan" 4.5 mg/kg, "Virospan" at a dose of 13 mg/kg does not stimulate the release of histamine-producing cells into the blood and is therefore not allergenic.

The analysis of the data from the Table 2 demonstrates that the total number of leukocytes statisti-

cally significantly increases to 3.08 ± 0.23 to 6 days, to 10.04 ± 0.23 to 30 days and statistically significantly decreases to 60 days to 2.07 ± 0.23 , which has the opposite effect compared with a concentration of "Virospan" 4.5 and 13 mg/kg.

So, red blood indices increased, including the level of erythrocytes in dynamics reached $9.69 \pm 0.20 \times 10^{12}/L$, and the hemoglobin concentration 165.12 ± 2.34 g/l, however, the hematocrit remained within the normal range and statistically did not change and amounted to $49.95 \pm 2.32\%$.

Table 2 – Hematological parameters of rats on the background of the dosage of "Virospan" 39mg/kg

Indicators	Control	6 days	30 days	60 days
WBC	2.49 ± 0.24	$3.08 \pm 0.23^*$	$10.04 \pm 0.23^*$	2.07 ± 0.3
RBC	7.95 ± 0.45	8.13 ± 0.20	$9.34 \pm 0.20^*$	$9.69 \pm 0.20^*$
HGB	135.00 ± 4.82	141.2 ± 2.34	$161.12 \pm 2.34^*$	$165.12 \pm 2.34^*$
HCT	46.18 ± 1.73	46.35 ± 2.32	50.35 ± 2.32	49.95 ± 2.32
MCV	55.46 ± 1.34	56.76 ± 0.19	$53.66 \pm 0.19^*$	$51.26 \pm 0.19^*$
MCH	16.18 ± 0.27	$17.09 \pm 0.18^*$	$17.09 \pm 0.18^*$	$16.89 \pm 0.18^*$
MCHC	29.24 ± 0.29	$30.81 \pm 0.93^*$	$32.51 \pm 0.93^*$	$33.51 \pm 0.93^*$
RDW	13.78 ± 0.51	$12.79 \pm 0.18^*$	$12.09 \pm 0.18^*$	$11.39 \pm 0.18^*$
PLT	911.60 ± 31.27	$1125.80 \pm 39.82^*$	891.80 ± 39.82	$639.80 \pm 39.82^*$
MPV	6.98 ± 0.08	6.79 ± 0.18	$7.49 \pm 0.18^*$	$6.09 \pm 0.18^*$
NEUTRO %	17.50 ± 4.98	$10.86 \pm 0.26^*$	$4.26 \pm 0.26^*$	$17.56 \pm 0.26^*$
NEUTRO abs	0.42 ± 0.17	0.42 ± 0.18	0.50 ± 0.18	0.45 ± 0.18

Continuation of table 2

Indicators	Control	6 days	30 days	60 days
LYMPHO %	0.34±0.19	0.44±0.41*	4.74±0.50*	0.44±0.41*
LYMPHO abs	0.14±0.08	0.19±0.10	0.55±0.18	0.19±0.10
MONO%	27.00±2.37	10.48±0.29*	66.28±0.35*	25.70±1.08
MONO abs	4.36±1.22	3.44±0.35	6.82±0.35*	5.69±0.35
BASO %	0.20±0.09	0.39±0.18	0.59±0.18*	0.29±0.18
BASO abs	0.10±0.06	0.17±0.11	0.20±0.11	0.17±0.11
EOS %	0.94±0.95	1.29±0.18	2.89±0.18*	4.99±0.18*
EOS abs	0.08±0.05	0.20±0.11	0.39±0.15*	0.24±0.11

Note: * statistically significant with respect to the control (P≤0.001)

The average volume of the erythrocyte, the average hemoglobin content in a single erythrocyte, the average concentration of hemoglobin in the erythrocyte mass, the calculated width of the distribution of erythrocytes by volume did not change significantly. Red blood indicators in this case indicate a better tolerance of the drug concentration at 39 mg/kg, as well as probably the inclusion of compensatory mechanisms and the absence of dehydration of the organism of experimental animals. The total number of platelets reaches its peak by 6 days – 1125.80±39.82 and by the end of the experiment it decreases 2-fold to 639.80±39.82. In terms of white blood, it should be noted that the percentage of neutrophils in the dynamics is statistically significantly reduced by 30 days to 4.26±0.26, but by 60 days it increases again to control values – 17.56±0.26. The level of lymphocytes varies slightly and the highest value is by 30 days – 4.74±0.50%, decreasing by 60 days to 0.44±0.41%. Analyzing the level of monocytes, it should be noted that the highest value – 66.28±0.35% was also noted on the 30th day of the experimental study. As in the case with the dosage of “Virospan” 4.5 mg/kg, 13 mg/kg at a dose of 39 mg/kg, a significant increase in the level of eosinophils and basophils was not observed.

Conclusion

Thus, according to a detailed analysis of peripheral blood against the background of the dosage of the drug Virospan, it was found that under experimental conditions, at 4.5 and 13mg/kg, “Virospan” causes a statistically significant increase in the level of white blood cells, red blood cells, hemoglobin and hematocrit. Against the background of a statistically

significant decrease in the level of polymorphonuclear neutrophils, an increase in the level of lymphocytes was observed. “Virospan” at a concentration of 39 mg/kg demonstrates a statistically significant decrease to 60 days of the total number of leukocytes, the absence of pronounced changes in the indicators of red blood and the absence of changes in the level of eosinophils and basophils. In general, to exclude the general toxic effect of the studied drug, a comprehensive assessment of their properties in vivo, namely, biochemical, anatomical and morphological parameters is necessary.

References

1. Baydaulet I.O. (2013) Faktory riska dlya zdorovia naseleniya v napryazhennykh ekologicheskikh usloviyakh zagryazneniya [Risk factors for public health in tense environmental pollution conditions]. *Gigiyena i sanitariya*, vol. 6, pp. 64-69.
2. Geha R., Notarangelo L. (2015) Primary immunodeficiency diseases: an update from the International Union of Immunological Societies Primary Immunodeficiency Diseases Classification Committee. *J Allergy Clin Immunol.*, vol. 120, pp. 776-794.
3. White B.T. (2012) Effects of temperature stress on grow the performance and bacon quality in grow-finish pigs house dattwo densities. *J Anim Sci.*, vol.86, pp.1789-1798.
4. Petrov R.V., Khaitov R.M., Pinegin V.P. (1997) Immunodiagnostika immunodefitsitov [Immunodiagnosis of immunodeficiencies]. *Immunologiy*, vol.4, pp. 4-7.
5. Kono H., Rock K. (2008) How dying cells alert the immune system to danger. *Annu Rev Immun.*, vol. 8, pp. 279-289.

6. Leskov V.P. (1999) Immunostimulyatory [Immunostimulants]. *Allergiya, astma i klinicheskaya immunologiya*, vol.4, pp. 12-25.
7. Khaitov R.M., Pinegin B.V. (2003) Immunomodulyatory: mekhanizm deystviya i klinicheskoye primeneniye [Immunomodulators: mechanism of action and clinical use]. *Immunologiya*, vol. 2, pp. 196-203.
8. Zemskov V.M., Ivanov A.M. (1996) Printsipy differentsirovannoy immunokorreksii [Principles of differentiated immunocorrection]. *Immunologiya*, vol. 3, pp. 4-6.
9. Rock K. (2014) The inflammatory response to cell death. *Annu. Rev. Pathol.*, vol. 3, pp. 99-116.
10. Mutwiri G. Gerdt V., Lopez M. (2007) Innate immunity and new adjuvants. *Rev Scient Techn.*, vol. 26, pp. 147-156.
11. Fraser C. K., Diener K. R., Brown M. P. (2007) Improving vaccines by incorporating immunological adjuvants. *Expert Rev. Vaccines.*, vol. 6, pp. 559-578.
12. Ulmer J. B. (2006) Vaccine manufacturing: challenges and solutions. *Nat Biotechnol.*, vol. 24, pp. 1377-1383.
13. Petrov R.V. Khaitov R.M. (2009) Korrektsiya immunodefitsitnykh sostoyaniy s pomoshchyu immunomodulyatora polioksidoniy [Correction of immunodeficiency states with polyoxidonium immunomodulator]. *Allergiya, astma i klinicheskaya immunologiya*, vol.9, pp. 3-7.
14. Tompkins W.A. (2009) Immunomodulation and therapeutic effects of the oral use of interferon – alpha: mechanism of action. *J Interferon Cytokine Res.*, vol. 19, pp. 817-828.
15. Werner G.H. (1996) Immunostimulating agents: what next? A review of their present and potential medical applications. *Eur J Biochem.*, vol. 242, pp. 1-19.

IRSTI 31.21.25: 61.51.17

¹Y.A. Aubakirov, ¹L.R. Sassykova, ¹Zh.Kh. Tashmukhambetova,
¹S.Y. Karymbayev, ²S. Sendilvelan, ¹M. Zharkyn, ¹A.K. Zhussupova,
¹A.A. Batyrbayeva, ¹Sh.A. Kayrdynov

¹Faculty of Chemistry and Chemical technology, Al-Farabi Kazakh National University, 050040, Almaty, Kazakhstan.

²Department of Mechanical Engineering, Dr.M.G.R. Educational and Research Institute,
 University, Chennai-600095, Tamilnadu, India.

*e-mail: larissa.rav@mail.ru

Catalytic reduction of aromatic nitro compounds: general questions, equipment, enlarged laboratory tests

Abstract: The article is devoted to issues of amines production from nitro compounds. The processes of catalytic reduction of aromatic nitrocompounds by hydrogen to amines have practically superseded all other methods for the production of aromatic amines in large-tonnage plants. Aromatic mono-, di- and polyamines, due to their high reactivity, are widely used in the production of various compounds (photochemicals, fuel stabilizers and additives lubricating oils, in the paint and varnish industry, for painting natural and synthetic fibers). Authors compare methods of nitro compounds reduction and show different variants of apparatus design. The article also describes the results of enlarged laboratory examinations of the deposited catalysts synthesized by authors in reactions of p-phenylenediamine, p-amino-diethylaniline, o- and p-aminophenols production. By using relatively small amounts of catalysts (0.48-0.6 g of catalyst by hydrogenating 50 g of an aromatic nitro compound) were obtained high amine yields of 90-98.7%.

Key words: catalytic reduction, nitro compounds, amines, p-phenylenediamine, p-amino-diethylaniline, aminophenol.

Introduction

Aromatic nitro compounds are used mainly in the composition of explosives or as solvents. In general, these compounds are applied to reduce the aniline derivatives used in the production of paints, pigments, insecticides, textiles, plastics, resins, elastomers (polyurethane), pharmaceuticals, plant growth regulators, fuel additives and vulcanization accelerators for rubber and antioxidants [1]. The most important property of the nitro group is its ability to be reduced to an amino group. By this method aromatic amines are produced.

Aromatic mono-, di- and polyamines, due to their high reactivity, are widely used in the production of various compounds: synthetic dyes of various shades (for photography, in the paint and varnish industry, for painting natural and synthetic fibers), photochemicals, fuel stabilizers and additives lubricating oils, chemical plant protection products, synthetic fibers, sorbents, medicines, etc. [2-8]. Taking into account the extremely high volumes of commercial production of aniline and toluene diamines, the total

production of which in the world is more than 3-4 million tons/year, the problem of improving the technology of obtaining these compounds can be considered actual [9-13].

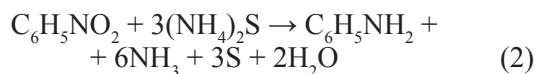
Aromatic nitro compounds reduction

The catalytic reduction of organic compounds, including aromatic mono- and polynitro compounds, to the corresponding amines is carried out in many variants, differing in the composition of the reaction masses, the aggregate state of the phases, the nature and type of the hydrogenation catalyst, the apparatus design of the process, the conditions of its conduct, etc. [14].

The reaction of aromatic nitro compounds reduction to amines by the action of ammonium sulphide on heating was discovered by N.N. Zinin in 1842 ("Zinin reaction") [15]. Zinin's reaction is a method of obtaining aromatic amines by reduction of nitro compounds (1):



Zinin acting on nitrobenzene with ammonium sulfide, obtained aniline (2):



Hydrogenation of aromatic nitro compounds can be implemented in the liquid or gas phase on the solid catalysts [16-18].

By the first option higher-boiling substances (dinitro-compounds, fats) are hydrogenated because their transfer to a gas form requires a large amount of hydrogen [19].

The second option is applied for the reduction of substances, the volatility of which at a reaction temperature is sufficient to create the necessary partial pressure of substances in the vapor mixture. By the second variant, for example, benzene, nitrobenzene, phenol can be hydrogenated [20, 22]. In all the variants heterogeneous catalysts are used. The most widespread catalysts are catalysts on the base of Group VIII metals and mixed catalysts.

In the case of a process in the vapor phase, copper is most often used on carriers, because the hydrogenation of the aromatic ring does not occur when using this catalyst.

In the papers [23-25] a catalytic method for the synthesis of aniline by hydrogenation of nitrobenzene in the vapor phase has been developed. Peculiarity of this method was mixing of aluminum hydroxide with a vanadium compound in the presence of water and nitric acid, then procedures of extruding, drying, calcination and then impregnation of the prepared mass with a solution of nickel and copper salts. In the work [26] a vapor-phase hydrogenation reaction of benzene on a Ni/Al₂O₃ catalyst with a small Ni content (up to 5 wt%) was carried out. In the works [27, 28] advantages and disadvantages of the vapor phase catalytic hydrogenation in industry are considered. Authors claimed that it is expedient to use modified heteropolycompounds for further improvement. They wrote that the film palladium catalysts may be the best for the selective reduction of acetylenic compounds to olefins. The authors have presented data on the selective hydrogenation of aromatics over these catalysts. In [29] authors offered to obtain aniline in the presence of a catalyst: Pd or Pt, supported on lipophilic carbon. The promoter is alkali metal hydroxide, carbonate or bicarbonate, Zn(OAc)₂, Zn(NO₃)₂, at a temperature of 150-250°C. A method is also known for the production of aniline by hydrogenating nitrobenzene in the gas phase in the presence of a nickel-copper-vanadium catalyst [30].

In [31] the process for the preparation of a catalyst for the producing aromatic amines R-R₁C₆H₃NH₂ (wherein R can be additionally NH₂) is patented. By this method the desired product is obtained by hydrogenating the corresponding nitroaromatic hydrocarbons with hydrogen in the gas phase in the presence of a catalyst Pd (0.001-7% by wt of the catalyst) and Pb (0.1-50%) on graphite or graphite-containing coke as a substrate, which has a surface of 0.2-10 m²/g. Hydrogen is introduced in excess: 30-600 equivalents per equivalent of NO₂-group.

The disadvantages of hydrogenation processes in the gas phase are:

- a high hydrogenation temperature (it contributes to the formation of a significant amount of by-products, a deterioration in the quality of the resulting catalyst and a decrease in the yield of the target products);
- a high pressure;
- the complexity of the process design of the reactions proceeding at high temperatures (which leads to a process cost increase, reactor designs and process diagrams);
- a relatively low catalyst load;
- the use of a large excess of hydrogen;
- a short inter-regenerative period of operation of the catalyst;
- a partial destruction of the catalyst;
- a partial loss of catalytic activity (and as a result of which the yield of aromatic amine products decreases);
- at high temperature of hydrogenation (up to 300-350°C) some nitro compounds can be decomposed, mono- and dinitro compounds in the mixture during evaporation can be converted into explosives;
- at high temperatures can be the aromatic ring hydrogenation;
- can be reactions of gumming and a deamination, which to a large extent deactivate the catalyst.

The liquid-phase catalytic reduction of nitro compounds

The application of liquid-phase catalytic reduction of nitro compounds makes it possible to perform the reaction at sufficiently low temperatures, which leads to a significant reduction in energy costs and the explosion of the system.

In general, the reduction reactions of organic compounds can be divided into two groups:

1. The reduction by molecular hydrogen in the presence of hydrogenation catalysts;

2. The reduction with other inorganic and organic reagents is “a chemical” reduction.

Nitro compounds reduction by molecular hydrogen

The most important way of amines producing from nitro compounds is catalytic reduction by hydrogen on catalysts. For the first time thanks to this method Zaitsev carried out such a reaction, passing over the platinum black nitrobenzene and hydrogen vapor. Later Sabatier implemented the such reaction over nickel and a number of other metals [32, 33]. A major contribution to the study of the catalytic reduction of nitro compounds was made by scientists from the USSR, the CIS, Russia and Kazakhstan [3, 4, 8-10, 12, 13, 22-25, 27, 28, 30, 32-42].

The reduction of nitro compounds can be carried out in the presence of both heterogeneous and homogeneous catalysts, but in the industry to date use only solid-phase heterogeneous catalysts [40, 43-46]. This is mainly due to the difficulty in isolating and regenerating the homogeneous catalyst for subsequent use.

Laboratory equipment for the hydrogenation of aromatic nitro compounds

A widespread installation for hydrogenation of aromatic nitro compounds is installation on a basis

of “catalytic duck” (fig.1). Fig. 1, 2 show the installations with “a catalytic duck” for hydrogenation at atmosphere and elevated pressure.

Today hydrogenation at elevated and high pressures is widely used. The process is carried out in special apparatuses – high-pressure autoclaves, circulating apparatuses and other reactors.

Autoclaves are devices in which reactions under pressure are carried out. They come in two classes – low-pressure autoclaves designed for pressures up to 10 atm, and high pressure autoclaves up to 1000 at. The latter are more often used in chemical laboratories. Autoclaves are thick-walled metal vessels, often cylindrical or spherical. The autoclave is closed with a lid, the sealing is achieved by a shutter with the help of a cone seal or sealing rings made of non-ferrous metals (copper, aluminum, etc.) or plastics (rubber, asbestos, etc.).

High-pressure autoclaves were first widely applied by Ipatiev, whose work in this area dates back to 1903 (fig. 3). The Ipatyev autoclave (or bomb) is a forged cylinder with a flange head that joins the autoclave body with the help of the Ipatyev shutter. Mixing of the contents is achieved by tilting the autoclave and its slow rotation. Such an autoclave is very convenient to handle. It is easy to wash. An example of using such a device may be the process of hydrogenation of benzene to cyclohexane [49].

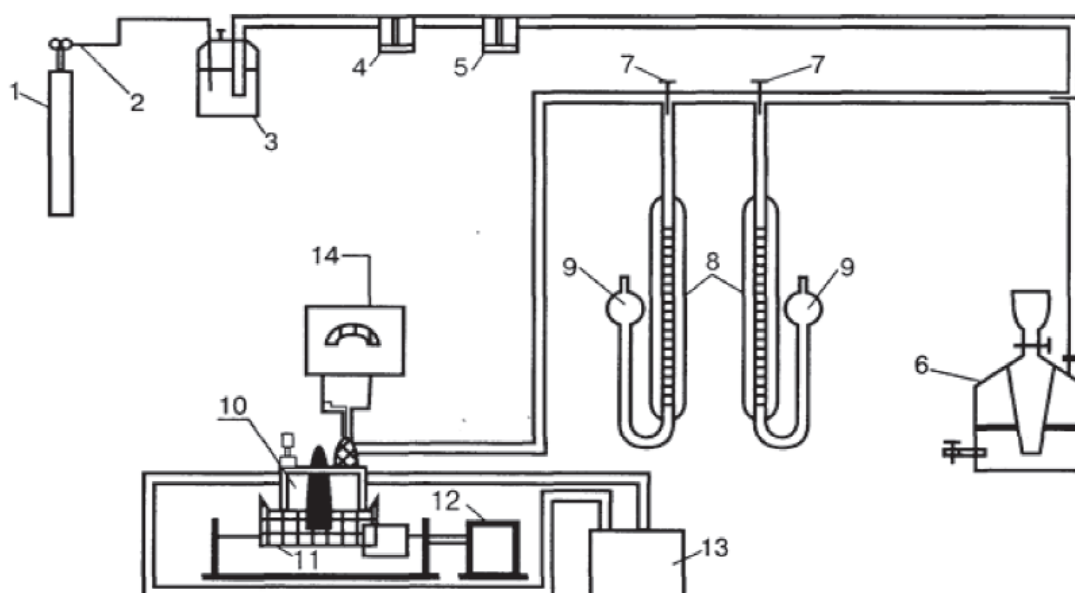


Figure 1 – Scheme of the unit for the catalytic hydrogenation of aromatic nitro compounds:

1 – hydrogen generator; 2, 7 – the crane; 3, 4, 5 – cleaning bottles; 6 – gas meter; 8 – measuring burettes; 9 – pear; 10 – catalytic “duck”; 11 – rocking chair; 12 – electric motor; 13 – thermostat; 14 – potentiometer

In general, the autoclave is a steel cylinder with a spherical bottom and a bolted spherical cover. The lid is provided with a valve for supplying hydrogen and descending the pressure (in separate designs, a valve for sampling from the gas and liq-

uid phases), a thermowell sleeve and a manometer. Desirably, the autoclave was made of acid resistant steel.

There are known different types of autoclaves: rotating, swinging, horizontal, vertical and column.

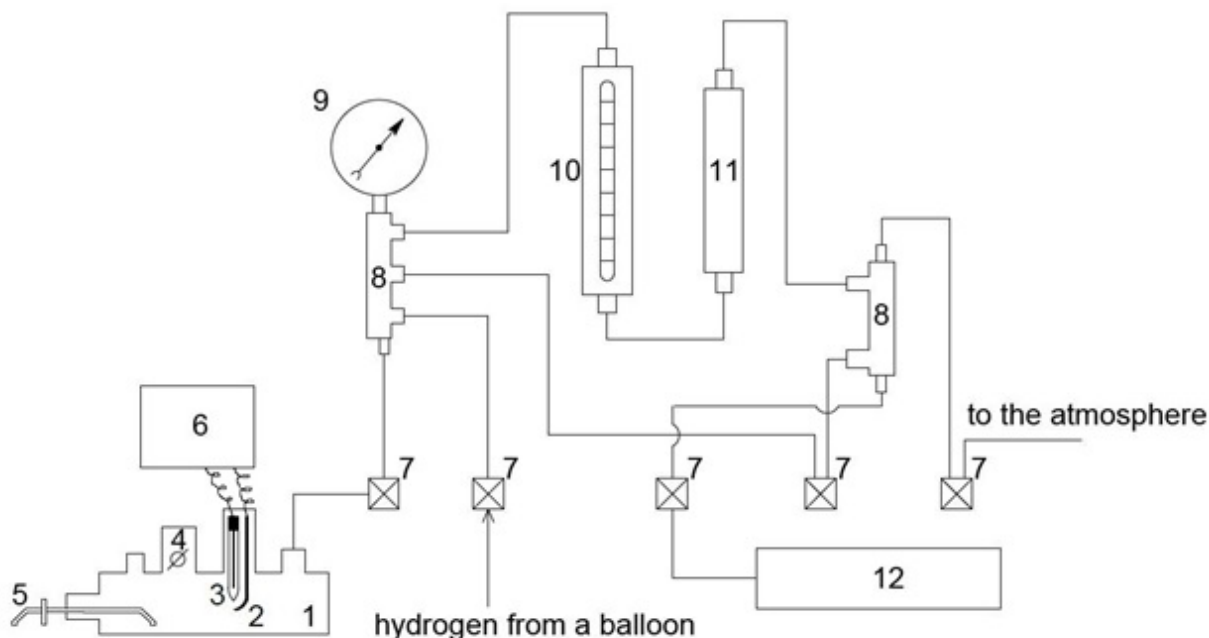


Figure 2 – An installation for liquid-phase hydrogenation at elevated pressure on the basis of catalytic “duck”: 1 – high-pressure device “duck”, 2 – platinum electrode, 3 – chlorine silver reference electrode, 4 – feed opening, 5 – sampler, 6 – potentiometer, 7 – fine adjustment valves, 8 – combs, 9 – gauge manometer, 10 – measuring burette, 11 – equalizing capacity, 12 – buffer capacity [47, 48]

In an autoclave with a magnetic stirrer of the N.E. Vishnevsky’ system (fig. 4) an electric motor rotating the stirrer is placed in a high-pressure zone. The magnetic flux of the stator located on the outside rotates the rotor placed inside the autoclave housing made of non-magnetic chromium-nickel steel. The rotor is fitted tightly onto the agitator shaft and rotates it through the bearings at high speed. Such an autoclave with a propeller stirrer is operated at a pressure of up to 300 atm and temperatures up to 300°C with a stirring speed of up to 3,000 per minute. In the autoclave, the sample can be sampled during the reaction, for which there is a special fitting connected to the siphon tube. The autoclave is heated by an electric furnace. To regulate the temperature of the autoclave, there is a water jacket and a pocket for the thermocouple. Through a special fitting, the reagents are loaded, and there is a discharge opening at the bottom. This design allows the autoclave to be fixed permanently and to perform its loading and unloading without disassembly. The autoclave is closed with a

lid and sealed with special pins with nuts.

Flow systems are also used for the hydrogenation of aromatic nitrocompounds. Continuous flow reactions have advantages over periodic reactions in terms of productivity, heating and mixing efficiency, as well as safety and reproducibility; in addition, automatic and multistage reactions are possible. The amount of waste can be minimized by using continuous flow conditions using solvents, free reagents, which leads to environmentally sustainable chemistry [50, 51].

Continuous flow reactions using heterogeneous catalysts (continuous flow catalytic reactions) can be ideal reaction systems, since the desired products that are easily separated from the catalysts are obtained continuously [52-54]. The authors of papers [55-57] develop various continuous flow systems with immobilized catalysts: hydrogenation of aromatic nitrocompounds using new palladium catalysts based on polysilane. The flow installation used by the authors of these works (fig. 5) is effective for the synthesis of

a number of nitrogen-containing compounds, which are key intermediates of many biologically active compounds and functional materials [58, 59]. The selective reduction of the nitro group proceeded quantitatively in the case of carbonyl compounds, such as esters and ketones. It is interesting to note that the ketone part was tolerant under the reaction conditions. Dinitro compounds can also be used in this flow-through reaction without inhibiting the product. The reduction of 2-nitroanisole was carried out quantitatively to obtain 2-aminoanisole under pure conditions without deactivating the catalyst. It is noted that the leaching of palladium was not observed in any of the reactions.

Enlarged laboratory tests

For enlarged laboratory examinations we used installation on the basis of “catalytic duck” (fig.1, 2) and a high-pressure kinetic unit (HPKU), consisting of an advanced Vishnevsky autoclave with intensive mixing and a measuring part (fig.6). This installation is one of the most widely used in the hydrogenation of various compounds. The main part of the HPKU is an autoclave (fig. 4). The efficiency of the catalysts was calculated by the amount of hydrogen absorbed per unit time (60 seconds). During the reaction, samples are taken – after reaching the absorption of 1, 2 and 3 moles of hydrogen – for analysis of the hydrogenation products. The autoclave device allows to take samples for analysis without disturbing the equilibrium conditions of the experiment.

After the end of the reaction (as indicated by the stopping of hydrogen absorption), stirring is turned off and the hydrogen pressure is released to the atmosphere, and the catalyst is filtered off from the catalyst and the final analysis is carried out. In some cases, the final product is isolated to determine the % yield of the amine from the theoretically calculated reaction amount. To do this, after separating the catalyst filter, the solvent is evaporated, then the remaining material is washed on the filter with distilled water and dried at 40-50°C.

Chromatographically pure, prepared by distillation in vacuum or by recrystallization nitrobenzene (NB), ortho, para-, ortho-nitrophenols (o-NP, p-NP, o-NP), ortho, meta-, para-nitroanilines (o-NA, m-NA, p-NA) and p-nitrodiethyl aniline (p-NDA) were hydrogenated. Physicochemical parameters of the starting compounds corresponded to the reference. Distilled water, C₁-C₅ alcohols of the grade “CP” were used as solvents.

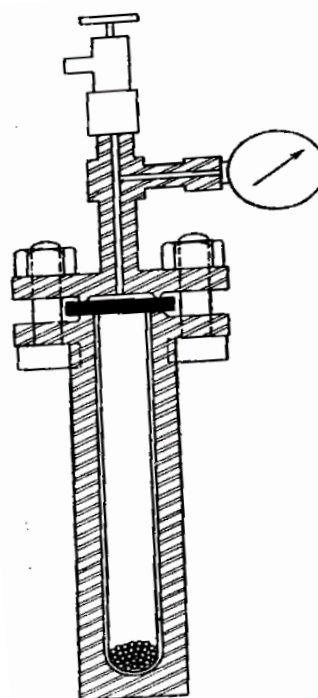


Figure 3 – Ipatiev' autoclave

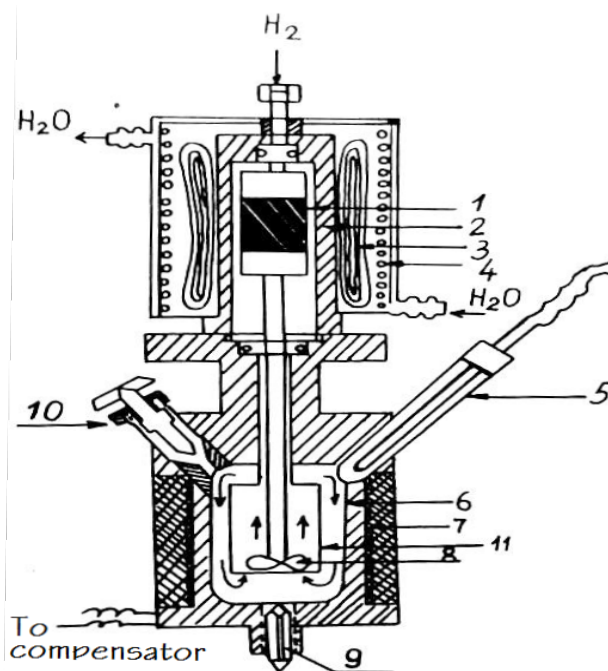


Figure 4 – The improved autoclave Vishnevsky with hermetic electric drive: 1 – rotor, 2 – a shielding sleeve, 3 – stator, 4 – cooling of the stator, 5 – thermocouple, 6 – reactor vessel, 7 – electrical heating, 8 – spiral mixer, 9 – lower cone valve, 10 – unit for enter the catalyst, the solvent and hydrogenated compounds, 11 – guiding glass

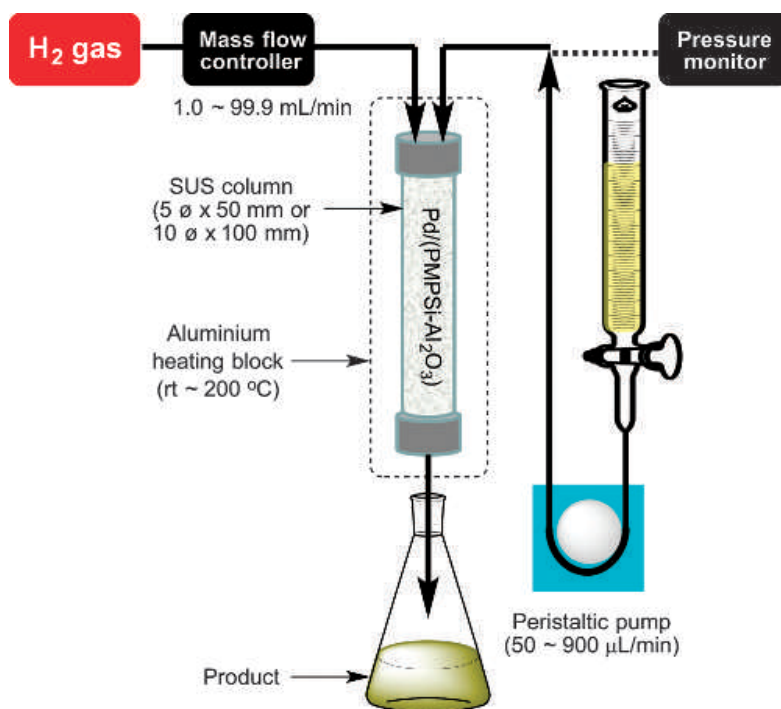


Figure 5 – Continuous-flow reactor

The reaction was carried out with electrolytic hydrogen from a balloon (99.8%), for gas-liquid chromatography (GLC), helium (99.992%) was used from a balloon.

For the calculations, the reaction rates for the first points and for the moment of absorption of

1MH_2 (or 2MH_2 , or 4MH_2 , depending of a reaction) are taken.

The selectivity of the process is calculated by the formula:

$$S_m = \frac{\text{The yield of the primary amine} \cdot 100\%}{\text{The yield of the primary amine} + \text{Yield of by-products}}$$

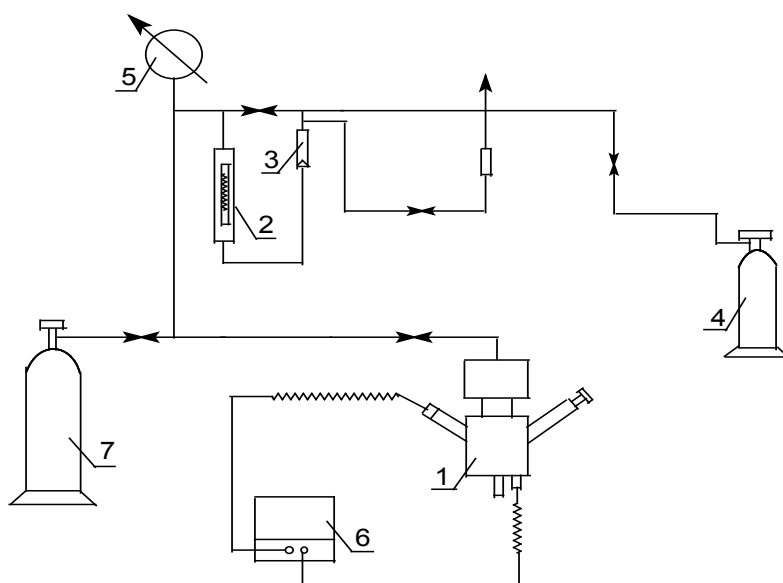


Figure 6 – High-Pressure Kinetic Unit: 1 – an autoclave of Vishnevsky; 2 – measuring burette; 3 – leveling capacity; 4 – buffer tank; 5 – gauge manometer; 6 – a device for determining and maintaining the temperature in the system; 7 – cylinder with hydrogen

For laboratory tests, catalysts deposited on $\gamma\text{-Al}_2\text{O}_3$, coal (C) of various grades, CaCO_3 (shell) catalysts based on Pt and Pd, were prepared by applying appropriate compounds to the carrier by impregnation. To prevent hydrolysis using PdCl_2 , a solution of NaCl was added to the solution. In the synthesis of Pd-Pt catalysts, 2% solution of Na_2CO_3 was used in some cases.

Qualitative and quantitative analysis of the initial compounds and reaction products was carried out by TLC, GLC, diazometric titration, voltammetric titration, and oscillographic polarography [60-64]. An IR spectroscopic analysis was used. Physicochemical methods of studying catalysts (BET, electron microscopy) were also applied in the work.

Results and Discussion

As a result of the hydrogenation of p-NDA in a catalytic “duck”, it was found that the change in the

mass of the sample of p-NDA does not affect the reaction rate, the initial reaction rate does not depend on the amount of hydrogenated material, i.e. the reaction order for the substance is zero. The activity of the Pd catalysts deposited on C is higher than for the samples of catalysts deposited on Al_2O_3 , which agrees with a decrease in the basicity of the carrier, which affects the degree of electron interaction of the metal-carrier. By reducing the activity, the prepared catalysts are arranged in a row: $\text{Pd} / \text{C} > \text{Pd} / \text{CaCO}_3 > \text{Pd} / \gamma\text{-Al}_2\text{O}_3$.

The high catalytic activity of Pd-based catalysts compared to the Ni catalyst allowed the reaction to be carried out under milder conditions. Enlarged tests of p-NDA in an autoclave were carried out on 2% Pd/C in methanol at hydrogen pressures of 0.5-3.0 MPa (tab.1).

For hydrogenation of NB, p-NP, o-NP, m-NA, p-NA an autoclave with a total volume of 400 ml was used. For the charge, 50 g of the substance and 200 ml of solvent were taken (tab.2).

Table 1 – Enlarged tests of p-NDA hydrogenation (31.5 g) in methanol p-ADA – para-amino-diethylaniline

T, K	P_{H_2} , MPa	Amount of acatalyst, q_{cat} , g	Yield of amine, p-ADA, %*	Duration of reaction, min.
2%Pd/C				
358	2.5	0.2	86.0	18.0
358	2.5	0.15	84.0	12.0
360	2.8	0.15	90.0	14.0
360	3.0	0.2	91.0	14.5
363	3.0	0.15	91.2	14.0
368	2.8	0.2	92.0	14.0
368	2.8	0.15	92.1	13.5
industrial Ni-Raney				
358-372	2.5-3.0	1.0-1.2	83.5-84.1	35.0- 45.0

*- result of 5 parallel experiments

Table 2 – Enlarged laboratory tests of NP and NA AP- Aminophenol, PhDA – Phenylenediamine

#	The starting compound, the resulting product (catalyst)	Yield, g*(%)	Amount of acatalyst, g	The temperature of the experiment, °C	Pressure of hydrogen, MPa	Duration of the test, min.
1	p-NP, p-AP (Pd/g)	114.0 (97,5%)	0,6	50-70	1.0-4.0	12-40
2	p-NP, p-AP (Pd-Pt/C)	105.1 (90%)	0.48	30-60	2.0-3.0	10-34

Continuation of table 2

#	The starting compound, the resulting product (catalyst)	Yield, g*(%)	Amount of acatalyst, g	The temperature of the experiment, °C	Pressure of hydrogen, MPa	Duration of the test, min.
3	p-NP, p-AP (Pd/g)	116.9 (98.5%)	0.55	50-70	1.0-4.0	14-38
4	o-NP, o-AP (Pd/g)	112.0 (96%)	0.6	50-70	1.0-4.0	30-44
5	o-NP, o-AP (Pd-Cu/g)	116.0 (98%)	0.6	50-70	4.0-5.0	35-52
6	p-NA, p- PhDA (Pd/g)	110.8 (95.2)	0.5	30-60	2.0-3.0	10-29
7	p-NA, p- PhDA (Pd-Pt/g)	115.0 (98.7%)	0.5	50-70	1.0-4.0	12-22

*- Yield (g) – the sum of 3 parallel experiments

Conclusion

The article summarized general issues of aromatic amine production from the corresponding nitro compounds. The authors described also own laboratory researches. The results of enlarged tests show that using relatively small amounts of catalysts (0.48-0.6 g of catalyst by hydrogenating 50 g of an aromatic nitro compound) it is possible to obtain high amine yields of 90-98.7%. The process time on bimetallic catalysts at hydrogenation of substances under identical conditions was lower than in the case of using only a monometallic Pd-containing catalyst. When comparing hydrogenation of the big batches of compounds the authors found that the reduction process p-NA is faster than for p-NP and, especially, for o-NP. It was also noted that 5-7% o-aminocyclohexanol appeared in the product samples. For this reason, the yield of the target product – p-AP was lower than expected (90%).

References

1. <http://chem21.info/info/667763/>
2. Charushin V.N. *Sorovsky educational journal*. 2000. – Volume 6, No. 3. – Pages 64-72.
3. Sassykova L.R., Masenova A.T., Bizhanov F.B. *Inst. org. Katal Elektrokim*, 1995, 3, 21-26.
4. Sassykova L.R. Catalytic reduction of aromatic mono- and dinitrocompounds. Diss...chem. sci. // Kazakhstan, Almaty, 1996, 223 p.
5. Rafiq K.A., Mohammad K.K., Shahnaz P.J. *Pharm. and Biomed. Anal.* 2002. Vol. 29, № 4. – P. 723-727.
6. Abdullaev M.G., Klyuev M.V. *Pharm. Chem. J* – 2005. Vol. 39, № 12. – P. 655-657.
7. Jurgen H. (ed) *Encyclopedia of Industrial Chemistry, Ullmann's, Wiley*, Florida, 1985.
8. Aubakirov Y.A. Development of methods for the catalytic synthesis of industrially important amino products. Author's abstract. diss... cand. chem. sciences, Kazakhstan, Almaty, 1996, 27 p.
9. Kozlov A.I., Zbarsky V.L. *Russ. Chem J.* – 2006. – V.L, No. 4. – Page 131.
10. Sokolsky D.V. Hydrogenation in solutions. Alma-Ata: Publishing House of the Academy of Sciences of Kaz. SSR. 1962. 457 p.
11. Ashmore P. *Catalysis and inhibition of chemical reactions*. Translation from English A.A. Slinkin, Moscow: The World, 1966. – P. 151-237.
12. Shmonina V.P. in: Catalytic reduction and hydrogenation in the liquid phase. – Ivanovo, 1970. – P. 8-17.
13. Sassykova L.R. Theory and technology of catalytic petrochemical productions. – Almaty, Qazaq University, 2018. – 296 P. ISBN 978-601-04-3249-9.
14. Berkman B.E. Industrial synthesis of aromatic nitro compounds and amines. – Moscow: Publishing house “Chemistry”, 1964.
15. Zinin N.N. Works on organic chemistry. – M.: Science, 1982. – 262 p.

16. Zhilin V.F., Zbarsky V.L., Kozlov A.I. Reduction of aromatic nitro compounds, – M.: RCTU. Published. center, 2004. – 92p.
17. Gates B., Quetzir J., Schuit G. Chemistry of catalytic processes. – Translated from English. – M.: Mir, 1981. – 552 p.
18. Gildebrand E.I., Fasman A.B. Skeletal catalysts in organic chemistry. – Alma-Ata: Science, 1982. – 136 p.
19. Masters K. Homogeneous catalysis by the transitional metals. – Translated from English – M.: Mir, 1983. – 552 p.
20. Gankin V.Yu., *New general theory of a catalysis*. – L.: Chemistry, 1991. – 80 p.
21. Tanabe K. Catalysts and catalytic processes. – M.: Mir, 1993. – 176 p.
22. Patent 2083540 Russian Federation, C 07 B 31/00. Method for hydrogenation of organic compounds. Datsevich L.B., Mukhortov D.A.– publ.1997. – 6 pp.
23. Pat. 2207335 Russian Federation, C 7 C 211/48, 211/46, 209/36. A process for the preparation of aromatic amines by reduction of the corresponding nitro compounds. Vinokurov V.A., Stycenko V.D., Patapenkov S.A., publ. 2003. – 6 pp.
24. Patent 2102138 Russian Federation, 6 B 01 J 23/847, 37/04. Method for the preparation of catalyst for the synthesis of aniline. Kladova N.V., Borisova T.V., Korobko L.N., publ. 1998, Bull. No. 2. – 14 p.
25. Patent 2093262 Russian Federation, 6 B 01 J 23/847, 37/02, 37/04. Method for the preparation of catalyst for the synthesis of aniline. publ.1997, Bull. No. 29. – 10 p.
26. Land Y., Fan Z., Li Y., Tang D., Li Y., Coug Y., Guofang Kejialaxuexuebao = Y. Nat. Univ. Def. Technol. – 1997. – 19(3), p.109 – 113.
27. Novalikhina M.D., Krylov O.V. Journal of Kinetics and Catalysis. – 2001. – 42 (1). – P. 86 – 98.
28. Novalikhina M.D., Krylov O.V. Uspekhi Khimii. – 1998. – 67 (7) – pp. 656 – 683.
29. Pat. 5283365 USA. *A method for obtaining aniline of high purity. Process for preparing high-purity aniline* / Nagata Teruyuki, Kobayashi Takashi, Watanabe Katsuji, KonoYoshitsugu, Tamaki Akihiro; Mitsui Toatsu; publ. 1944.
30. Author's Certificate 302333 USSR, C 07 C 85/10, C 07 87/52. Method for the production of aniline / Tsatsko IM; publ. 28.04.71. Bul. № 15. – 2 p.
31. Application 19521587 Germany, MKI6 S 07 C 211/45, B 01 J 23/62. Method and catalyst for the preparation of aromatic amines by hydrogenation in the gas phase. *Verfahren und Katalysator zur Herstellung von aromatischem Amin durch Gasphasenhydrierung* / Langer Reinhard, Buysch Hans – Josef, Pentling Ursula; publ. 19.12.96.
32. Fasman A.B., Sokolsky D.V. Structure and physico-chemical properties of skeleton catalysts. – Alma-Ata: Science of KazSSR, 1968. – P.115-140.
33. Nikolaev Yu.T., Yakubson A.M. Aniline, M.: Chemistry, 1984. 148 p.
34. Sokolsky D.V., Druz B.A. Introduction to the theory of heterogeneous catalysis. M.: High School. 1981. 216 p.
35. Sokolsky V.D. in: Hydrogenation catalysts. Alma-Ata: Science of KazSSR, 1975. pp. 7.
36. Sokolsky D.V. Hydrogenation in solutions. Alma-Ata: AN Kaz. SSR. 1962. 457 p.
37. Klyuev M.V. *Journal of Organic Chemistry*. 1987. Vol. 23. p. 581-585.
38. Tereshko L.V. Synthesis of aromatic and fatty aromatic amines on palladium-containing catalysts. Diss...chem. sciences. – Ivanovo, 1990, 163 p.
39. Kochetova L.B., Klyuev M.V., Petrochemistry. 1997. Vol.37. № 5. P.420-426.
40. Sokolsky D.V. in: *The mechanism of catalysis*, part 1. Novosibirsk. Science. 1984. p. 87-101.
41. Klyuev M.V., Vainstein E.F., *Proc. 6-th European Symp. on Organic reactivity*. Louvain-la-Neuve. 24-29 juli 1997. P. 143.
42. Klyuev M.V., *Russian polymer news*. 1998. V. 3. № 3. P. 27-29.
43. Pernoud L., Candy J.P., Didillon B., Jacquot R., Basset J.M. *Studies in Surface Science and Catalysis*. – 2000. – No 130. – P. 2057 – 2062.
44. Voronin M.V., Nasibulin A.A., Klyuev M.V. *Journal of Organic Chemistry*. 1997. Vol.33. №11. P. 1696-1698.
45. Johnstone R.A., Wilby A.H., Entwistle I.D. *Chemical Reviews*, **85(2)**, 1985, 129-170.
46. Masenova A.T., Sassykova L.R., Bizhanov F.B. “*Europacat-2*”, Netherlands, Maastricht, 1995.
47. Sassykova L.R., Otzhan U.N., Kurmansitova A.K., Serikkanov A.A., Aubakirov Y.A., Zhumakanova A.S., Kenzhebekov A.S. *News of ASRK, series of chemistry and technology*, 2017, 422 (2), 147-156.
48. Otzhan U.N., Kurmansitova A.K., Sassykova L.R., Serikkanov A.A., Kenzhebekov A.S., Starikov E.B. *Intern J of Biology and Chemistry*, 2016, 9(2), 40-44.
49. Wikipedia contributors. (2018, March 5). *Autoclave*. In Wikipedia, The Free Encyclopedia. Retrieved March 29, 2018, from <https://en.wikipedia.org/w/index.php?title=Autoclave&oldid=828918578>
50. Puglisi A., Benaglia M., Chirolì V. *Green Chemistry*, 2013, 15(7), 1790.

51. Rebrov E.V., Schouten J.C., Croon M. H.J.M. *Chemical Engineering Science*, 2011, 66 (7), 1374-1393.
52. Aijaz A., Xu Q., *Journal of Physical Chemistry Letters*, 2014, 5(8), 1400-1411.
53. Matsumoto T., Ueno M., Wang N., Kobayashi Sh., *Chemistry – An Asian Journal*, 2008, 3(2), 196-214.
54. Javaid R., Kawasaki Sh., Suzuki A., Suzuki T.M., *Beilstein Journal of Organic Chemistry*, 2013, 9, 1156-1163.
55. Masaharu Ueno, Yasuharu Morii, Kiyoko Uramoto, Hidekazu Oyamada, Yuichiro Mori, Shū Kobayashi, *Journal of Flow Chemistry*, 2014, 4(4), 160-163.
56. Naiwei Wang, Tsutomu Matsumoto, Masaharu Ueno, Hiroyuki Miyamura, Shū Kobayashi, *Angewandte Chemie International Edition*, 2009, 48(26), 4744-4746.
57. Juta Kobayashi, Yuichiro Mori, Shū Kobayashi, *Chemical Communications*, 2005, 20, 2567.
58. Tetsu Tsubogo, Yasuhiro Yamashita, Shū Kobayashi, *Topics in Catalysis*, 2014, 57(10-13), 935-939
59. Hidekazu Oyamada, Ryo Akiyama, Hiroyuki Hagio, Takeshi Naito, Sh. Kobayashi, *Chem. Comm.*, 2006, 41, 4297.
60. Sassykova L.R., Kasenova D.Sh., Masenova A.T., Bizhanov F.B., *Russ. J. Appl. Chem.*, 71, 1401-1403(1998).
61. Sassykova L.R., *Chemical and biochemical engineering quarterly*, 2017, 31(4), 447-453.
62. Heyrovsky M., *J. Electroanal. Chem.*, 1970, v. 28, №2, p. 409-420.
63. Sassykova L., Aubakirov Y., *Chiang Mai Journal of Science*, 45, 1, 2018, 474-483.
64. Stradyn J.P. **Polarography of organic nitro-compounds**, Riga, Acad Latv. SSR, 1961.

IRSTI 61.51.29

¹K. Bhaskar, ²S. Sendilvelan, ³L.R. Sassykova

¹Department of Automobile Engineering, Rajalakshmi Engineering College, Chennai 602105, India

²Department of Mechanical Engineering, Dr. M.G.R. Educational and Research Institute, Chennai 600095, India

³Institute of Combustion Problems, Almaty, Kazakhstan.

*e-mail: larissa.rav@mail.ru

Research of the performance and emission characteristics of Jatropa Oil Methyl Esters (JOME) and diesel blends in a partially premixed charge compression ignition engine

Abstract: In this article for reducing NO_x and particulate matter (PM) were used partially premixed charge compression ignition (PPCCI) combustion of diesel fuel with external mixture formation technique and Jatropa oil methyl ester (JOME) blend in the main injection. Diesel fuel was injected into the intake manifold for formation of homogeneous pre-mixture beforehand and the pre-mixture is burnt in the cylinder with the balance quantity of fuel directly injected into the cylinder by a conventional injection system. For obtaining homogeneous mixture, diesel fuel was injected in the intake manifold using a solenoid-operated injector controlled by electronic control unit (ECU). Exhaust gas recirculation (EGR) technique was adopted for controlling of the start of combustion (SOC). Experiments were carried out with 10%, 20%, and 30% EGR for premixed ratio (Rp) 25% and results are compared with conventional diesel fuel operation. It was found that diesel manifold injection and JOME blend in main injection results in better mixture preparation and lower emissions. It was shown that due to homogenous lean operation, significant reduction in NO_x and PM was achieved with the PPCCI combustion mode at Rp 25% and EGR 20% in the JOME-Diesel mode of operation.

Key words: exhaust gas recirculation, jatropa methyl ester, diesel premix, charge compression ignition

Introduction

Energy is the major factor for economic growth of any country. The need for the energy is increasing day by day with the growth of population and requirement of modern energy consuming equipment for comfort living. The invention of internal combustion engine and developments in engine technology resulted in exploitation of the petroleum-based reserves which is depleting at a rapid rate [1]. Combustion of these fuels in engines release substantial amount of pollutants such as carbon dioxide (CO_2), carbon monoxide (CO), unburned hydrocarbon (UBHC), nitrogen oxides (NO_x) and particulate matter (PM) [2]. Reducing the such emissions and increasing the fuel economy of IC engines are the primary concern for all developing nations. There has been a world-wide interest in the search of alternatives to petroleum derived fuels due to their depletion and concern for the environment. Bio-diesel derived from edible, non-edible oils and animal fats can be used in diesel engines with little or no modifications [3-5].

It is known that Jatropa oil methyl esters are well proven alternative fuels to petroleum diesel. Unfortunately cultivation of jatropa requires huge land area and good quality jatropa plant seed for generating sufficient oil. Even though biodiesel offers reduction in Smoke, UBHC and CO emission due to the molecular oxygen present in it, NO_x emissions are higher which can be reduced by using exhaust gas recirculation.

Homogeneous charge compression ignition (HCCI) is a promising alternative combustion technology for diesel engines with high efficiency and lower NO_x and particulate matter emissions. Relative to compression ignition direct ignition engines, HCCI engines have substantially lower these emissions [6-8]. The low emissions of PM and NO_x in HCCI engines are a result of the dilute homogeneous air and fuel mixture in addition to low combustion temperatures. The change in HCCI engine may be made dilute by being very lean, by stratification, by using exhaust gas recirculation (EGR), or combination of these methods [9, 10].

In case of using HCCI engines can be some challenges:

- high CO and UBHC emissions because of incomplete oxidation.
- the operating range of automotive engine using HCCI mode is found to be too narrow [11, 12].
- improper combustion or misfire under fuel-lean conditions limits the minimum power output at which the engine can operate.
- high heat release rates and high in-cylinder pressure may cause more wear and damage to the components.
- it is difficult to control an auto-ignition [13].

In HCCI combustion, control over the start of combustion (SOC) is the main problem [14, 15]. Conventional control techniques are not applicable, indirect methods like variable EGR technique, variable compression ratio (VCR), variable valve timing (VVT), increased intake charge temperature, equivalence ratio variation, injection timing, modulating two or more fuels, fuel additives [16-18] which alter the compression process are necessary. Since HCCI engine operates on lean mixtures, the peak temperatures always lower in comparison to spark ignition and diesel engines. Low peak temperatures prevent the formation of NO_x . However, they also lead to incomplete burning of fuel especially near the walls of the combustion chamber.

It was proposed to study the effect of partially premixed charge compression ignition (PPCCI) combustion mode a variant of HCCI combustion mode in diesel engines. In this method generally two fuels are used [19-21]. One fuel is injected in to the intake air, upstream of the intake valve to obtain a premixed charge. Remaining fuel is injected into the combustion chamber through conventional injection system. The PPCCI technique reduces NO_x and PM using partially premixed charge compression ignition (PPCCI) combustion. In this method of combustion, diesel, petrol, methanol, liquefied petroleum gas (LPG), compressed natural gas (CNG), methyl tert-butyl ether (MTBE) and acetylene are commonly used as premixed fuel or main fuel (in-cylinder injection).

In this work investigation to study the effect of Jatropha methyl ester biodiesel as main fuel and diesel as premixed fuel was carried.

In PPCCI, combustion takes place predominantly in premixed manner than in diffusive manner due to homogeneous mixture formation by fuel-air premixing [22-24]. In addition, premixed mixture combustion is faster than conventional diesel combustion as it occurs at multiple points in the cylinder.

This sudden combustion causes a sharp increase in pressure and temperature leading to high maximum values. By this reason, in PPCCI combustion takes place with a highly diluted mixture to maintain the temperature and pressure low in the cylinder and is normally restricted to low loads. That's why it is possible to avoid engine damage while NO_x emissions are lowered by low temperatures.

In this work, the performance, emission and combustion characteristics have been studied using jatropha oil methyl esters in CIDI and HCCI modes for determination of the optimum blend ratio of JOME with diesel in CIDI mode, the optimum EGR percentages for better tradeoff of soot and NO_x emissions for JOME. It was studied the effect of PPCCI combustion mode with diesel and biodiesel blends.

Various experiments were carried out using PPCCI mode of combustion with diesel as premixed fuel with premixed ratio of 0.25 and 20% JOME as main fuel with 10%, 20% and 30% EGR. The performance characteristics (brake thermal efficiency, exhaust gas temperature), emission characteristics (UBHC, CO, NO_x and soot emissions) and combustion parameters (in-cylinder pressure, ignition delay and heat release rate) are presented.

Materials and Methods

The tests were performed on a single cylinder, four stroke, naturally aspirated, air-cooled diesel engine coupled with an electrical swinging field dynamometer. The detailed technical specifications of the engine are given in tab.1. Fig. 1 shows the schematic diagram of the experimental set-up. The intake manifold of the engine is modified to fit the primary fuel injector. AVL 415 Variable Sampling Smoke meter is used to measure the particulate matter in the exhaust. MRU delta 1600 L Exhaust Gas Analyzer is used to measure HC, CO and NO_x emissions.

AVL 615 indimeter system is used to get pressure crank angle diagram at various loads using piezoelectric pressure transducer and angle encoder and to process the same for getting various parameters such as heat release rate curve, peak pressure, angle of occurrence of peak pressure, imep, etc.

The engine was started with diesel and allowed to warm up till steady state conditions were achieved. Engine Speed, fuel consumption rate, exhaust emissions (HC, CO, and NO_x), smoke intensity, pressure-crank angle diagram and exhaust gas temperature were measured at various loads. The experiment was repeated at various loads with 20% JOME blends with diesel. The experiments were conducted on

a CIDI engine maintained at 25%, 50%, 75% and 100% of brake power output at the speed of 1500 rpm with modified inlet manifold to operate the engine in PPCCI combustion mode. The experiment was repeated with premixed ratios of 0.25 at various power outputs.

In PPCCI mode the notations are used:

D-20J mode – Diesel (manifold injection)-20% JOME and 80%.

Diesel blends (main injection).

R_p – the ratio of energy of premixed fuel Q_p to the total energy Q_t .

$$R_p = Q_p / Q_t = (m_p \cdot CV_p) / (m_p \cdot CV_p + m_d \cdot CV_d)$$

where m is the mass of fuel and CV is the lower calorific value and subscripts p and d refer to premixed and directly injected fuel, respectively.

Table 1 – Test Engine Specifications

Engine Type	Four stroke, Air cooled, stationary, constant speed, direct injection, CI engine
No. of cylinders	1
Maximum power	4.4 kW at 1500 rpm
Maximum torque	28 N-m at 1500 rpm
Bore	87.5 mm
Stroke	110 mm
Displacement	661.5cc
Compression Ratio	17.5: 1
Injection Timing	23.40 bTDC
Loading type	Swinging field dynamometer

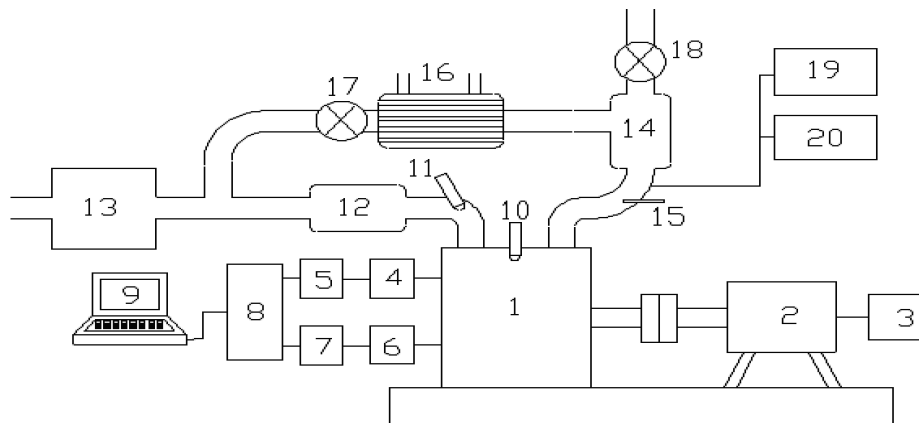


Figure 1 – Experimental setup: 1 – diesel engine, 2 – electrical, 3 – dynamometer, 4 – pressure pickup, 5 – charge amplifier, 6 – TDC position, 7 – TDC amplifier, 8 – A/D Card, 9 – personal, 10 – main injector, 11 – premixed fuel, 12 – mixing chamber, 13 – air flow, 14 – settling chamber, 15 – thermocouple, 16 – EGR cooler, 17 – EGR valve, 18 – back pressure, 19 – exhaust gas, 20 – AVL smoke

Results and Discussion

In the present work, reduction of NO_x and PM with partially premixed charge compression ignition (PPCCI) combustion was investigated. Diesel was used as a premixed fuel with premixed ratio of 0.25 along with 20% jatropha oil methyl ester (JOME) blend as main fuel with 10%, 20% and 30% EGR. Diesel fuel was injected into the intake manifold using a solenoid operated injector controlled by electronic control unit (ECU) to form premixed charge. The pre-mixed charge was burnt in the cylinder along with the fuel directly injected into the cylinder by a conventional injection system [25]. To control the start of combustion

and NO_x emissions, EGR was adopted and the exhaust gas was varied from 10% to 30% in steps of 10%.

Investigation of specific energy consumption and brake thermal efficiency

The variation of SEC and brake thermal efficiency with brake power for CIDI mode and D-20J mode with premixed ratio of 0.25 without EGR and with 10%, 20% and 30% EGR are demonstrated in fig.2, 3. As the percentage of EGR increases, the SEC increases and brake thermal efficiency decreases compared to CIDI mode. When EGR is introduced the fuel air mixture is diluted and the decrease in the availability of oxygen retards the combustion. The heat release in combustion reactions is decreased and

the quantity of unburned fuel is relatively large. As EGR increases, the brake thermal efficiency decreases [26, 27].

The SEC varies from 13,420 to 14,417 kJ/kWh in D-20J for premixed ratio of 0.25 without EGR and

with 10%, 20% and 30% EGR compared to 12,661 kJ/kWh in CIDI mode at rated power output. The brake thermal efficiency varies from 26.8 % to 25.0% in D-20J mode for above mode compared to 28.4% in CIDI mode.

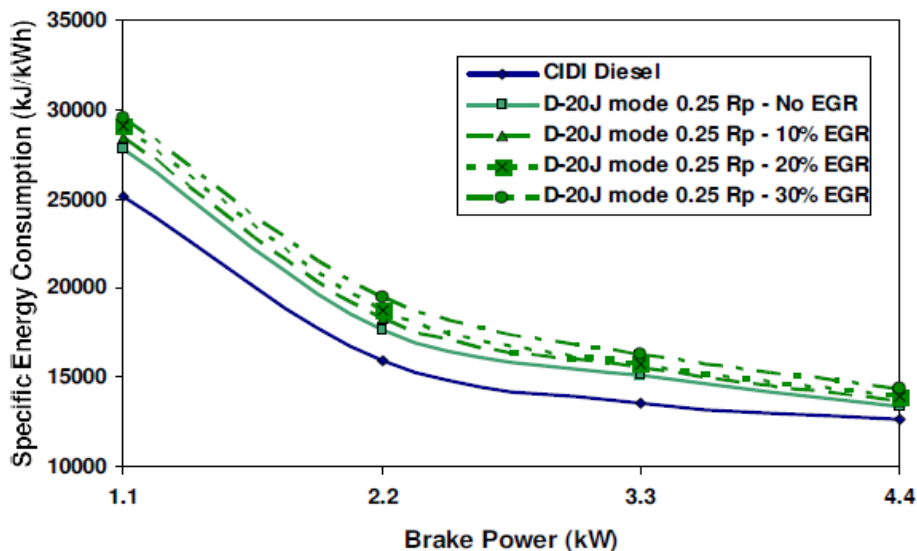


Figure 2 – Variation of specific energy consumption with brake power

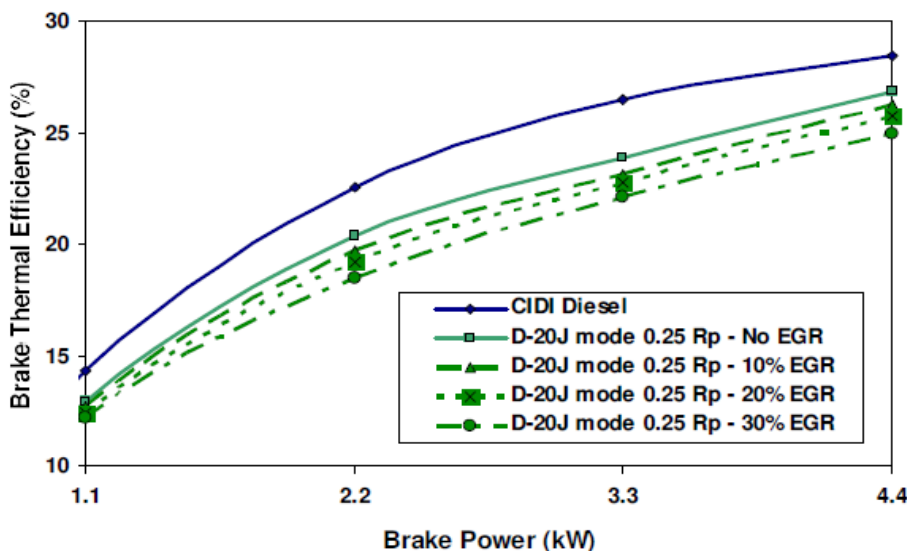


Figure 3 – Variation of Brake Thermal Efficiency with Brake Power

Impact of temperature of exhaust gas

Research the variation of exhaust gas temperature with brake power for D-20J with premixed ratio of 0.25 with 10%, 20% and 30% EGR and without EGR compared with CIDI mode is shown

in fig. 4. The combustion starts earlier resulting in higher in-cylinder temperature and pressure. These results in higher exhaust gas temperature at rated power output with premixed ratio of 0.25 without EGR compared to base line diesel mode. With EGR,

the specific heat capacities of re-circulated H_2O and CO_2 constituents increase resulting in lower peak combustion temperature. The effect is more pronounced at higher EGR percentages. At rated power

output, the exhaust gas temperature varies from $444^\circ C$ to $431^\circ C$ with 10%, 20% and 30% EGR for premixed ratio of 0.25 compared to $485^\circ C$ without EGR in D-20J mode.

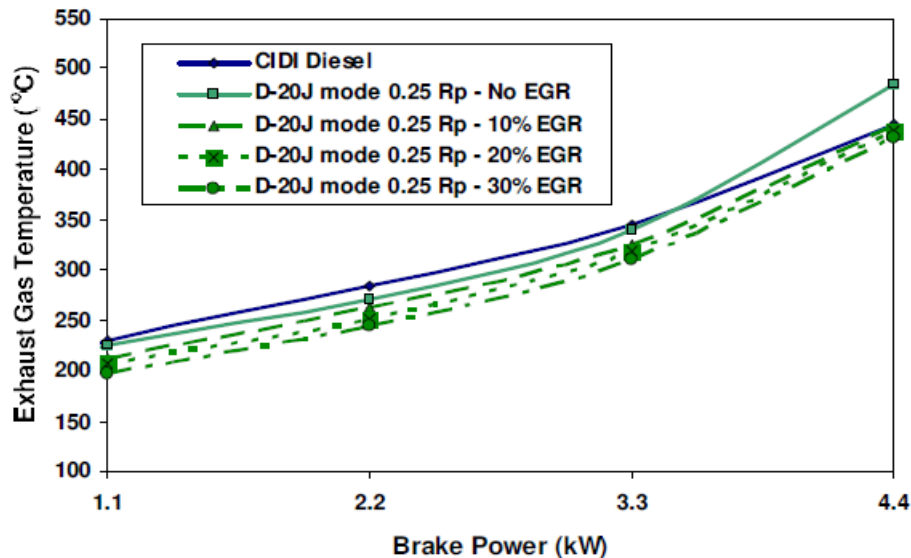


Figure 4 – Research the variation of temperature of exhaust gas with brake power

Studying unburnt hydrocarbon and emissions of CO

Fig.5 shows the variation of UBHC with brake power for CIDI mode, for PPCCI mode with D-20J 10, 20 and 30% EGR and without EGR. The variation of CO emissions is shown in figure 6 for the same operating conditions. Reduction of oxygen with EGR reduces the combustion reaction rate and temperature inside the cylinder. The burned gas temperature is low which results in increased emissions of UBHC and CO compared to CIDI mode. The peak temperatures are also relatively low to complete the oxidation of CO to CO_2 [28].

Because of lower inlet temperatures, premixed diesel fuel and in-cylinder injection of methyl ester blends are not completely evaporated which also leads to higher UBHC and CO [29, 30]. The effects of crevice volume and flame quenching may also be responsible for high UBHC and CO emissions. The UBHC emissions vary from 0.9 to 1.2 g/kWh in D-20J for premixed ratio of 0.25 without EGR and with 10%, 20% and 30% EGR compared to 0.7 g/kWh in CIDI mode at rated power output and the CO emissions vary from 17.6 to 30.9 g/kWh in D-20J mode compared to 16.7 g/kWh in CIDI mode.

Research of NO_x emissions

Fig. 7 shows the variation of NO_x emissions with brake power for CIDI mode and PPCCI mode with D-20J with 10, 20 and 30% EGR and without EGR.

The combustion starts earlier resulting in higher heat release rate, in-cylinder temperature and pressure at rated power output. These results in higher NO_x formation at rated power output for D-20J mode with premixed ratio of 0.25 without EGR compared to base line diesel mode. Recirculation of exhaust gas reduces the NO_x emission at all the power outputs compared to CIDI mode as oxygen available for the formation of NO_x is reduced when using EGR [31, 32]. Peak combustion pressure and temperatures are reduced as EGR percentage increases. At rated power output in D-20J mode with 10%, 20% and 30% EGR the NO_x emissions range from 6.2 to 3.33 g/kWh compared to 9.1 g/kWh without EGR.

Investigation of soot emissions

The variation of soot emission with brake power for PPCCI mode of operation with D-20J with 10, 20 and 30% EGR and without EGR is shown in fig.8. Soot emission in PPCCI mode with EGR is higher compared to that of without EGR. The increase in soot emission is due to reduction in oxygen content

and decrease in heat release rate with EGR at all power outputs [33].

It was found that with 10% EGR and 20% EGR, soot emissions are lower than that of CIDI mode but higher than PPCCI mode without EGR. Soot emissions are higher than that of CIDI mode when EGR is creased beyond 20%. Hence, the quantity of EGR

that can be re-circulated in PPCCI mode with pre-mixed ratio of 0.25 is limited to 20% in the present work. In PPCCI mode, the soot emissions in D-20J mode at rated power output vary from 82 to 208 mg/m³ with 10%, 20% and 30% EGR while it is 75 mg/mg³ without EGR compared to 166 mg/m³ in CIDI mode.

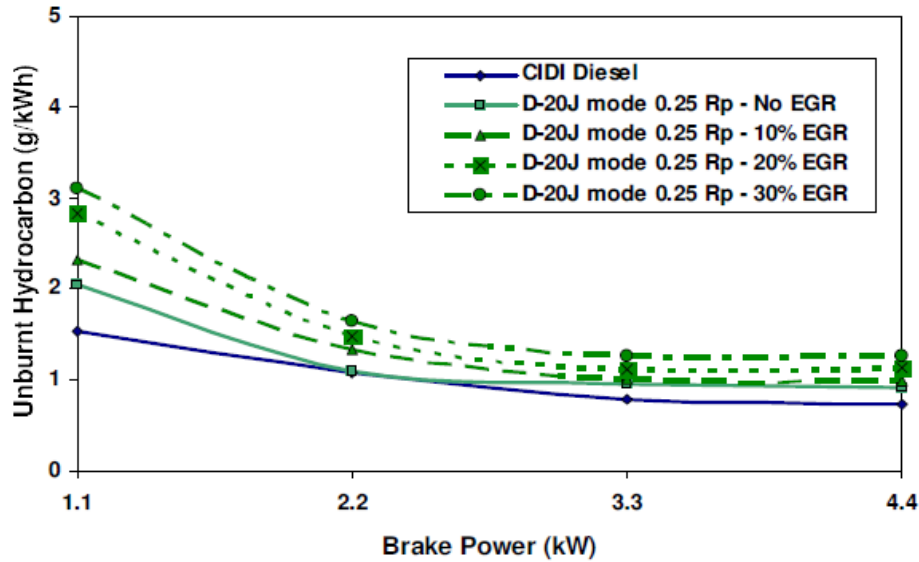


Figure 5 – Influence of variation of unburnt hydrocarbon with brake power

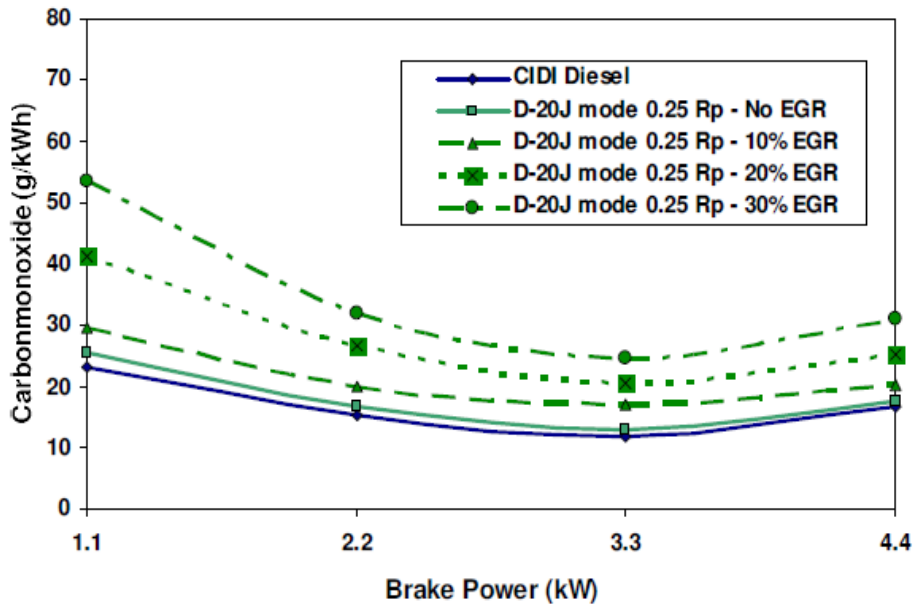


Figure 6 – Influence of variation of carbonmonoxide with brake power

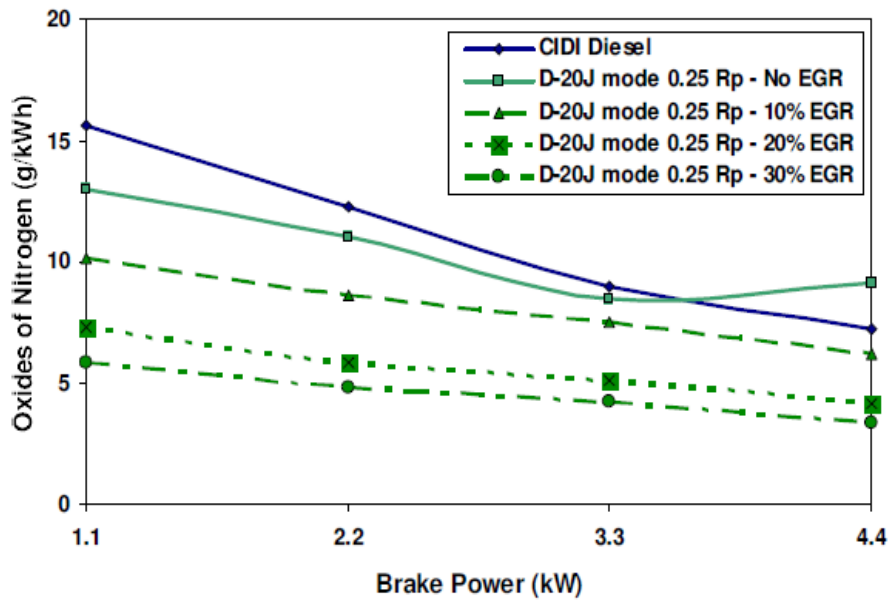


Figure 7 – Variation of NO_x with brake power

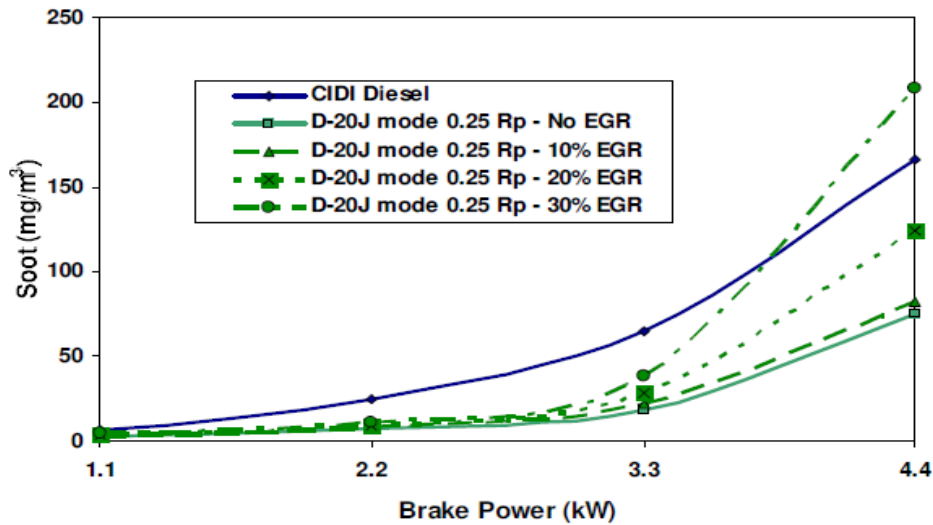


Figure 8 – Variation of soot with brake power

Research of heat release rate

Fig. 9 shows the heat release rate at rated power output for various premixed ratios in PPCCI mode compared to CIDI mode. It can be observed that the heat release curves show two peaks—one smaller magnitude and another peak of greater magnitude near TDC. The first stage of heat release is associated with low-temperature kinetic reactions (cool flames) named low temperature reactions (LTR). The second stage of heat release rate is the main heat release and named as high temperature reactions (HTR). The

time delay between the LTR and HTR is named as negative temperature coefficient (NTC) region [34–38].

The negative temperature coefficient regime is characterized by a decrease in the overall reaction rate even though in-cylinder temperature increases. This leads to a lower reactivity of the system. For diesel (lower octane number fuel) the heat release in the low temperature combustion (LTC) is predominant compared to gasoline (higher octane number fuel) [39].

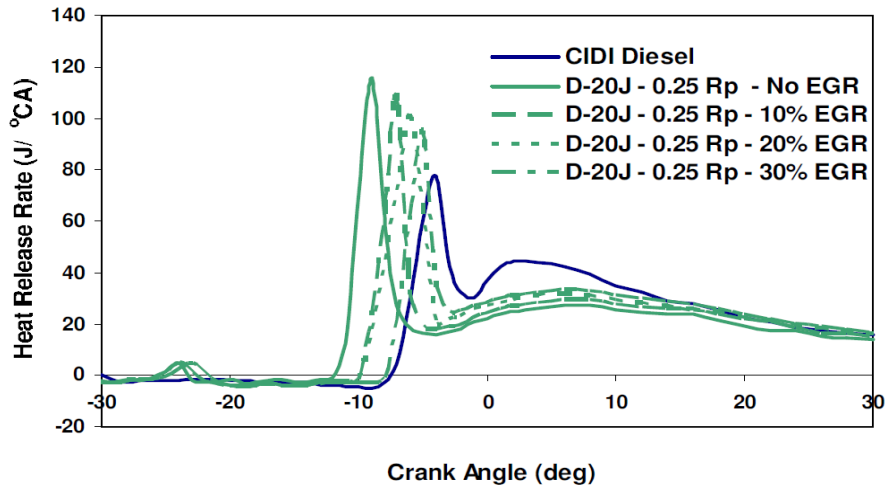


Figure 9 – Variation of Heat Release Rate with Brake Power

Fig. 10 shows the LTR, HTR and interval between LTR and HTR in D-20J mode at rated power output for premixed ratio of 0.25 without EGR and with 10, 20 and 30% EGR. It is observed that the peak LTR is not affected with increase in EGR per-

centage. But peak of HTR is significantly decreased as the percentage of EGR is increased. Increasing EGR percentage can delay both, the start of LTR and HTR. The EGR act as a thermal sink absorbing the heat present and lowers the heat release rate.

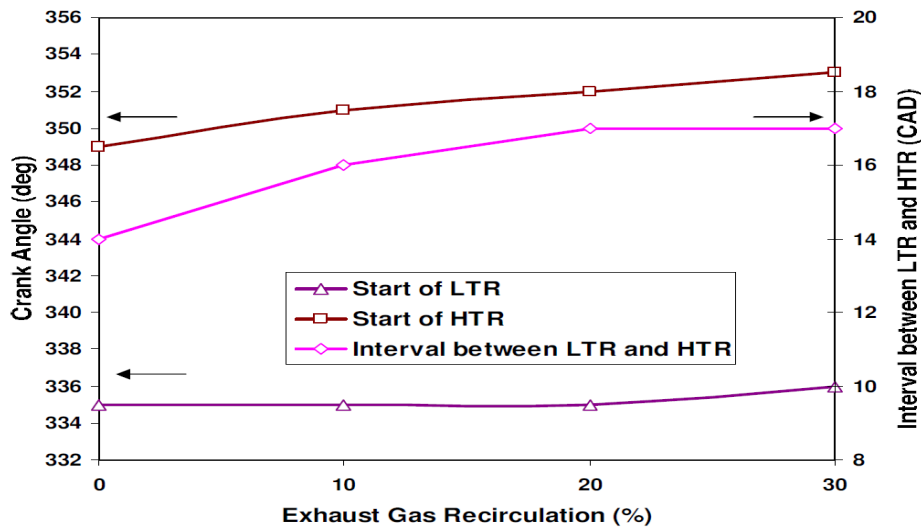


Figure 10 – LTR, HTR and Interval between LTR and HTR with Various Percentages of EGR at Rated Power Output for D-20J mode

The peak heat release rates during HTR at rated power in D-20J are 115.8, 109, 101.2 and 95.2 J/°CA occurring at 11 to 7 °CA bTDC for premixed ratios of 0.25 without EGR and with 10, 20 and 30% EGR while the peak heat release rates during LTR vary from 4.8 to 5.1 J/°CA occurring at nearly 25°CA bTDC for all premixed ratios. The time interval between LTR and HTR varies from 14 to 17°CA.

Conclusions

Thus as a result of the performed experimental work it was found that brake thermal efficiency decreases with increase in EGR percentages. UBHC and CO emissions are higher in PPCCI mode. NO_x emissions are lower and the percentage decreases are 14.8%, 42.8% and 54.3% compared to baseline die-

sel mode. Soot emission decrease up to 20% EGR and increases when EGR is increased above 20% compared to CIDI mode. In D-20J the peak pressure increases up to 20% EGR and decrease when EGR is increased to 30% compared to CIDI mode. The percentage increases in peak heat release rate in D-20J are 40.6%, 30.6% and 22.8 % compared to CIDI mode. Premixed ratio of 0.25 with 20% EGR is observed to be optimum in D-20J comparing the performance, combustion and emission characteristics.

References

1. Kakaee A-H., Paykani A., Ghajar M. (2014) *Renew Sustain Energy Rev.*, vol. 38, pp. 64–78.
2. Sassykova L.R. (2018) Technogenic emissions into the atmosphere: impact on the environment and neutralization by catalytic methods. *Qazaq university*.
3. Murugesan A., Umarani C., Chinnusamy T.R., Krishnan M., Subramanian R., Neduzchezain N. (2009) *Renew Sustain Energy Rev.*, vol. 13, pp. 825–834..
4. Murugesan A., Umarani C., Subramanian R., Nedunchezian N. (2009) *Renew Sustain Energy Rev.*, vol. 13, pp. 653–662.
5. Kumar S., Chaube A., Jain S.K. (2012) *Int J Energy Environ.*, vol. 3, pp. 471–484.
6. Gan S., Ng H.K., Pang K.M. (2011) *Appl Energy*, vol. 88, pp. 559–567.
7. Sassykova L., Nalibayeva A. (2018) *J. Chem. Technol. Metall.*, vol. 53(2), pp. 289-295.
8. Lu X., Qian Y., Yang Z., Han D., Ji J., Zhou X. (2014) *Energy*, vol. 64, pp. 707–718.
9. Fang Q., Fang J., Zhuang J., Huang Z. (2012) *Appl Therm Eng*, vol. 48, pp. 97–104.
10. Tsolakakis A., Megaritis A., Yap D. (2008) *Energy*, vol. 33, pp. 462–470.
11. Cinar C., Uyumaz A., Solmaz H., Topgul T. (2015) *Energy Convers Manag.*, vol. 94, pp. 159–168.
12. Yao M., Zheng Z., Liu H. (2009) *Prog Energy Combust Sci*, vol. 35, pp. 398–437.
13. Machrafi H., Cavadias S., Gilbert P. (2008) *Fuel Process Technol*, vol. 89, pp. 1007–16.
14. Bendu H., Murugan S., (2014) *Renew Sustain Energy Rev*, vol. 38, pp. 732–746.
15. Maurya R.K., Agarwal A.K. (2011) *Appl Energy*, vol. 88, pp. 1153–1163.
16. Bhaskar K., Sassykova L.R., Prabhahar M., Sendilvelan S. (2018) *International Journal of Mechanical and Production Engineering Research and Development*, vol. 8(1), pp. 399-406.
17. Murata Y., Kusaka J., Daisho Y., Kawano D., Suzuki H., Ishii H. (2008) *SAE Int J Engines*, vol. 1, pp. 444–456.
18. Roberts M., (2002) *SAE Tech Pap*, vol. 03, pp.–227.
19. Arana C.P., Pontoni M., Sen S., Puri I.K. (2004), *Combust Flame*, vol. 138, pp. 362–372.
20. Sassykova L.R., Aubakirov Y.A., Bunin V.N., Sendilvelan S. (2017), *International Journal of Biology and Chemistry*, vol. 10(2), pp. 54-61.
21. Jacobs T.J., Assanis D.N. (2007), *Proc Combust Inst*, vol. 31 II, pp. 2913–2920.
22. Mohamed I.M., Varuna N.J., Ramesh A. (2015) *Energy*, vol. 89, pp. 990–1000.
23. Musculus M.P.B., Miles P.C., Pickett L.M. (2013) *Prog Energy Combust Sci*, vol. 39, pp. 246–283.
24. Bray K., Domingo P., Vervisch L. (2005) *Combust Flame*, vol. 141, pp. 431–437.
25. Chen Z., Yao C., Wang Q., Han G., Dou Z., Wei H. (2016), *Fuel*, vol. 170, pp. 67–76.
26. Thangavelu S.K., Ahmed A.S., Ani F.N. (2016) *Renew Sustain Energy Rev*, vol. 56, pp. 820–835.
27. Tsolakakis A., Megaritis A., Wyszynski M.L., Theinnoi K., (2007) *Energy*, vol. 32, pp. 2072–2080.
28. Pandey R.K., Rehman A., Sarviya R.M. (2012), *Renew Sustain Energy Rev*, vol. 16, pp. 1562–1578.
29. Vijayaraj K, Sathiyagnanam AP. (2016) *Alexandria Eng J*, vol. 55, pp. 215–221.
30. Agarwal A.K., Dhar A., Gupta J.G., Kim W.I., Choi K., Lee C.S. (2015) *Energy Convers Manag*, vol. 91, pp. 302–314.
31. Verschaeren R., Schaepdryver W., Serruys T., Bastiaen M., Vervaeke L., Verhelst S. (2014) *Energy*, vol. 76, pp. 614–621.
32. Yasin M.H.M., Mamat R., Yusop A.F., Idris D.M.N.D., Yusaf T., Rasul M. (2017) *Energy Procedia*, vol. 110, pp. 26–31.
33. Li X., Xu Z., Guan C., Huang Z. (2014), *Appl Therm Eng*, vol. 68, pp. 100–106.
34. Sendilvelan S., Bhaskar K. (2017) *World J Eng*, vol. 14(4), pp. 348-352
35. Kathirvelu B., Subramanian S. (2017) *Environ Eng Res*, vol. 22, pp. 294–301.
36. Chen Z., Liu J., Wu Z., Lee C. (2013) *Energy Convers Manag.*, vol. 76, pp. 725–731.
37. Mostafa K. D. K., Sajad R., Maryam E., Talal Y., Subramanian S. (2018), *Energy Conversion and Management*, vol. 165, pp. 344-353.
38. Zhang P., Ji W., He T., He X., Wang Z., Yang B. (2016) *Combust Flame*, vol. 67, pp. 14–23.
39. Wang B., Wang Z., Shuai S., Xu H. (2015) *Appl Energy*, vol. 160, p. 769.

IRSTI 31.25.19

^{1,2}Ye.A. Dauletov, ¹M. Bajayo-Lugo, ²K. Abdiyev, ^{2,3}Zh. Toktarbay and ^{1*}N. Nuraje¹Department of Chemical Engineering, Texas Tech University, Lubbock, TX 79409²Department of Chemical Technologies of Organic Compounds and Polymers,

K. Satbayev Kazakh National Research Technical University (Satbayev University), Almaty 050013, Kazakhstan

³Specialized gymnasium for gifted children teaching in three languages named after Al-Farabi, Almaty, Kazakhstan

*e-mail: nurxat.nuraje@ttu.edu

Poly (DADMAC-co- VEMEA): Synthesis and Flocculation Properties

Abstract: Flocculants are widely investigated chemicals, which can be utilized to remedy or purify waste water from industries including petroleum, fabric, mining. Although many types of flocculants have been explored, each flocculant has its merits and demerits. Thus, we investigated poly (N,N-diallyl-N,N-dimethylammonium chloride) cationic flocculants. This work reports a novel flocculant which was developed based on the widely used flocculant, poly (N,N-diallyl-N,N-dimethylammonium chloride) (DADMAC) cationic polymers. This newly developed flocculant has not only enhanced flocculant performance, but also provided reusability of this polymer with insertion of crosslinking groups. The new developed copolymer, Poly (DADMAC-co- VEMEA), was synthesized via random radical polymerization approach and characterized by NMR and FTIR. The flocculation performance for these polymers were evaluated and studied by turbidity experiments and zeta-potential measurements. Their flocculation performance over poly (DADMAC) homopolymer can be improved by adding a VEMEA unit to the polymer chain and partially crosslinking the copolymer. This newly developed flocculant can provide new direction in developing flocculants potentially.

Key words: Flocculant, DMDAAC, VEMEA, Zeta potential, Turbidity

Introduction

The supply of pure water is still one of many urgent matters which our society faces worldwide at present [1-3]. For example, based on the United Nation's statistics, one out of seven people do not have a proper clean water source to use [4]. Water contamination is the main obstacle to accessing a pure water source, which is mainly caused by waste water from fabric factories and petroleum oilfields, and leakage from mining and other industry failures [5]. Thus, water purification techniques have been developed based on the concept of distillation [6], filtration [7], reverse osmosis [6], and electrodialysis [3]. All treatment techniques can be utilized in terms of the nature of the contaminants. However, due to physical chemical properties of the contaminants, filtration membranes or permeable active barriers can be easily contaminated by different types of contaminants [6]. For examples, filtration membranes are easily blocked and lose performance due to the attachment of positively or negatively charged organic pollut-

ants. Therefore, it is very important to precipitate or remove via coagulants [8, 9] before filtration.

Polyelectrolytes have been broadly explored to neutralize colloidal contaminants or pollutants via a coagulation process [10]. The principle is that organic or inorganic colloidal contaminants can be precipitated from waste water via addition of flocculants, which have high affinity to remove colloidal contaminants with physical forces such as electrostatic and other forces. This binding between colloidal contaminants and flocculants creates large particles of flocs, which further induce the precipitation of the pollutants. This treatment is usually applied before filtration of industrial waste water and other water treatment [10, 11]. In recent years, cationic flocculants like poly (N,N-diallyl-N,N-dimethylammonium chloride) (DADMAC) have been explored [8-9, 12]. This flocculant is widely used in the treatment of pulp and paper mill industrial wastewater [13].

In this work, to increase the flocculation performance of P(DADMAC), we plan to synthesize a copolymer of N,N-diallyl-N,N-dimethylammonium

chloride (DADMAC) and vinyl ether of monoethanolamine (VEMEA) (Scheme 1) and improve water purification performance based on the hypothesis that copolymers containing double amine groups can provide better flocculation properties (Scheme 2), and at the same time self-crosslinking between monomers further improve flocculation quality (Scheme 1). Regarding this, Cationic polystarch flocculant was investigated for flocculating activity, which was improved until the optimal degree of crosslinking [14]. We used random radical polymerization techniques to synthesize copolymers of Poly (DADMAC-co-VEMEA) under different conditions, including varying monomer ratio, and characterized them using FTIR and NMR. The resulting polymers are further applied to test waste water containing bentonite. Flocculation performance was further evaluated and explained via turbidity measurements and zeta potential approaches.

Materials and Methods

Materials

N, N-Diallyl, N, N-dimethyl ammonium chloride (65 wt % in water), ammonium persulfate (APS, 99.7 wt% purity), Silver Nitrate (99.8 wt % purity), Sodium Chloride (97 wt %), Hydrochloric Acid (37 wt %) were purchased from Sigma Aldrich Inc., (USA) and used without any further purification. The comonomer VEMEA was provided by JSC “Carbit” (Kazakhstan). Before use, it was purified by distillation at temperature range 112-116°C and its refractive index was recorded as 1.4382 at 298 K. Acetone was purchased from “Labchimprom” Ltd. (Kazakhstan) and used as it is. Ultra-high pure (99.995 wt %) purging gas, Argon was owned from “Ikhsan” Ltd. (Kazakhstan). During all synthesis and purification process of polymers, the Mili-Q water with resistivity at least $15 \text{ M}\Omega \times \text{cm}$ at 298 K was used. For flocculation experiments Bentonite, main component of which is montmorillonite (90-100% conc.) was purchased from Sigma Aldrich Inc., (USA).

Synthesis and purification of polymers

Copolymers of DADMAC and VEMEA were synthesized at different monomer molar ratios and

different initiator molar concentrations as mentioned in previous publications [1]. Initially the solution of monomers was purged for 15 minutes with ultra-high pure argon, which was sealed in a glass ampoule after adding a specific amount of initiator. The ampoule was kept in a water bath heated at 60°C for 5 hours. After 5 hours the ampoule was cooled immediately, and the product was precipitated with fresh acetone. After drying in the vacuum oven, the solid mass was placed in dialysis tubing with a molecular weight cut-off of 1200 Da for further analysis such as FTIR, NMR, and flocculation. Dialysis tubing with polymer was kept in water for three days while being stirred with a magnetic stirrer at 400 rpm. The water was replaced with pure water thrice a day. This part of the work was described in more detail in our previous publication[15]. For this work only two samples of polymers were selected: with initial monomer ratio DADMAC: VEMEA 80:20 and DADMAC: VEMEA 95:5 and with molar concentration of initiator 0.2% and 0.03% accordingly.

FTIR

FTIR was carried out in a Vertex 70 FTIR using diffuse reflectance Fourier transform spectroscopy (DRIFT) mode where scan time was 64, and resolution was 4. Samples for this analysis were prepared in a 1:200 mass ratio where KBr is the diluent. The FTIR spectra was detected in the spectral range between 400 cm^{-1} and 4000 cm^{-1} . The sample was characterized in a powder state in the atmosphere of nitrogen gas.

^1H and ^{13}C -NMR

The ^1H and ^{13}C NMR analysis were performed using a Varian Unity INOVA 500 in D₂O media at 298 K. The solvent contained reference standard 1 wt. % DSS (4,4-dimethyl-4-silapentane-1-sulfonic acid). The concentrations of sample were 10 mg and 30 mg of sample per 1 g of solvent for ^1H -NMR and ^{13}C -NMR analysis accordingly.

Flocculation Measurements

For flocculation experiments, a 0.5 wt. % solution of bentonite with effective diameter 158.43 nm was prepared. The commercial bentonite received from Sigma Aldrich Inc. has following composition (Table 1):

Table 1 – Composition of Sigma-Aldrich bentonite

Components	Al ₂ O ₃	SiO ₂	TiO ₂	Fe ₂ O ₃	MnO	CaO	K ₂ O	MgO	Na ₂ O	P ₂ O ₅	SO ₃
Wt. %	21	60.5	0.153	3.83	0.009	1.02	0.318	2.76	2.11	0.04	0.74

Flocculants were purified by using dialysis tubing with a MW cut-off 1200 Da. Flocculation of suspensions were done in 40 ml graduated cylinders. Suspension of bentonite was tested at 3 different acidic pH's (2, 3, 4) and with original polymer without adding acid. For analysis two polymers were selected with initial monomer concentrations of 80:20 (0.2% APS) and 95:5 (0.03% APS). Dosage of flocculant solution varied from 1 ml to 7 ml per 40 ml of bentonite solution, where polymer concentration was 0.1 wt. %. All flocculation experiments lasted 4 hours before measurement of residual turbidity and zeta potential of supernatant of treated suspension.

Residual Turbidity of supernatants of treated suspension was measured by recording optical density before treatment and after treatment. For performing this experiment, the spectrophotometer Genesys 6 (USA) was set for 740 nm wavelength and deionized water was used as a reference standard. The residual turbidity of treated samples was found using the following formula (1):

$$RT = \frac{OD_{740s}}{OD_{740i}} * 100\% , \quad (1)$$

where OD_{740s} is optical density of supernatant and OD_{740i} is optical density of initial suspension.

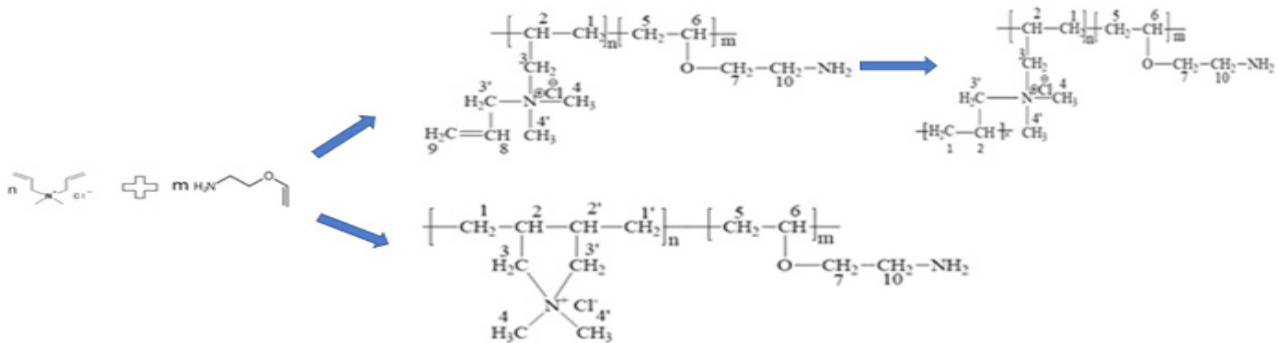
Determination of zeta-potentials of treated solutions

Zeta potentials of both suspension and supernatant of treated samples were measured in Brookhaven Nano Omni. An eluent solution of potassium chloride (0.1M) was used. The sample for zeta-potential measurement was prepared by adding one drop of supernatant to the 20 ml eluent which was filtered with a 0.1-micron syringe filter. The mixture was homogenized by sonicating for about 10 seconds. Afterwards, 3 ml of this mixture was placed in a plastic BI-SCP cell which was rinsed with the same mixture twice beforehand. All zeta potential measurements were performed at 298.15 K. The zeta potential of bentonite which was received from Sigma Aldrich doesn't change significantly with the changing suspension pH [16].

Since the zeta potential of bentonite changes with pH, it is essential to find out its zeta potential and isoelectric point for flocculation tests (2-4). The zeta potential of samples was calculated using the Smulchovski model which has following formula (2):

$$\xi = \frac{\mu_e \eta}{\epsilon} , \quad (2)$$

where μ_e is electrophoretic mobility, ϵ is permittivity of vacuum and η is viscosity of liquid.



Scheme 1 – Possible reactions in the copolymerization of DADMAC with VEMEA



Scheme 2 – Interaction of amine group of the copolymer with hydrochloric acid

Results and Discussion

We plan to synthesize a copolymer of DADMAC and VEMEA which not only provides densely-packed positive ions, but also increases the collection efficiency of flocculants based on our hypothesis mentioned previously (scheme 1 and 2). As mentioned in our previous publication [15], the copolymer based on DADMAC and VEMEA may have two possible molecular structures where DADMAC polymerizes either by forming a five-membered cycle or a pendant group with double bond (Scheme 1). In the latter case, the pendant group with a double bond at high temperature can cause partial cross-linkage [17]. Additionally, the cross-linking degree increases with increasing initiator concentration in the initial reaction mixture.

The resulting copolymers from the above reaction were further characterized by both NMR and FTIR. For the $^1\text{H-NMR}$, $^{13}\text{C-NMR}$ and FTIR spectra analyses, the copolymer with initial monomer ratio of 80:20 with 0.2 wt.% initiator was selected. The

$^1\text{H-NMR}$ spectrum (Figure 1) after purification with dialysis tubing still shows multiplet signals at ranges 5.89-5.90 ppm and 5.52-5.60 ppm which belong to hydrogens of carbons with double bonds. As the polymer partially cross-linked, the resulting product usually sophisticated with ability of water absorption and showed the presence of singlet 4.66 ppm which indicates some bound water due to strong interaction of an amine group with D_2O . Multiplets between 3.00-3.18 ppm corresponds to methyl groups which are located at positions 4 and 4'. Peaks at 0 ppm, 0.50 ppm, 1.5-1.64 ppm, and 2.74-2.77 ppm belong to 4,4-dimethyl-4-silapentane-1-sulfonate which is a reference standard as the solvent. As hydrogens in the amine group of the vinyl ether of monoethanolamine are replaced with hydrogens of deuterated water, it is not possible to see hydrogens belonging to the amine group in $^1\text{H-NMR}$ spectrum of the copolymer. Another important thing which is worthwhile to mention is the singlet corresponding to 3.69 ppm belongs to the peaks of hydrogens on positions 3 and 3'.

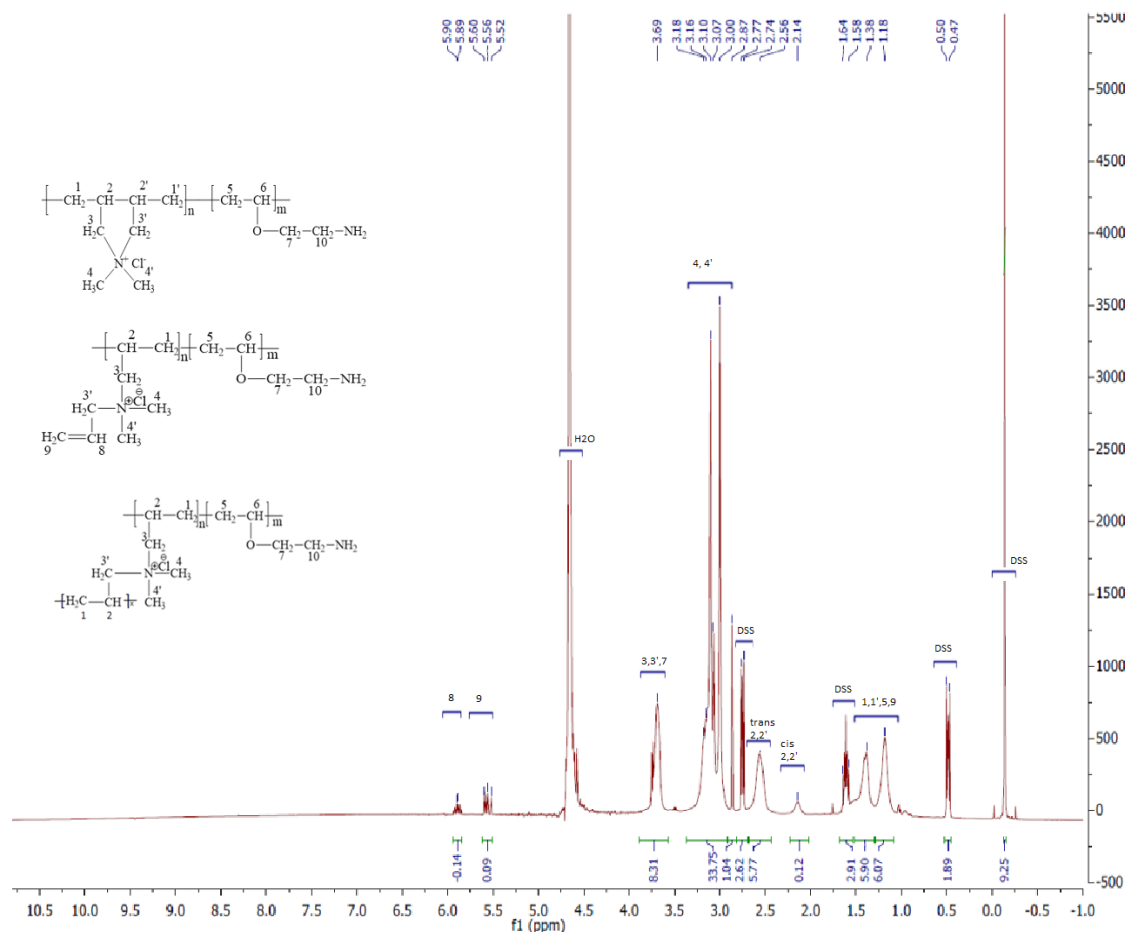


Figure 1 – $^1\text{H-NMR}$ spectra of poly (DADMAC-VEMEA 80:20 (0.2% in.))

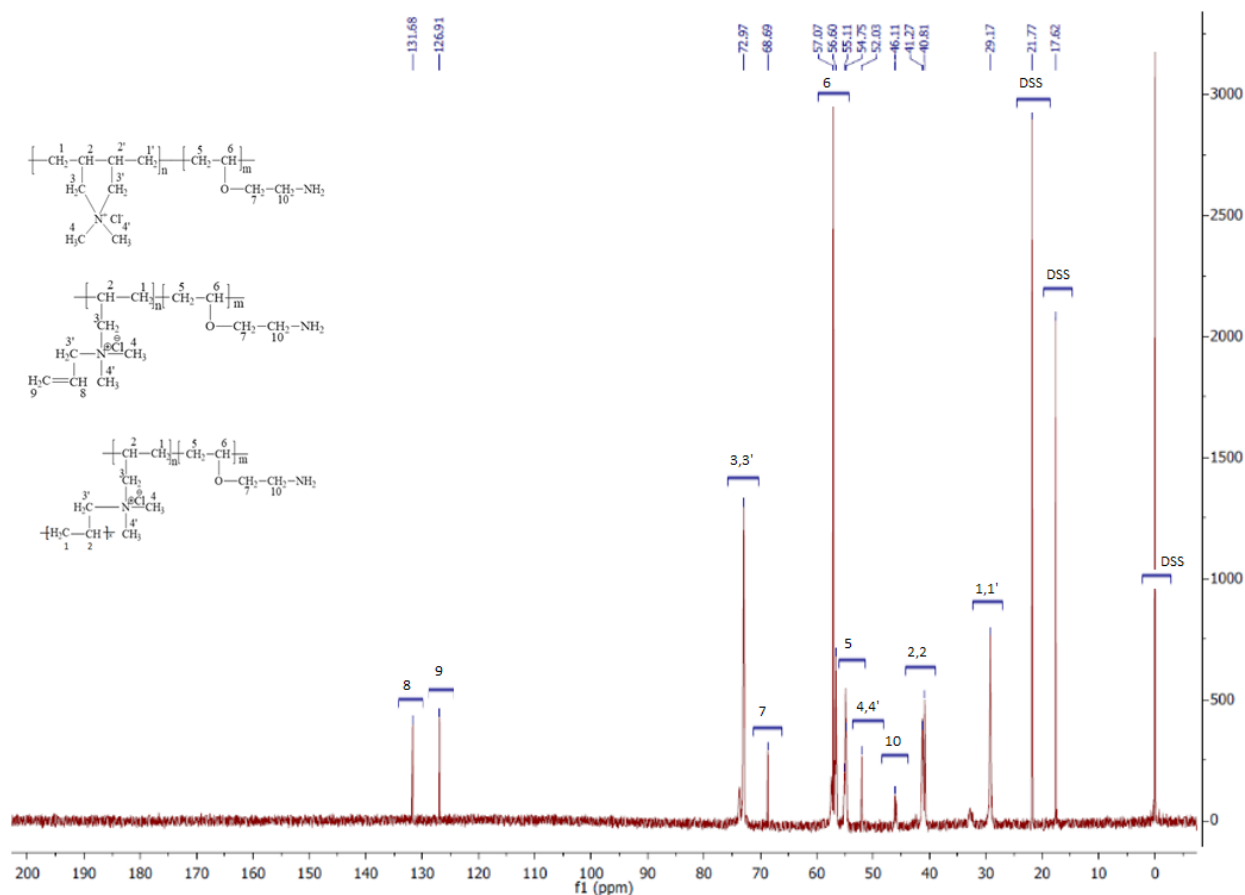


Figure 2 – ^{13}C -NMR spectra of poly (DADMAC-VEMEA 80:20 (0.2% in.))

At the same time, it coincides with the peak of hydrogens on position 7, which makes it difficult to prove the involvement of VEMEA in the copolymerization. The rest of the peaks on 1.38 ppm and 1.18 ppm belong to hydrogens at positions 1, 1', 5, 9'. In the case of cyclo-structure of DADMAC, hydrogens in positions 2 and 2' can be located in such a way to form cis-trans isomers of the monomer unit, so the peaks 2.56 ppm and 2.14 ppm correspond to hydrogens which are trans and cis isomers of the monomer accordingly. The peak 2.56 ppm also covers the hydrogens on position 10.

In ^{13}C -NMR spectrum (Figure 2), peaks at 0 ppm, 17.62 ppm, 21.77 ppm, and 57.07 ppm belong to the reference standard. The peaks at positions of 29.17 ppm (1 and 1' carbons), 40.81-41.27 ppm (2 and 2' carbons), 52.03 ppm (4 and 4' carbons), and 72.97 ppm (3 and 3' carbons) can be interpreted as signals of the carbons of the DADMAC unit. The copolymer containing carbons with double bonds shows singlets on position 126.91 ppm and 131.68 ppm correspond to $\text{CH}_2=\text{CH}$ - group of DADMAC. In the case of the VEMEA monomer, the carbon at position 10 which

is attached to the amine group appears at 46.11 ppm. Other peaks at 56.60-57.07 ppm and 68.69 ppm are characteristic to an ether group, indicating carbons at positions 6 and 7 correspondingly. The last peaks in the range 54.75-55.11 ppm belong to the carbon at position 5.

The FTIR spectrum of the copolymer (Figure 3) is clearer and easier to interpret for proving VEMEA involvement. The broad peak at 3434.2 cm^{-1} corresponds to the O-H and N-H stretching vibration. As mentioned above, water peaks show up because of material hygroscopicity. The broad peak observed at 1629.6 cm^{-1} is assigned to the scissoring of amine groups and the stretching vibration of $\text{C}=\text{C}$. The signal for the double bond in the copolymer can be observed at peak 800 cm^{-1} , which was identified as the out of plane bending of $=\text{CH}_2$. Peaks at 2868.7 cm^{-1} , 2931.7 cm^{-1} , 2987.1 cm^{-1} belong to the stretching vibrations of CH_3 , CH_2 , and CH functional groups. The signal at 1472.9 cm^{-1} is related to the interaction of counterions in DADMAC unit [18]. The C-O stretching vibration of the VEMEA group corresponds to the broad peak at position 1037.7 cm^{-1} .

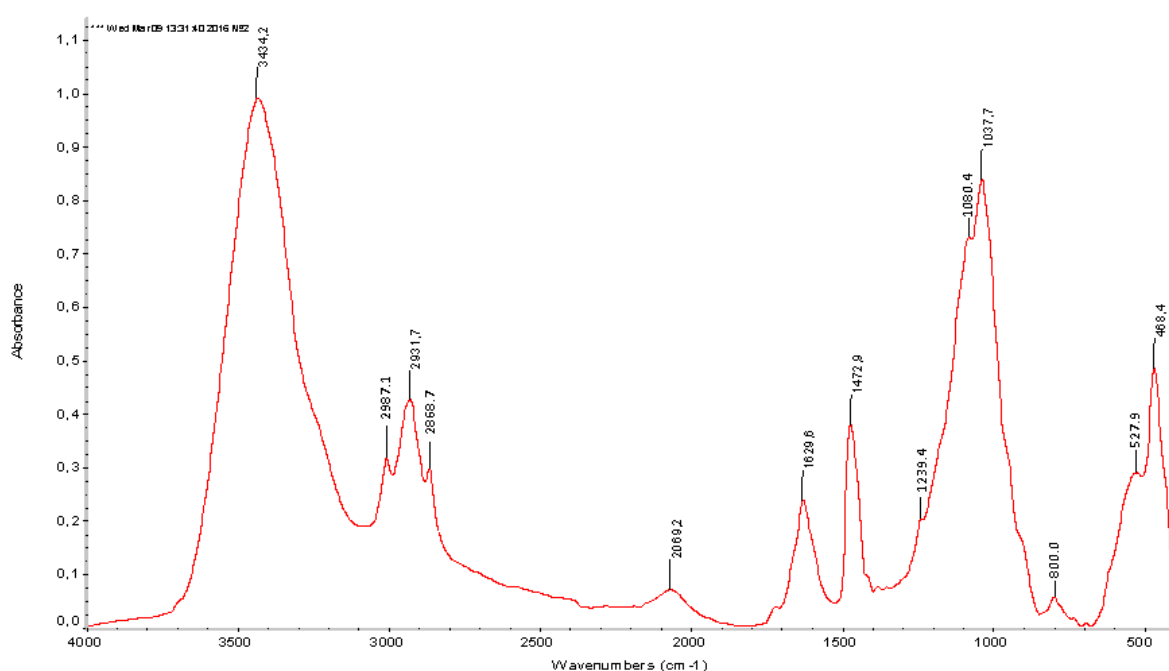


Figure 3 – FTIR spectra of poly (DADMAC-VEMEA 80:20 (0.2% in.))

The selection of copolymer with a different portion of VEMEA monomer is rationalized by the influence of the VEMEA unit on the flocculation ability of the copolymer based on our hypothesis. PolyDADMAC is a very popular flocculating agent in different areas of industry [13, 19-20]. The effect of cross linkage on the flocculating quality of the copolymer is another thing worth mentioning about the copolymer of DADMAC. PolyDADMAC itself is a cationic polymer and is partially cross linked, so it swells at low pH [21]. At the same time, VEMEA reacts with acid-giving cations in aqueous media (Scheme 2). In overall, acidic media is preferred for the flocculation process with synthesized copolymers.

Poly (DADMAC-VEMEA 80:20) (0.2% in.) is characterized with a higher content of VEMEA which gives a better effect at the lowest pH (Figure 4). As initiator amount increases, the resulting copolymer contains higher cross-linkage and a higher content of VEMEA. As bentonite itself is stable at acidic pH, the efficiency of the copolymer at lower pH is only ascribed to the mentioned copolymer behaviors at lower pH. From the graph, it is shown that this copolymer works best at pH 2 in a 4-ml dosage.

Poly (DADMAC-VEMEA 95:5) (0.03% in.) shows the best flocculation performance at pH 4 (Figure 5), which is related to less cross-linkage as the polymer was synthesized with lower initiator

concentration with respect to the previous one. Also, it doesn't have much VEMEA, which is sensitive to acid presence. The polymer also has a higher molecular weight because of decreased initiator concentration. This copolymer works best at pH 4 with a 3-ml dosage, which shows that the copolymer with a higher molecular weight is preferred for the flocculation process. It was assumed that this copolymer, because of its higher molecular weight, swells in such a way that during attachment to bentonite particles, it precipitates earlier before becoming neutral.

Pure solution of the above two copolymers works in the same way, but better efficiency was observed for the second one because of the higher molecular weight. Both samples in the case of pure copolymer solution show destabilization of suspension with a higher dosage of flocculant because of repulsion between copolymers in the solution [25-27, 29, 31]. From the zeta-potential measurements (Figure 6), it becomes clear that Poly (DADMAC-VEMEA 80:20 (0.2% in.)) at pH 2 is more effective in terms of quality of supernatant and dosage amount than the pure solution of Poly (DADMAC-VEMEA 95:5 (0.03% in.)). Consequently, we can be more confident that the copolymer with some degree of cross-linkage and some amount of VEMEA monomer at lower pH works better than the copolymer with less cross-linkage and decreased amounts of the VEMEA unit.

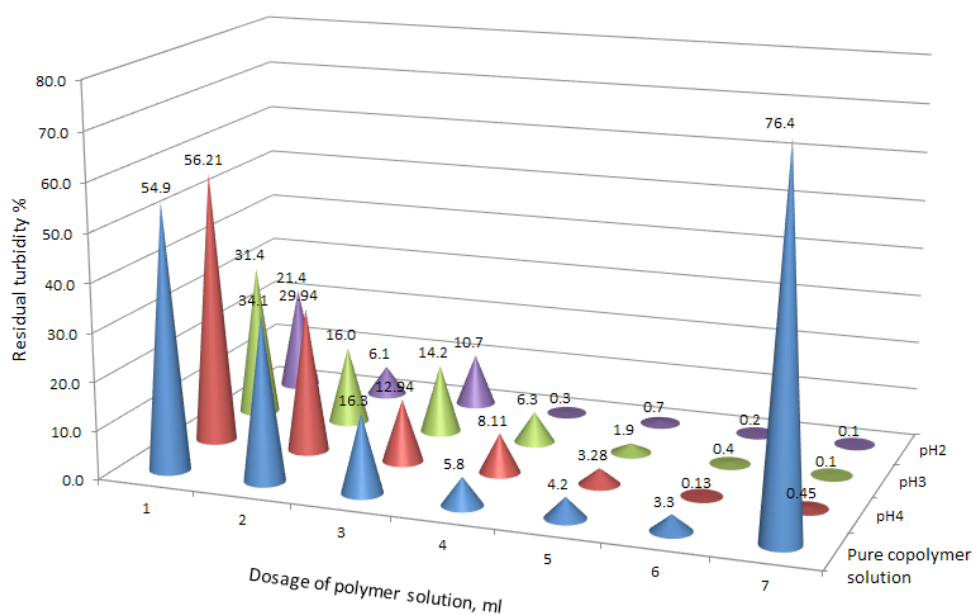


Figure 4 – Flocculation property of poly (DADMAC-VEMEA 80:20 (0.2% in.))

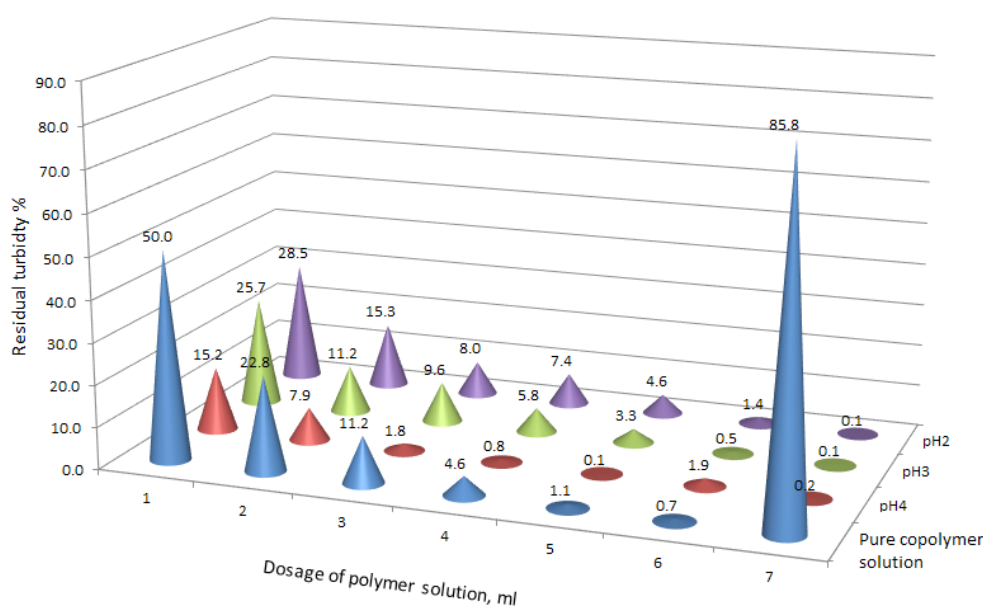


Figure 5 – Flocculation property of poly (DADMAC-VEMEA 95:5 (0.03% in.))

Considering the above results obtained from flocculation experiments, we can propose a flocculation mechanism. Based on the widely accepted three flocculation mechanisms [22], two mechanisms can be used to explain the flocculation of bentonite suspension with DADMAC-VEMEA copolymer, which are charge neutralization and polymer bridging mechanisms (Fig-

ure 7). At low pH the VEMEA unit in the copolymer gains a positive charge in addition to DADMAC, which makes the copolymer more positively charged.

As copolymers are cross-linked in some degree and swell under acidic pH, they overlap the suspended bentonite particles which precipitate due to gravitational force [28, 30].

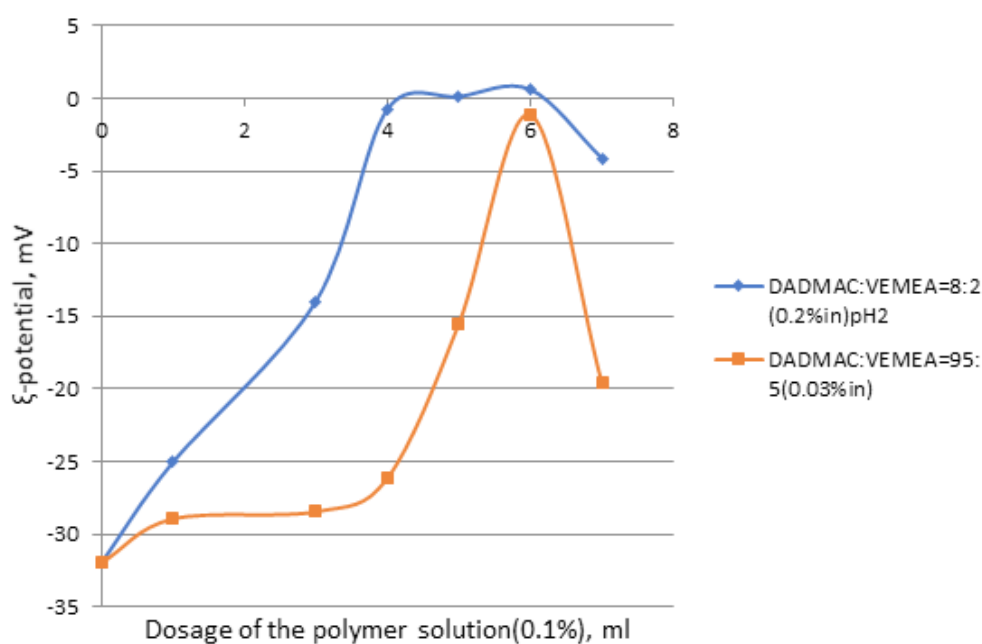


Figure 6 – Zeta potential of supernatants after treatments of copolymers

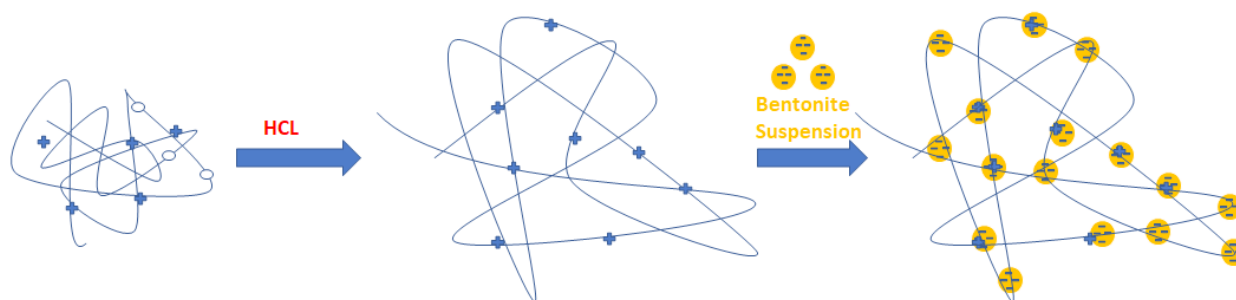


Figure 7 – Suggested flocculation mechanism for treatment of bentonite suspension with poly (DADMAC-VEMEA) copolymer

Conclusion

From the results of performed experiments it can be concluded that the flocculation ability of poly (DADMAC) homopolymer can be improved by adding a VEMEA unit to the polymer chain and making the copolymer partially crosslinked. As mentioned above, the VEMEA monomer becomes positively charged in acidic media, which is preferred in wastewaters containing negatively charged mechanical particles, and the optimized cross linkage degree of the copolymer help to overlap large areas by the flocculant, which initiates flocculation by bridging mechanism. The copolymerization of DADMAC with a VEMEA-containing primary amine has big potential in developing effective flocculants, which can be utilized in the primary steps of wastewater purification, and at

the same time partial cross linkage of the copolymers yield purified water with less residual polymer.

References

1. Welgemoed, T. J. and Schutte, C.F., Capacitive 2005 Desalination 183:327-340.
2. Suss, M. E., Porada, S., Sun, X., Biesheuvel, P. M., Yoon, J., Presser, V., 2015 *Energy & Environmental Science* 8:2296-2319.
3. Anderson, M. A., Cudero, A. L., Palma, J 2010 *Electrochimica Acta*, 55:3845-3856.
4. Porada, S., Zhao, R., van der Wal, A., Presser, V.; Biesheuvel, P. M. 2013 *Progress in Materials Science* 58:1388-1442.
5. Nuraje, N., Asmatulu, R., Mul, G., Green Photo-Active Nanomaterials: Sustainable Energy and

Environmental Remediation; *Royal Society of Chemistry*, 2015.

6. Asatekin Alexiou, A. Improved Filtration Membranes through Self-Organizing Amphiphilic Comb Copolymers. Massachusetts Institute of Technology, 2009.

7. Asmatulu, R.; Muppalla, H.; Veisi, Z.; Khan, W.; Asaduzzaman, A.; Nuraje, N. 2013 *Membranes* 3:375.

8. Abdiyev, K. Z.; Toktarbay, Z.; Zhenissova, A. Z.; Zhursumbaeva, M. B.; Kainazarova, R. N.; Nuraje, N. 2015 *Colloids and Surfaces A: Physicochemical and Engineering Aspects* 480:228-235.

9. Wang, Y.; Banziger, J.; Dubin, P. L.; Filippelli, G.; Nuraje, N. 2001 *Environmental Science & Technology* 35, 2608-2611.

10. Ghaly, A. E. S., A.; Faber, B.E. 2007 *American Journal of Environmental Sciences* 3:19-29.

11. Konieczny, K.; Rajca, M.; Bodzek, M.; Kwiecińska, A., Water Treatment Using Hybrid Method of Coagulation and Low-Pressure Membrane Filtration 2009 *Environment Protection Engineering*, 35:5-22.

12. Wandrey, C.; Hernández-Barajas, J.; Hunkeler, D., Diallyldimethylammonium Chloride and Its Polymers. In Radical Polymerisation Polyelectrolytes, Capek, I.; Hernández-Barajas, J.; Hunkeler, D.; Reddinger, J. L.; Reynolds, J. R.; Wandrey, C., Eds. Springer Berlin Heidelberg: Berlin, Heidelberg, 1999; pp 123-183.

13. Razali, M. A. A.; Ahmad, Z.; Ahmad, M.; Ariffin, A. 2011 *Engineering Journal* 166:529-535.

14. You, L.; Lu, F.; Li, D.; Qiao, Z.; Yin, Y. 2009 *Journal of Hazardous Materials*, 172:38-45.

15. Dauletov, Y.; Abdiyev, K.; Toktarbay, Z.; Nuraje, N.; Zhursumbaeva, M.; Kenzhaliyev, B. 2018 *Fibers and Polymers* 19:2023-2029.

16. Au, P.-I.; Leong, Y.-K. 2013 *Colloids and Surfaces A: Physicochemical and Engineering Aspects* 436:530-541.

17. Jaeger, W.; Hahn, M.; Wandrey, C.; Seehaus, F.; Reinisch, G. 1984 *Journal of Macromolecular Science—Chemistry* 21:593-614.

18. Mwangi, I. W.; Ngila, J. C.; Ndungu, P.; Msagati, T. 2014 *Physics and Chemistry of the Earth, Parts A/B/C* 72:54-60.

19. Ariffin, A.; Razali, M.; Ahmad, Z. 2012 *Chemical Engineering Journal* 179:107-111.

20. Razali, M.; Ariffin, A. 2015 *Applied Surface Science* 351:89-94.

21. Khare, A. R.; Peppas, N. A.; Massimo, G.; Colombo, P. 1992 *Journal of controlled release* 22:239-244.

22. Lee, C. S.; Robinson, J.; Chong, M. F. 2014 *Process Safety and Environmental Protection*, 92:489-508.

23. Nurkeeva, Z.S., Mun, G.A., Koblanov, S.M., Yermukhambetova, B.B., Abdykalykova, R.A., & Khutoryanskiy, V.V. (2002) *Radiat. Phys. Chem.*, 64:9-12.

24. Vorob'eva, A.I., Sagitova, D.R., Sadykova, G.R., Parshina, L.N., Trofimov, B.A., Monakov, & Yu.B. (2007) Copolymerization of N,N-diallyl-N,N-dimethylammonium chloride with ethylene glycol vinyl ether in aqueous medium. *Polymer Science, Series B*, 49:80-84. 25. T. Harif, M. Khai, A. Adin 2012 *Water Res.* 46:3177-3188.

26. T. Harif, A. Adin 2011 *Water Res.* 45:6195-6206.

27. M.L. Christensen, M. Hjorth, K. Keiding 2009 *Water Res.* 43:773-783. 28. L. Besra, D.K. Sengupta, S.K. Roy, P. Ay, 2002 *J. Miner. Process.* 66:183-202. 29. B. Bolto, J. Gregory 2007 *Water Res.* 41:2301-2324.

30. Zhenbei Wang, Jun Nan, Xiaoyu Ji, Yueming Yang 2018 *Science of The Total Environment* 633:1183-1191

31. Hua Wei, Boqiang Gao, Jie Ren, Aimin Li, Hu Yang 2018 *Water Res.* 143:608-631.

IRSTI 31.23.99

¹A. Kurmanbayeva, ³Zh. Shynykul, ²Yang Ye, ¹M.A. Dyusebaeva, ^{1*}J. Jenis¹Faculty of Chemistry and Chemical Technology, Al-Farabi Kazakh National University, Almaty, Kazakhstan, *e-mail: janarjenis@mail.ru²Shanghai Institute of Materia Medica, Chinese Academy of Science, Shanghai, China³Key Laboratory of Animal Models and Human Disease Mechanisms of Chinese Academy of Sciences and Yunnan Province, Kunming Institute of Zoology, Kunming, Yunnan, China.

Chemical Constituents of *Artemisia sublessingiana*

Abstract. One of the main interests of research in the field of medicinal plants is based on the results of potentially active properties of medicinal plants, one of which is current plant – *Artemisia sublessingiana* known among the locals in Kazakhstan and other Central Asian countries as having healing properties. Definitely, detailed chemical constituents of this herb have not been explored yet. In this study, we have investigated the main bioactive contents of the whole plant *A. sublessingiana* in terms of its moisture content (10.00 %), total ash (12.42 %), and extractives (22.88 %), also have analyzed the chemical constituents. Therefore, eleven macro- and microelements were identified in the ash of *A. sublessingiana* by using the method of multi-element atomic emission spectral analysis, and the main elements were K (47.310 %), Ca (41.910 %), Fe (4.984 %), Zn (0.126 %), and Mg (0.3475 %). Moreover, 8 fatty and 20 amino acids were identified from the further chemical investigation of the medicinal plant. Among of them, linoleic acid and oleic acid were recorded as the main components of fatty acids at C_{18:2} (69.1 %) and C_{18:1} (18.3 %) respectively, while glutamate, aspartate and alanine were the major contents of the amino acids at 640 mg/100 g, 1120 mg/100 g and 890 mg/100 g respectively.

Key words: *Artemisia sublessingiana*, bioactive constituents, macro-micro elements, GC-MS.

Introduction

Artemisia sublessingiana is a flowering plant of the family Compositae (Asteraceae). Within this family, *Artemisia* is included in the tribe Anthemideae and comprises over 500 species, which are mainly widespread found in Asia, Europe and North America. Asia has the greatest concentration of *Artemisia* species, with 150 accessions for China, 174 in the ex-USSR, about 50 reported for Japan, 35 species in Iran and 81 species of the genus found in Kazakhstan [1-3]. The genus *Artemisia* is known for its medicinal and aromatic properties, and used for the production of essential oils beneficial in medicine, food and cosmetics. Based on the phytochemical and pharmacological studies, *Artemisia* is a valuable medicinal source with neuroprotective, gastroprotective, anti-oxidative, anti-inflammatory, and anti-cancer effects. Farther, extensive studies on the chemical compounds composition of *Artemisia* have led to the identification of bioactive flavonoids, coumarins, sesquiterpen lactones, oxygenated monoterpenes, and sesquiterpenes [4-6].

Humans with inadequate or monotonous nutrition, poor quality of drinking water, decreased amount of mineral substances due to bleeding, disease, alcohol and some drugs that bind or cause loss of trace elements are the main causes of the lack of the biologically necessary essentials. At the same time, humans and animals can only acquire the irreplaceable essential nutrients (for example: niacin or choline) by feeding on plants or plant-based products. [7]. **Minerals, amino acids, fatty acids and vitamins** are the essential nutrients for humans.

The importance of obtaining “mineral salts” with food lies in the fact that these elements are part of the enzymes and other substances necessary for the body – participants in biochemical reactions. Consequently, in order to maintain optimal health, appropriate levels of consumption of certain chemical elements are required. Minerals are extensively divided into major minerals (macro-minerals) and trace minerals (micro-minerals). Major minerals include calcium (Ca), magnesium (Mg), potassium (K), and iron (Fe) among others [8]. As a result of the deficiency of essential amino acids in the human

body, synthesis of proteins is violated, which leads to weakening of memory and mental abilities, and a decrease in immunity (resistance of the organism to diseases) [9]. Essential fatty acids are important for the cardiovascular system: they inhibit the development of atherosclerosis, improve blood circulation, and have cardio protective and antiarrhythmic action. Polyunsaturated fatty acids reduce inflammatory processes in the body and improve the nutrition of tissues. The daily human need is estimated at 5-10 grams [10-11]. All essential amino acids, fatty acids and minerals can be found in plants and plant-based foods. A suitable combination of vegetarian or vegan products provides a person with a sufficient amount of essential nutrients [12-15].

Herbal application of species *Artemisia* as a treatment tool have been known around from immemorial time with many of them being tested through several generations because of widely distributed genus of the plant family *Asteraceae*. Nowadays, *Artemisia* species are an estimable source of sesquiterpenes, essential oils and other pharmacological active compounds which have been reported to carry various biological activities including, anti-tumor, anti-oxidant, antibacterial, anti-viral, anti-fungal, anti-cancer and to possibly solve some serious disease [16-17]. In addition, modern research in various fields of science, beside medicine, find a unique application of species *Artemisia* as a depurative, disinfectant, insecticidal anti-feedant, digestive and counteracting agent to insect poison [18-20]. However, most species of *Artemisia* have not been fully explored.

In current study has been made the investigation of chemical constituents, in intent to determine the amount of essential substances as a natural source from Kazakh medicinal plant of *A. sublessingiana* grown in Almaty region of Kazakhstan for the first time.

Materials and Methods

A. sublessingiana plants were collected in September 2017 at Kapchagay Lake of Almaty region, Kazakhstan and identified by Dr. Alibek Ydyrys. Voucher specimens (9358-S) were deposited in the Herbarium of Laboratory Plant Biomorphology, Faculty of Biology and Biotechnology, Al-Farabi Kazakh National University, Kazakhstan.

The quantitative and qualitative analysis of the biologically active constituents of the plant were carried out according to the methods reported in the State Pharmacopeia XI edition techniques.

The elemental constituents of the ash of *A. sublessingiana* were analyzed using multi-element atomic emission spectral analysis method in Shimadzu 6200 series spectrometer. These experiments were carried out in the "Center of Physico-Chemistry methods of research and analysis" of the Republican State Enterprise Kazakh National Al-Farabi University.

To determine the amino acid composition, renow of the raw material was made using GC/MS device. GC-MS analysis involves the test of the aerial part of *A. sublessingiana* by Gas Chromatograph coupled with Mass Spectrometer using polar mixture of 0.31% carbowax 20 m, 0.28% silar 5CP and 0.06% lexan in chromosorb WA-W-120-140 mesh column (400x3mm). The column temperature was programmed from 110 °C (held for 20min) at 6°C/min from 110 °C to 180 °C at 32 °C /min from 185 °C to 290 °C. When it reached 250 °C, it was left to stay constant till the end of the output of all amino acids.

To determine the fatty acid composition of the raw material, dried plant extract of *A. sublessingiana* was extracted with a chloroform-methanol mixture (2: 1) for 5 minutes, the extract was filtered through a paper filter and concentrated to dryness. Then, to taken extract add 10 ml of methanol and 2-3 drops of acetyl chloride and undergo further methylation at 60-70° C in a special system for 30 minutes. The methanol was removed by rotary evaporation and the samples were extracted with 5 ml of hexane and analyzed for 1 hour using a gas chromatograph «CARLO-ERBA-420» allocated in the Kazakh Academy of Nutrition. As a result, chromatograms of methyl esters of the fatty acids were obtained. 8 fatty acids were identified, by comparison with authentic samples by the time of exit from column.

Results and discussion

The moisture content (10.00 %), total ash (12.42 %), extractives (22.88 %) and the quantitative-qualitative contents of the biologically active constituents of the aerial parts of *A. sublessingiana* were determined (Table 1). Ash content makes it possible to judge the content of organic and mineral substances in the sample qualitatively. As a rule, the lower the content of organic substances, the higher the ash content. The content of the ash substances reveals the dependence on the properties of the test sample to certain organs and tissues of plants. Thus, the proportion of the ash component is high in tissues rich in catalytically active proteins using activator ions and ions in the cytosol composition. Mois-

ture content is mostly water, with its participation, the dissolved nutrients enter the plant through the roots and move from one cell to another, in the aqueous medium, electrolytic dissociation of these compounds occurs and the assimilation of ions containing the necessary elements of mineral nutrition by plants.

The percentage of extractives gives an idea about the content of metabolic substances in the organic extract of the plant; this is the total amount of phenolic compounds, terpenes, and polysaccharides, together with coumarins, sesquiterpen lactones, oxygenated monoterpenes, and sesquiterpenes.

Table 1 – Quantitative analysis of the main bioactive contents of *A. sublessingiana*

Contents, %					
Moisture content	Ash	Extractives	Organic acids	Flavonoids	Duplicates
10.00	12.42	22.88	0.446	0.057	0.60

In the present study, eleven macro-, micro-elements such as K (47.310 %), Ca (41.910 %), Fe (4.984 %), Zn (0.126%), Mg (0.347 %), Cu (0.081 %), Cd (0.010 %), Pb (0.060 %), Ni (0.00720 %), Mn (0.347 %), and Na (4.890) were determined in the ash of *A. sublessingiana* (Table 2). Trace elements are necessary for living organisms to ensure normal life activity. With a lack of potassium, there are disruptions in the work of the heart and skeletal musculature. Prolonged potassium deficiency can cause acute neuralgia. Prolonged deficiency of calcium and vitamin D in the diet leads to an increased risk of osteoporosis, and in infancy causes rickets. In living organisms, iron is an important microelement that catalyzes the processes of oxygen exchange (respiration). The main

intracellular depot of iron is the globular protein complex – ferritin. Lack of iron is manifested as a disease of the body: chlorosis in plants and anemia in animals. Zinc is essential for the production of sperm and male hormones, is essential for the metabolism of vitamin E, important for the normal functioning of the prostate, involved in the synthesis of various anabolic hormones in the body including insulin, testosterone and growth hormone, and necessary for the breakdown of alcohol in the body, alcohol dehydrogenase. **Magnesium is necessary** in maintaining the normal function of the nervous system and heart muscle, has a vasodilation effect, stimulates bile secretion, and increases the motor activity of the intestines, which helps to eliminate cholesterol from the body.

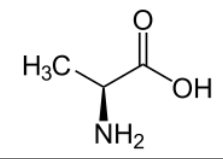
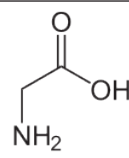
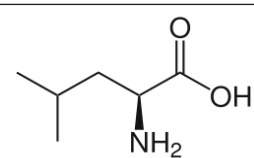
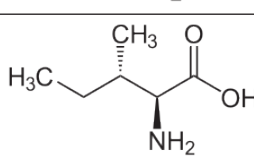
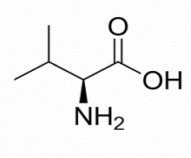
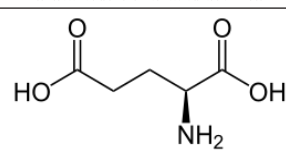
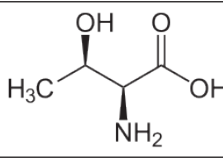
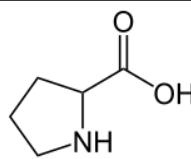
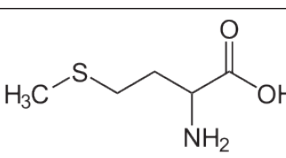
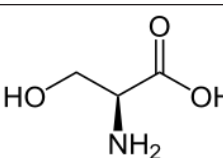
Table 2 – Composition of macro-micro elements from the ash of *A. sublessingiana*

Element	Cu	Zn	Cd	Pb	Fe	Ni	Mn	K	Na	Mg	Ca
%	0.0810	0.126	0.010	0.060	4.984	0.0072	0.347	47.31	4.89	41.91	10.82

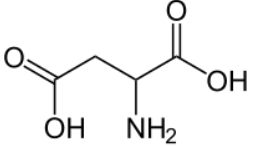
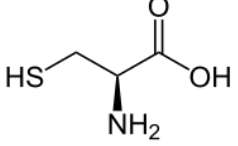
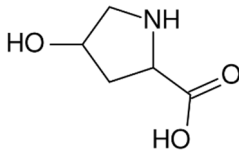
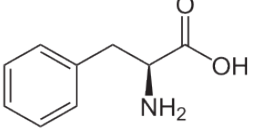
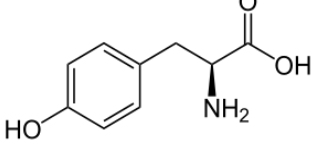
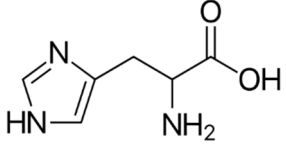
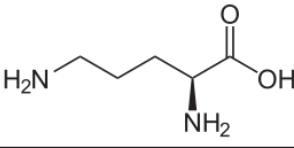
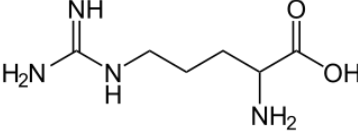
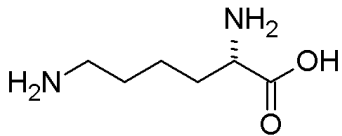
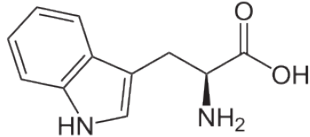
In the composition of amino acids mainly was glutamate (2640 mg/100g), aspartate (1120 mg/100g) and alanine (890 mg/100g) (Table 3). Glutamic acid is used as a chiral building block in organic synthesis, in particular, the dehydration of glutamic acid leads to its lactam-pyroglutamic acid (5-oxoproline), which is a key precursor in the synthesis of unnatural amino acids, heterocyclic compounds, biologically active compounds and so forth. Aspartate itself and

its salts are used as components of medicines. For example, the drug containing aspartate of potassium and magnesium, is used in the therapy of cardiovascular disorders. α -Alanine is part of many proteins, β -alanine is part of a number of biologically active compounds. Alanine is easily converted into the liver in glucose. This process is called the glucose-alanine cycle and is one of the main ways of gluconeogenesis in the liver.

Table 3 – Amino acid contents of *A. sublessingiana*

№	Amino acids	Molecular formula	Structure	MW	Amount in plant, mg/100g
1	Alanine	$C_3H_7NO_2$		89	890
2	Glycine	$C_2H_5NO_2$		75	452
3	Leucine	$C_6H_{13}NO_2$		131	420
4	Isoleucine	$C_6H_{13}NO_2$		131	390
5	Valine	$C_5H_{11}NO_2$		117	342
6	Glutamate	$C_5H_9NO_4$		147	2640
7	Threonine	$C_4H_9NO_3$		119	320
8	Proline	$C_5H_9NO_2$		115	760
9	Methionine	$C_5H_{11}NO_2S$		149	115
10	Serine	$C_3H_7NO_3$		105	372

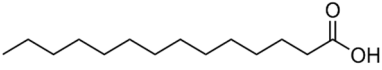
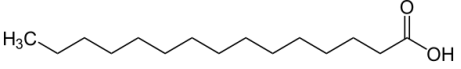
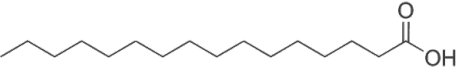
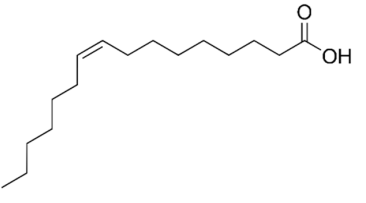
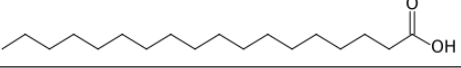
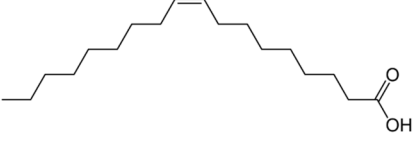
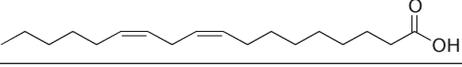
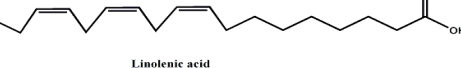
Continuation of table 3

№	Amino acids	Molecular formula	Structure	MW	Amount in plant, mg/100g
11	Aspartate	$C_4H_7NO_4$		133	1120
12	Cysteine	$C_3H_7NO_2S$		121	56
13	Oxyproline	$C_5H_9NO_3$		131	7
14	Phenylalanine	$C_9H_{11}NO_2$		165	326
15	Tyrosine	$C_9H_{11}NO_3$		181	354
16	Histidine	$C_6H_9N_3O_2$		155	270
17	Ornithine	$C_5H_{12}N_2O_2$		132	2
18	Arginine	$C_6H_{14}N_4O_2$		174	486
19	Lysine	$C_6H_{14}N_2O_2$		146	318
20	Tryptophan	$C_{11}H_{12}N_2O_2$		204	100

Results of determining the quantitative composition of the fatty acids showed that in *A. sublessingiana* from the major contents were: linoleic acid $C_{18:2}$ (69.1%) and oleic acid $C_{18:1}$ (18.3%) (Table 4). Palmitic acid is used in the production of stearin, detergents, cosmetics, lubricating oils and plasticizers; calcium palmitate is used as a component of the com-

positions for hydrophobization of tissues, skin, wood, emulsifier in cosmetic preparations, and lubrication in the production of tablets. Increased consumption of linoleic acid associated with dietary recommendations may reduce the risk of cardiovascular disease. Linoleic acid has a long-term positive effect on the prevention of type 2 diabetes mellitus.

Table 4 – Fatty acid contents of *A. sublessingiana*

№	Fatty acids	Molecular formula	Structure	MW	Amount in plant, %
1	Meristic acid $C_{14:0}$	$C_{14}H_{28}O_2$		228	0.7
2	Pentadecanoic acid $C_{15:0}$	$C_{15}H_{30}O_2$		242	1.2
3	Palmitic acid $C_{16:0}$	$C_{16}H_{32}O_2$		256	5,7
4	Palmitoleic acid $C_{16:1}$	$C_{16}H_{30}O_2$		254	0.3
5	Stearin acid $C_{18:0}$	$C_{18}H_{36}O_2$		284	4.2
6	Oleic acid $C_{18:1}$	$C_{18}H_{34}O_2$		282	18.3
7	Linoleic acid $C_{18:2}$	$C_{18}H_{32}O_2$		280	69.1
8	Linolenic acid $C_{18:3}$	$C_{18}H_{30}O_2$	 Linolenic acid	278	0.5

Conclusion

In conclusion, we investigated the main bioactive chemical contents of the whole plant *Artemisia sublessingiana* in terms of its moisture content (10.00 %), total ash (12.42 %), and extractives (22.88 %) as well as identified the composition of the macro- and microelements from its ash. Eleven macro- and

microelements in the ash of *A. sublessingiana* were analyzed using the method of multi-element atomic emission spectral analysis in the “Center of Physico-Chemistry methods of research and analysis”, and the main elements were K (47.310 %), Ca (41.910 %), Fe (4.984 %), Zn (0.126 %), Mg (0.347 %). Farther, 8 fatty and 20 amino acids were identified from the chemical investigation of the medicinal plant.

Moreover, Linoleic acid C_{18:2} (69.1%) and oleic acid C_{18:1} (18.3 %) were recorded as the main components of the fatty acids, while glutamate (2640 mg/100g), aspartate (1120 mg/100g) and alanine (890 mg/100g) were determined as the main amino acid components.

Acknowledgement

The work was supported by grants from Ministry of Education and Science of Kazakhstan (0118PK00458).

References

- Mukhitdinov N.M., Parshina G.N. (2002) Medical plants.
- Bora, K.S., Sharma, A. (2011) The genus *Artemisia*: A comprehensive review. *Pharm. Biol.* vol. 49, pp. 101–109.
- Mukhitdinov N.M., Mamurova A.T. (2013) Medical plants.
- Ahuja A., Yi Y.S., Kim M.Y., Cho J.Y. (2018) Ethnopharmacological properties of *Artemisia asiatica*: A comprehensive review. *Journal of Ethnopharmacology*, pp.117-128.
- Bayzakova G. L. (2016) Investigation of chemical compounds of *Artemisia Dracunculus*.
- Aitkazovich N. (2008) Research of chemical constituents of *Artemisia Leucodes* and *Artemisia Pontica*.
- Nosratpour M., Jafari S.M. (2018) Bioavailability of Minerals (Ca, Mg, Zn, K, Mn, Se) in Food Products. *Reference Module in Food Science*.
- Taghi Gharibzahedi S.M., MahdiJafar S. (2017) The importance of minerals in human nutrition: Bioavailability, food fortification, processing effects and nanoencapsulation. *Trends in Food Science & Technology*, vol. 62, pp.119-132
- Mc Dougall J. (2002) Plant Foods Have a Complete Amino Acid Composition. *Circulation*, vol. 105, iss. 25. pp. 197.
- Schagen Silke K., Vasiliki A. Zampeli, E. Makrantonaki and Christos C. Zouboulis. (2012) Discovering the link between nutrition and skin aging. *Dermatoendocrinol, iss. 4, no. 3, pp. 298-307.*
- Doni C, Sharma P, Saikia G, Longvah T. (2018) Fatty acid profile of edible oils and fats consumed in India, *Food Chemistry*, vol. 238, pp. 9-15.
- Baiseitova M.A., Aisa H., Jenis J. (2015) Chemical constituents of *Dracocephalum nutans*. *International Journal of Biology and Chemistry*, vol. 8, iss. 2, pp. 90-97.
- Abilova Zh.A., Baiseitova A.M., Jenis J. (2017) Investigation of chemical constituents of *Bergeria Crassifolia*. “News of the NAS RK, Series of Chemistry and Technology”, pp. 24-30.
- Muzichkina R.A., Abilov Zh.A., Korulkin D.Yu. (2010) Basics of Chemical Natural Compounds. Almaty.
- Burasheva G.Sh., Eskalieva B.K., Kipchakbayeva A.K. (2016). Medical plants of Kazakhstan. Almaty.
- Altunkaya A., Yildirim B., Ekici K., Terzioğlu O. (2014) Determining essential oil composition, antibacterial and antioxidant activity of water wormwood extracts. *The Journal of FOOD*, vol. 39, iss. 1, pp. 17-24.
- Shafi G., Hasan T.N., Syed N.A., Al-Hazzani A.A., Alshatwi A.A. (2012) *Artemisia absinthium* (AA) a novel potential complementary and alternative medicine for breast cancer. *Journal Molecular biology reports*, vol. 39, iss. 7, pp. 7373–7379.
- Gohari A.R., Kurepaz-Mahmoodabadi M., Saeidnia S. (2013) Volatile oil of *Artemisia santolina* decreased morphine withdrawal jumping in mice. *Journal Pharmacognosy Res.*, vol. 5, pp.118-120.
- Martinez-Diaz R.A., Ibáñez-Escribano A., Burillo J., Heras L.D.L., Prado G.D. (2015) Trypanocidal, trichomonocidal and cytotoxic components of cultivated *Artemisia absinthium* Linnaeus (Asteraceae) essential oil. *Journal Mem Inst Oswaldo Cruz*, vol. 110, pp. 693-699. (in Brazil)
- Lee J.Y., Chang E.J., Kim H.J., Park J.H., Choi S.W. (2002) Antioxidative flavonoids from leaves of *Carthamus tinctorius*. *Arch Pharm Res*, vol. 25, pp. 313-319.

IRSTI 31.23.99

¹Y. Mekesh, ¹G.A. Seitimova, ²Y.S. Ikhsanov, ¹Y.A. Litvinenko,
¹G.Sh. Burasheva, ²M.K. Nauryzbaev, ³X.A. Aisa

¹Al-Farabi Kazakh National University, Almaty, Kazakhstan

²Center for Physical and Chemical Methods of Research and Analysis, Almaty, Kazakhstan

³The Xinjiang Technical Institute of Physics and Chemistry, Xinjiang, China

Development of a method for isolating carotenoids from tomato mass

Abstract. The article discusses a method for isolating carotenoids from tomato paste unsuitable for use in the food industry. It is known that the content of lycopene in tomatoes of various varieties varies in wide ranges, therefore, to obtain a natural preparation of lycopene, it is necessary to select varieties of tomatoes with its high content. Carotenoids are practically the only and relatively affordable source of vitamin A (retinol), and in most cases, their use does not lead to an overdose of this vitamin. It should also be noted that despite the wide range of biological activity of carotenoids and the fact that the substances of this class are non-toxic, readily available and relatively cheap to obtain, only some foreign medicines based on β -carotene are known (usually in combination with vitamins E and C). However, the development of effective means of drug therapy based on this class of compounds requires a detailed comparative study of their biological activity. Currently, carotenoids such as beta-carotene, lycopene, lutein, and astaxanthin have been widely used as biologically active components. This is due to their antioxidant, immunostimulating, anticarcinogenic and other features. The difficulty of isolating carotenoids is that representatives of this class in the plant world are in the form of associates with various biopolymers. One of the important organic compounds of natural origin is a fat-soluble carotenoid – lycopene. It is a tetraterpene, which consists of eight isoprene units, a valuable food coloring and antioxidant. The special value of lycopene is that, being a strong antioxidant, it effectively helps to reduce the concentration of harmful cholesterol in the blood. Taking lycopene, a person enhances his defense related to the violation of acid-base balance in the body, as well as problems of the prostate and potency. Also, according to several studies, lycopene can slow down the aging process. We have developed a method for the isolation of lycopene and β -carotene from the tomato mass, selected the optimal extraction conditions. Of all the tested solvents, the optimal extractants were: methyl chloride, acetone and chloroform, since the carotenoids are most completely extracted in these solvents. The extraction process, the amount of carotenoids from the tomato mass was carried out by hot maceration. Also, methods of standardization of isolated substances have been developed; UV-spectrometry has been selected as the most convenient and sufficiently accurate method.

Key words: tomato masses, carotenoids, lycopene, extraction, UV spectrometry

Introduction

Currently, it is well known that reactive oxygen species and free radicals are actively involved in the pathogenesis of many diseases. The flow of free radical reactions in the lipid phase of biomembranes leads to a violation of their physicochemical properties and changes in the operation of membrane enzyme systems.

Under normal conditions, aerobic organisms are protected from such effects by the coordinated functioning of various antioxidant systems, as well as a certain correspondence between the rates of metabolic processes and catabolism occurring in the cell.

However, during shifts in the stationary course of radical processes, the modulation of the antioxidant status of the organism is required. In this regard, a great interest has recently manifested itself in carotenoids – natural pigments synthesized by plants and microorganisms.

Carotenoids are organic compounds made up of eight isoprene fragments. The activity of carotenoids, as antioxidants, is associated with the presence of a functional polyene chain in them. The main function of carotenoids in the plant cell is to protect its structures from the damaging effects of free radicals formed during photosynthesis. In animals, carotenoids are not synthesized *in vivo*; however, when

ingested with a plant diet and involved in cell metabolism, they exhibit a certain biological activity. In addition to the provitamin function recently detected in β -carotene and other carotenoids, antioxidant activity helps to explain their role in preventing the development of cataracts, radiation damage, the occurrence and development of cardiovascular diseases, and in inhibiting mutagenesis and transformation of eukaryotic cells [1].

Carotenoids are practically the only and relatively affordable source of vitamin A (retinol), and in most cases their use does not lead to an overdose of this vitamin, because the synthesis of retinol during the metabolism of carotenoids is enzymatically limited [2].

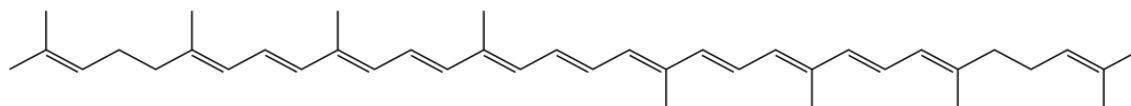
It should also be noted that despite the wide range of biological activity of carotenoids and the fact that the substances of this class are non-toxic, readily available and relatively cheap to obtain, only some foreign medicines based on β -carotene are known (usually in combination with vitamins E and C).

In the Republic of Kazakhstan, drugs, both on the basis of β -carotene, the most popular representative of the carotenoid class, and on the basis of its structural analogues, do not exist. Along with this, it is known that other carotenoids similar in structure to β -carotene, such as astaxanthin, canthaxanthin and lycopene, are stronger antioxidants [1].

However, the development of effective means of drug therapy based on this class of compounds requires a detailed comparative study of their biological activity.

Currently, carotenoids such as beta-carotene, lycopene, lutein, and astaxanthin have been widely used as biologically active components. This is due to their antioxidant, immunostimulating, anticarcinogenic and other features.

The body's need for a rational and balanced diet increases dramatically. An important role in the regulation of metabolic processes is played by such components of foodstuffs as biologically active lipids, and, in particular, carotenoids. Existing methods for the isolation of drugs – the amount of carotenoids from plant materials are few. The difficulty of isolating carotenoids is that representatives of this class in the plant world are in the form of associates with various biopolymers. One of the important organic compounds of natural origin is a fat-soluble carotenoid – lycopene. It is a tetraterpene, which consists of eight isoprene units, a valuable food coloring and antioxidant. The presence of 11 conjugated double bonds causes the light-absorbing property of lycopene and its ability to easily oxidize, therefore, during the oxidation of lycopene, epoxides of different composition are formed. Lycopene absorbs all wavelengths of visible light, so it has a red color [3].



Lycopene

The special value of lycopene is that, being a strong antioxidant, it effectively helps to reduce the concentration of harmful cholesterol in the blood. Taking lycopene, a person enhances his defense related to the violation of acid-base balance in the body, as well as problems of the prostate and potency. Also, according to several studies, lycopene can slow down the aging process. The main function of lycopene in the human body is antioxidant. Reducing oxidative stress slows down the development of atherosclerosis, and also provides DNA protection that can prevent oncogenesis. The consumption of lycopene, as well as lycopene-containing products leads to a significant decrease in markers of oxidative stress in humans. Lycopene is the most powerful an-

tiioxidant carotenoid present in human blood. Several pilot studies suggest a signaling role for lycopene in relation to certain cell cultures. In particular, it is assumed that lycopene can slow down cell proliferation as a signal metabolite [3-7].

Lycopene – refers to carotenoids and is synthesized by plants, algae and fungi. It has a thick pink color, turning into a purple hue, which is of great interest for the food industry, which is in dire need of natural harmless dyes of this hue. The use of lycopene for imparting pink color to food products provides them with an improved presentation and allows you to simultaneously enrich the products with valuable biological properties that contribute to the preservation of health [8-9].

Materials and methods

Tomato mass has a dark red color, with a specific smell.

The object of study is tomato paste with expired shelf life, prepared according to the following procedure:

Tomato paste was dried at room temperature for 10 days;

the resulting product has a burgundy color. Figure 1 shows the object of study.



Figure 1 – Dried Tomato Mass

Selection of conditions for the isolation of carotenoids: To isolate carotenoids from the tomato mass, work was carried out to select the optimal extractant.

For the extraction process we have chosen the following solvents: Acetone, hexane, ethanol, chloroform and methylene chloride

The extracts were prepared according to the following procedure: A tomato (exact weight) mass and extractant were placed in a 25 ml flask in a ratio of 1:5, then the flasks were closed and placed in a cabinet without sunshine for 24 hours.

The extract obtained after infusion must be filtered from the insoluble fraction.

Then the obtained extracts need to be placed in porcelain cups brought to constant weight and the extractant is completely evaporated, then, based on the

weight of the dry residue, to calculate the proportion of extractives.

In parallel, according to a similar method, samples are prepared for qualitative and quantitative analysis by spectrometry and thin layer chromatography.

Carotenoid separation and lycopene detection in the proposed extracts: To this end, we have carried out work on the selection of systems for dividing the sum of carotenoids. The following solvents were used to prepare the systems: chloroform, hexane, acetone, ethyl, butyl alcohol, methyl chloride and acetic acid.

The deceleration rate (Rf) is determined - a characteristic of the relative speed of movement of a component in a thin layer (also known as retention coefficient (Rf) in planar chromatography). The deceleration factor is equal to the ratio of the distance from the sample application point to the center of the adsorption zone and the distance traveled by the solvent front from the sample application point. For chromatography, we used the solvent systems hexane - acetone and hexane - chloroform.

In addition, a quantitative analysis of carotenoids and lycopene was performed by UV spectrophotometry by the following method:

Approximately 1 g (exact mass) of the drug is dissolved in a mixture of these solvents in a 50 ml volumetric flask, diluted to the mark with the same mixture and stirred.

The optical density of the solution is measured at a wavelength of 450 nm in a cuvette with a layer thickness of 10 mm, using as a reference solution a mixture of hexane-ethyl alcohol 96%.

In parallel, measure the optical density of the solution with potassium dichromate.

Results and discussion

The results of the study of the extract content of substances from the tomato mass and data on the qualitative composition of carotenoids are presented in table 1 and in figure 2.

Table 1 – The effect of solvents on the quality of the extraction of carotenoids in tomato mass

Solvents	Indicators			
	The amount of extractives, %	Carotenoids	Lycopene	Terpenes and other classes of compounds
Acetone	33,15	++	++	+++
Ethanol	34,20	+	+	+++
Hexane	30,35	+	+	+++

Continuation of table 1

Solvents	Indicators			
	The amount of extractives, %	Carotenoids	Lycopene	Terpenes and other classes of compounds
Chloroform	34,45	++	++	+++
Methyl chloride	38,25	+++	+++	+++

Note: "+" intensity of spots on a thin-layer chromatogram

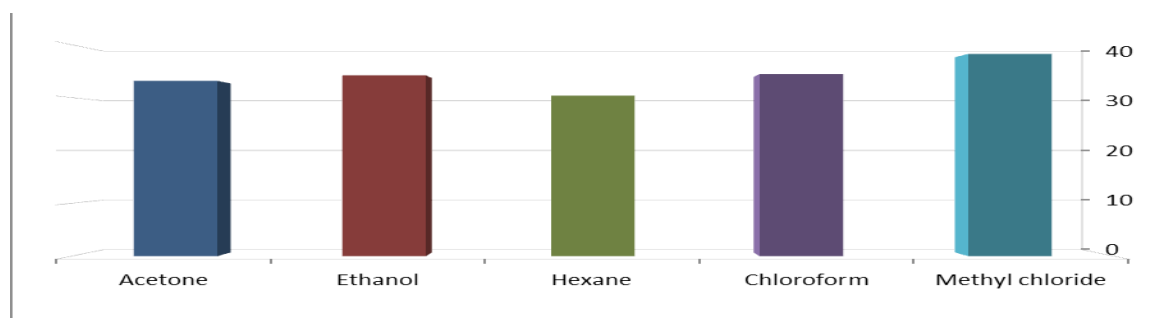


Figure 1 – The yield of extractives from raw materials, depending on solvents



Figure 2 – Analysis of carotenoid concentrate from tomato mass by thin layer chromatography

Of all the tested solvents, the optimal extractants were: methyl chloride, acetone and chloroform, since the carotenoids are most completely extracted in these solvents.

The extraction process, the amount of carotenoids from the tomato mass was carried out by hot maceration.

The basic flow chart of the production of the amount of carotenoids from tomato includes the following technological processes (TP):

TP.1 – harvesting plant materials;

TP.2 – drying of vegetable raw materials in a ventilated room at a temperature of 200 ° C without direct sunlight;

TP.3 – control of the good quality of crushed vegetable raw materials;

TP.4 – grinding of plant materials at the mill-carved type SM 100 comfort with a 5 liter receiver, rotor and filter bag to a particle size of 1-2 mm;

TP.5 – supercritical fluid extraction using a Thar SFE-1000 instrument;

TP.6 – removal of ballast substances;

TP.7 – final purification (chromatographic analysis) and isolation of the final product.

The extract obtained is concentrated and subjected to chromatography on a thin layer of silica gel.

Carotenoid separation and lycopene detection in the proposed extracts. To this end, we have carried out work on the selection of systems for dividing the sum of carotenoids. The following solvents were used to prepare the systems: chloroform, hexane, acetone, ethyl, butyl alcohol, methyl chloride and acetic acid.

The deceleration rate (Rf) is defined as a characteristic of the relative speed of movement of a component in a thin layer (also known as retention coefficient (Rf) in planar chromatography). The deceleration factor is equal to the ratio of the distance

from the sample application point to the center of the adsorption zone and the distance traveled by the solvent front from the sample application point.

Currently, we have studied about 40 systems, of which the best were: hexane – acetone (9: 1), hexane – chloroform (9: 1) and it was established that in

the system hexane – acetone (10: 0.5) lycopene has $R_f = 0.62$.

In addition, a quantitative analysis of carotenoids and lycopene was performed by UV spectrophotometry.

The research results are summarized in table 2.

Table 2 – The quantitative content of carotenoids in tomato mass (mg%)

λ , nm	β -carotene	Lycopene
474	-	13,30
474	-	13,37
474	-	13,36
450	15,14	-
450	14,86	-
450	14,88	-

It was established that at $\lambda = 474$ nm, the content of lycopene is 13.34 mg%, and the content of β -carotene at $\lambda = 450$ nm was 14.96 mg%.

Conclusions

– Thus, the tomato mass, obtained from tomato paste, which has expired, dried under a plaster, at room temperature for 10 days. Tomato mass has a dark red color, a specific smell.

– Tomato pulp was treated with hexane, ethyl alcohol, acetone – ethyl alcohol mixture at a ratio of (5: 1) and methyl chloride. The most saturated extract is obtained by methyl chloride. The number of extractives in the studied solvents.

– Using the TLC method, a system was selected where it is possible to qualitatively determine the presence of lycopene and other carotenoids in the plant object.

– Quantitative analysis of carotenoids and lycopene was determined by UV spectrophotometry.

References

1. Nesterova O.A. Antioksidantnye i gipolipidemicheskie svoystva likopina: ... avtoref. kand. biol. nauk.: 03.00.04 – Biohimija 14.00.16 – Patologicheskaja fiziologija – M.: NII FHM MZ RF, 1996. – 16 s. (in Russian)
2. Kuregjan A.G., Pechinskij S.V., Zilfikarov I.N. Sposoby poluchenija karotinoidov, lekarstvennyh preparatov i biologicheski aktivnyh

dobavok k pishhe na ih osnove (obzor) // *Zhurn. Farmaceuticheskaja tehnologija*. 2014. – Vyp. 6, №1. – S. 36-45 (in Russian). Hartal D. Lycopene: a bioactive carotenoid and its use in foods // *The Intern. Review of Food Science and Technology*. – 2006. – P. 75-78.

3. Li W., Wang G., Lu X., Jiang Y., Xu L., Zhao X. Lycopene ameliorates renal function in rats with streptozotocin-induced diabetes // *Int. J. Clin. Exp. Pathol.* – 2014. – Vol. 7(8). – P. 5008-5015.

4. Visioli F., Riso P., Grande S., Galli C., Porrini M. Protective activity of tomato products on in vivo markers of lipid oxidation // *Eur. J. Nutr.* – 2003. – Vol. 42 (4). – P. 201-206.

5. Devaraj S., Mathur S., Basu A., Aung H.H., Vasu V.T., Meyers S., Jialal I. A dose-response study on the effects of purified lycopene supplementation on biomarkers of oxidative stress // *J. Am. Coll. Nutr.* – 2008. – Vol. 27(2). – P. 267-273.

6. Rao A.V., Agarwal S. Role of Antioxidant Lycopene in Cancer and Heart Disease // *Journal of the American College of Nutrition*. – 2000. – Vol. 19, № 5. – P. 563-569.

7. Narushin V.G. Funkcional'nye hlebobulochnye izdelija s dobavleniem natural'nyh karotinoidov // *Produkty i ingredijenty*. – 2007. – № 6. – S. 45 (in Russian).

8. Nich P. Funkcional'nye produkty. Likopin kak funkcional'naja dobavka v varenye i livernye kolbasy // *Mjasnoj Biznes*. 2007. – №6. – S. 26-30 (in Russian).

IRSTI 31.23.99

¹D.S. Nurpeisova, ¹M. Toktarbek, ^{1*}G.A. Seitimova, ¹B.K. Yeskaliyeva,
¹G.Sh. Burasheva, ²M. Iqbal Choudhary

¹Al-Farabi Kazakh National University, Faculty of Chemistry and Chemical Technology, Almaty, Kazakhstan

²H.E.J. Research Institute of Chemistry, International Center for Chemical and Biological Sciences,
University of Karachi, Karachi-75270, Pakistan

*e-mail: sitigulnaz@mail.ru

Phytochemical analysis of *Petrosimonia sibirica* grown in Kazakhstan

Abstract. In this study, complete phytochemical analyses of the component composition of *Petrosimonia sibirica* was conducted for the first time. Phytochemical screening showed the presence of a variety of primary and secondary metabolites. The data for quantitative determination of biologically active compounds were presented. The qualitative composition of amino, fatty acids of the plant *Petrosimonia sibirica* has been studied by using the method of paper chromatography (PC) and thin-layer chromatography (TLC), their quantitative composition of amino, fatty acids have been identified by gas chromatography. The composition of 20 amino, 8 fatty acids of *Petrosimonia sibirica*, family *Chenopodiaceae* have been established. The major amino acids in studied plant were glutamic acid (2.440%), alanine (0.618%), aspartic acid (1.254%), arginine (0.405%), tyrosine (0.340%), and proline (0.306%). The dominant fatty acids in plant with respect to quantity were oleic (48.3%) and linoleic (26.7%) acids. In order to optimize the extraction process technological parameters (extracting solvent, a ratio between solvent and solid plant material and process temperature) were selected. The most suitable solvent is 70% ethyl alcohol, solid – solvent ratio (1: 6-8), extraction time (3 days), and extraction temperature (20-25 °C). In addition, Kazakh species of *Petrosimonia sibirica* plant are valued as a rich source of saponins and flavonoids. Quercetin 3-O-β-D-glucopyranoside (isoquercitrin) was isolated from *Petrosimonia sibirica*. Flavonoid glycoside was identified by ¹H NMR, ¹³C NMR, and MS, and compared with the data in the literature. The results revealed the presence of medicinally important constituents in the studied plant. Therefore, extracts from these plants could be seen as a good source for useful drugs.

Key words: *Petrosimonia sibirica*, halophytes, amino acids, fatty acids, flavonoids, quercetin 3-O-β-D-glucopyranoside (isoquercitrin).

Introduction

Despite the intensive growth of medicinal products, plants continue to occupy a significant place in the arsenal of medicines, since their lesser side effect, accumulation in the body, as well as the effectiveness in the treatment of certain diseases, have been proved.

The importance of plants is known to us well. The flora of the Republic of Kazakhstan has the richest reserves of plant resources, but it is not used enough in medical practice, which requires more in-depth study and introduction into the domestic medicine of effective medicines derived from plant materials.

Plant cells produce two types of metabolites: primary metabolites involved directly in growth and metabolism (carbohydrates, lipids, and proteins), and

secondary metabolites considered as end products of primary metabolism and not involved in metabolic activity (alkaloids, phenolics, sterols, steroids, essential oils, lignins, and tannins, etc.). They act as defense chemicals [1]. Secondary metabolites are also relevant to medicine and agriculture.

Therefore, the study of the chemical composition of the plant materials, development of methods for the isolation of biologically active substances and the study of biological activity in order to isolate new drugs and herbal remedies is an important task.

Plants of the family *Chenopodiaceae*, which occupy the predominant part of the landscape of the Republic of Kazakhstan, are of great interest. Chemical studies of most plants of this family indicate their high nutritional value. From the literature, it is known that plants growing in arid zones have

an interesting chemical composition and practical significance.

Petrosimonia sibirica (Pall.) Bunge belongs to the family *Chenopodiaceae*, a family comprising of probably about 100 genera and 1400 species, which is represented in Kazakhstan by 47 genera and 218 species. There are 11 species of the plant genus *Petrosimonia*; 10 of these are indigenous to Kazakhstan. *Petrosimonia* is the basic fodder for camels in the autumn [2, 3]. According to literary studies, phenolic compounds, an alkaloid, quinone, lactone, and esters have been isolated from plant *Petrosimonia sibirica*, which grown in China [4, 5]. However, there are no reports on phytochemical analysis of Kazakh species of the plant genus *Petrosimonia*.

The investigation of the chemical constituents from the aerial part of *Petrosimonia sibirica* was reported for the first time.

Materials and methods

Melting points were determined in open capillary tubes on Buchi M-560 melting point apparatus and are uncorrected. NMR spectra were recorded using CD₃OD as solvent on Avance AV 400 MHz Instrument (Bruker Co., Switzerland). Chemical shifts are given in δ (ppm), and coupling constants are reported in Hz. The ¹H, ¹³C-NMR and ESI-MS spectra were recorded at HEJ Research Institute of Chemistry, University of Karachi, Pakistan. Thin layer chromatography (TLC) was performed by using silica gel plates Alugram SIL G/UV 254 (Macherey-Nagel, Germany) and identification of the spots on the TLC plate was carried out by spraying *ceric sulfate*.

Plant material. The aerial part of *Petrosimonia sibirica* was collected during flowering period from saline soils at Karatal district of Almaty region, Kazakhstan. The plant material was taxonomically identified, authenticated by professors of botany at Institute of Botany and Phytointroduction, Almaty. The aerial parts of the plant were air dried, powdered to particle size in the range 6.0-8.0 mm, according to regulatory documents, sieved, weighed and transferred into airtight containers with proper labeling for future use.

Extraction and Isolation. The air-dried and finely powdered aerial parts of the plant (1.0 kg) was exhaustively extracted by maceration for 72 hrs. at room temperature with ethanol (70%) till complete exhaustion. Extraction is repeated twice. The ethanolic extract was concentrated under reduced pressure using rotary vacuum evaporator to obtain a dark brown residue (130 g). The combined extract was

dissolved in a least amount distilled water/alcohol mixture (9:1) and successively extracted with hexane, chloroform, ethyl acetate, and *n*-butanol. Each extract was separately evaporated to dryness using rotary vacuum evaporator under reduced pressure at a temperature not exceeding 45 °C. Each of the obtained fractions was subjected to thin layer (TLC) and paper (PC) chromatographic techniques and then column chromatography for isolation of its major constituents. The ethyl acetate soluble extract of *Petrosimonia sibirica* (28 g) was chromatographed on silica gel column using different ratio of chloroform and methanol in gradient elution manner followed by Sephadex LH-20 with MeOH to yield 17 mg of compound 1.

Acid hydrolysis of the compound carried by 2% HCl on a boiling water bath, while mild acid hydrolysis was sampled at a certain time interval. The hydrolysis products were identified by m.p., PC, and TLC in appropriate solvent systems with authentic samples.

Fatty acids analysis. The composition of the saturated and unsaturated carboxylic acids (fatty acids) in plants is determined by gas-liquid chromatography apparatus Carlo-Erba-4200 using helium as a carrier gas, flame ionization detector, carrier gas velocity 30 ml/min, detector temperature 188 °C, oven temperature 230 °C, adsorbent Cellite 545 on Chromosorb WAW. The chloroform extract of plant species is added to 10 ml of methanol and 2-3 drops of acetyl chloride and then carried out methylation at 60-70 °C in a special system for 30 minutes. Methanol was removed using a rotary evaporator, and the samples are extracted with 5 mL of *n*-hexane and analyzed by gas chromatography for 1 hour [6].

Amino acids analysis. Analysis of amino acids was carried out chromatographically using helium as carrier gas, flame ionization detector 300 °C and condenser temperature 250 °C on Chromosorb WAW. Aqueous extract of the plant was hydrolyzed in HCl for 24 hours. The resulting hydrolyzate was evaporated to dryness in a rotary evaporator at 40 °C, after centrifugation at 2.5 thousand revolutions per minute the resulting precipitate was dissolved in sulfosalicylic acid and amino acids are eluted through an ion exchange column Dausk-50. On freshly obtained elutes 2, 2-dimethoxypropane and propanol saturated with HCl were added. The resulting mixture is heated at 110 °C for 20 minutes, then addition of a freshly prepared acylating reagent (1 volume of acetic anhydride and 2 volumes of triethylamine and 5 volumes of acetone), evaporation of the sample to dryness, addition of ethyl acetate and saturated aqueous solution

of NaCl. Finally, the ethyl acetate layer is analyzed on the amino acid analyzer (Carlo-Erba) [7].

Vitamin analysis. The contents of vitamins A (retinol) and E (tocopherol) were determined by fluorimetry on a spectrofluorometer (Hitachi, Japan). The vitamin C content in the biological samples was determined by titration [8-10]. Fatty and amino acids, vitamin analyses were performed at the laboratories of The Kazakh Academy of Nutrition.

Results and discussion

The moisture content, total ash, extractives, qualitative and quantitative contents of biologically active constituents of *Petrosimonia sibirica* were determined according to methods reported in the State Pharmacopoeia of the Republic of Kazakhstan I edition techniques [11].

Moisture content is an important factor because the appearance and stability of dried plants depend on the amount of water they contain and the propensity of microorganisms to grow depends on their water content. Medicinal plant materials should not contain moisture above the permissible norms; since at high humidity, during storage conditions are created that contribute to a decrease in its quality. For most types of medicinal plant materials, the permissible limit of moisture is usually 12–15%. The results in table 1 showed low moisture content of the aerial part in *Petrosimonia sibirica* (7.8%).

The amount and composition of ash remaining after combustion of plant material vary considerably according to the part of the plant, age, environment etc. The ash content is a measure of the total amount of minerals present within a plant, whereas the min-

eral contents are a measure of the amount of specific inorganic components present within it [12].

The extractives of medicinal plants conventionally called complex organic and inorganic substances extracted from plant material with an appropriate solvent and quantified as a dry residue.

The methods of two- and one-dimensional chromatography on paper, as well as TLC in various solvent systems established for the first time that the following main groups of biologically active substances are contained in the studied plant: flavonoids, amino acids, alkaloids, saponins, coumarins, and carbohydrates.

Vitamins are defined as relatively low-molecular-weight compounds which humans, and for that matter, any living organism that depends on organic matter as a source of nutrients, require small quantities for normal metabolism. There are more than 30 such substances, and all of them are vital for the human body, entering into the composition of all tissues and cells, activating and determining the course of many processes. Vitamins increase the body's resistance to infectious diseases, inhibit the aging process, determine the activity of enzymes, participate in the metabolism of amino acids, fatty acids, hormones, microelements [10]. Vitamins are classified as either fat-soluble (vitamins A, D, E and K) or water-soluble (vitamins B and C). The results indicated that vitamin C dominated over vitamins E and A (table 1).

The data quantitative determination of *Petrosimonia sibirica* is shown in Table 1. The results revealed the presence of biologically active compounds in the plant studied.

From table 1, it could be seen the predominance of saponins and flavonoids in *Petrosimonia sibirica*.

Table 1 – Qualitative and quantitative screening of the powdered aerial parts of *Petrosimonia sibirica*

Plant	Contents, %												
	Moisture content	Ash	Extractives materials 70% – aqueous alcohol	Saponins	Flavonoids	Tannins	Alkaloids	Carbohydrates	Organic acids	Coumarins	Vitamin A	Vitamins C	Vitamins E
<i>Petrosimonia sibirica</i>	7.8	24.7	52.9	0.6	2.0	0.1	0.4	4.2	3.5	0.3	0,00016	0,011	0,0022

It is known that amino acids occupy a special place in modern medicine. By their action, many of them belong to central neurotransmitters, both stimulating and inhibiting the transmission of nerve impulses in the synapses of the central nervous system, which determines their pharmacological orientation. In total, about 300 amino acids have been found in nature, however, only 20, which are called protein or proteinogenic amino acids, are found in proteins. Having a wide range of pharmacological actions and the ability to enhance the digestibility of other substances, amino acids are attracting more and more attention of researchers as potential drugs. One of the most important func-

tions of amino acids is their participation in the synthesis of proteins that perform catalytic, regulatory, spare, structural, transport, protective and other functions [13, 14].

GC analysis of the amino acids constituents of the aerial part of *Petrosimonia sibirica* (table 2) revealed the presence of twenty amino acids but differs in their percentages; the major amino acids in studied plant were glutamic acid (2.440%), alanine (0.618%), aspartic acid (1.254%), arginine (0.405%), tyrosine (0.340%), and proline (0.306%).

Petrosimonia plants can be used in autumn and winter as wild feed for sheep and cattle owing to the high contents of glutamic and aspartic acids.

Table 2 – Amino acids composition of *Petrosimonia sibirica*, %

Amino acids	Relative percentage %	Amino acids	Relative percentage %
Alanine	0.618	Cysteine	0.032
Glycine	0.296	Oxyproline	0.001
Valine	0.274	Phenyl alanine	0.290
Leucine	0.380	Glutamic acid	2.440
Isoleucine	0.362	Ornithine	0.001
Threonine	0.202	Tyrosine	0.340
Serine	0.204	Histidine	0.260
Proline	0.306	Arginine	0.405
Methionine	0.060	Lysine	0.202
Aspartic acid	1.254	Tryptophan	0.094

Probably, the appearance of fatty acids in plant extract is associated with the hydrolysis of lipids in plants. Fatty acid glycerides are physiologically active, especially glycerides of some unsaturated fatty acids. These include linoleic and linolenic acids, which are necessary for the vital activity of a living organism (vitamin F factor) [15, 16].

Fatty-acid analyses for studied plant detected eight fatty acids (table 3). The dominant fatty acids in studied plant with respect to quantity were oleic (48.3%) and linoleic (26.7%) acids. This fact and the rapidly renewable properties together with high drought and freezing resistance and broad distributions on low and highly saline soils, i.e., those of little value for agriculture, supported our hypothesis about the feed value of *Petrosimonia* plants.

In order to optimize the extraction process of biologically active compounds from *Petrosimonia sibirica* technological parameters were selected. Extracting solvent, a ratio between solvent and solid

plant material and process temperature are the most important optimum extraction parameters. A quantitative measure for this is the valuable compounds extraction yield from plant material. The most suitable solvent is 70% ethyl alcohol, solid – solvent ratio (1: 6-8), extraction time (3 days), and extraction temperature (20-25 °C), under these conditions, up to 60% of biologically active compounds are extracted.

Powdered plant material of *Petrosimonia sibirica* was soaked in 70% ethanol, and then ethanolic extract was concentrated. It was then divided into *n*-hexane, chloroform, ethyl acetate, *n*-butanol, and aqueous fractions.

The *n*-hexane fraction contains large amounts of chlorophyll which hindered the isolation of its contents, together with fatty acids, sterols, and resins. The chloroform fraction has shown the presence of several secondary metabolites such as coumarins, alkaloids along with fat-soluble vitamins. The ethyl

acetate fraction was found rich in polyphenolics and terpenoids. Saponins were found in the *n*-butanol fraction.

Table 3 – Composition of the saturated and unsaturated carboxylic acids (fatty acids) in *Petrosimonia sibirica*, %

Fatty acids	Content, %
Linoleic acid [C _{18:2}]	26.7
Oleic acid [C _{18:1}]	48.3
Palmitic acid [C _{16:0}]	14.7
Stearin acid [C _{18:0}]	5.2
Palmitoleic acid [C _{16:1}]	0.9
Pentadecanoic acid [C _{15:0}]	1.6
Myristic acid [C _{14:0}]	1.3
Linolenic acid [C _{18:3}]	1.3

Since the purpose of this work is to isolate flavonoids, ethyl acetate soluble fraction has been studied more deeply. The ¹H NMR, ¹³C NMR spectrum of compound 1 revealed the characteristic signals of flavonol glycosides. Compound 1 was identified by ESI-MS, which gave molecular ion peak at *m/z* 464, corresponding to the molecular formula C₂₁H₂₀O₁₂.

Compound 1 – yellow crystals, m.p. 230-232 °C, have a dark glow in UV light. IR spectrum (KBr, ν_{max}, cm⁻¹): 3350-3256, 1645, 1115-1061. UV spectrum (MeOH, γ_{max}, nm): 362, 264. The position on the two-dimensional paper chromatogram (*n*-butanol–acetic acid–water (BAW), 40:12.5:29, 6 % acetic acid) of compound indicates their glycosidic nature [17]. From the products of acid hydrolysis of compound 1, the corresponding aglycone was isolated, in the hydrolysate by the PC method using *o*-toluidine as a developer, glucose were identified in comparison with reliable samples.

In the products of alkaline destruction of the aglycone of compound 1, it has been found that rings A have the structure of phloroglucinol, i.e. in the C-5 and C-7 positions, there are free hydroxyl groups, and ring B of compound 1 is defined as protocatechuic acid [18].

¹H NMR (500 MHz, CD₃OD, δ, ppm): 7.68 (1H, d, J=2.0, H-2'), 7.61 (1H, d, H-6'), 7.30 (1H, d, J=8.0, H-5'), 6.64 (1H, d, J=2.0 Гц, H-8), 6.45 (1H, d, J=2.0, H-6), 5.54 (d, J=8.0, H-1').

From the data of ¹H NMR spectroscopy, it follows that carbohydrate residue in compound 1 is in

the β-form. To determine the place of addition of sugar, ¹³C-NMR and HMBC two-dimensional spectra were taken. Based on modern spectral analysis methods and comparison with the literature data, accordingly, compound 1 was proved to be quercetin 3-O-β-D-glucopyranoside (isoquercitrin) [19, 20].

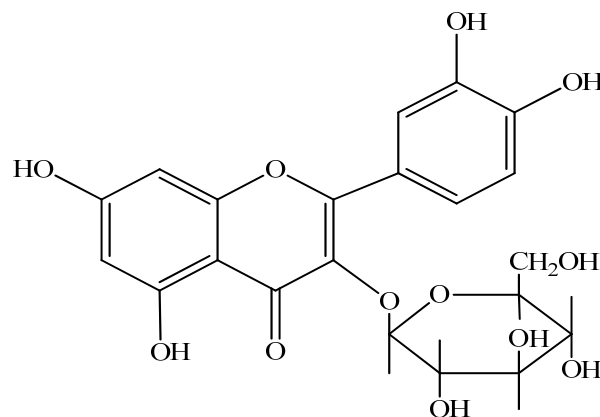


Figure 1 – Quercetin 3-O-β-D-glucopyranoside (Compound 1)

Conclusion

A phytochemical study of *Petrosimonia sibirica* was carried out. The qualitative composition of amino, fatty acids of the plant *Petrosimonia sibirica* has been studied by using the method of paper chromatography (PC) and thin-layer chromatography (TLC), their quantitative composition of amino, fatty acids have been identified by gas chromatography.

Column chromatography of ethyl acetate soluble fraction obtained from the ethanolic extract afforded quercetin 3-O-β-D-glucopyranoside (isoquercitrin), which was identified by comparison of its NMR with reported data. Flavonoid glycoside was isolated from *Petrosimonia sibirica* for the first time.

Acknowledgements

This research was supported and funded by the Ministry of Education and Science of the Republic of Kazakhstan (Grant No. AP05131716).

References

1. Irchhaiya R., Kumar A., Yadav A., Gupta N., Kumar S., Gupta N., et al. (2015) Metabolites in plants and its classification. *World J. Pharm. Pharmacol. Sci*, vol. 4, pp. 287-305.

2. Pavlova N.V. (1960) Flora of Kazakhstan [Flora Kazakhstana], *Akad. Nauk KazSSR*, Alma-Ata; vol. 3, pp. 306-311 (in Russian)
3. Komarov V.L. (1955) Flora of the USSR [Flora SSSR], *Akad. Nauk SSSR*, Moscow, Leningrad; vol. 6, pp. 316-326 (in Russian)
4. Sun W., Ma Z.Y., Zhang X., Yang H.B., Sun W.F. (2015) Secondary metabolites of *Petrosimonia sibirica*. *Chem. Nat. Compd.*, vol. 51, pp. 530.
5. Wang Y., Zhang H., Su X., Yang H.B., Sun W.F. (2016) Flavonoids and phenolic compounds of *Petrosimonia sibirica*. *Chem. Nat. Compd.*, vol. 52, pp. 482.
6. Chamberlain J., Nelson G., Milton K. (1993) Fatty acid profiles of major food sources of howler monkeys (*Alouatta palliata*) in the neotropics. *Experientia*, vol. 49, pp. 820-823.
7. Adams R.F. (1974) Determination of amino acid profiles in biological samples by gas chromatography. *Journal of Chromatography A*, vol. 95 (2), pp. 189-212.
8. Neeld J.B., Pearson W.N. (1963) Macro- and micromethods for the determination of serum vitamin A using trifluoroacetic acid. *The Journal of Nutrition*, vol. 79(4), pp. 454-462.
9. Omaye S.T., David Turnbull J., Sauberlich H.E. (1979) Selected methods for the determination of ascorbic acid in animal cells, tissues, and fluids. *Vitamins and coenzymes*, Part D, pp. 3-11.
10. Pegg R.B., Landen W.O., Eitenmiller R.R. (2010) *Vitamin Analysis. Food Analysis*, pp. 179-200.
11. State Pharmacopoeia of the Republic of Kazakhstan [Gosudarstvennaia farmakopeia Respubliki Kazakhstan], (2008) *Zhibek Joly*, Almaty (in Russian)
12. Seitimova G.A., Alzhanbayeva A.M., Burasheva G.Sh., Yeskaliyeva B.K., Choudhary M.I. (2016) Phytochemical study of *Kochia prostrata*. *International Journal of Biology and Chemistry*, vol. 9 (2), pp. 51-54.
13. McKee T., McKee J.R. (2012) *Biochemistry: The molecular basis of life*, 5th edition. *Oxford University Press*, Oxford, New York.
14. Tiukavkina N.A., Baukov Yu.A. (2004) *Bioorganic chemistry [Bioorganicheskaia khimiia]. Drofa*, Moscow (in Russian)
15. Watson R.R., Fabien De Meester (2016) *Handbook of lipids in human function: Fatty acids. Academic Press and AOCS Press*, USA, 809 p.
16. Kurkin V.A. (2004) *Pharmacognosy: Textbook for Students of Pharmaceutical Higher Educational Institutes [Farmakognoziia]. OOO Ofort*, Samara, pp. 141-186 (in Russian)
17. Mabry T.I., Markham K.R., Thomas M.B. (1970) *The Systematic Identification of Flavonoids. Springer-Verlag*, Berlin-Heidelberg-New-York, pp. 3-14.
18. Burasheva G.S., Mukhamed'yarova M.M., Chumbalov T.K. (1976) Polyphenols of *Alhagi kirgisorum*. III, *Chem. Nat. Compd.*, vol. 12(5), pp. 596.
19. Markham K.R. (1982) *Techniques of flavonoid identification. Academic Press*, London-New York, 113 p.
20. Kim H.Y., Moon B.H., Lee H.J., Choi D.H. (2004) Flavonol glycosides from the leaves of *Eucommia ulmoides* O. with glycation inhibitory activity. *Journal of Ethnopharmacology*, vol. 93(2-3), pp. 227-230.

IRSTI 61.31.57

¹*N.A. Nursapina, ¹I.V. Matveyeva, ¹B.A. Shynybek

¹al-Farabi Kazakh National University, Almaty, Kazakhstan,

*e-mail: nurgulya13@mail.ru

AMP and Ambersep 920 IRA anion exchange resins for recovery of uranium from productive solution

Abstract: In the process of uranium production, one of the most important stages affecting the completeness of uranium extraction from productive solutions is the sorption stage. In order to study the effectiveness of ion exchange resins under dynamic conditions, sorption and desorption characteristics of anion exchangers, which used for recovery of uranium from sulfuric acid production solutions were studied.

In laboratory conditions, sorption and desorption of uranium from productive solution on anion exchange resins of the brands Ambersep 920 IRA and AMP were carried out. During the research work, sorption and desorption characteristics were studied, as well as sorption capacity of the resins. Despite the fact that dynamic exchange capacities of the resins are equal, the sorption characteristics are different. The concentration of uranium in the desorption eluate for Ambersep 920 IRA and AMP was 856.00 and 268.00 mg/l, respectively, which is 5 and 1.5 times higher than the initial concentration of uranium in the productive solution. The most efficient anion exchanger, Ambersep 920 IRA, has been identified, which has good sorption and desorption characteristics compare to AMP.

Key words: uranium industry, ion exchange resins, underground leaching, sorption – desorption of uranium.

Introduction

In contemporary world, the need of electricity is growing every year. These days many countries are view nuclear power as acceptable. According to the IAEA, annual report [1] 447 nuclear power reactors are in operation nowadays. In nearest future 60 more reactors will be built in 15 countries. The global capacity of nuclear power plants will grow by 42% in 2030, by 83% in 2040 and by 123% in 2050, as compared to the level of 2016. The increases of nuclear power plants in the world lead to produce significant amount of nuclear fuel.

For present time, uranium is still recognized as a leading fission material. It is most often considered as the irreplaceable raw material for nuclear industry [2] and demand for uranium is expected to continue to rise in the near future [3].

Better separation of uranium from ores is one of the leading tasks nowadays. One of the most essential stages in the processing of uranium ore is its sorption on ion-exchange resins. The ion-exchange resin plays an important role for the production of uranium. Today the market of ion-exchange resins is represented by a wide range of resins. The selection of ion-exchange resin which have the high sorption

and desorption, as well as kinetic characteristics is an urgent task for ensuring the maximum performance of this technological process. The sorption of uranium from sulphuric acid solutions by strongly basic anion exchange resin is widely described in literature [4-6]. Strongly basic anionic exchangers were often utilized in uranium industry and are even recognized as the most suitable ion exchangers for uranium recovery [7].

In this study we examined the sorption and desorption characteristic of two brands of anion exchangers from productive solutions: AMP (Smoly State Company, Ukraine) and Ambersep 920 IRA (® TMTrademark of The Dow Chemical Company (“Dow”) or an affiliated company of Dow). In the study [5] during the investigation of resins of two brands was revealed that AMP exchanger was the one with preferred characteristics, whereas in the course of this work AMP showed worse results comparing with Ambersep 920 IRA exchanger.

Materials and Methods

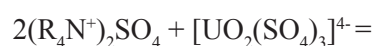
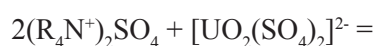
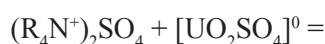
Preparation of productive solution

The laboratory agitation leaching was carried out for obtaining real uranium productive solution from

ore sample [8]. The sulfuric acid 2.5 % was used as a leaching reagent. The uranium productive solution with concentration of uranium equal to 173.12 mg/l was obtained as a result of leaching.

Strongly based ion – exchange resins

The sorption recovery of uranium from sulfuric acid leaching solutions by strongly basic anion exchangers can be described by reactions of complexation and ion exchange [9]:



In our case, strongly basic ion exchange resins AMP and Ambersep 920 IRA were set in columns (0.5x3) (Figure 1) for investigation of sorption and desorption process of uranium under dynamic conditions. The productive solution was passed through the resin (Figure 1) with a rate of 1 ml/min until the completely uranium saturation by the sorbent.

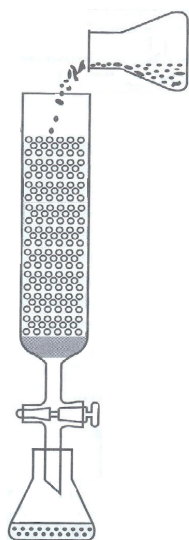


Figure 1 – Scheme of sorption under dynamic condition

Since significant amount of sulfate anion complexes of uranium formed at a pH of 2, as a result the pH of productive solution was brought to this value. The obtained fractions after sorption and desorption of uranium were collected every 5 ml of volume for establishing the breakthrough point. 1.8 M solution of ammonium nitrate was used as a desorbing solution [10].

Determination of uranium concentration

The titanium-phosphate-vanadate titration method was used for determination of the uranium concentration in the sorption cells and desorption eluates.

This measurement technique establishes a volumetric titrimetric titanium-phosphate-vanadate method of determination of the uranium concentration in uranium productive solutions in the range of mass concentrations from 0.001 g/l to 1.00 g/l.

An aliquot of the sample (2-10 ml), depending on the expected uranium concentration, was placed in a 100 ml conical flask then distilled water was added to a total volume of 10 ml. 1-2 drops of urea were added, mixed, and then 10 ml of concentrated phosphoric acid was added. After that, chloride of tetravalent titanium was added for appearing a violet color. The solution was cooled and a solution of sodium nitrate was added, the excess of which was destroyed by the addition of urea. Sodium salt of diphenylamine-4-sulfonic acid was added as an indicator. The following reaction occurs as a result of titration:



The mass concentration of uranium (X) g/l calculated by the following formula:

$$X = \frac{T \cdot (V_2 - V_1) \cdot 1000}{A}$$

where: V_1 is volume of ammonium metavanadic acid solution, consumed for titration of a blank sample with addition of Mohr salt, ml; V_2 is volume of a solution of ammonium metavanadic acid, spent on titration of uranium, ml; A is aliquot of the analyzed sample, ml; T is the titer of a solution of ammonium metavanadic acid in uranium g/ml.

Determination of the dynamic exchange capacity

Determination of the exchange capacity of resins under dynamic conditions fully represents the sorption process in practice. It makes possible to determine the working exchange capacity, which is equivalent of dynamic exchange capacity, before the

breakthrough point. Dynamic exchange capacity is calculated by the following formula [11]:

$$DEC = C \cdot \frac{V_{ps}}{V_{resins}}$$

where: V_{ps} is volume of the passed solution, l; V_{resins} is volume of the resins, cm^3 ; C is concentration of the uranium in the productive solution, mg/l.

Results and discussions

Based on the obtained data (Table 1), after the titration of the sorption cells of uranium on the an-

ion exchange resin AMP, the dependence shown in Fig. 1 was constructed.

According to the curve shown in Figure 2, the breakthrough point of uranium is observed in the first 5 ml of the volume of the productive solution. The concentration of the uranium slightly increases to equalize the concentrations in the influent and effluent solutions. The plateau was established on the volume of the passed solution equal to 200 ml. Desorption of the uranium from the ion exchanger was carried out after completely saturation of the resin. The uranium concentration in the desorption eluates was determined titrimetrically (Table 2). The desorption curve was constructed (Figure 3).

Table 1 – Data obtained after titration of the sorption cells of uranium on the anion exchange resin AMP (measurement error is 0.25 ml).

Sample	$V_{Pr,s}, ml$	$C_u, mg/l$
1	5	62.9
10	50	131.27
20	100	134.00
25	125	142.21
30	150	142.21
40	200	142.24
45	225	139.47
50	250	139.47

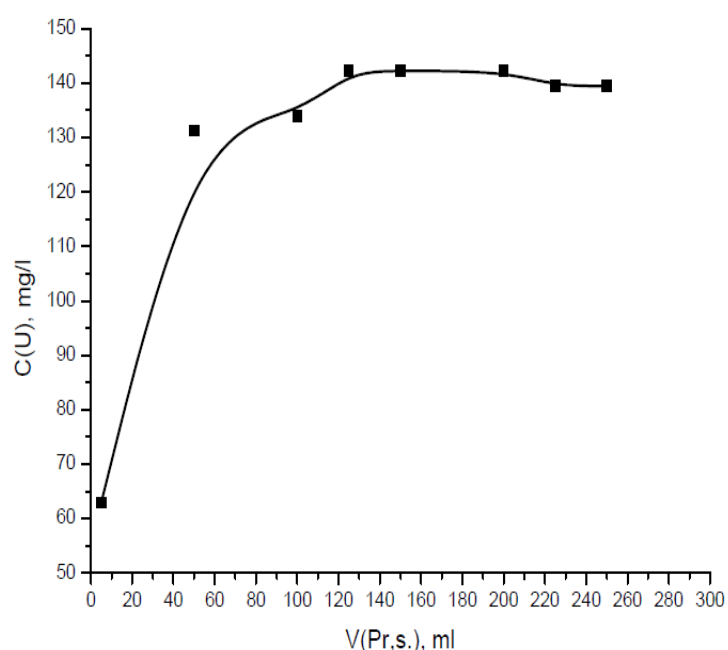


Figure 2 – The output curve of the uranium sorption on the anion exchange resin AMP (measurement error it 0.25 ml)

Table 2 – Data obtained after titration of uranium desorption eluates on the anion exchange resin AMP (measurement error is 0.25 ml).

Sample	$V_{\text{desorp.el.}}, \text{ ml}$	$C_{\text{U}}, \text{ mg/l}$
1	5	268.01
2	10	103.92
5	25	5.469
10	50	0

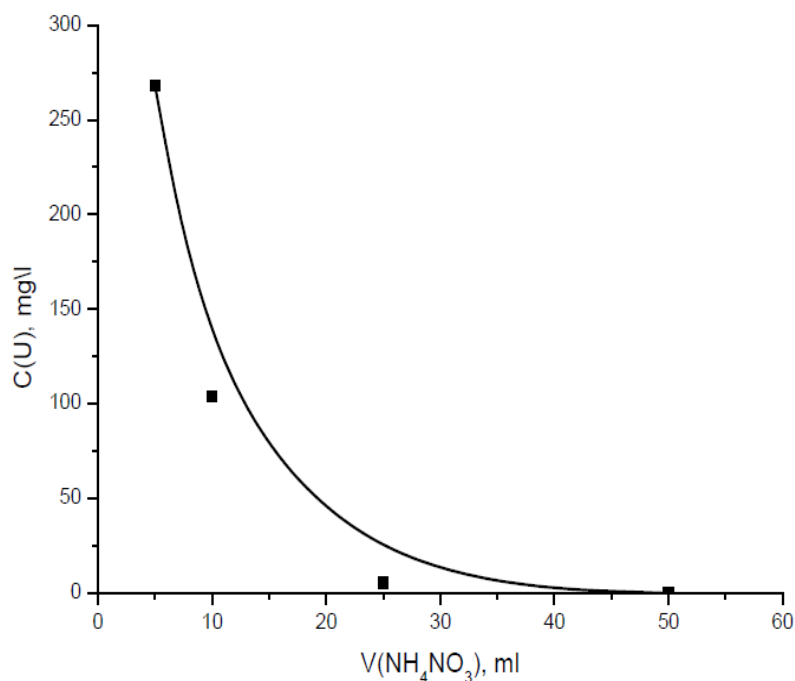
**Figure 3** – The output curve of uranium desorption on the anion exchange resin AMP (error of measurement it 0.25 ml)

Figure 3 shows that uranium is elutriated first by 5 ml of a desorbing solution. The maximum amount of uranium in the eluate was 268.00 mg/l, which is almost 1.5 times higher than the concentration of uranium in the initial productive solution. According to the data on the curve, the resin reaches a zero value of the uranium concentration when 50 ml of desorbing solution passes, this indicates a good

desorption characteristic of the AMP resin. Based on the experimental data, the DEC (dynamic exchange capacity) was calculated, which was equal to 1.47 mg/cm³.

Based on the obtained data (Table 3), after the titration of the sorption cells of uranium on the anion exchange resin Ambersep 920 IRA, the dependence shown in fig. 3 was constructed.

Table 3 – Data obtained after titration of the sorption cells of uranium on the anion exchange resin Ambersep 920 IRA (measurement error is 0.25 ml).

Sample	$V_{\text{Sorp.cells}}, \text{ ml}$	$C_{\text{U}}, \text{ mg/l}$
1	5	13.67
10	50	87.51
15	75	84.77
20	100	101.19

Continuation of table 3

Sample	$V_{\text{Sorp.cells}}, \text{ ml}$	$C_U, \text{ mg/l}$
25	125	131.27
30	150	139.47
35	175	123.07
40	200	134.00
45	225	131.27
50	250	155.88
55	275	150.41
60	300	164.09
65	325	134.00
70	350	150.41
75	375	150.41
80	400	161.31

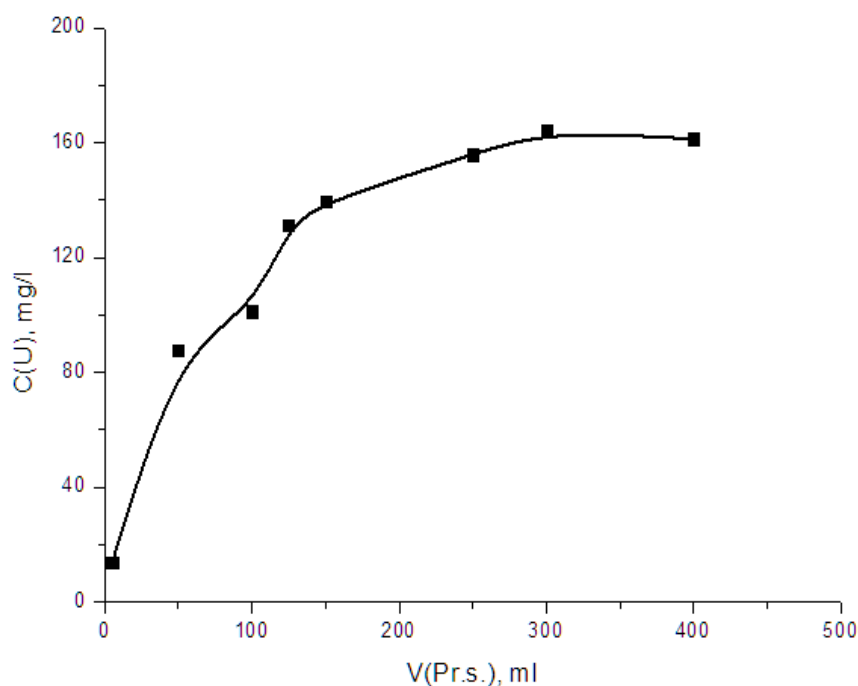


Figure 4 – The output curve of the uranium sorption on the anion exchange resin Ambersep 920 IRA (measurement error it 0.25 ml)

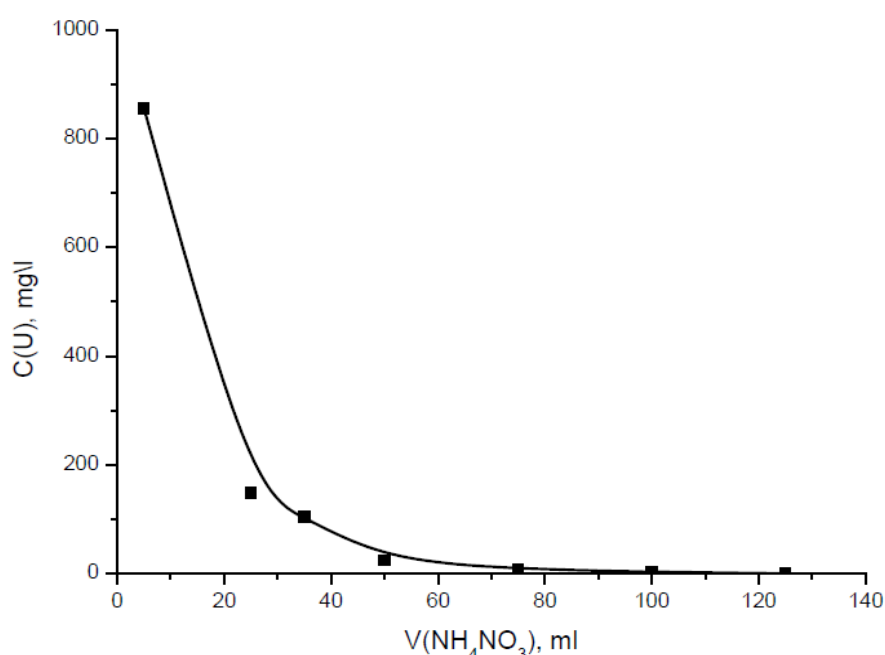
This curve shows a breakthrough point in the first 5 ml of the volume of the productive solution. The concentration of the uranium slightly increases to equalize the concentrations in the influent and effluent solutions. The plateau was established on the volume of the passed solution equal to 350 ml. The uranium was eluted from the column, and the data given in Table 4 were obtained. The uranium concentration in desorption eluates was determined titrimet-

rically. The output desorption curve was constructed (Figure 5).

Figure 5 shows that uranium is elutriated first by 5 ml of a desorbing solution. The maximum amount of uranium in the eluate was 856.00 mg/l, which is almost 5 times higher than the concentration of uranium in the initial productive solution. Based on the experimental data, the DEC (dynamic exchange capacity) was calculated, which was equal to 1.47 mg/cm³.

Table 4 – Data obtained after titration of uranium desorption eluates on the anion exchange resin Ambersep 920 IRA (measurement error is 0.25 ml)

Sample	$V_{\text{Desorp. el.}}, \text{ ml}$	$C_U, \text{ mg/l}$
1	5	856.00
5	25	147.68
7	35	103.92
10	50	24.6
15	75	8.2
20	100	2.7
25	125	0

**Figure 5** – The output curve of uranium desorption on the anion exchange resin Ambersep 920 IRA (error of measurement is 0.25 ml)**Table 5** – Comparative characteristics of the obtained results

Ion – exchange resin	DEC, mg/cm^3	C_U at the time of breakthrough point, mg/l	C_U in the desorption eluates, mg/l	C_U in the productive solution, mg/l
Ambersep 920 IRA	1.47	13.67	856.00	173.12
AMP	1.47	62.90	268.00	

Based on Table 5, it can be seen that the dynamic exchange capacity for both resins has the same value, but the value of the uranium content at the time of breakthrough for the resins is different. So, for the Ambersept 920 IRA, the concentration of uranium in the sorption cell at the time of the breakthrough is 13.67

mg/l , while the same value for the anion exchanger AMP is 62.9 mg/l . In addition, it should be noted the preferential desorption characteristics of the ion-exchange resin Ambersept 920 IRA, where the uranium content in the desorption eluate is 3 times higher than the uranium content in the AMP desorption eluates.

Conclusion

Based on the sorption and desorption characteristics of the strongly basic ion-exchangers AMP and Ambersep 920 IRA, it was found that the Ambersep 920 IRA anion exchanger has greater sorption and desorption advantages in comparison with AMP exchanger. Thus, the final uranium content in the desorption eluate for Ambersep 920 IRA and AMP was 856.00 and 268.00 mg/l, respectively, which is 5 and 1.5 times higher than the initial uranium content in the production solution. The breakthrough of uranium for the Ambersep 920 IRA resin is observed with lower concentration of uranium than the AMP resin, which indicates better sorption ability of the resin. Thus, the results of the conducted studies show the prospects of using the Ambersep 920 IRA anion exchange resin in the sorptional extraction of uranium from productive solutions of sub-surface leaching.

References

1. IAEA Annual Report for 2016. GOV/INE/2017/12 – GC (61)/INF/ 8.1
2. Ahmed, S. H., Sharaby, C. M., & El Gammal, E. M. 2013. Uranium extraction from sulfuric acid medium using trioctylamine impregnated activated carbon. *Hydrometallurgy* 134/135: 150–157.
3. Bożena Danko, Rajmund S. Dybczyński, Zbigniew Samczyński, Dorota Gajda, Irena Herdzik-Koniecko, Grażyna Zakrzewska-Kołtuniewicz, Ewelina Chajduk, Krzysztof Kulisa. 2017. Ion exchange investigation for recovery of uranium from acidic pregnant leach solutions. *Nukleonika* 62(3): 213-221.
4. Zagorodnyaya, A. N., Abisheva, Z. S., Shari-pova, A. S., Sadykanova, S. E., Bochevskaya, Y. G., Atanova, O. V. 2013. Sorption of rhenium and uranium by strong base anion exchange resin from solutions with different anion compositions. *Hydrometallurgy* 131/132: 127–131.
5. Kolomiets, D. N., Troshkina, L. D., Sheremet'ev, M. F., Konopleva, L. V. 2005. Sorption of uranium from sulfuric acid leaching solutions by strongly basic anion exchangers. *Russ. J. Appl. Chem.* 78(5): 722–726.
6. Ikeda, A., Aida, M., Fujii, Y., Kataoka, S., Annen, S., & Sato, J. 2002. Ion exchange separation for decontamination of centrifuge enrichment plant. *J Nucl. Sci. Technol.* 39(10): 1099–1105.
7. Carr, J., Zontov, N., & Yamin, S. 2008. Meeting the future challenges of the uranium industry. In ALTA 2008 Uranium Conference, p. 20.
8. Sadyrbayeva G.A., Myrzabek K.A., Zhatkanbayev E.E., Daurenbekov S.D. 2011. *Mining information analytical bulletin* (scientific and technical journal) [Gornyj informacionnyj analiticheskij byulleten' (nauchno-tehnicheskij zhurnal)] 11: 216 – 222 (In Russian).
9. Beletskii, I.V., Bogatkov, L.K., Volkov, N.I. 1997. *Handbook of Uranium Geotechnology* (Spravochnik po geotekhnologii urana) Moscow: Energoatomizdat (In Russian).
10. Shokobayev N.M., Dauletbaev T.S., Zhumbabayeva D.S. 2014. *Mountain magazine of Kazakhstan* [Gornyi zhurnal Kazakhstana] 18 (112): 30-37 (in Russian).
11. State standard №20255.2-89 (2002) Ion exchange resins. Methods of determining dynamic ion-exchange capacity. Moscow: publishing standards. (In Russian).

IRSTI 31.15.25, 31.15.35, 52.45.19

*Sh. Amerkhanova, R. Shlyapov, A. Uali

L.N. Gumilyov Eurasian National University, Faculty of Natural Sciences, Astana, Kazakhstan

*e-mail: amerkhanova_sh@mail.ru

Adsorption and flotation of copper sulfide ore with diisopropyldithiophosphate collector

Abstract: One of the topical problems of the enrichment industry is the evaluation of the influence of pulp chemistry on the sorption and flotation properties of sodium diisopropyl dithiophosphate. The affinity of the collector with respect to copper ore by the method of static sorption and flotation tests has been studied in this paper. The results of investigation adsorption mechanism of diisopropyldithiophosphate collector on the surface of the sulfide copper ore and flotation has been discussed. The investigation of composition and structure of sulphide copper ore has been carried out by using FT-IR-spectroscopy, X-ray diffraction spectroscopy and ICP-MS method. Based on the results of the analysis, the main minerals of copper ore, chalcocite and bornite, were selected. Also the analytical expressions of the real solubility constants of chalcocite and bornite, which connect the product of the solubility of hydroxocompounds at the phase interface with the solubility of copper diisopropyldithiophosphates and the oxidation-reduction ability of minerals, were obtained taking into account that the results showed that sorption capacity of ore at pH 10.5-11.5 is a maximum. The role of the oxidation-reduction processes in fixing of diisopropyldithiophosphate ion on the surface of ore was established. It was shown that data of extraction of copper to concentrate and adsorption value of diisopropyldithiophosphate ion are correlating. The IR-Fourier spectroscopic analysis showed that collector is coordinated with the ions of the metal of the crystal lattice of copper-containing minerals through the sulfur atoms of the dithiophosphate group.

Key words: sulfide copper ore; diisopropyldithiophosphate; adsorption; pulp chemistry; flotation.

Introduction

The polymetallic raw materials currently being processed are characterized by a fine dissemination of minerals and complex structural characteristics that make the flotation process more difficult. The diameter of the characteristic minerals – chalcocite, covellin, bornite in the copper sulfide ore varies: 0.2 mm for chalcocite and to 0.03 μm for bornite. The chalcocite inclusions have equigranular structure [1]. Theoretical substantiations and experimentally confirmed optimal conditions for flotation enrichment processes of sulfide polymetallic ores are the basis for creating innovative flotation technologies and ensuring the efficiency and complexity of mineral raw materials. The provision of an optimal reagent enrichment regime is referred to the problems that need to be solved, namely, the influence of the composition of copper ore and flotation reagents on the process of its processing [2-9], and the features of the flotation agent fixing mechanism on the mineral surface [10-

13]. The purpose of this work is to study the flotation behavior of sulfide copper ore using sodium diisopropyldithiophosphate as a collector, to study the structure and composition of the ore and their effect on the interaction between collector and ore.

Materials and methods

Materials and reagents. Sulfide copper ore was obtained from a copper mine in Central Kazakhstan. The samples were wet-ground and elutriated. Size fractions were ± 0.074 mm. The sodium diisopropyldithiophosphate (the content of pure substance is 78%) was prepared in a laboratory by diluting to a concentration of $4.25 \cdot 10^{-5}$ M and used as a main collector. Flotation reagent Oksal T-92 (mixture of polyhydric alcohols, aqueous solution) was used as a foam-forming agent (concentration $1 \cdot 10^{-5}$ M). The sodium hydroxide (1 M) and hydrochloric acid (1 M) of analytical purity were used as pH adjusters.

Distilled water was used in all experimental studies.

Adsorption tests. The amount of adsorbed collector on the ore was measured by potentiometric titration of the collector solution after the separation of the solid phase by the solution of copper (II) sulfate, Cu_2S was used as the indicator electrode [14]. 1 g of ore was immersed into 50 ml of an aqueous solution, containing the main collector ($4.25 \cdot 10^{-5}$ M) at a fixed pH for 30 min at 25°C. After that, the sample was centrifuged for 10 min at a rate of 9000 rpm/min.

Flotation tests. Flotation tests for sulfide copper ore were conducted by using a laboratory FML-1 (237 AK) flotation machine with cell (volume of 0.5 L). 100 grams of a copper ore were firstly mixed with 0.5 L distillate water in the flotation cell for 1 min with an impeller speed of 2000 rpm/min. The sodium hydroxide (1 M) or hydrochloric acid (1 M) was added to adjust the pulp pH to a predetermined pH. Collecting reagent and foam-forming agent were then added and conditioned for 8 min. The pulp pH was then adjusted slightly before flotation and was assumed to be the slurry pH at the end of flotation. The total flotation time was 9 min, and the concentrates were collected by manually scraping.

Both the concentrates collected and the tailings remaining in the cell were dried and weighed for calculating flotation recoveries. All recovery results presented are the average of duplicate flotation tests.

Characterization. FT-IR spectroscopic measurements were carried out by the device FSM 1201. X-ray diffraction spectroscopy (XRD) spectra of samples of initial ore and concentrates were carried out by the X-ray powder diffraction D8 Advance (Bruker, Germany) with the Cu-k_α line of 0.15406 nm. ICP-MS study of elemental composition of sulfide copper ore was carried out by the spectrometer ICP MS Agilent 7500.

Results and discussion

Investigation of composition and structure of ore. The chemical composition of sulfide copper ore was determined for its description. Quantitative data on the content of chemical elements of rock-forming minerals were obtained by the method of inductively coupled plasma mass spectrometry (ICP-MS). Approximate values were obtained from the average of five test sites of each sample from heterogeneous rock materials. The results of the ore analysis are presented in Table 1.

Table 1 – Elemental composition of sulfide copper ore by results of chemical analysis

Element	Amount, %	Element	Amount, g·t ⁻¹	Element	Amount, g·t ⁻¹
Cu	1.99	Au	<0.01	La	26.90
Pb	0.04	Ag	15.02	Ce	55.82
Zn	0.01	Be	1.50	Pr	6.69
S	0.58	Sc	17.80	Nd	26.50
		Ti	5938.10	Sm	5.20
		V	146.35	Eu	1.50
		Cr	83.10	Gd	4.80
		Co	25.40	Tb	0.74
		Ni	68.59	Dy	4.20
		Rb	21.80	Ho	0.83
		Sr	558.70	Er	2.20
		Y	18.83	Tm	0.32
		Zr	171.30	Yb	2.10
		Nb	12.90	Lu	0.31
		Cd	1.90	Hf	4.60
		Cs	0.86	Pb	11.30
				Th	6.62
				U	2.10

The results of the chemical analysis show that the average copper content in the ore is 1.99%, and accordingly refers to the average. Besides copper, lead and zinc, the ore contains a relatively large amount of titanium, strontium, vanadium,

zirconium. The presence of scattered elements was found in the sample. It also shows that ore contains lanthanides and actinides in a total amount of 162.73 g·t⁻¹. Table 2 contains data on the mineralogical composition of sulfide copper ore.

Table 2 – Mineral composition of sulfide copper ore

Mineral (-s)	Mass fraction, %	Mineral (-s)	Mass fraction, %
Feldspar	65.71	Pyroxene	Rare grains
Chlorites	19.12	Azurite	
Quartz	7.82	Pyrite	
Calcite	0.85	Galena	
Epidotes	0.34	Magnetite	
Hematite	1.74	Covellite	
Bornite	1.01	Chalcopyrite	
Chalcocite	1.69	Iron hydroxides	
Malachite	0.09	Rutile, anatase	
Apatite	0.95	Zircon	
Totally	95.88		

It can be seen that rock-forming minerals are represented in the ore as feldspars, chlorites and quartz. Sulfide copper is presented in the form of chalcocite (1.69%) and bornite (1.01%), in the form of rare grains there are covellite and chalcopyrite.

Copper is represented by 13.57% of oxides and 84.92% of secondary sulfides, on 0.50% of primary sulfides. Sulfide copper ores consist mainly of ore minerals (containing 5.48%), rock-forming minerals (quartz, feldspar, chlorite and epidotes) with a content of 93.84%. Phase analysis was performed to establish the copper phases (Table 3) [15].

The main mass of copper is concentrated in sulfide form (85.43%), which in turn is divided into primary sulfides (0.50%) and secondary copper sulfides (84.92%). Oxidized copper amounts 14.57%.

The predominance of copper sulfides in the composition of the ore allows using of sulfhydryl collectors, namely sodium diisopropyldithio-phosphate at evaluating sorption and flotation in these systems.

Flotation and Adsorption. The results of the investigation of sodium diisopropyldithiophosphate adsorption and flotation of copper sulfide ore are shown in Figure 1.

Table 3 – Phase analysis of copper in the initial ore

Cu _{com} , %	Cu in the oxidized form			Cu in the sulfide form				Cu water-soluble
	Cu _{com. oxid.}	Cu _{bound. oxid.}	Cu _{free oxid.}	Cu _{com. sulph.}	Cu _{bound. Chalcocite.}	Cu _{bound. Bornite}	Cu _{carb. Chalcopyrite}	
1.99	0.28	0.26	0.02	1.69	1.16	0.52	0.01	0.02
100	14.07	13.07	1.01	84.92	58.29	26.13	0.50	1.01

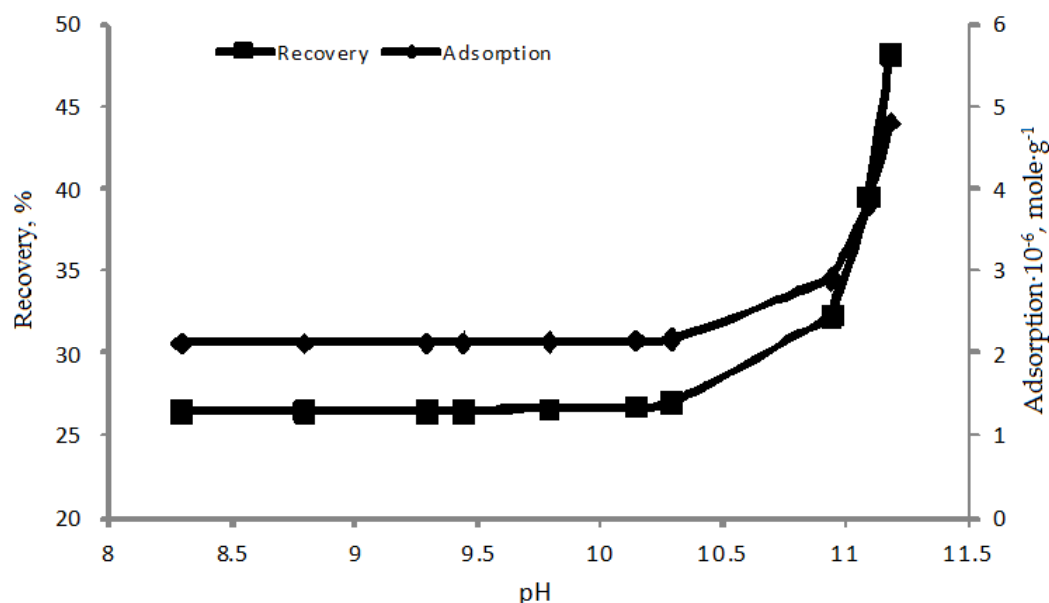


Figure 1 - The effect of pH on copper recovery and the adsorption of sodium diisopropyldithiophosphate ($C=4.25 \cdot 10^{-5}$ mole \cdot L $^{-1}$) on copper sulfide ore

Analysis of the data shown in Figure 2 showed that the maximum copper recovery into the concentrate and the sorption of diisopropyldithiophosphate ions on the surface is observed at pH 11; this is due to oxidation-reduction processes involving sulfide minerals (chalcocite) and the replacement of sulfate ions by diisopropyldithiophosphate ions with the formation of less soluble compounds. The oxidation of sulfide ions occurs with low intensity at pH 8-10. Since in the ore the main copper-containing minerals are chalcocite and bornite, consideration of the equilibrium involving collectors will be carried out using the example of these minerals whose surface

after immersion in aqueous solutions consists of three layers, the outer layer is represented by copper hydroxides, the middle layer - by elemental sulfur, the inner surface - by copper (I) sulfide. The outer layer dissolves at low and high pH of the medium; therefore, in the oxidation-reduction processes in the presence of oxygen, a layer of elemental sulfur participates. At low pH of medium 1-6, the oxidation-reduction pair S^{2-}/S predominates, at high pH 8-14, sulfur is oxidized to sulfate ions. Possible reactions (I-XIX) and equilibrium constants for the presented system are given in Table 4, where L is a diisopropyldithiophosphate ion ($i-C_3H_7O)_2PS_2^-$.

Table 4 - Oxidation-reduction reactions and equilibriums in systems $Cu_2S-H_3O^+/OH^- - L^-$, $Cu_5FeS_4 - H_3O^+/OH^- - L^-$

Reactions	The equilibrium constant / Standard potential, V
$Cu_2S_{(s)} = 2Cu^+ + S^{2-}$ (I)	$K_{sp1} = 10^{-48.12}$
$Cu_5FeS_4 = 5Cu^+ + Fe^{3+} + 4S^{2-}$ (II)*	$K_{sp2} = 10^{-134.29}$
$Cu^{2+} + e^- \rightarrow Cu^+$ (III)	$E_{Cu^{2+}/Cu^+}^0 = 0.167$
$S^{2-} + 2e^- \rightarrow S^0$ (IV)	$E_{S^{2-}/S^0}^0 = -0.48$
$2S^{2-} + 3H_2O + 8e^- \rightarrow S_2O_3^{2-} + 6H^+$ (V)	$E_{S^{2-}/S_2O_3^{2-}}^0 = -0.547$
$S^{2-} + 8OH^- + 8e^- \rightarrow SO_4^{2-} + 4H_2O$ (VI)	$E_{S^{2-}/SO_4^{2-}}^0 = -1.23$
$Cu^{2+} + OH^- = CuOH^+$ (VII)	$K_1 = 10^7$
$Cu^{2+} + 2OH^- = Cu(OH)_2$ (VIII)	$K_2 = 10^{13.68}$
$Cu^{2+} + 3OH^- = Cu(OH)_3^-$ (IX)	$K_3 = 10^{17}$
$Cu^{2+} + 4OH^- = Cu(OH)_4^{2-}$ (X)	$K_4 = 10^{18.5}$
$Fe^{2+} + OH^- = FeOH^+$ (XI)	$K_5 = 10^{5.5}$

Continuation of table 4

Reactions	The equilibrium constant / Standard potential, V
$Fe^{2+} + 2OH^- = Fe(OH)_2$ (XII)	$K_6 = 10^{7.4}$
$Fe^{2+} + 3OH^- = Fe(OH)_3^-$ (XIII)	$K_7 = 10^{11}$
$Fe^{2+} + 4OH^- = Fe(OH)_4^{2-}$ (XIV)	$K_8 = 10^{10}$
$Cu(OH)_{2(s)} = Cu^{2+} + 2OH^-$ (XV)	$K_{sp3} = 10^{-19.25}$
$Fe^{3+} + e^- \rightarrow Fe^{2+}$ (XVI)	$E_{Fe^{3+}/Fe^{2+}}^0 = 0.771$
$CuL_{2(s)} = Cu^{2+} + 2L^-$ (XVII)	$K_{sp4} = 10^{-19.42}$
$FeL_{2(s)} = Fe^{2+} + 2L^-$ (XVIII)	$K_{sp5} = 10^{-20.29}$
$L^- + H_3O^+ \leftrightarrow HL + H_2O$ (XIX)	$K_A = 10^{-5.59}$
<p>* The value of K_{sp2} is calculated by the method of comparative calculation from dependence (reaction (II))</p> $-\Delta_s \bar{G}_{298}^0 = -1.0469 \cdot (-\Delta_f \bar{G}_{298}^0) + 118.85,$ <p style="text-align: center;">where:</p> $-\Delta_s \bar{G}_{298}^0 = (8.314 \cdot 2.303 \cdot 298 \cdot \ln K_{sp2})/10$ $-\Delta_f \bar{G}_{298}^0(Cu_5FeS_4) = 32.2 \text{ kJ/mole} \cdot \text{atom} [16]$ <p>The equation is derived from the data on the solubility product for the following minerals: $Cu_3(OH)_2(CO_3)_2$ (azurite), FeS_2 (pyrite), Cu_2S (chalcocite), $CuFeS_2$ (chalcopyrite), $Cu_2(OH)_2CO_3$ (malachite) and the average atomic energy of Gibbs. The correlation coefficient of the dependence is $R = 0.99$.</p>	

The mole fraction of the free anions of the precipitant (diisopropyldithiophosphate ions) [17]:

$$x_L = \frac{\frac{K_A^2}{[H_3O^+]^2}}{\left(1 + \frac{K_A}{[H_3O^+]}\right)^2} = \frac{1}{\left(1 + \frac{[H_3O^+]}{K_A}\right)^2} \quad (1)$$

where K_A is the equilibrium constant of the reaction (XIX).

The mole fraction of the free metal ions:

$$x_{Kt} = \frac{1}{1 + K_1[OH^-] + K_2[OH^-]^2 + K_3[OH^-]^3 + K_4[OH^-]^4} \quad (2)$$

where K_1, K_2, K_3, K_4 are the stability constants of metal hydroxocomplexes (reactions (VII-X) for Cu(II) ions, (XI-XIV) for Fe(II)).

The real solubility constant of metal diisopropyldithiophosphates is:

$$K_{KtL_2}^{S,r} = \frac{K_{KtL_2}^S}{x_{Kt}x_L^2} \quad (3)$$

where x_{Kt} is the mole fraction of the free metal ions, x_L is the mole fraction of the free anions of the precipitant (diisopropyldithiophosphate ions), $K_{KtL_2}^S$ is the solubility constant of metal (II) diisopropyldithiophosphate (reactions (XVII-XVIII)).

In acidic medium, copper sulfides are oxidized to elemental sulfur by reaction (IV), sulfide sulfur is oxidized to thiosulfate and sulfate ions in neutral (V) and alkaline (VI) mediums. Then the free

concentration of metal ions not bound to a poorly soluble compound with a diisopropyldithiophosphate ion is:

$$x'_{Kt} = \frac{1}{1 + (1/K_{KtL_2}^{S,r})[L^-]^2} \quad (4)$$

where $K_{KtL_2}^{S,r}$ is the real solubility constant of metal diisopropyldithiophosphates, $[L^-]$ is concentration of diisopropyldithiophosphate-ions in solution.

The mole fraction of hydroxide-ions, not bounded with metal ions, is:

$$x_{OH^-} = \frac{1}{\left(1 + \frac{10^{-pH}}{K_w}\right)^2} \quad (5)$$

where K_w is the ionic product of water.

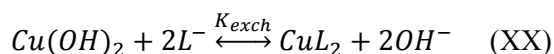
The real dissolution constant of copper (II) hydroxide is calculated by formula:

$$K_{Kt(OH)_2}^{S,r} = \frac{K_{Kt(OH)_2}^S}{x_{Kt}x_{OH^-}^2} \quad (6)$$

where $K_{Kt(OH)_2}^S$ is the solubility constant of metal (II) hydroxide (reaction XV), x_{Kt} is the mole fraction of metal ions, not bounded to hydroxocomplexes, x_{OH^-} is the mole fraction of hydroxide-ions not bounded with metal ions.

The formation of the copper (II) hydroxide on the surface of the mineral is possible when chalcocine is dissolved in an alkaline solution. $Cu(OH)_2$ in the presence of diisopropyldithiophosphate ions forms a slightly

soluble copper (II) diisopropyldithiophosphate as a result of the substitution reaction:



The exchange constant (K_{exch}) is calculated by formula:

$$K_{exch} = \frac{[OH^-]}{[L^-]} = \frac{K_{Cu(OH)_2}^{c,r}}{K_{CuL_2}^{c,r}} \quad (7)$$

where $K_{Cu(OH)_2}^{c,r}$ is the real solubility constant of copper (II) hydroxide, $K_{CuL_2}^{c,r}$ is the real solubility constant of copper (II) diisopropyldithiophosphate.

From the data shown in Figure 2, it is evident that the most complete exchange process occurs at low pH of the medium from one to five pH units, in this medium, the mole fraction of copper (II) hydroxides is negligible, and copper (II) ions are bound to aqua-complexes.

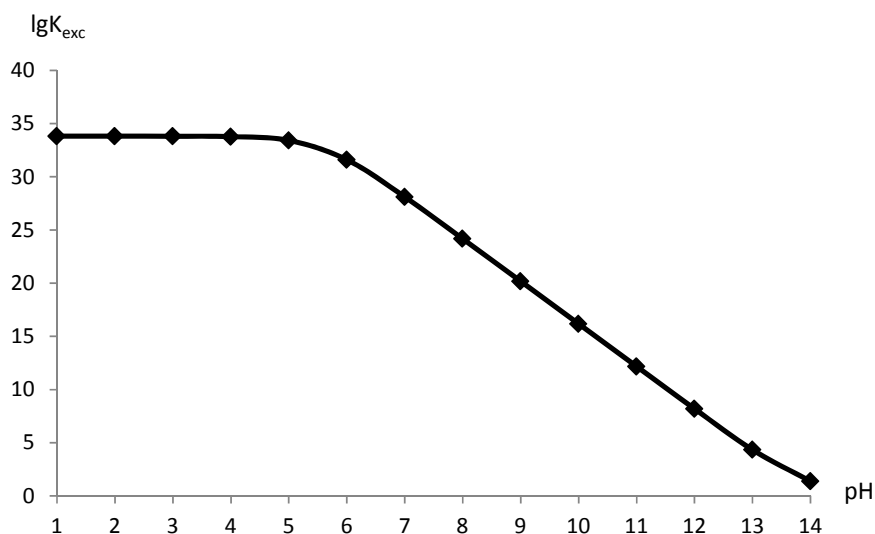


Figure 2 - The effect of pH on the exchange constant of hydroxide-ions on diisopropyldithiophosphate ions in the composition of a poorly soluble compound

However, as a result of red-ox processes involving copper (I) ions and sulfide ions, the formation of significant amounts of copper (II) ions and, consequently, diisopropyldithiophosphate complexes on the mineral surface is hampered by the formation of a film of elemental sulfur that reduces access of ligand ions to the mineral surface.

It was found that as the pH of the medium increases, the molar fraction of copper (II) hydroxides increases, this leads to a decrease in the

exchange constant. However, the logarithm of the exchange constant at pH 14 is greater than zero, which indicates the predominance of the replacement of hydroxide ions by diisopropyldithiophosphate ions.

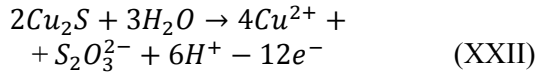
In connection with this, the real oxidation-reduction potential of the pair Cu^{2+}/Cu^+ , was calculated, taking into account the influence of oxidation-reduction potentials of sulfide ions in acidic (8), neutral (9) and alkaline (10) mediums for chalcocite according to the equations:



$$E^{\circ,r} = E_{S^{2-}/S^0}^{\circ} + E_{Cu^{2+}/Cu^+}^{\circ} + 0.059 \cdot z_{Cu^{2+}} \cdot \lg \gamma_{Cu^{2+}} + 0.059 \cdot z_{Cu^{2+}} \cdot \lg x'_{Cu^{2+}} \quad (8)$$

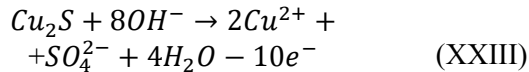
where $z_{Cu^{2+}}$ is the amount of Cu (II) ions' moles, E_{Cu^{2+}/Cu^+}° is the standard potential of reaction III.

Chalcocite oxidizes in neutral medium by reaction:



$$E^{\circ,r} = E_{Cu^{2+}/Cu^+}^\circ + \left(\frac{0.059}{z}\right) \cdot \lg \frac{\gamma_{S_2O_3^{2-}} \cdot \gamma_{H_3O^+}^{z_{H_3O^+}}}{\gamma_{S^{2-}}^2} - \left(\frac{0.059 \cdot z_{H_3O^+}}{z}\right) \cdot pH + E_{S^{2-}/S_2O_3^{2-}}^\circ + 0.059 \cdot z_{Cu^{2+}} \cdot \lg x'_{Cu^{2+}} + 0.059 \cdot z_{Cu^{2+}} \cdot \lg \gamma_{Cu^{2+}} \quad (9)$$

where $z_{Cu^{2+}}$ is the amount of Cu (II) ions' moles, $z_{H_3O^+}$ is the amount of hydroxonium ions' moles according to oxidation-reduction reaction, z is the number of electrons by reaction. Chalcocite oxidizes in alkaline medium according to the reaction:

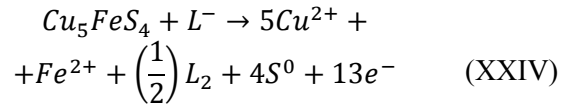


$$E^{\circ,r} = E_{Cu^{2+}/Cu^+}^\circ + \left(\frac{0.059}{z}\right) \cdot \lg \frac{\gamma_{SO_4^{2-}} \cdot \gamma_{OH^-}^{z_{OH^-}}}{\gamma_{S^{2-}}} - \left(\frac{0.059 \cdot z_{OH^-}}{z}\right) \cdot pH + \left(\frac{0.826 \cdot z_{OH^-}}{z}\right) + E_{S^{2-}/SO_4^{2-}}^\circ + 0.059 \cdot z_{Cu^{2+}} \cdot \lg x'_{Cu^{2+}} + 0.059 \cdot z_{Cu^{2+}} \cdot \lg \gamma_{Cu^{2+}} \quad (10)$$

where $z_{Cu^{2+}}$ is the amount of Cu(II) ions' moles, z_{OH^-} is the amount of hydroxide ions' moles

according to oxidation-reduction reaction, z is the number of electrons according to the reaction.

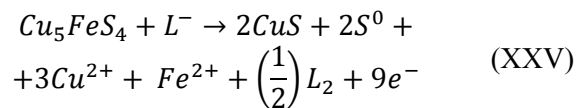
Analogous calculations of the real oxidation-reduction potential of the Cu(II)/Cu(I) pair, taking into account the oxidation of sulfide and diisopropyldithiophosphate ions, the reduction of Fe(III) ions were carried out for bornite in acidic and weakly acidic mediums (11, 12) [18], neutral and alkaline mediums (13) [19]:



$$E^{\circ,r} = E_{S^{2-}/S^0}^\circ + E_{Cu^{2+}/Cu^+}^\circ - E_{Fe^{3+}/Fe^{2+}}^\circ + E_{L_2/2L^-}^\circ + \left(\frac{0.059}{z}\right) \cdot z_{Cu^{2+}} \cdot \lg \gamma_{Cu^{2+}} + \left(\frac{0.059}{z}\right) \cdot z_{Cu^{2+}} \cdot \lg x'_{Cu^{2+}} + \left(\frac{0.059}{z}\right) \cdot z_{Fe^{2+}} \cdot \lg \gamma_{Fe^{2+}} + \left(\frac{0.059}{z}\right) \cdot z_{Fe^{2+}} \cdot \lg x'_{Fe^{2+}} - z_{L^-} \cdot \left(\frac{0.059}{z}\right) \cdot \lg x_{L_2} - z_{L^-} \cdot \left(\frac{0.059}{z}\right) \cdot \lg \gamma_{L_2} \quad (11)$$

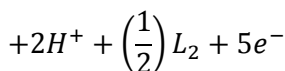
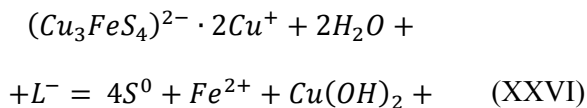
where $E_{L_2/2L^-}^\circ$ is the oxidation-reduction potential of pair of diisopropyldithiophosphate-ion – disulfide equals to 0.196 B, x_{L^-} is the mole fraction of not bounded ligands, γ_{L_2}'' is the activity coefficient of ligand in the solution, z_{L^-} is the number of ligand moles, participating in the reaction, $E_{Fe^{3+}/Fe^{2+}}^\circ$ is the standard potential of reaction XVI.

In weakly acidic medium pH 2-5 bornite oxidizes according to the reaction:



$$\begin{aligned}
E^{\circ,r} &= E_{Cu^{2+}/Cu^+}^{\circ} - E_{Fe^{3+}/Fe^{2+}}^{\circ} + E_{L_2/2L^-}^{\circ} + \\
&+ \left(\frac{0.059}{z}\right) \cdot \lg \frac{\gamma_{Cu^{2+}}^3 \cdot \gamma_{H_3O^+}^{z_{H_3O^+}}}{1} - \\
&- \left(\frac{0.059 \cdot z_{H_3O^+}}{z}\right) \cdot pH + E_{S^{2-}/S^0}^{\circ} + \\
&+ \left(\frac{0.059}{z}\right) \cdot z_{Cu^{2+}} \cdot \lg x'_{Cu^{2+}} + \left(\frac{0.059}{z}\right) \cdot z_{Cu^{2+}} \cdot \\
&\cdot \lg \gamma_{Cu^{2+}} + \left(\frac{0.059}{z}\right) \cdot z_{Fe^{2+}} \cdot \lg \gamma_{Fe^{2+}} + \\
&+ \left(\frac{0.059}{z}\right) \cdot z_{Fe^{2+}} \cdot \lg x'_{Fe^{2+}} - z_{L^-} \cdot \left(\frac{0.059}{z}\right) \cdot \\
&\cdot \lg x_{L^-} - z_{L^-} \cdot \left(\frac{0.059}{z}\right) \cdot \lg \gamma_{L^-}''
\end{aligned} \quad (12)$$

For bornite, the process of surface oxidation under the action of dissolved oxygen in the pH range 5-14 proceeds according to the reaction:



$$\begin{aligned}
E^{\circ,r} &= E_{Cu^{2+}/Cu^+}^{\circ} - E_{Fe^{3+}/Fe^{2+}}^{\circ} + E_{L_2/2L^-}^{\circ} + \left(\frac{0.059}{z}\right) \cdot \\
&\cdot \lg \frac{\gamma_{H_3O^+}^{z_{H_3O^+}}}{1} - \left(\frac{0.059 \cdot z_{H_3O^+}}{z}\right) \cdot pH + E_{S^{2-}/S^0}^{\circ} + \\
&+ \left(\frac{0.059}{z}\right) \cdot z_{Fe^{2+}} \cdot \lg \gamma_{Fe^{2+}} + \left(\frac{0.059}{z}\right) \cdot z_{Fe^{2+}} \cdot \\
&\cdot \lg x'_{Fe^{2+}} - z_{L^-} \cdot \left(\frac{0.059}{z}\right) \cdot \lg x_{L^-} - \\
&- z_{L^-} \cdot \left(\frac{0.059}{z}\right) \cdot \lg \gamma_{L^-}''
\end{aligned} \quad (13)$$

The real potential of the oxidation-reduction process depends on the molar fraction of the potential-determining ions, copper (II) ions, which are not bound to a poorly soluble compound, calculated by formula (2) and the mole fraction of sulfide ions, which is calculated according to the formulas (14-16):

$$\begin{aligned}
&\text{pH 1-6} \\
x_{S^{2-}} &= \frac{1}{1 + 10^{\frac{(E^{\circ,r} - E_{S^{2-}/S^0}^{\circ}) \cdot z}{0.059}}} \quad (14)
\end{aligned}$$

where $E^{\circ,r}$ is the real standard potential of pair Cu^{2+}/Cu^+ , E_{S^{2-}/S^0}° is the real standard potential of pair S^{2-}/S^0 , z is the number of electrons participating in the oxidation of sulfide sulphur.

$$\begin{aligned}
&\text{pH 7} \\
x_{S^{2-}} &= \frac{1}{1 + 10^{\frac{(E^{\circ,r} - E_{S^{2-}/S_2O_3^{2-}}^{\circ}) \cdot z}{0.059}}} \quad (15)
\end{aligned}$$

where $E_{S^{2-}/S_2O_3^{2-}}^{\circ}$ is the real standard potential of pair $S^{2-}/S_2O_3^{2-}$.

$$\begin{aligned}
&\text{pH 8-14} \\
x_{S^{2-}} &= \frac{1}{1 + 10^{\frac{(E^{\circ,r} - E_{S^{2-}/SO_4^{2-}}^{\circ}) \cdot z}{0.059}}} \quad (16)
\end{aligned}$$

where $E_{S^{2-}/SO_4^{2-}}^{\circ}$ is the real standard potential of pair S^{2-}/SO_4^{2-} .

For bornite the mole fraction of sulfide ions at pH 1-14 is calculated by formula:

$$x_{S^{2-}} = \frac{1}{1 + 10^{\frac{(E^{\circ,r} - E_{S^{2-}/S^0}^{\circ}) \cdot z}{0.059}}} \quad (17)$$

Since an insoluble compound is formed on the surface of the chalcocite, the real solubility constant which is calculated taking into account the influence of the pH of the medium, in formula (3), instead of the solubility constant of copper (II) diisopropylidithiophosphate, the solubility constant of chalcocite is used, and the mole fraction of the anion is replaced by the mole fraction of the sulfide ion, manifesting as a precipitator.

The real solubility constant of copper (I) sulfide:

$$K_{Cu_2S}^{S,r} = \frac{K_{Cu_2S}^S}{x_{Cu^+}^2 x_{S^{2-}}} \quad (18)$$

where $K_{Cu_2S}^S$ is the solubility product of copper sulfide (I) (reaction I), $x_{S^{2-}}$ is the mole fraction of sulfide ions (14-16), x_{Cu^+} is the mole fraction of copper (I) ions, determining by equation:

$$x_{Cu^+} = \frac{1}{1+10^{\frac{(E^{\circ,r}-E^{\circ}_{Cu^{2+}/Cu^+}) \cdot z}{0.059}}} \quad (19)$$

where z is the number of electrons participating in the reaction I.

$pK^{S,r}$ is calculated by equation:

$$pK^{S,r} = -\log K_{Cu_2S}^{S,r} \quad (20)$$

The real solubility constant of bornite:

$$K_{Cu_5FeS_4}^{S,r} = \frac{K_{Cu_5FeS_4}^S}{x_{Cu^+}^5 x_{Fe^{3+}} x_{S^{2-}}^4} \quad (21)$$

where $K_{Cu_5FeS_4}^{S,r}$ is the solubility product of bornite (reaction II), $x_{S^{2-}}$ is the mole fraction of sulfide ions (17), x_{Cu^+} is the mole fraction of copper (I) ions (19).

$x_{Fe^{3+}}$ is the mole fraction of iron (III) and calculated by equation:

$$x_{Fe^{3+}} = \frac{1}{1+10^{\frac{(E^{\circ}_{Fe^{3+}/Fe^{2+}}-E^{\circ,r}) \cdot z}{0.059}}} \quad (22)$$

where z is the number of electrons participating in the reaction XVI.

$pK^{S,r}$ is calculated by equation:

$$pK^{S,r} = -\log K_{Cu_5FeS_4}^{S,r} \quad (23)$$

The results of calculating the changes in the real solubility constant ($pK^{S,r}$) of chalcocite and bornite in the presence of a flotation agent - sodium diisopropyldithiophosphate from the pH of the medium are shown in Figures 3-4.

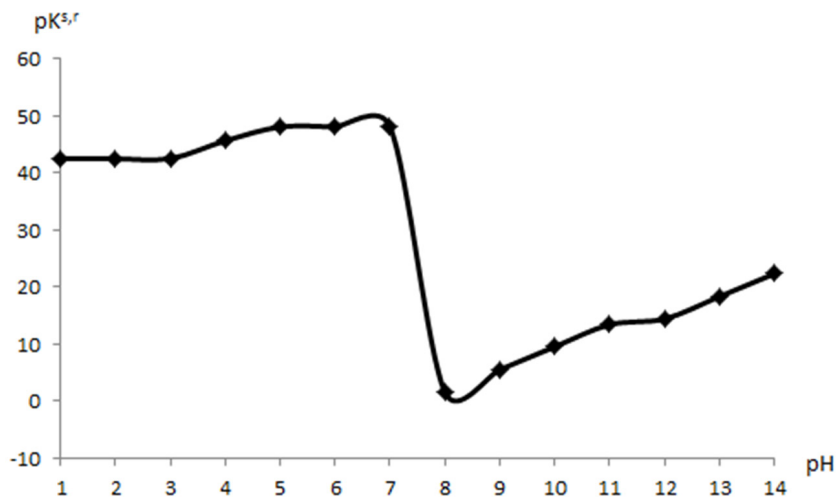


Figure 3 – Dependence of the real solubility constant ($pK^{S,r}$) of chalcocite in the presence of a flotation agent ($C=4.25 \cdot 10^{-5}$ mole \cdot L $^{-1}$) on the pH of the mineral suspension

Analysis of the real solubility constant ($pK^{S,r}$) showed that the stability of chalcocite in the presence of sodium diisopropyldithiophosphate with increasing pH of the solution in acidic media remains constant up to pH 3, in the pH range 4-7, chalcocite stability increases. The maximum solubility constant for chalcocite is observed at pH

7, which is associated with oxidation to thiosulfate ions in the presence of oxygen, since copper (II) thiosulfate is less soluble. In the transition to a slightly alkaline medium pH 8, the real solubility constant decreases sharply, this process corresponds to the formation of sulfate ions and copper (II) ions on the chalcocite surface, followed

by the replacement of diisopropyldithiophosphate ion and the formation of copper (II) ion complexes that are physically adsorbed. At pH 8-14, there is an

increase in solubility of chalcocite $pK^{s,r}$, associated with the formation of sparingly soluble copper (II) diisopropyldithiophosphates.

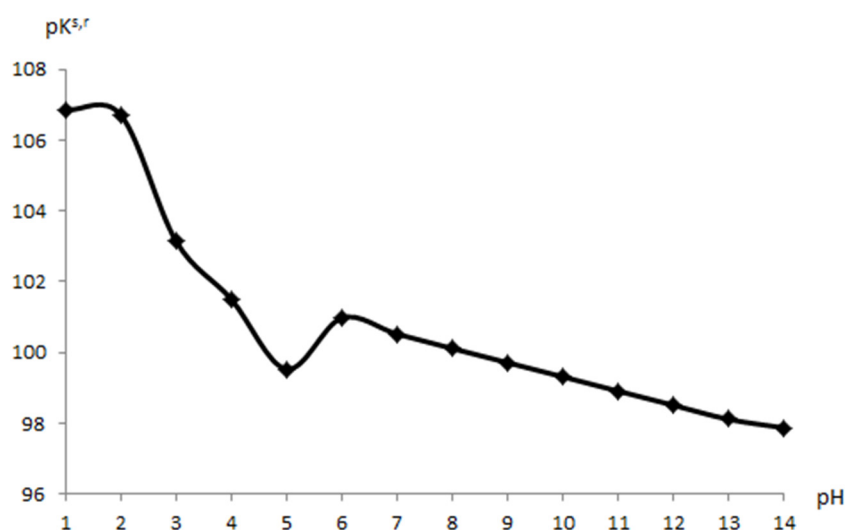


Figure 4 – Dependence of the real solubility constant ($pK^{s,r}$) of bornite in the presence of a flotation agent ($C=4.25 \cdot 10^{-5}$ mole \cdot L $^{-1}$) on the pH of the mineral suspension

It is shown that in an acid medium pH 1-2 bornite has minimal solubility due to the presence of elemental sulfur on the surface. Increasing pH of the solution to 5 leads to an increase in solubility due to the formation of iron (III) hydroxide, which forms iron (III) diisopropyldithiophosphate, then this compound disproportionates to iron (II) diisopropyldithiophosphate and disulfide. Covellite is also formed on the surface of bornite particles at pH 5.

It is shown that in the pH range 6-14, the iron (III) diisopropyldithiophosphate formed enters oxidation-reduction reactions, the product of which is the disulfide, which is fixed on the surface by means of van-der-Waals bonds, this causes the sorption of the collector.

Therefore, flotation of chalcocite and bornite in acidic and neutral mediums is impossible, flotation ability of chalcocite and bornite increases in the pH range 8-12. This also indicates the dependence of the reactivity of the mineral on the pH of the solution. Further, infrared spectra of flotation agents on the surface of the ore were removed.

FT-IR spectroscopy. To explain the mechanism of adsorption of the flotation agent on the surface of the ore, the IR spectra of the flotation agent, ore and ore after the sorption of the flotation agent were considered (Figure 5).

The IR spectrum of sodium diisopropyldithiophosphate there are absorption bands in the region of 2888-2963 cm^{-1} , which corresponds to stretching vibrations of CH-bonds. The dithiophosphate radical is characterized by absorption bands at 520-560 cm^{-1} and 630-680 cm^{-1} , related to the $\nu(\text{P-S})$ and $\nu(\text{P=S})$ coordinated PS_2 -groups, respectively. IR-Fourier spectrum (cm^{-1}): 1458, 1430, 1307 (νCH_2); 1085, 1034, 990 pl., 966 ($\nu\text{C-O}$); 778, 736 pl. ($\nu\text{P-O}$), 2370 cm^{-1} ($\nu\text{S-H}$). The absorption bands at 989 and 969 cm^{-1} are characteristic for the P-O-R fragment oscillation. The figure also shows the IR-Fourier-spectrum of sulfide copper ore. The spectrum contains a broad absorption band in the region of 3000-3500 cm^{-1} , which corresponds to OH-groups, absorption bands at 1105, 983 cm^{-1} are characteristic for SO_4^{2-} groups, 879 cm^{-1} for CO_3^{2-} groups, 1080 cm^{-1} for PO_4^{3-} groups. Analysis of the IR Fourier spectrum of the ore treated with a flotation agent solution showed that there is an absorption band at 1000 cm^{-1} that is characteristic of the P-O-R fragment oscillation. In the region of 2800-3000 cm^{-1} , new absorption bands appear which characterizes the trace amounts of a flotation reagent of an organic nature. Perhaps this flotation agent has not entered into a chemical interaction with the mineral, but only physically

adsorbed on the surface of its particles. After contact of the ore with $1 \cdot 10^{-5}$ M solution of dithiophosphate in a weakly alkaline medium, the maxima of the characteristic frequencies of the P=S ($680, 669 \text{ cm}^{-1}$) and PS ($590, 560, 525.5 \text{ cm}^{-1}$), toward low frequencies by 10 cm^{-1} for P=S bond and by $2-5 \text{ cm}^{-1}$ for PS bond, on the basis of which it is possible to assume the formation of bidentate-cyclic coordination of ligands with a metal via both sulfur atoms. The formation of additional bands with maxima in the frequency range of 610

and 575 cm^{-1} indicates, possibly, the formation of bonds of ore components with sulfur atoms of the reagent. The position of these bands is shifted in comparison with the position of similar bands in the IR spectrum of the flotation agent this indicates the coordination of $(i\text{-C}_3\text{H}_7\text{O})_2\text{PS}_2^-$ ions on the ore surface. The position of the bands $\nu(\text{PS}_2)$ is shifted by $3-4 \text{ cm}^{-1}$ to the low frequency region, and the position of the bands $\nu(\text{P-O-R})$ has shifted by 6 cm^{-1} and 31 cm^{-1} to the high-frequency region.

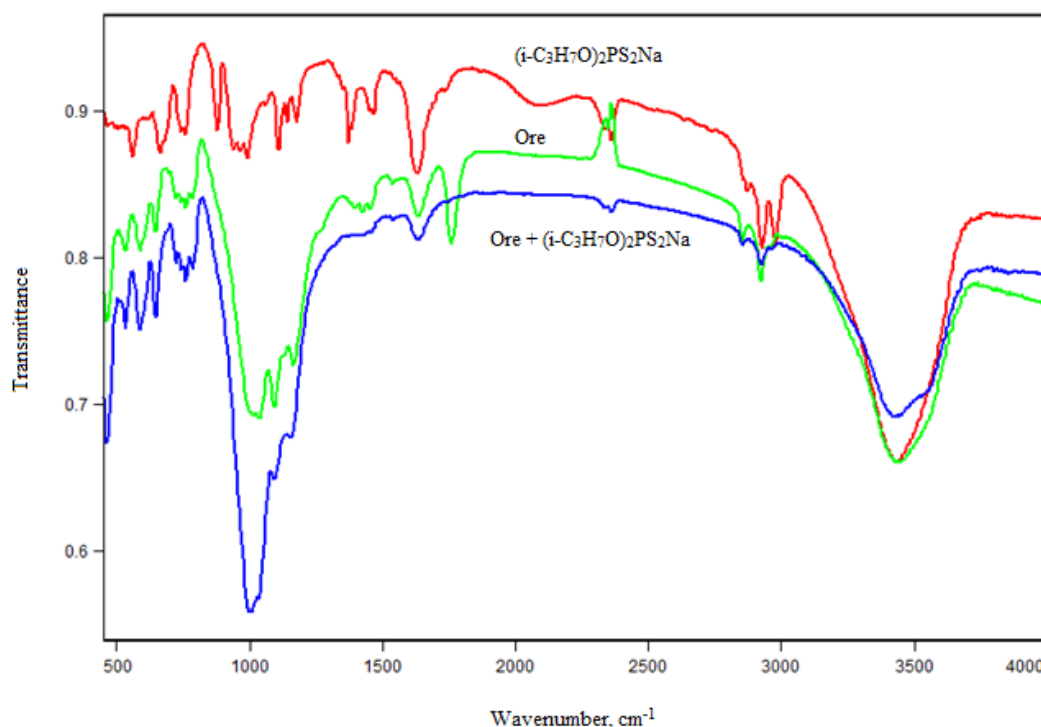


Figure 5 – FT-IR spectra of collector, sulfide copper ore and sulfide copper ore treated with collector after treatment

Conclusion

Elemental analysis of samples of copper sulfide ore was carried out, copper content in ore equals to 1.99%. According to the results of the mineralogical analysis, copper-containing sulfide minerals contain chalcocite, bornite. It is shown that the sorption capacity increases with increasing pH of the medium from 10.5-11.5. It has been established that oxidation-reduction processes play the main role in fixing the collector of diisopropyldithiophosphate ion. In a weakly alkaline medium, the sorption of the collector does

not change with increasing pH, which is due to the formation of copper (II) complexes, as well as the disulfide fixed through Van-der-Waals bonds. While in the alkaline medium the collector anion forms strong coordination bonds with the metal ions of the crystal lattice of the mineral. Correlation of extraction of copper in concentrate during flotation enrichment with the value of sorption is revealed, which indicates a high sorption capacity of the collector at pH 10.5-11.5. FT-IR-spectroscopic analysis of ore samples was conducted, according to which it was established that the collector is coordinated with the ions of the

metal of the crystal lattice of copper-containing minerals through the sulfur atoms of the dithiophosphate group.

References

- Gusev A.I. (2014) Tipizaciya ehndogenogo orudeneniya koksairskogo rudnogo polya gornogo altaya [Typification of endogenous mineralization koksair ore field of the Altai mountains]. *Uspekhi sovremennogo estestvoznaniya*, no. 5-1, pp. 98-102.
- Corin K.C., Kalichini M., O'Connor C.T., Simukanga S. (2016) The recovery of oxide copper minerals from a complex copper ore by sulphidisation. *Minerals engineering*, vol. 102, pp.15-17.
- Sousa R., Futuro A., Pires C.S., Leite M.M. (2017) Froth flotation of Aljustrel sulfide complex ore. *Physicochemical problems of mineral processing*, vol. 53, pp.758-769.
- Azizi A. (2015) A study on the modified flotation parameters and selectivity index in copper flotation. *Particulate science and technology*, vol. 35, pp.38-44.
- Jacques S., Greet C.J., Bastin D. (2016) Oxidative weathering of a copper sulphide ore and its influence on pulp chemistry and flotation. *Minerals engineering*, vol. 99, pp.52-59.
- Thompson P. (2016) Laboratory testing for sulfide flotation process development. *Minerals & metallurgical processing*, vol. 33, pp.200-213.
- Wei S., Haisheng H., Hongbiao T., Runqing L. (2015) Study on the flotation technology and adsorption mechanism of galena-jamesonite separation. *International Journal of Mining Science and Technology*, vol. 25, pp.53-57.
- Wiese J., Harris P., Bradshaw D. (2011) The effect of the reagent suite on froth stability in laboratory scale batch flotation tests. *Minerals Engineering*, vol. 24, pp.995-1003.
- Avdokhin V., Morozov V.A. (1998) System for Control of Complex Ores Flotation Based on Measuring Pulp Ionic Composition. *IFAC Proceedings Volumes*, vol. 31, pp.125-128.
- Zhang T., Qin W., Yang C., Huang Sh. (2014) Floc flotation of marmatite fines in aqueous suspensions induced by butyl xanthate and ammonium dibutyl dithiophosphate. *Transactions of Nonferrous Metals Society of China*, vol. 24, pp.1578-1586.
- Piao Zh., Wei D., Liu Zh., Liu W., Gao Sh., Li M. (2013) Selective depression of galena and chalcopyrite by O,O-bis(2,3-dihydroxypropyl) dithiophosphate. *Transactions of Nonferrous Metals Society of China*, vol. 23, pp.3063-3067.
- Buckley A.N., Hope G.A., Parker G.K., Steyn J., Woods R. (2017) Mechanism of mixed dithiophosphate and mercaptobenzothiazole collectors for Cu sulfide ore minerals. *Minerals Engineering*, vol. 109, pp.80-97.
- Zhong H., Huang Zh., Zhao G., Wang Sh., Liu G., Cao Zh. (2015) The collecting performance and interaction mechanism of sodium diisobutylidithiophosphinate in sulfide minerals flotation. *Journal of Materials Research and Technology*, vol. 4, pp.151-161.
- Amerkhanova Sh.K. (2005) Eelektrohimicheskie i fiziko-himicheskie svojstva hal'kogenidov podgruppy medi i metallov pervogo perehodno-go rjada [Metal chalcogenides' electrochemical and physico-chemical characteristics in the subgroup of copper and metals of first transitional row]: Sum. dis. ... doct. chem. sci., Karaganda, p. 50.
- Filippova N.A. (1975) Fazovyj analiz rud i produktov ih pererabotki [Phase-analysis of ores and their treatment products], 2nd ed, Chem: Moscow, p. 280.
- Ospanov Kh.K. (2004) Theory of controlling a physico-chemical process-taking place at the interface solid-liquid, 1st ed., Flint River: London, p. 129.
- Yanson Je. Ju, Putnin' Ja.K. (1980) Teoreticheskie osnovy analiticheskoy himii [Theoretical foundations of analytical chemistry], High sch.: Moscow, p. 260.
- Pesic B. (1984) Dissolution of bornite in sulfuric acid using oxygen as oxidant. *Hydrometallurgy*, vol. 12, pp.195-215.
- Gautier J., Ortiz J., Heller-Ling N., Poillerat G., Chartier P. (1998) Oxygen reduction on bornite in alkaline medium. *Journal of Applied Electrochemistry*, vol. 28, pp.827-834.

IRSTI 31.17.15

^{1,2*}G. Xanthopoulou and ¹G. Vekinis

¹Institute of Materials Science, NCSR “Demokritos”, Aghia Paraskevi, 15310, Greece

²Department of Theory of Aircraft Engines, Samara National Research University, 34 Moskovskoe shosse, 443086 Samara, Russia

*e-mail: gxantho@ims.demokritos.gr

Self-propagating high-temperature synthesis of nial intermetallic compounds

Abstract. In this work, the self-propagating high-temperature synthesis (SHS) method was utilized for the synthesis of the B2 NiAl compound. Elemental nickel and aluminum powders were mixed, die-pressed, and pre-heated in a furnace in which the SHS reaction was initiated and propagated. The influence of pre-heating temperature was evaluated against the final composition, phase formation, microstructure and hardness of the final compact. Conditions were found under which, the final product forms through solidification from the melt and (irrespective of the furnace temperature) consists only of the B2 NiAl. The NiAl compacts formed consisted of a core which is essentially pore free and accounts for ~80% of the total volume and a high porosity shell around it. The microstructure consists of large, equiaxial grains with linear grain boundaries indicative of high phase stability. Finally, it was found that as the pre-heating temperature increases the hardness of the NiAl compact decreases; a transient temperature analysis enabled to interpret this observation.

Practical significance of the results: NiAl is an extremely useful industrial material with many high temperature applications.

Key words: self-propagating high-temperature synthesis, NiAl

Introduction

The B2 ordered intermetallic NiAl compounds exhibit a wide range of physical and mechanical properties which show promise for applications ranging from high-pressure turbine blades to buried interconnects in electronic components [1]. NiAl forms an adherent film on oxidation in air at temperatures up to 1200°C, indicating good corrosion resistance as demonstrated by its use as a base for some protective coatings on nickel-based superalloys. The structure remains fully ordered up to the melting point, implying a resistance to diffusion-controlled processes, such as precipitation, grain growth, oxidation and creep deformation. The large phase width of NiAl suggests a potential for substitutional alloying to improve strength and oxidation resistance. NiAl is approximately 30% less dense than nickel (a common superalloy base) and has a melting point 200°C higher. On the other hand, drawbacks of this type of intermetallics include low ductility and toughness [1, 2].

Conventionally intermetallics are fabricated by processes such as vacuum arc melting and their final

microstructure is refined by several thermomechanical treatments. To reduce costs and complexity, Self-Propagating High-Temperature Synthesis (SHS) and thermal explosion, has also been used [3-7]. In the SHS method, the exothermic reaction between the powder constituents is initiated and becomes self-sustaining to yield the final product progressively without requiring additional heat. Compared to conventional processing methods, the main advantages of SHS are: (i) higher purity products because of the high reaction temperature which can volatilize and hence “remove” low boiling point impurities, (ii) simplicity since there is no need for expensive processing facilities and equipment, (iii) low operating and processing costs due to the short exothermic reaction times, (iv) ability to fabricate non-equilibrium or metastable phases because of the high thermal gradients and rapid cooling rates and (v) capability for producing a wide range of inorganic materials consolidated into a final product in one step by utilizing the chemical energy of the reactants [8-10]. However, there are some disadvantages of the method such as high porosity (which may be reduced by simultane-

ous compression [11]), microstructural inhomogeneities, etc. Several reviews of the combustion synthesis technique and its prospects have appeared in the literature [12-22].

Thermodynamics

During the combustion synthesis reaction there are four important temperatures which affect the process of the reaction and the properties of the final product: 1) the initial or preheating temperature T_o , which is the temperature of the powder compact of the reactant sample before the reaction is initiated, 2) the ignition temperature T_{ig} , which represents the point at which the SHS reaction is spontaneously activated without further external heat supply, 3) the adiabatic combustion temperature T_{ad} , which is the maximum combustion temperature achieved under adiabatic conditions and (4) the actual combustion temperature T_c , achieved normally under non-adiabatic conditions [23].

The amount of heat, $H(R)$ required to raise the temperature of the reactants from the initial temperature T_o to the ignition temperature T_{ig} (i.e. the tem-

perature at which the exothermic reaction initiates) is given by the following equation:

$$H(R) = \int_{T_o}^{T_{ig}} \sum n_i C_p(R_i) dT + \sum_{T_o-T_{ig}} n_i L(R_i) \quad (1)$$

where n_i , $C_p(R_i)$, and $L(R_i)$ represent the reaction stoichiometric coefficients, heat capacities and the phase transformation enthalpies (if the reactants go through a phase change such as from solid to liquid) of the reactants respectively. At a certain distance from the heat source, the reactant compact reaches steady state conditions; in this state the heat of the reaction $\Delta H(T_{ig})$ is only used to heat the adjacent layer from T_o to T_{ig} . At this point, the amount of heat available to be absorbed by the products under adiabatic conditions is, therefore, $H(P)$, which raises the temperature from T_{ig} to the adiabatic temperature $T_{ad}(T_o)$, i.e.

$$\Delta H(T_{ig}) = - [H(R) + H(P)] \quad (2)$$

where $H(P)$ is given by:

$$H(P) = \int_{T_{ig}}^{T_{ad}(T_o)} \sum n_j C_p(P_j) dT + \sum_{T_{ig}-T_{ad}(T_o)} n_i L(P_j) \quad (3)$$

where n_j , $C_p(P_j)$, and $L(P_j)$ represent the reaction stoichiometric coefficients, heat capacities and the phase transformation enthalpies (if the products go through a transformation phase change) of the products respectively. The increase of the initial (average) temperature T_o will decrease $H(R)$ and increase both $H(P)$ and the adiabatic temperature. Increasing T_o to T_{ig} , will decrease $H(R)$ to zero and

all of $\Delta H(T_{ig})$ will be available to be absorbed by the products [14,23].

Materials and Methods

Processing and synthesis

Used in the experiments Ni powder characteristics presented in table 1.

Table 1 – Nickel Powder Characteristics

Composition							
C	Mn	Cu	Fe	S	Si	Ni	
0.017	<0.01	<0.01	0.04	0.0002	0.31	Bal.	
Size Distribution							
Mesh Size	+100	+120	+140	+200	+270	+325	-325
Percent	4.2	3.0	6.1	15.2	15.9	13.7	41.9

Aluminum powder MERCK, max. particle size 125 micron, purity 99.5%.

Stoichiometric fractions of elemental powders to produce the NiAl phase (38.5wt%Ni + 61.5wt%Al) were mixed thoroughly and die-pressed at a pressure of 30 bars to form cylindrical compacts (diameter c. 15 mm and height c. 20 mm) of green density about 60% of theoretical. The cylindrical specimens were then pre-heated in a furnace where the exothermic reaction between the Ni and the Al particles initiates as soon as any area of the compact reaches the ignition temperature. In all of our experiments, the reaction was initiated at the top surface of the specimens after exposure to the furnace temperature for a period between 1 and 4 minutes, depending on pre-heating temperature. As the SHS combustion zone moves through the specimen, a series of reactions take place and the compact melts, since the combustion temperature (approaching 2000 °C is well above the melting temperature of the NiAl phase (1640 °C). Once the SHS reaction is completed, the specimen is removed from the furnace and air-cooled.

The microstructure of the NiAl product, its chemical homogeneity and its mechanical properties usually depend on the processing conditions as well as the compact geometry, because of their effect on

the actual average compact temperature at the time of ignition and on the cooling rate of the NiAl melt. The dimensions and the initial density of the specimens were kept fixed, while the furnace temperature T_{fur} was varied from 700 to 1000°C. The time to reaction initiation t_{in} was not constant in the experiments but decreased with increasing the furnace temperature as the initiation temperature was reached quicker.

Characterization

The NiAl materials synthesized were characterized by a number of techniques including X-ray diffraction, optical and scanning electron microscopy, electron dispersive spectroscopy, and hardness testing.

Results and Discussion

Modelling of the compact temperature

The time to ignition t_{in} , defined as the period that the specimen remains inside the furnace until the reaction initiates depends upon the initial temperature of the furnace. The variation of t_{in} versus the furnace temperature T_{fur} as determined from the SHS experiments is shown in Figure 1.

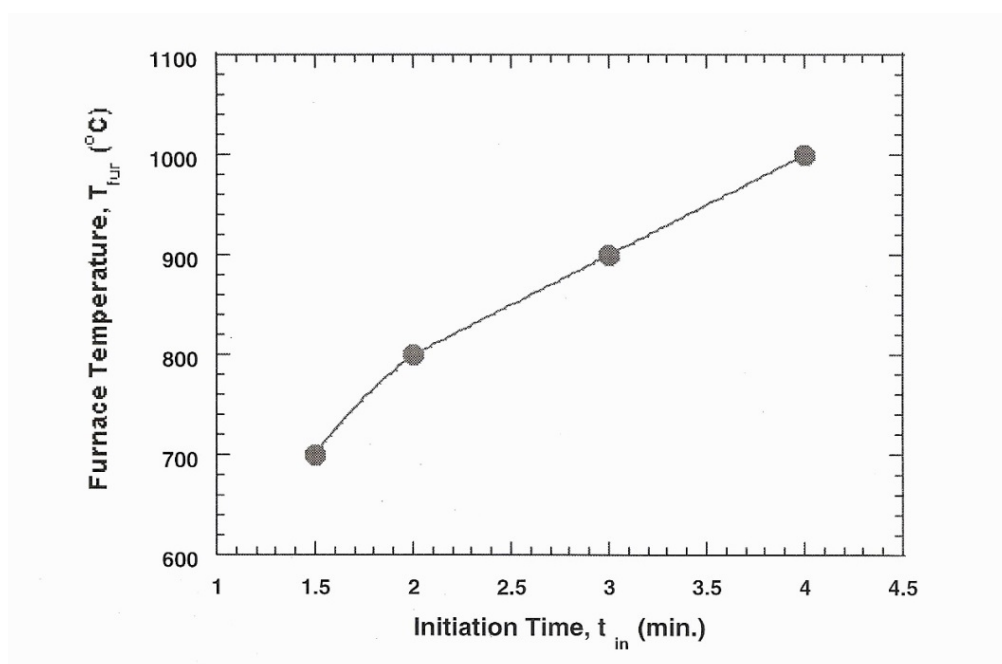


Figure 1 – The variation of initiation time t_{in} as a function of the furnace temperature T_{fur}

It is seen that as the furnace temperature increases the initiation time decreases because the ignition temperature (on the top surface of the sample) is reached faster. After ignition, the time required to propagate

the reaction front along the specimen is less than 1 second, i.e. the reaction speed is quite high^{1*}. Thus,

^{1*}in fact, earlier work[16] on the synthesis of the 50% Ni – 50% Al system it was measured as being equal to XXX m/sec

with regard to the microstructure formation and evolution, it we accept that at the end of the reaction and prior to solidification, the material is at the liquid state. The microstructure obtained from the solidification process is dependent upon the difference between the temperature of the melt (which is related to the combustion temperature of the reaction) and the furnace temperature. Therefore, to interpret the microstructural features the combustion temperature (or likewise the average compact temperature) must be estimated.

As mentioned above in the section of “Thermodynamics”, the maximum adiabatic temperature de-

pends upon the average temperature of the compact. Evidently, the latter should be related to the furnace temperature and the time of exposure inside the furnace t_{in} . In order to gain a comparative estimate of the average compact temperature right before the reaction initiation for the various T_{fur} and t_{in} , a transient temperature analysis was conducted. In particular, the temperature at the center of the compact T_{cen} for the specific T_{fur} and t_{in} was calculated following the procedure which is outlined in the Appendix.

The variation of the temperature at the center of the compact versus the furnace temperature is shown in Figure 2.

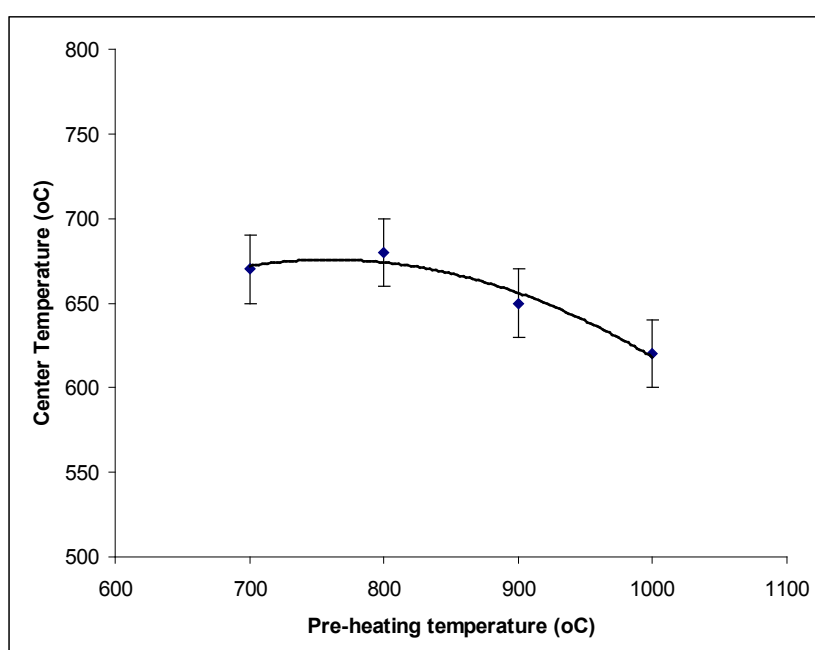


Figure 2 – The temperature at the center of the compact versus the furnace temperature

It is seen that, within the limits of the estimation error (which mainly arises from factors such as the accuracy of the calculation of the thermal properties of the porous compact) T_{cen} does not appear to vary with the furnace temperature. In other words T_{fur} and t_{in} are combined such that the temperature of the specimen's center has the same temperature irrespectively of the processing conditions. Therefore, since the temperature at the center of the specimen reflects its average temperature, it is deduced that the combustion temperature was the same for all of the experimental conditions. Given the fact that the ignition temperature (which in the experiments of this work was first reached on the top surface of the specimen) is dependent only upon the composi-

tion of the compact, the above analysis is important as it provides an indication that the average temperature of the specimen right before the ignition does not vary with the furnace temperature.

Characterization

a. X-ray Diffraction (XRD)

Figure 3 shows the XRD spectrum of a material fabricated by self-propagating synthesis of nickel and aluminum powder under the following processing conditions: furnace temperature 1000 °C, green compact density 60% of the theoretical, and initial dimensions 20 mm diameter and 15 mm height.

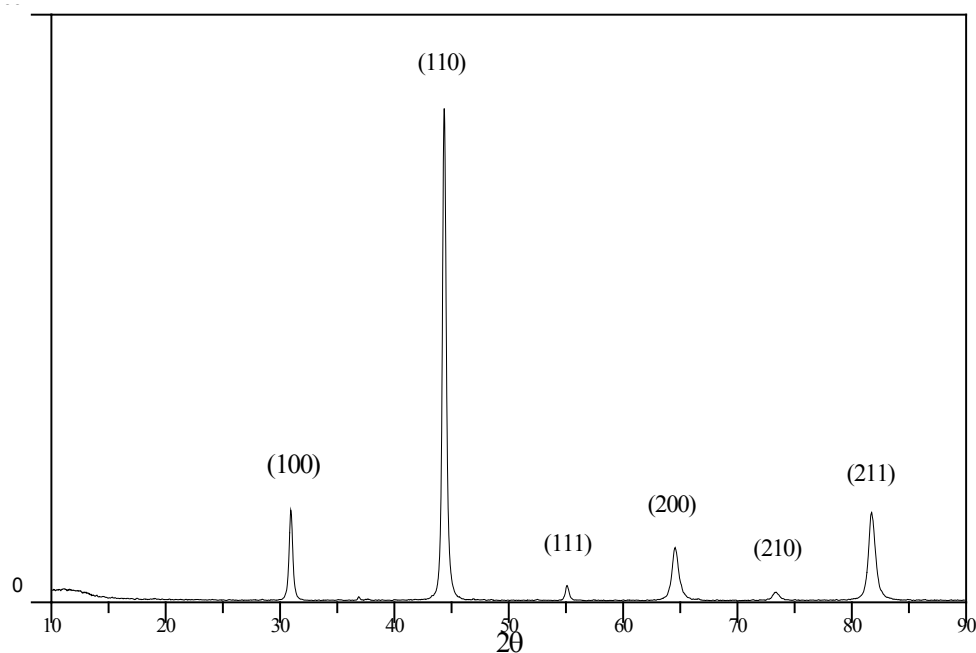


Figure 3 – Typical XRD spectra of NiAl produced by self-propagating high-temperature synthesis

In order to eliminate possible effects of the texture developed during the solidification of the melt, the specimen was pulverized, and its powder was used for the XRD characterization. All peaks that appear in the graph correspond to the NiAl intermetallic phase; no other intermediate phases between nickel and aluminum, or any oxides were detected, and no further elemental aluminum and nickel are present. In addition, materials synthesized under different processing conditions (i.e. furnace temperature, time exposed inside the furnace, etc.) were also examined by XRD, giving identical spectra to that shown in Figure 3. Therefore, in all cases pure monophase NiAl with the B2 ordered cubic structure with a lattice parameter $a = 2.88\text{\AA}$ was fabricated.

Earlier characterization work on the formation of NiAl compounds using differential thermal analysis (DTA) and synchrotron radiation techniques revealed that during the SHS synthesis several intermediate phases such as Ni_3Al and Ni_3Al_2 are formed prior to the formation of the final, stoichiometric NiAl phase[23-24]. The formation as well as the presence of residues of the intermediate phases depends upon the combustion temperature. In particular, the proportion of the Ni_3Al and Ni_3Al_2 phases decreases as the combustion temperature increases. Therefore, the above results indicate that a high combustion temperature was achieved in our experiments.

Microstructure

As mentioned above, the NiAl formation proceeds through the formation of a melt. Examination of the microstructure at lower magnifications showed that the final product comprises two regions, a core which accounts for ~80% of the total volume of the compact, and a “shell” of high porosity (of the order of 20%) material around the core. This outer shell, whose microstructure is shown in Figure 4, owes its formation to the gravitational flow of a small portion of the liquid, since in our experiments the specimen stood free inside the furnace, thus flow of the melt was possible.

It is observed that the structure comprises large (~150 μm) grains of equiaxed shape. The fact that the NiAl grains have linear grain boundaries with no curvature indicate the high stability of the formed compound, the absence of secondary phases, and a very rapid crystallization of the primary melt. Although, no pores can be discerned from this micrograph; the higher magnification micrograph in Figure 6 shows that there are a few spherical with a size of less than 10 μm inside the material.

Although at low magnifications the microstructure of the core appears to be quite uniform, microstructural nonuniformities may be distinguished at higher magnifications. In particular, the SEM micrograph of Figure 6 reveals the presence of spherical particles within a fine grained matrix.

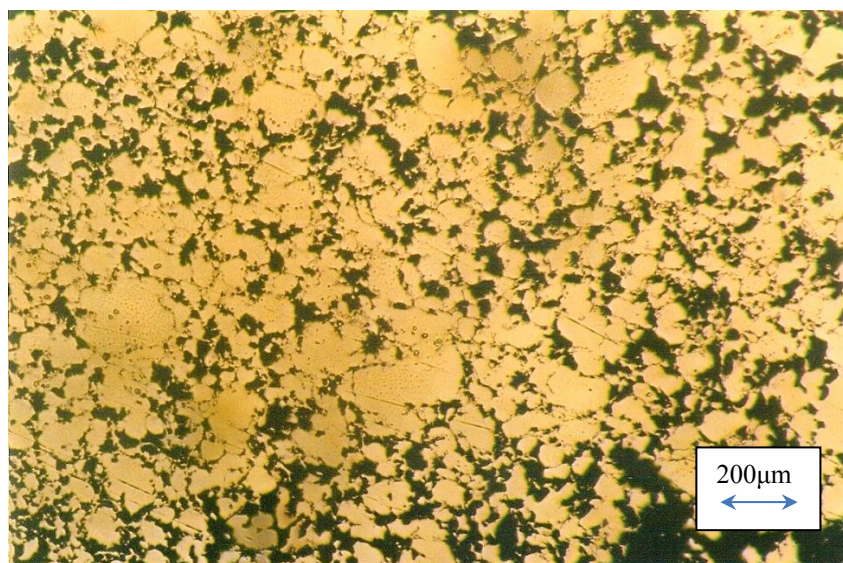


Figure 4 – Microstructure of NiAl-rich outer shell

A typical, low magnification, optical micrograph of the core is shown in Figure 5.

In conjunction with the XRD results it can be deduced that both the particles as well as the fine matrix are of pure NiAl. It is also seen that the pores are mainly located at the particle/matrix boundaries,

which indicated that the large particles solidified first inside the matrix which was in the liquid state.

Hardness

The Vickers hardness of the NiAl compounds versus the furnace temperature at which they were synthesized is presented in Figure 8.



Figure 5 – Microstructure of the core

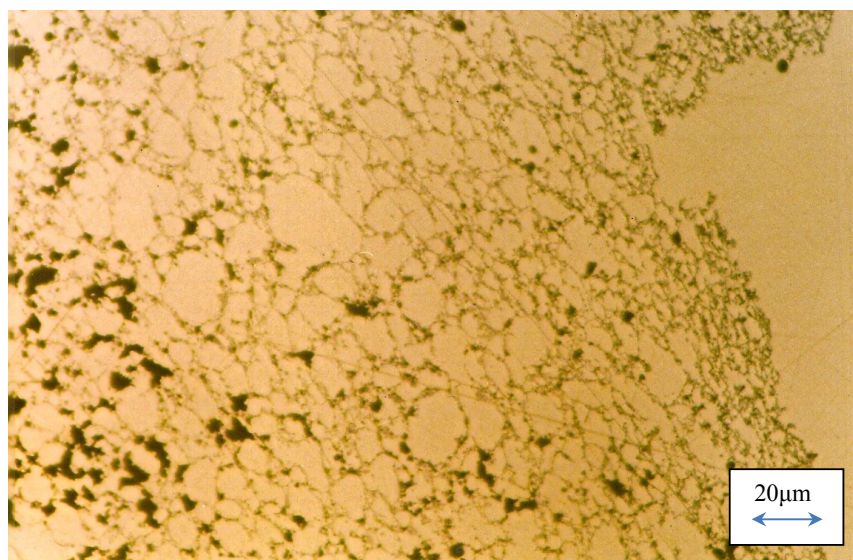


Figure 6 – Microstructure of semi-spherical particles within a fine grained matrix

The particles have a wide distribution of sizes ranging between 4 and 15 μm . The chemical composition of the particles as well as the composition of the matrix were determined by EDS analysis. The EDS spectra shown in Figure 7 do not reveal any essential differences on the peaks of nickel and aluminum between the particles and the matrix.

The results revealed a trend of decreasing hardness with increasing the furnace temperature. This hardness variation can be interpreted with regard to the cooling rate of the NiAl melt which is proportional to the difference ΔT between the temperature of the melt T_m and the temperature of the furnace T_{fur} . If it is assumed that the temperature of the melt is near the combustion temperature, (which as discussed in

the previous sections is essentially constant for all conditions used) then ΔT increases as the furnace temperature decreases. Therefore, at lower T_{fur} the cooling rate is higher, resulting to a more brittle and harder microstructure. SEM micrographs of the fracture surface of NiAl compacts fabricated at furnace temperatures of 700 and 1000 $^{\circ}\text{C}$ are shown in Figures 9a and b respectively. The micrograph of Figure 9a shows a brittle type of fracture, while areas which have undergone plastic deformation are observed in Figure 9b. Interestingly, NiAl fibres were also found to have formed inside pores and are also visible in Figure 9a and b. This is the first time such fibres have been observed and the exact conditions of formation and characteristics are under investigation at present.

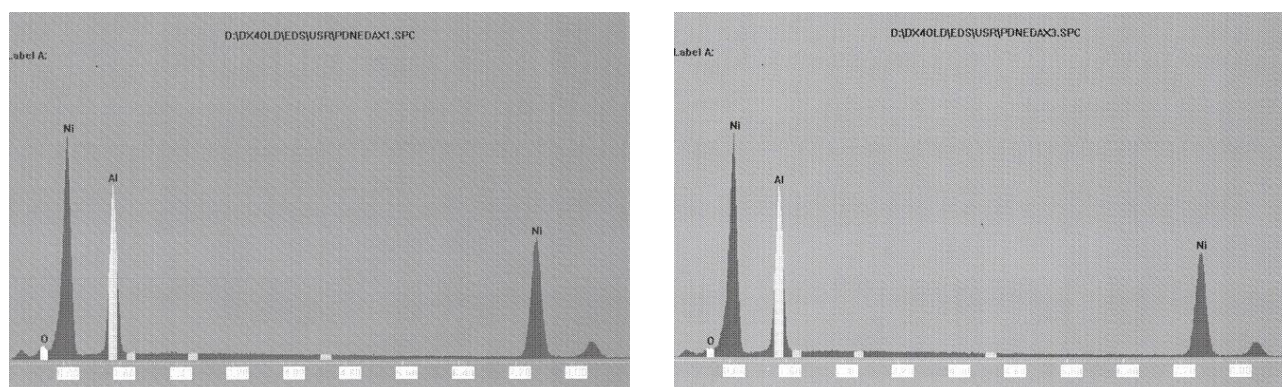


Figure 7 – The EDS spectra of the particles (left) and the matrix (right) showing that they have almost identical elemental composition

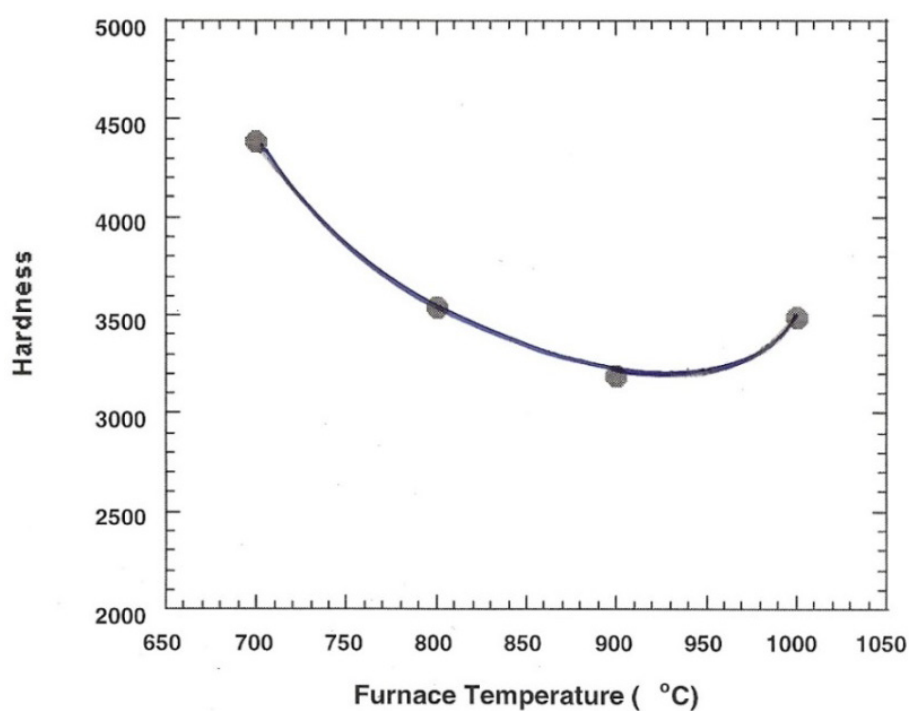


Figure 8 – The Vickers hardness of the NiAl compounds versus the furnace temperature.

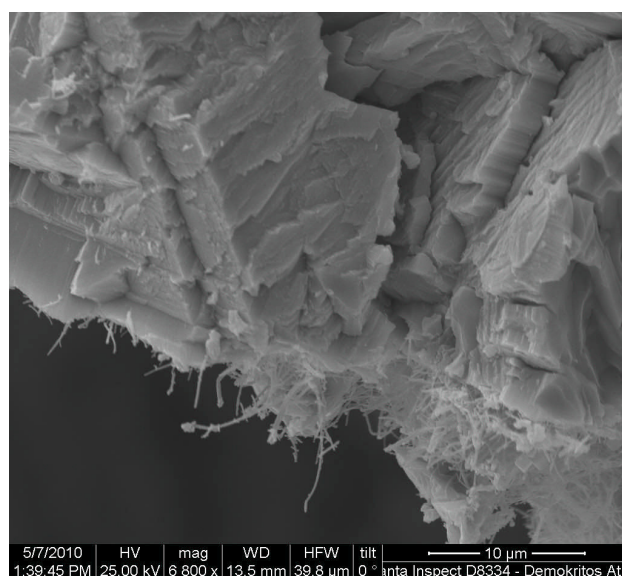
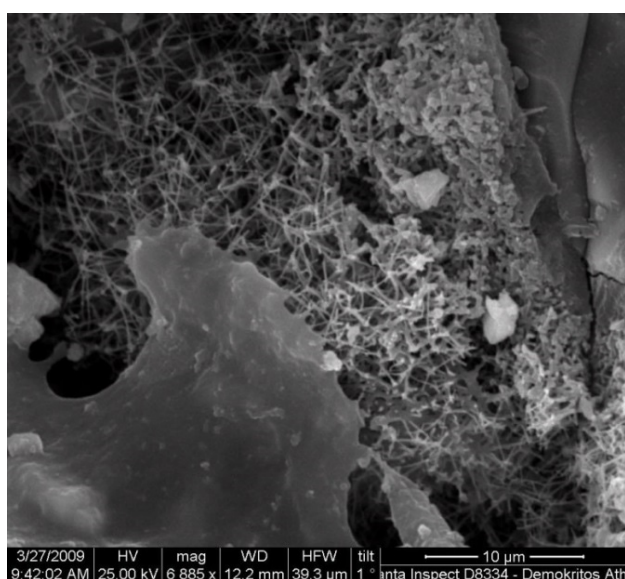


Figure 9 – SEM of SHS NiAl (initial mixture 60%Al- 40% Ni). Brittle fracture with some localized areas where limited plastic deformation are visible. NiAl fibres are also visible

In summary, the low sensitivity of the material hardness (and hence strength) upon the furnace temperature represents a significant technological advantage of the process from the industrial

point of view, because it does not pose great difficulties in scale-up, and also the material quality does not vary greatly with the processing furnace temperature.

Summary and conclusions

The SHS method was used to synthesize the B2 NiAl compound from elemental nickel and aluminum powders. The main conclusions of this work may be summarized as follows:

1. X-ray diffraction showed that the NiAl is the only phase formed (through solidification of a melt) when the powder compacts are processed at a furnace temperature is at the 700-1000 °C range.

2. The microstructure consists of large equiaxed grains with linear grain boundaries. The latter indicate the high stability of the compound synthesized and a very rapid crystallization of the primary melt.

3. The hardness of the final product was found to decrease with the increase of the furnace temperature because of the lower cooling rate of the melt.

4. The process used has shown that NiAl fibres can form inside pores of the material.

Acknowledgements

We'd like to thank Dr P. Nikolaou for his contribution in this work.

References

1. C.T. Liu and K.S. Kumar, Ordered Intermetallic Alloys, Part I: Nickel and Iron Aluminides, JOM, May 1993, pp. 38-41.
2. R.D. Noebe, R.R. Bowman, and M.V. Nathal, Review of the Physical and Mechanical Properties and Potential Applications of the B2 Compound NiAl, NASA Technical Memorandum 105598.
3. D.E. Alman, J.A. Hawk, A.V. Petty, and J.C. Rawers, "Processing Intermetallic Composites by Self-Propagating, High Temperature Synthesis", JOM, March 1994, 31-35.
4. A. Varma, C.R. Kachelmyer, and A.S. Rogachev, Mechanistic Studies in the Combustion Synthesis of Aluminides and Silicides, *Int. J. of Self. Prop. High-Temp. Synth.*, vol. 5, No 1, 1996, pp. 1-25.
5. T.S. Dyer and Z.A. Munir, The Synthesis of Nickel Aluminides by Multilayer Self-Propagating Combustion, *Metall. Mater. Trans. B*, vol. 26B, 1995, pp. 603-610.
6. Z.A. Munir, Reaction Synthesis Processes: Mechanisms and Characteristics, *Metall. Trans. A*, vol. 23A, 1992, pp. 7-13.
7. B. Michelic, M. Dakic, R. Djekic, and D. Uskokovic, Processing of Compact Materials by the Use of Self-Propagating High-Temperature Synthesis and Pseudo-Hot Isostatic Pressing, *Mater. Lett.*, vol. 13, 1992, pp. 391-395.
8. H. Doty and R. Abbaschian, Reactive Hot Compaction of NiAl with in situ Alumina Reinforcement, *mat. Scie. Eng. A*, vol. A195, 1995, pp. 101-111.
9. J.J. Moore, D.W. Ready, H.J. Feng, K. Monroe, and B. Mishra, The Combustion Synthesis of Advanced Materials, JOM, November 1994, pp. 72-78.
10. D.E. Alman, C.P. Dogan, J.A. Hawk, and J.C. Rawers, Processing, Structure and Properties of Metal-Intermetallic Layer Composites, *Mater. Scie. Eng. A*, vol. A192/193, 1995, pp. 624-632.
11. Z.P. Xing, J.T. Guo, G.Y. An, and Z.Q. Hu, Hot Pressing Aided Exothermic Synthesis and Densification of NiAl and NiAl-TiC Composite, *Int. J. of Self. Prop. High-Temp. Synth.*, vol. 5, No 1, 1996, pp. 51-56.
12. A.G. Merzhanov, Worldwide Evolution and Present Status of SHS as a Branch of Modern R&D, *Int. J. of Self. Prop. High-Temp. Synth.*, vol. 6, No 2, 1997, pp. 119-163.
13. J.J. Moore and H.J. Feng, Combustion Synthesis of Advanced Materials: Part II. Classification, Applications and Modeling, *Prog. Mater. Scie.*, vol. 39, 1995, pp. 274-316.
14. Z.A. Munir, Synthesis of High Temperature Materials by Self-Propagating Combustion Methods *Ceram. Bull.*, vol. 67, No 2, 1988, pp. 342-349.
15. Shushan Dong, Ping Hou, Haiyong Cheng, Haibin Yang and Guangtian Zou, Fabrication of intermetallic NiAl by self-propagating high-temperature synthesis reaction using aluminium nanopowder under high pressure, 2002 *J. Phys. Condens. Matter* 14 11023
16. Effects of TiC addition on combustion synthesis of NiAl in SHS mode YEH C. L., SU S. H., CHANG H. Y., *Journal of alloys and compounds* 2005, vol. 398, pp. 85-93
17. Iris V. Rivero, Michelle L. Pantoya, Karthik Rajamani, Simon M. Hsiang, Correlation of reactant particle size on residual stresses of nanostructured NiAl generated by self-propagating high-temperature synthesis *Materials Research Society*, v.24, n.6, pp. 2079- 2088
18. Roy, S. K. and Biswas, A'Combustion of Powder Mixtures Forming Reaction Products -Synthesis of NiAl', *Mineral Processing and Extractive Metallurgy Review*, 22: 2, 567 – 596.(2001)

19. D. Tingaud, L. Stuppfler, S. Paris, D. Vrel, F. Bernard, C. Penot and F. Nardou, Time-resolved X-ray diffraction study of SHS-produced NiAl and NiAl-ZrO₂ composites *Int. Journal SHS*, 2007, Volume 16, Number 1, Pages 12-17
20. V. I. Vershinnikov and I. P. Borovinskaya, Fine TiAl and NiAl powders by SHS with a reduction stage *Int. Journal SHS*, 2009, Volume 18, Number 2, Pages 97-101
21. A. Biswas, S.K. Roy, Comparison between the microstructural evolutions of two modes of SHS of NiAl: key to a common reaction mechanism, *Acta Materialia* 52 (2004) 257–270
22. A. Shchukin, D. Vrel, A. Sytshev, Interaction of NiAl Intermetallic During SHS Synthesis with Ta Substrate, February 2018, Advanced Engineering Materials DOI: 10.1002/adem.201701077
23. J.J. Moore and H.J. Feng, Combustion Synthesis of Advanced Materials: Part I. Reaction Parameters, *Prog. Mater. Scie.*, vol. 39, 1995, pp. 243-273.
24. M.C. Dumez, R.M. Marin-Ayral, and J.C. Tedenac, La Synthèse Auto-Propagée Haute Pression Appliquée aux Intermétalliques de Type Nickel-Aluminium, *Mater. Res. Bull.* vol. 29, No 6, 1994, pp. 611-617.
25. A.V. Luikov, A.G. Slskov, L.L. Vasiliev, and Y.E. Fraiman, *Int. J/ Heat Mass Transf.*, vol. 11, pp. 117-125, 1968
26. W.D. Kingery, H.K. Bowen, and D.R. Uhlmann, Introduction to Ceramics, 2nd Edition, J. Wiley & Sons, New York, 1976.
27. A.D. Brailsford and K.G. Major, *Br. J. Appl. Phys.*, vol. 15, 1964, pp. 313-320.
28. G.H. Geiger and D.R. Poirier, Transport Phenomena in Metallurgy, Addison-Wesley Publishing Co, Reading MA, 1973.
29. F. P. Incropera and D.P. DeWitt, Fundamentals of Heat and Mass Transfer, 2nd Edition, J. Wiley & Sons, New York, 1985
30. D. Tingaud, L. Stuppfler, S. Paris, D. Vrel, F. Bernard, C. Penot and F. Nardou, Time-resolved X-ray diffraction study of SHS-produced NiAl and NiAl-ZrO₂ composites, *Int. Journal SHS*, 2007, Volume 16, Number 1, Pages 12-17
31. V. I. Vershinnikov and I. P. Borovinskaya, Fine TiAl and NiAl powders by SHS with a reduction stage *Int. Journal SHS*, 2009, Volume 18, Number 2, Pages 97-101
32. A. Biswas, S.K. Roy, Comparison between the microstructural evolutions of two modes of SHS of NiAl: key to a common reaction mechanism, *Acta Materialia* 52 (2004) 257–270
33. A. Shchukin, D. Vrel, A. Sytshev, Interaction of NiAl Intermetallic During SHS Synthesis with Ta Substrate, February 2018, Advanced Engineering Materials DOI: 10.1002/adem.201701077

IRSTI 61.33.39

¹O.A. Yessimova, ¹A.O. Adilbekova, M.Zh. Kerimkulova,
²G.D. Isenova, ³B. Lozowicka, ¹K. Sagymbekova

¹Al-Farabi National Kazakh University, Almaty, Kazakhstan

²LLP «Kazakh Institute of Protection and Quarantine of Plants named after Zh. Zhiembayev», Almaty, Kazakhstan

³Institute of Plant Protection, Poznan, Poland

e-mail: Orinkul.Esimova@kaznu.kz

Influence of mixed aqueous solutions of polyhexamethylene guanidine hydrochloride and OP-10 on vegetable crop seeds

Abstract. The effect of bactericidal and fungicidal polymer polyhexamethylene guanidine hydrochloride (PHMGH) and its mixture with non-ionic surfactant oxyethylated isooctylphenol (OP-10) on the germination of seeds of tomatoes, cucumbers and sugar beet was studied. PHMGH is known disinfectant. It is odorless, colorless, non-corrosive and non-toxic for humans, PHMGH can be applied to make an innovative product in the disinfection of plants and vegetables and preservation of food products. Vegetable seeds were treated with aqueous solutions of PHMGH, OP-10 and mixed solutions of PHMGH/OP-10. Tests were made in relation to the growth and development of plants treated with bactericides. PHMGH (0.05 %) aqueous solution favors for cucumber seed growth (the germination percentage equals to 94 %), PHMGH/OP-10 complex (at a ratio of 1:1 at initial component concentrations equaled to 0.01%) for tomato seeds (90%). The mixture of PHMG/OP-10 was effective on the growth and development for all of the studied vegetable crops (stem and leaf length). The effect of aqueous solutions of PHMGH, OP-10 and PHMGH/OP-10 on the content of chlorophyll in the leaves of the studied objects was studied. The increasing of chlorophyll amount was observed after treatment with PHMGH complexes that results in resistance of vegetables to action of environmental factors.

Key words: polyhexamethylene guanidine hydrochloride, oxyethylated isooctylphenol, bactericidal complexes, fungicidal complexes, germination, chlorophyll, seeds, surfactant.

Introduction

The consumption of fresh vegetables increases every year in our country. Wide using of chemicals on plant protection leads to the negative environmental, sanitary and other consequences. With the accumulation of negative impact factors, the development of improving methods and means of plant protection, the alternative ways preventing diseases of vegetable crops are growing. For this reason, the importance of the development and production of new bactericidal and fungicidal complexes increases [1].

Vegetable crops as other plants are exposed to diseases, which in turn interfere to obtaining of a stable and high yield. Traditional methods of crop increasing are complex, long-lasting and not always effective [2-3].

Recently, a method of film based on polymers has been successfully used in vegetable growing. This

method allows bactericidal and fungicidal complexes to fix on the surface of the culture, providing them the high germination, as well as further development of a plant. Moreover, the use of such agents eliminates the negative impact of microorganisms, being safe for the environment [4].

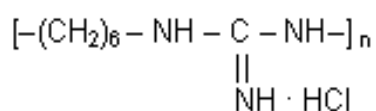
Currently, the environmentally correct, non toxic preparations are necessary for agriculture. In this perspective, complexes with high biological activity based on polyhexamethylene guanidine hydrochloride (PHMGH) and PHMGH/surfactant were used to improve the germination of vegetable seeds. Polymeric guanidines are widely used as disinfectants [5-8]. The many physical and chemical characteristics of this product: odorless, colorless, non-corrosive and non-toxic for humans with a neutral pH make an innovative product in the disinfection of plants and vegetables and preservation of food products. The antimicrobial activity of this product was shown on

many bacteria [9]. Also, PHMGH has a fungicidal activity on various fungal species [10]. Non-ionic surfactant OP-10 was used due to their surface properties and ability to wet the surface of plants (stem, leaves).

The main aim of this study was to show opportunity of using of polyhexamethylene guanidine hydrochloride with respect to the some vegetable crops cultivated in our country such as tomatoes, cucumbers and sugar beet. Therefore, the biological activity of PHGMH and its complexes with non-ionic surfactant was tested for the above vegetable cultures.

Materials and Methods

Materials. The water-soluble polymer PHMGH was used for the preparation the new bactericidal and fungicidal compounds. Polyhexamethylene guanidine hydrochloride (PHMGH) is an antimicrobial biocide of the guanidine group, produced in Russia at the Pokrovsky Plant of Biopreparations, $M_n = 1.7 \cdot 10^3$, has the following structural formula:



It is known that PHMGH is polyelectrolyte of cationic type and it keeps the bactericidal and fungicidal properties at interaction with other polyelectrolytes and surfactants [11-13].

As a surfactant, the oxyethylated isooctylphenol (OP-10) was used. OP-10 is a nonionic surface active agent, product of joining of ethylene oxide to the alkylphenol with formula $\text{C}_8\text{H}_{17}\text{C}_6\text{H}_4\text{O}(\text{CH}_2\text{CH}_2\text{O})_{10}\text{H}$ ($\text{C}_7\text{H}_{17}-\text{C}_6\text{H}_4-\text{O}-(\text{CH}_2-\text{CH}_2\text{O})_n$). Also the complexes of PHMGH/ OP-10 at a ratio of 1:1 were tested for the investigation.

Methods. The germination of seeds was studied in accordance with GOST 12038-84 "Seeds of agricultural crops. Methods for determination of germination". Four samples per 100 seeds of vegetable cultures were taken. Seeds were placed on moistened filter papers in Petri dishes. Petri dishes were previously sterilized in a desiccator SNOL 58/350 "Abutenos Elektrotechnika". The limit of reproducible temperatures ranges from 20 to 300 °C, the error of temperature stabilization is ± 2 °C for 1 hour at a temperature of 130 °C. Petri dishes wrapped in a tracing paper were placed in a thermostat for three days at a temperature of 27 °C. Germination of seeds was determined as a percentage. For the result of the

analysis, the arithmetic mean results of determining the germination capacity of all analyzed samples were taken.

The main regularities of plant growth and development were studied within thirty days by the standard method [14]. The length of the aerial part of the plants was measured during the experiment and a change of the external characteristics of the plant was observed. The thickness of the stalks of germinated plants was measured with the help of a caliper SHZ I – 125 mm, the division price 0.1 mm, class 2.

The chlorophyll content was determined on a SPEKOL 1500 spectrophotometer. The measuring error was $\pm 0.3\%$ according to biochemical methods for plant physiology study [15].

The effect of mixtures of PHMGH, OP-10 and PHMGH/OP-10 on seed germination was investigated by two methods:

1) Direct influence method on seeds.

Seeds were treated with mixtures of water solutions of PHMGH, OP-10 and PHMGH/OP-10 of 0.01%; 0.05 %; 0.1 % and 0.2 % concentrations. To determine the germination, the treated seeds were placed in a climatic chamber at a temperature of + 28 °C for 3-7 days;

2) Method of sprout watering. After germination of seeds in the soil, the irrigation was carried out with mixtures of PHMGH, OP-10 and PHMGH/OP-10 in water with 0.01 %; 0.05 %; 0.1 %; 0.2 % concentrations (50 ml).

Results and Discussion

One of the methods for assessment of the sowing quality of vegetable crops is to determine their productivity. In conditions of poor productivity, the possibility of obtaining a high yield reduces. Therefore, before sowing the crop, it becomes necessary to treat the seeds with bactericidal and fungicidal preparations.

1. *Effect of fungicidal and bactericidal complexes on the germination of vegetable seeds.*

The results of the studies of the effect of PHMGH, OP-10 and mixed solutions of PHMGH/OP-10 on seed germination are shown in Figures 1-3.

According to Figure 1, the best results were achieved by means of processing with a mixture of 0.05 % solution of PHGMH. Germination of seeds of cucumbers reached 90%.

The results of analyzes carried out with respect to tomato seeds are provided in Figure 2.

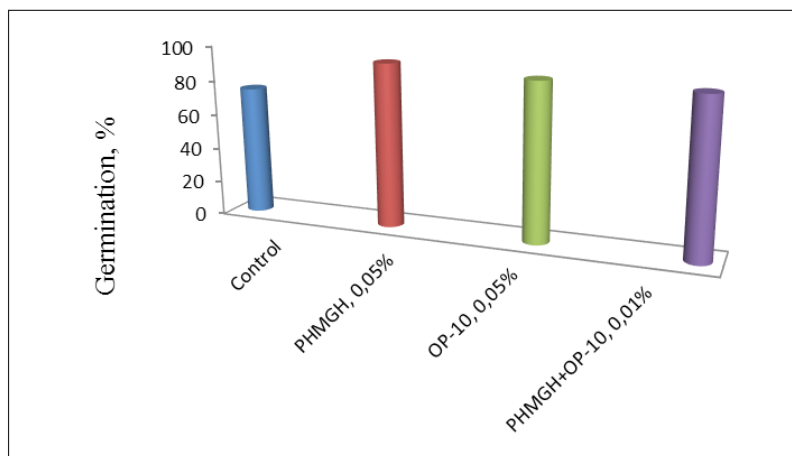


Figure 1 – The germination of cucumber seeds treated by solutions of PHGMH, OP-10 and PHMGH/OP-10

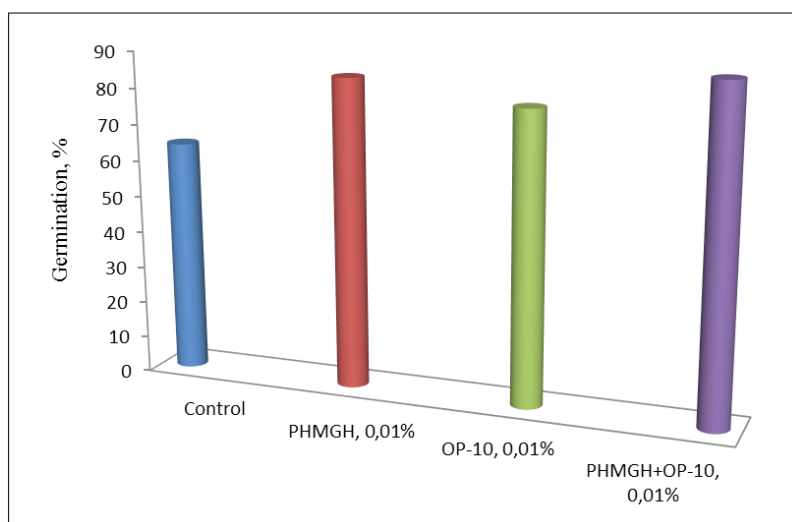


Figure 2 – The germination of tomato seeds treated by solutions of PHGMH, OP-10 and PHMGH/OP-10

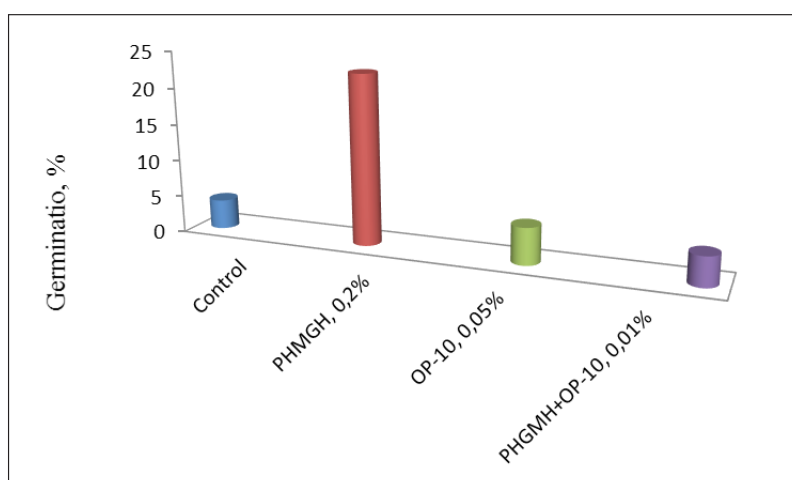


Figure 3 – The germination of sugar beet seeds treated by solutions of PHGMH, OP-10 and PHMGH/OP-10

As seen in Figure 2 the germination reached to 90 % after the treatment by PHGMH/OP-10 mixed solutions of 0.01 % at a ratio of 1:1 (vol.) of 0.01 % solutions. In the next experiment with respect to sugar beet seeds the concentrations of components were changed according to optimal data obtained

previously (Figure 3). As can be seen in Figure 3 the best results was observed after treatment by 0.2 % PHGMH.

Figure 4 presents the germination of seeds untreated and treated with mixed solutions of PHMGH/OP-10 at a ratio 1:1 (vol.)

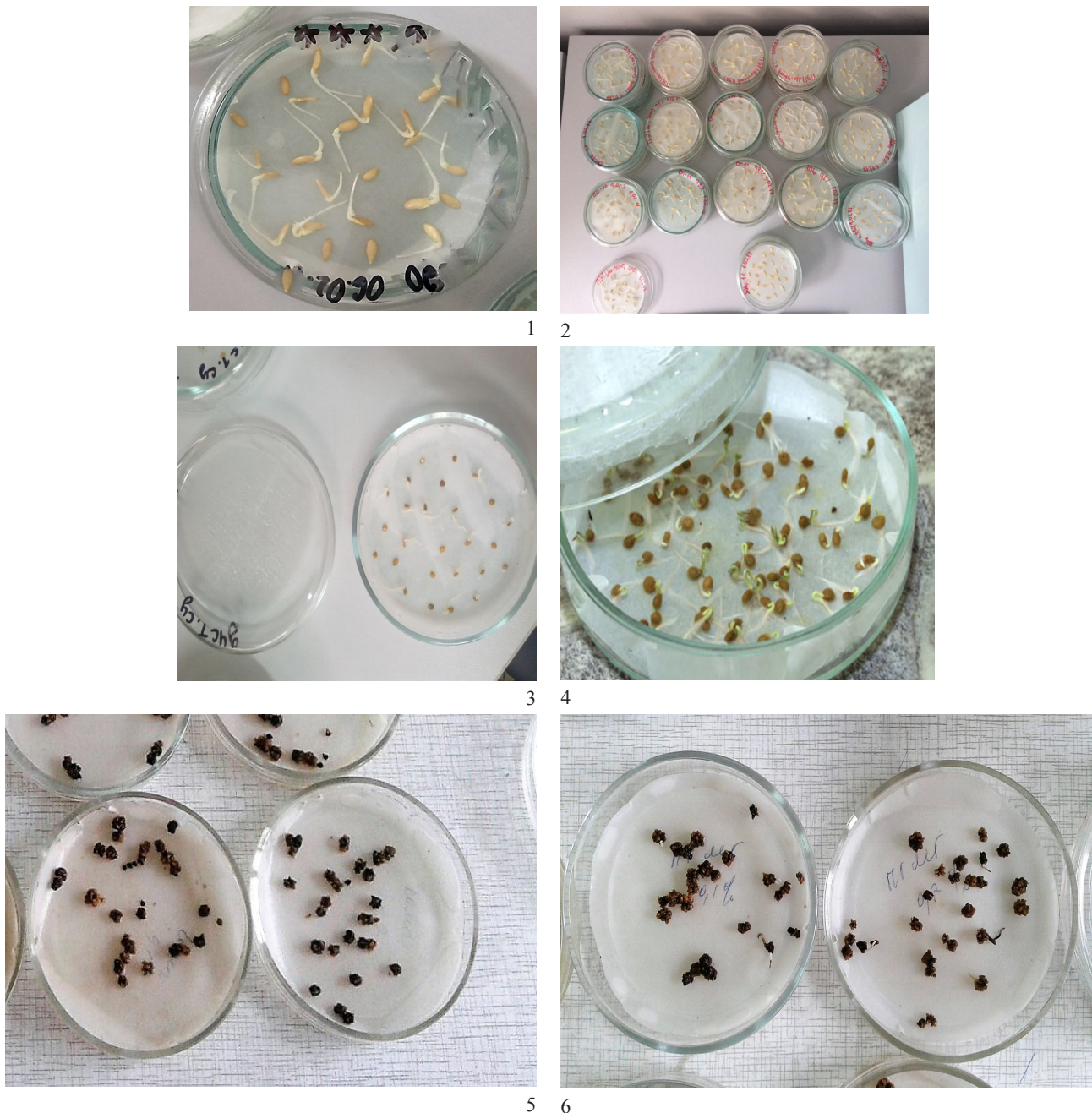


Figure 4 – Vegetable seeds untreated and treated with mixed solutions of PHMGH/OP-10 at a ratio 1:1
 (1 – untreated cucumber seeds, 2 – treated cucumber seeds, 3 – untreated tomato seeds,
 4 – treated tomato seeds, 5 – untreated sugar beet seeds, 6 – treated sugar beet seeds)

2. *The influence of bactericidal and fungicidal complexes on the growth and development of vegetable crops.*

To observe the growth and development of cultures, we carry out the following experiments: the seeds were planted in 500 g soil in four replicates. After emergence of seeds, the sprouts were watered with solutions of PHGMH, OP-10 and PHGMH/OP-

10 by 50 ml with different concentrations equaled to 0.01 %; 0.05 %; 0.1 %; 0.2 %. The results of the data obtained are presented in Figures 5-7.

As shown in Figure 5 the best results were reached after watering by PHGMH/OP-10 at initial concentrations of components equaled to 0.01 %.

Similar tests were carried out with relation to tomatoes (Figure 6).

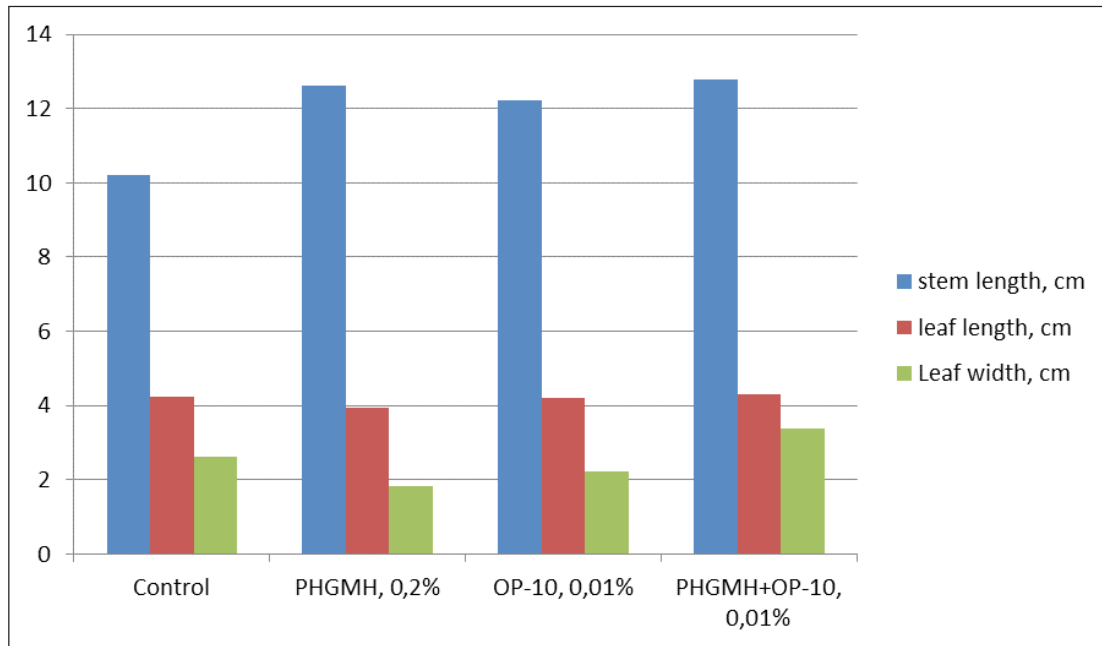


Figure 5 – Influence of solutions of PHGMH, OP-10 and PHGMH/OP-10 on growth and development of cucumber

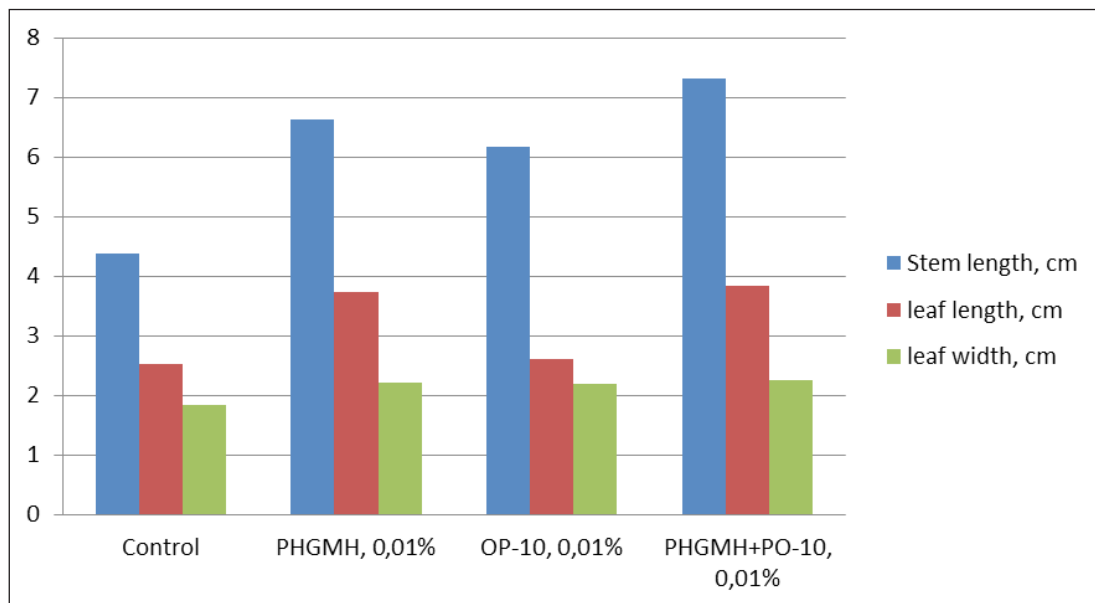


Figure 6 – Influence of solutions of PHGMH, OP-10 and PHGMH/OP-10 on growth and development of tomatoes

According to the results of the analysis of tomato samples, it can be seen from Figure 6 that the watering with complex of PGMG/OP-10 of 0.01% initial aqueous solutions positively influenced on the

growth of the stem length, the length and width of the leaf of the plant.

Similar results were obtained during experiments with sugar beet. The results are shown in Figure 7.

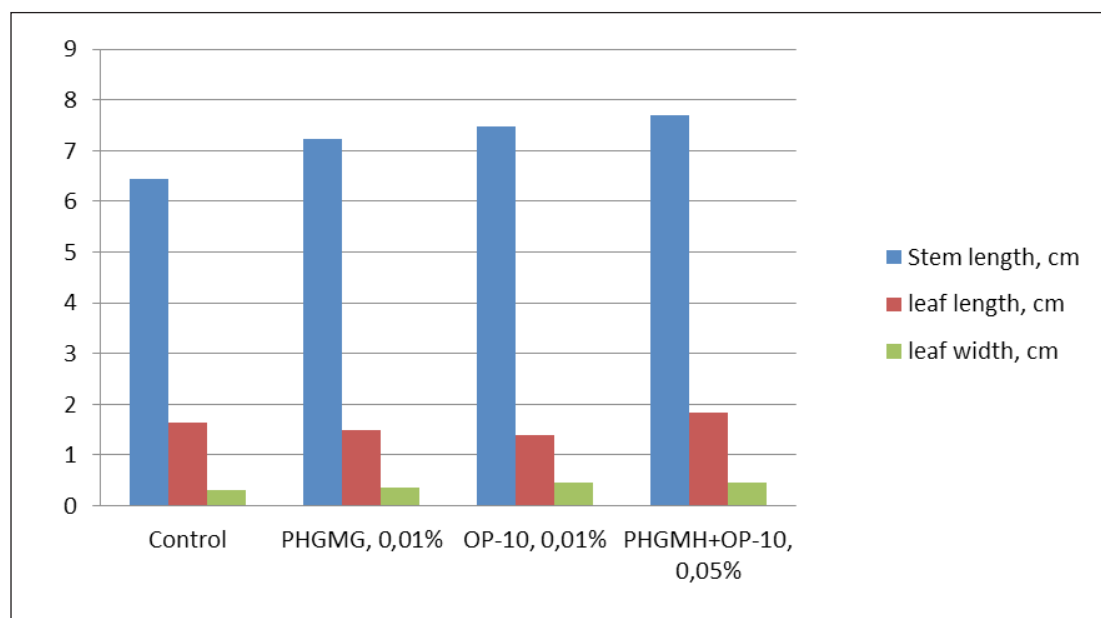


Figure 7 – Influence of solutions of PHGMH, OP-10 and PHGMH/OP-10 on growth and development of sugar beet

Figure 7 shows that good results as in previous tests complexes of PHGMH/OP-10 (0.05 %) exerted with respect to sugar beet growth.

3. Determination of chlorophyll on the leaves of cultures

Determination of the amount of chlorophyll in plants gives us the opportunity to assess their resistance to environmental factors. To determine the concentration of chlorophyll it is necessary to separate the pigment from the suspended filtrate of the substance. From the filtrate the chlorophyll concentration was determined by means of analysis conducted on a Spekol spectrophotometer. The results of the studies are presented in Figures 8-10.

As can be seen from Figure 8 that the amount of chlorophyll is most abundant in samples treated with PHGMH complexes (0.05%; 0.1%) and OP-10 (0.01%).

The following experiments were conducted in relation to tomato shoots (Figure 9).

As can be seen in Figure 9, a large amount of chlorophyll was detected in the leaf samples treated with PHGMH (0.01 %) and PHGMH/OP-10 (0.01 %), equaled to 2.6 and 2.97, respectively.

The results on determining the amount of chlorophyll in the leaves of sugar beet are shown in Figure 10.

Figure 10 shows that the most quantity of chlorophyll in the leaves of sugar beet was determined at processing with PHGMH (0.05 %) and OP-10 (0.1 %), equaled to 19.83 and 19.17%, respectively, when in the control sample while the chlorophyll content was 13.74%. The results of experiments confirmed that the crop shoots treated with aqueous solutions of PHGMH, surfactant and their mixture are resistant to environmental factors due to bactericidal and fungicidal activity of guanidine component while non-ionic surfactant provides the surface activity of composition [16-18].

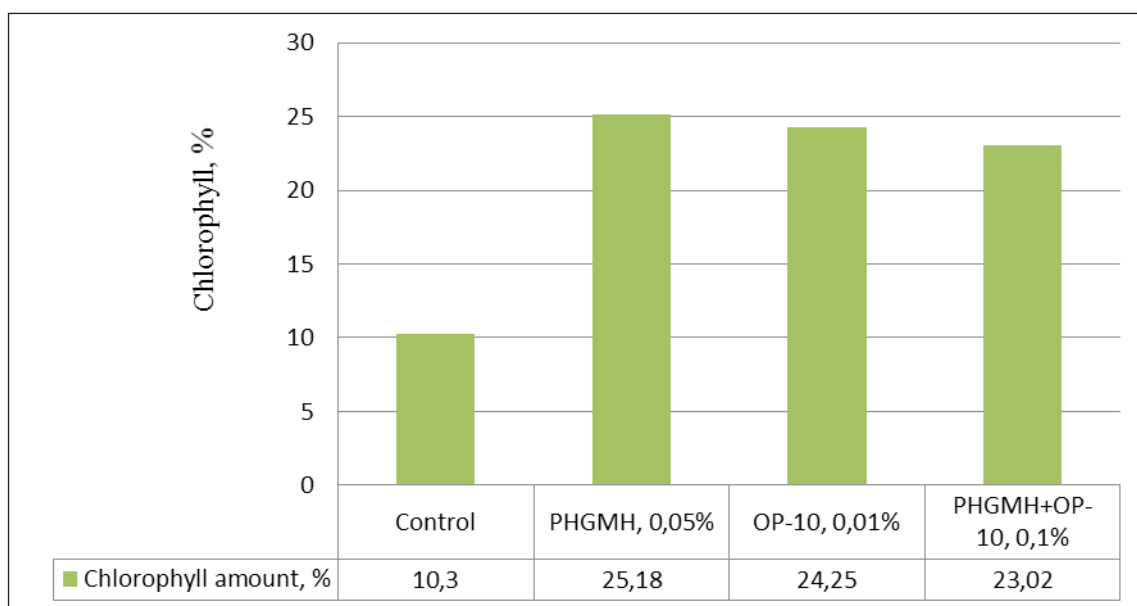


Figure 8 – Chlorophyll amount in cucumber leaf treated with PHGMH, OP-10 and PHGMH/OP-10 solutions

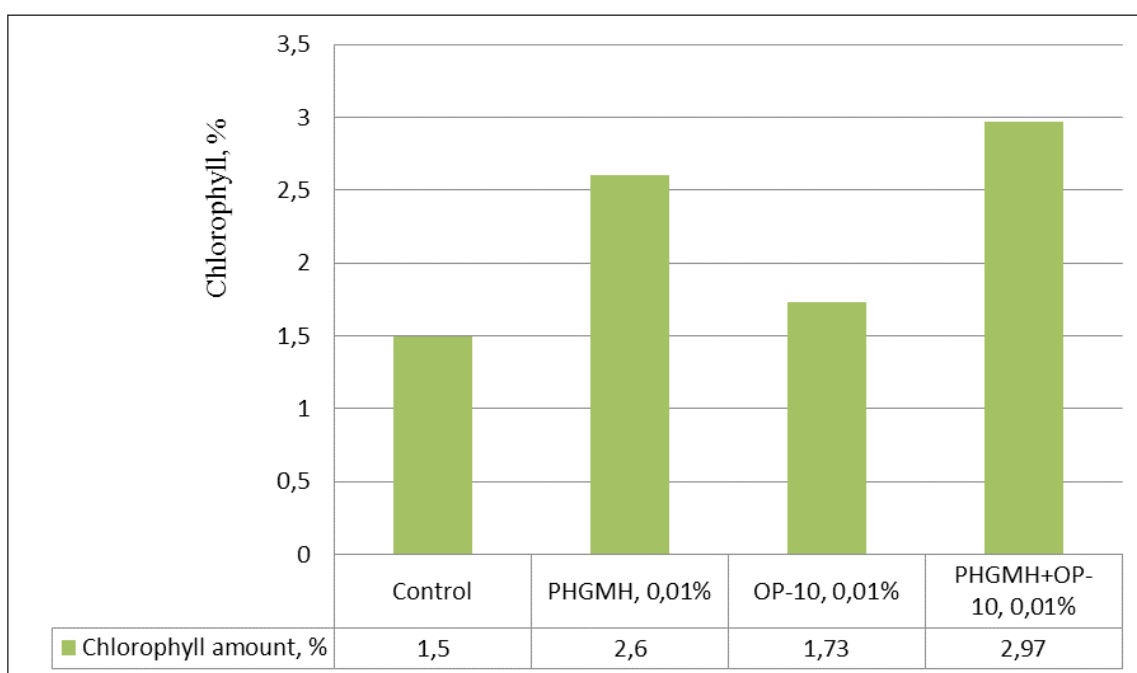


Figure 9 – Chlorophyll amount in tomato leaf treated with PHGMH, OP-10 and PHGMH/OP-10 solutions

Conclusions

PHGMH, OP-10 and PHGMH/OP-10 complex influence on the germination of vegetable seeds was studied. PHGMH (0.05 %) aqueous solution was more favorable for cucumber seeds (the germination

percentage equals to 94 %), PHGMH/OP-10 complex (at a ratio of 1:1 at initial component concentrations equaled to 0.01%) for tomato seeds (the germination percentage was 90%), and 0.2 % aqueous solution of PHGMH with respect to sugar beet seeds (the germination percentage was 23%).

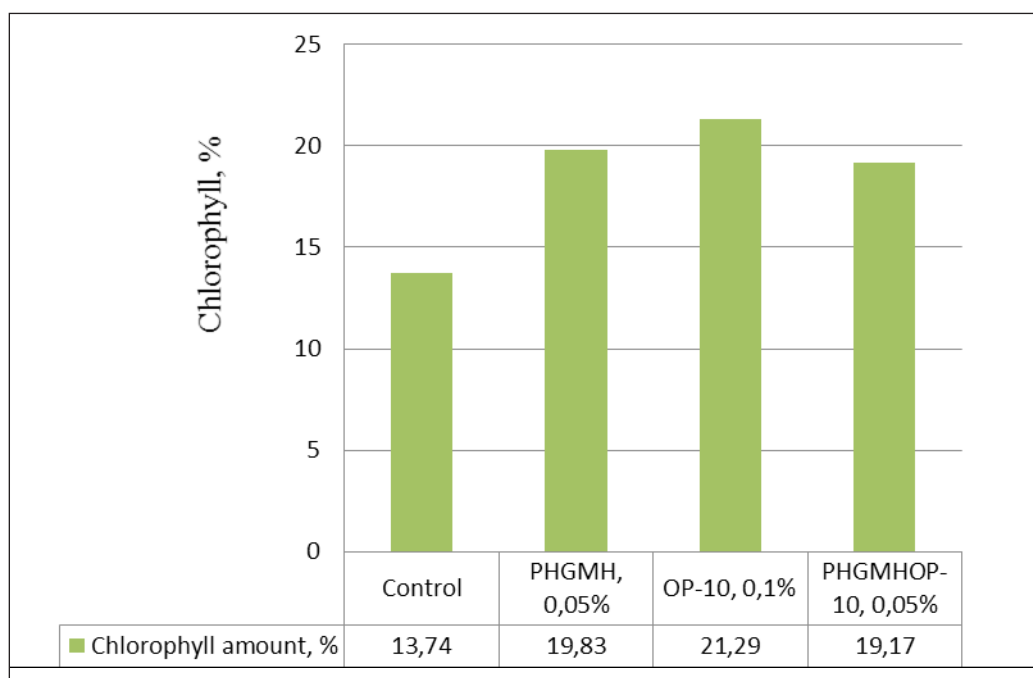


Figure 10 – Chlorophyll amount in sugar beet leaf treated with PHGMH, OP-10 and PHGMH/OP-10 solutions

The mixture of PHMG/OP-10 was effective on the growth and development for all of the studied vegetable crops (stem and leaf length). Thus, the sprouts of cucumbers and tomato show good results after treatment with a complex with initial concentration equaled to 0.01 % and sugar beet sprouts – at treating with 0.05% of complex of PHGMH/OP-10.

The amount of chlorophyll in the cultivated shoots of vegetables was determined after treatment with disinfectant and their complexes. The amount of chlorophyll was significantly higher in comparison with the control sample leaves (without treatment) of tomato, cucumber and sugar beet.

The results of the studies showed that the seeds treated with preparations are highly productive and show the increasing of the chlorophyll amount in the leaves providing the resistance of cultures to environmental factors.

References

1. Gnatenko A.V., Kovalenko V.L., Kulikova V.V., Ukhovskiy V.V. (2013) Ustojchivost' test-kul'tur leptospir k baktericidnomu preparatu «argicide» [Stability of the test cultures of leptospira against the bactericide "argicide"]. *Vestnik of the Altai State Agrarian Universit*, vol. 108, no 10, pp. 99-102.
2. Aprasyuhin A.I., Filonik I.A. The stimulator of growth and development of vegetable crops

and a way of stimulation of growth and development of vegetable cultures. [Stimulyator rosta i razvitiya ovoshchnyh kul'tur i sposob stimulyacii rosta i razvitiya ovoshchnyh kul'tur]. *Patent of the Russian Federation* No. 2006132114A, publ. 27.07.2008 (in Russian).

3. Malysheva Zh. N., Vershinin Yu. S., Ryzhova A. Yu., Novakov IA. (2013) Aggregating ability of polyelectrolytes and their mixtures with surfactants [Agregiruyushchaya sposobnost' polielektrolitov i ih smesey s poverhnostno-aktivnymi veshchestvami]. *Izvestiya Volgograd State Technical University*, vol. 10, no 4, pp. 140-145 (in Russian).

4. Anatolevich S.D. (2005) Biocidal preparations based on polyhexamethylenguanidine (2005) [Biocidnye preparaty na osnove poligeksametilen-guanidina]. *Zhizn' i bezopasnost' – Life and safety*, vol. 3, 4. pp, 46-48 (in Russian).

5. Gustavo F. de Paula, Germano I. Netto, Luiz Henrique C. Mattoso. (2011) Physical and Chemical Characterization of Poly(hexamethylene biguanide) Hydrochloride. *Polymers*, no 3, pp. 928-941. doi:10.3390/polym3020928

6. Zhou Z.X., Wie D.F., Guan Y., Zheng A.N., Zhong J.J. (2010) Damage of *Escherichia coli* membrane by bactericidal agent polyhexamethylene guanidine hydrochloride: micrographic evidences, *J Appl Microbiol.*, vol. 108, , pp. 898–907.

7. Kratzer C, Tobudic S, Graninger W, Buxbaum A, Georgopoulos A. (2006) In vitro antimicrobial activity of the novel polymeric guanidine Akacid plus. *J Hosp Infect.* vol. 63, no 3, pp. 316–322. doi: 10.1016/j.jhin.2006.01.024.
8. Wei D, Ma Q, Guan Y, Hu F, Zheng A, Zhang X, et al. (2009) Structural characterization and antibacterial activity of oligoguanidine (polyhexamethylene guanidine hydrochloride) *Mater Sci Eng, C.*, vol. 29, no 6, pp. 1776–1780. doi: 10.1016/j.msec.2009.02.005.
9. Dafu Wei, Qiangxiang Ma, Yong Guan, Fuzeng Hu, Anna Zheng, Xi Zhang. (2009) Structural characterization and antibacterial activity of oligoguanidine (polyhexamethylene guanidine hydrochloride). *Mater Sci Eng.*, vol. 29, no 6, pp. 1776-1780.
10. Konan M. Yao, Ollo Kambiré, Kouassi, C., Kouassi, Rose Koffi-Névry, Tagro, S. Guéhi. (2017) Risk Prevention of Fungal Contamination of Raw Cocoa Beans in Côte d Ivoire: Case of Polyhexamethylene Guanidine Hydrochloride (PHMGH). *Food and Public Health*, vol. 7, no 2, pp. 40-50. doi: 10.5923/j.fph.20170702.03
11. Vointseva I.I., Valetsky P.M. (2000) Interpolymers with biocidal properties based on polyhexamethyleneguanidine and chlorosulfonated polyethylene Proceedings of the 2nd All-Russian Karginy Symposium on Chemistry and Physics of Polymers in the early 21st Century, Chernogolovka, Russia, pp. 72.
12. Baimenova U.S., Musabekov K.B. (1998) Interaction of Metacide with Methacrylic Acid, Proceedings of the International Conference on Colloid Chemistry and Physical Chemical Mechanics, Moscow, Russia, pp. 107.
13. Vointseva I.I., Gembitsky P.A. (2009) Polyguanidines are disinfectants and polyfunctional additives in composite materials [Poliguanidiny dizañficiruyuschie i polifunkcional'nye dobavki kompozitnyh materialov], Moscow, LKM-press, p. 303.
14. Biddle K.L. (1989) Analysis of plant growth. Photosynthesis and bioproductivity: methods of determination. [Analyz roste rastenii. Fotosintez i bioproductivnost: metody opedeleniya] Moscow, Russia: Agropromizdat. pp. 53-61.
15. Shlyk, A.A. (1971) Determination of chlorophylls and carotenoids in extracts of green leaves. Biochemical methods in plant physiology. Moscow, Russia: Nauka. [in Russian].
16. Oulé, M.K., Richard, A., Anne-Marie, B., Tano, K., Anne-Marie, M., Stephanie, M., Rose, K.-N., Korami, D., Lorraine, F., Lamine, D. (2008). Polyhexamethylene guanidine hydrochloride-based disinfectant: a novel tool to fight meticillin-resistant *Staphylococcus aureus* and nosocomial infections. *Journal of Medical Microbiology*, 57:
17. Yao K.M., Koffi-Névry R., Guéhi S.T., Tano K. and Oulé M.K. (2012). Antimicrobial Activities of Polyhexamethylene Guanidine Hydrochloride Based Disinfectant against Fungi Isolated from Cocoa Beans and Reference Strains of Bacteria. *Journal of Food Protection*, vol 75, no 6, pp. 1167-71.
18. Goldfein M. D., Ivanov A.V. (2016) Applied Natural Science: Environmental Issues and Global Perspectives. CRC Press, pp. 458.

IRSTI 61.51.15

R.A. Fedorov, A.V. Akopyan, A.V. Anisimov, E.A. Karakhanov

Lomonosov Moscow State University, Chemistry Department, Moscow, Russia
e-mail: sulfur45@mail.ru

Peroxide Oxidative Desulfurization of Crude Petroleum in the presence of fatty acids

Abstract. Oxidative desulfurization of crude petroleum with hydrogen peroxide in the presence of fatty acids has been studied. A procedure for the recovery of oxidized sulfur-containing compounds from the petroleum by extracting the oxidation products with acetone has been selected. The influence of fatty acid on the residual sulfur content and oil viscosity was determined. As a result of oxidative desulfurization, up to 45% of total sulfur is recovered from petroleum, with the viscosity decreasing of crude oil.

Key words: petroleum, oxidative desulfurization, hydrogen peroxide, viscosity, fatty acids.

Introduction

Due to constant growth in the consumption of petroleum refinery products, the sulfur content in oil is subject to strict limitation. Nowadays is essential the search for costefficient technologies for decreasing the total sulfur content in refinery products and viscosity of crude oil [1]. Sulfur-containing compounds have a negative influence on many performance characteristics of petroleum products: stability and response to additives of motor gasolines decrease and their sooting tendency and corrosion activity increase; the service life of oil-refining equipment and transportation pipes decreases [2-4].

In the process of oxidative desulfurization with hydrogen peroxide, sulfur-containing compounds are oxidized first to sulfoxides and then to sulfones. This method allows to achieve low levels of sulfur in crude oil with a very simple technological design process [5] with the removal of chemically inactive benzothiophene derivatives and dibenzothiophene [6-8]. Currently, hydrogen peroxide is one of the most suitable oxidizing agents for the process of oxidative desulfurization. This is due to the fact that it has the highest percentage of active oxygen (47.1%), in addition, it has such technological and economic advantages as relatively low cost, environmental friendliness and commercial availability [9,10]. As additives to hydrogen peroxide, carboxyl compounds are effectively used, which significantly accelerate the oxidation of organic sulfur compounds and increase the degree of desulfurization of the feed-

stock [11, 12]. The combination of hydrogen peroxide with complexes of various metals also provides a high degree of petroleum fractions organic sulfur compounds oxidation [13–15]. Removing of oxidized sulfur-containing compounds from raw materials is carried out by extraction from oxidized oil fractions with polar solvents.

The reduction of viscosity is especially important for the transportation of oils with increased viscosity, since the process of pumping them requires an increase in the power of pumping units. The processing of such oil requires the improvement of technological schemes at all stages, which leads to an increase in the cost not only of its transportation, but also of production and refining [16]. The main characteristics that determine the technological processes associated with the oil processing with high viscosity are structural and mechanical properties, which are particularly influenced by the content in the oil of high-molecular compounds, including asphaltenes. In low-paraffinic oils, the important reason for high viscosity of oil is the presence of asphaltenes [17, 18]. To improve the rheological characteristics of viscous and highly viscous oils and increase their stability against delamination, synthetic surfactants, such as fatty acids, as well as specialized technological processes, such as aquatermolysis, are used [19]. The aim of this work was to develop a method for transferring oil from the medium-sour class to the low-sour class, without affecting the basic physico-chemical parameters, such as viscosity and density, applying the principles of oxidative desulfurization.

Materials and Methods

Crude oil from the Moscow refinery with a sulfur content of 1.24% was used in the study. This oil belongs to the medium and low-viscosity. The main physicochemical parameters are presented in table 1.

Table 1 – Physicochemical parameters of the crude oil

Parameter	Initial oil
Density, kg/m ³	872.7
Kinematic viscosity, cSt	2.623
Dynamic viscosity, mPa•s	2.3
Total sulfur, ppm	12400
Mercaptan sulfur, ppm	8
Asphaltenes, wt %	2.5
Water, vol %	0.1

Aqueous solutions of hydrogen peroxide (Prime Chemicals Group) were used as an oxidizing agents; formic acid (88% aqueous solution, analytical grade, Component-reagent), oleic (reagent grade, Reachim), stearic (97 %, Acros Organics) and lauric acid (reagent grade, Mas Albion). The following metal salts were used: Na₂MoO₄·2H₂O, Na₂WO₄·2H₂O (Aldrich Chemical), (NH₄)₂MoO₄ (AMX Line), C₁₀H₁₄MoO₆ (molybdenum acetylacetonate, DALHIM), Mo(CO)₆ (reagent grade, Reachim). Extractants served as solvents: acetone (analytical grade), methanol (reagent grade), N, N-dimethylformamide (reagent grade), acetonitrile (reagent grade), methyl ethyl ketone, dimethyl sulfoxide (reagent grade), N, N-dimethylacetamide (reagent grade). N-hexane (analytical grade, Ecos-1) was used as a solvent for determining the mass fraction of asphaltenes.

The sulfur content in the samples before and after desulfurization was determined on an ASE-2 X-ray energy dispersive sulfur analyzer (Burevestnik) with the relative error of no more than 5% and concentration range from 50 to 50000 ppm.

Crude oil desulfurization was carried out according to the following scheme: the required volume of the oxidizing system was added to a 10 ml sample of crude oil based on the molar ratios S: H₂O₂: acid: Me from 1: 1: 0: 0 to 1: 4: 1: 0.02. The reaction was carried out with constant stirring at 20 ° C for 2 to 6 hours. 10 mL of the oxidized petroleum were rinsed with 10 mL of water, extracted with 12 mL of the ex-

tracting agent with 20 vol % water, and the extracting agent and petroleum were separated by centrifugation. The operation was repeated twice, after which petroleum was rinsed with 10 mL of water, and the petroleum after extraction was analyzed for sulfur.

Determination of kinematic and dynamic of crude oil viscosity was carried out according to the method GOST 33-2016 using a glass viscometer at room temperature.

Fractional composition was determined by distillation according to GOST 2177-99.

Asphaltenes determination in the initial and oxidized crude oil was carried out according to the following procedure: 5 – 10 g of the sample were dissolved in 40-fold amount of n-hexane and left in the darkness for 18 – 20 h to precipitate asphaltenes. The solution was filtered, the precipitate was washed with hexane until the oil stains on the filter disappeared and until the flowing hexane was completely transparent. After that, the filter cake was dissolved in hot benzene and placed in a suspended flask, and benzene was distilled off to obtain a constant mass of the flask with an error of 0.01% [20]. The content of asphaltenes was found by the formula:

$$\text{Asphaltenes} = 100 * (a / A), \text{ wt. \%}$$

a – weight of the obtained sediment, A – weight of the sample.

Results and discussion

The process of oxidative desulfurization of hydrocarbon feedstock generally includes two steps: (1) oxidation of sulfur compounds present in the fraction and (2) the recovery of oxidation products from the fraction. Adsorption, extraction, or thermal methods are used to selectively remove oxidation products of sulfur compounds [21]. Previous studies have shown that the most effective method for extracting oxidized sulfur-containing compounds is extraction with polar solvents [5]. At the initial stage of work, the evaluation of extractants of various chemical nature was carried out.

The data obtained (Fig. 1) show that acetone and N, N-DMF most oxidized sulfur-containing compounds are extracted from oil, which is most likely due to the high polarity of the extracted compounds. Due to the simplicity of its regeneration and the best result on the residual sulfur content, acetone was used as extractation agent for oxidative products.

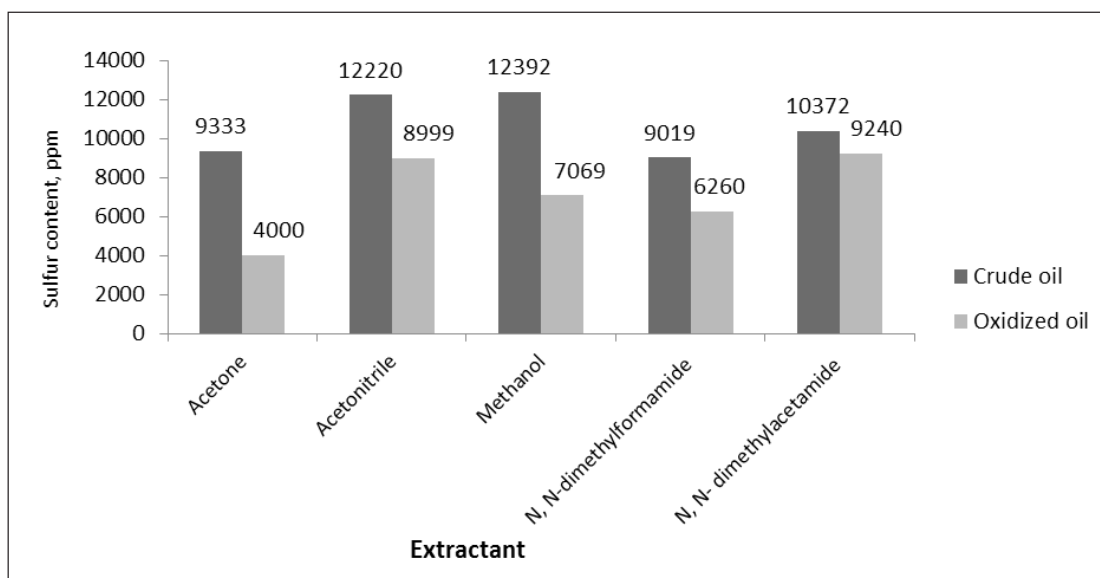


Figure 1 – Dependence of residual sulfur content on the nature of the extractant. (Conditions: S: H₂O₂ (50%): HCOOH = 1: 10: 6 (mol.), 20 ° C, 6 hours)

Aqueous solutions of hydrogen peroxide were used as oxidizing agents. To ensure optimal desulfurization conditions, the effect of the amount and concentration of hydrogen peroxide on the residual sulfur content was studied.

According to the data obtained (Table 2), 5 and 10% aqueous solutions of hydrogen peroxide are advisable to use in a molar ratio of 1: 1 for

10% hydrogen peroxide and 4: 1 and 2: 1 for 5% hydrogen peroxide. These solutions in combination with 88% formic acid and subsequent extraction can reduce the residual sulfur content in the oil to 5500 ppm. This is most likely due to the fact that at high concentrations of hydrogen peroxide, the mainly oxidized compounds which are difficult to extract.

Table 2 – The dependence of the residual sulfur content on the concentration and amount of hydrogen peroxide. (Conditions: S: HCOOH = 1: 1 (mol.), 20 ° C, 2 hours)

Molar ratio H ₂ O ₂ : S	Residual sulfur content, ppm				
	Hydrogen peroxide concentration, vol %				
	50	37	24	10	5
4 : 1	9000	8400	7800	8000	5500
2 : 1	8700	8700	7700	7600	6000
1 : 1	8000	8700	7800	7000	7700

It is known from the published data [11,12] that desulfurization in an acidic medium provides positive results on the residual sulfur content in the feedstock, and the use of fatty acids has a positive effect on the viscosity of oil. During the work, the effect of carboxylic acids on the residual content of oxidized sulfur-containing compounds, the mass fraction of asphaltenes and the viscosity of oil were investigated.

The data obtained indicate that the use of fatty acids can reduce the viscosity of oil, but does not provide oxidation of sulfur-containing compounds of oil compared with formic acid. The increase in the mass fraction of asphaltenes in oxidized oil is most likely due to the increase in the proportion of the fraction of insoluble asphaltenes.

The published data suggest that salts of transition metals forming peroxo complexes with H₂O₂

contribute to the reduction of the content of sulfur-containing compounds in the feedstock [22]. Sodium molybdate and sodium tungstate were used as salts containing transition metals.

Based on the data obtained, the use of sodium molybdate in the oxidative system in combination

with oleic acid can reduce the residual sulfur content to 6000 ppm as compared with tungstates.

In connection with obtaining a positive effect from the use of molybdenum as a catalyst for the oxidation of sulfur compounds of oil, various molybdenum salts were used in the work.

Table 3 – Effect of carboxylic acids on the residual sulfur content and oil viscosity. (Conditions: S: H₂O₂ (10%): acid = 1: 1: 1 (mol.), 20 ° C, 2 h, * – conditions: S: H₂O₂ (10%): mixture of acids = 1: 1: 2 (mol.), 20°C, 2 hours)

Acid	Residual sulfur content, ppm	Kinematic viscosity, cSt	Asphaltenes, wt %
Formic	7300	2.76	6.17
Acetic	8300	2.64	5.3
Stearic	9066	2.23	4.16
Oleic	9500	2.30	4.38
Lauric	11000	2.34	4.46
Stearic + formic*	9700	2.05	5.9
Oleic + formic*	8800	2.13	5.34
Lauric + formic*	9400	2.21	6.23

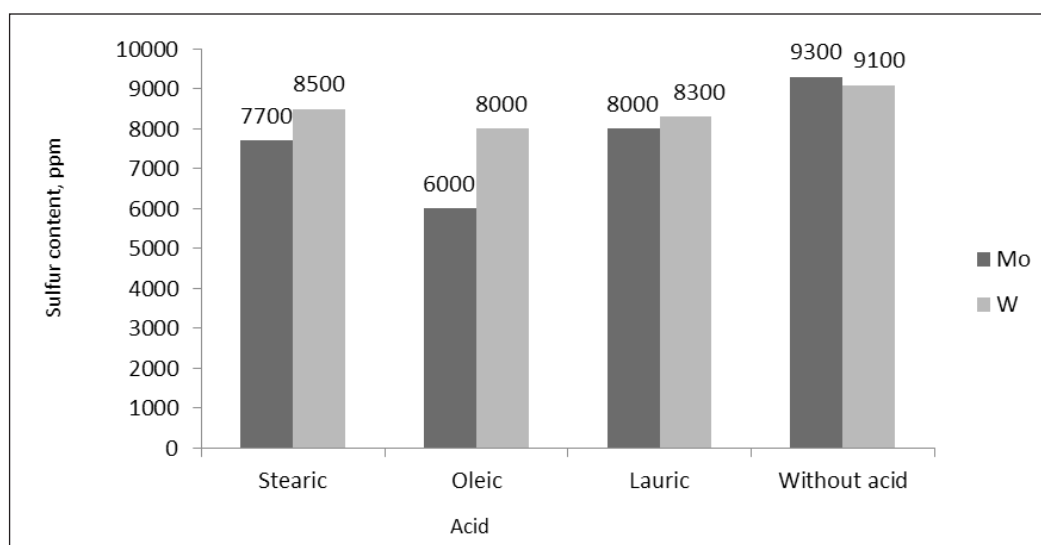


Figure 2 – The effect of transition metal salts and fatty acids on the residual sulfur content. (Conditions: S: H₂O₂ (10%): acid: Me = 1: 1: 1: 0.02 (mole), 20 ° C, 2 hours)

Based on the data obtained (Fig. 3), the use of sodium molybdate in a molar ratio of sulfur to 1: 200 is preferable compared with other salts of molybdenum and sodium molybdate in a molar ratio of 1: 100.

The work also determined the fractional composition of the original oil, oil after oxidation with

an excess of hydrogen peroxide and formic acid, as well as oil after its oxidation. The oxidizing system in the presence of oleic acid and sodium molybdate was used, followed by extraction of sulfur-containing compounds of oxidation products, as well as the of total sulfur content in each of the oil fractions was determined (Table 4).

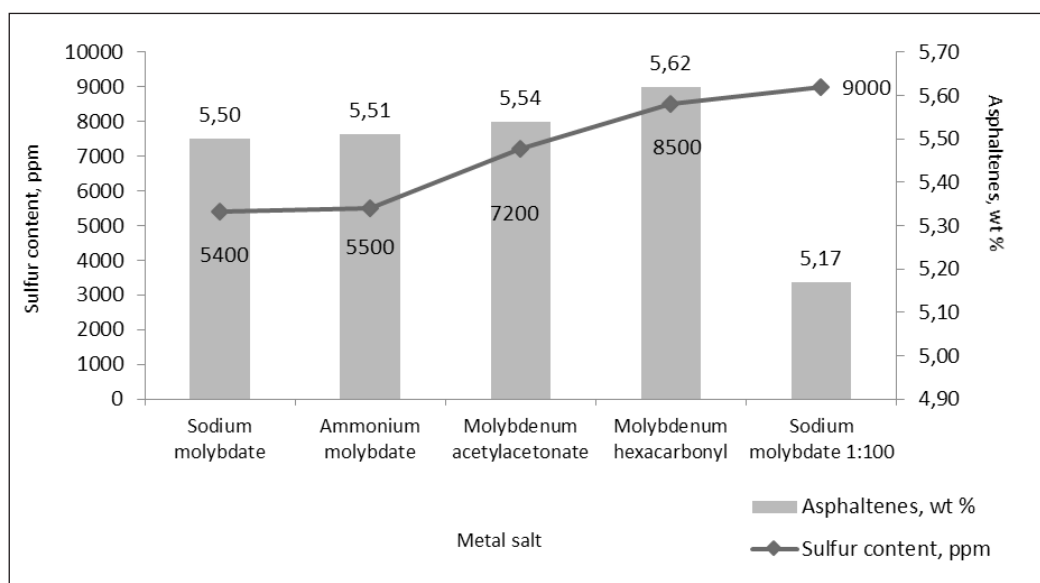


Figure 3 – The effect of molybdenum salts on the residual sulfur content and asphaltene content. (Conditions: S: H₂O₂ (10%): oleic acid: Me = 1: 1: 1: 0.02 (mole.), 20 ° C, 2 h, * – S: H₂O₂ (10%): oleic acid: Me = 1: 1: 1: 0.01 (mole), 20 ° C, 2 hours)

Table 4 – Fractional composition of the original and oxidized oil. (Conditions: 1) S: H₂O₂ (50%): HCOOH = 1: 10: 6 (mole), 20 ° C, 6 h; 2) S: H₂O₂ (10%): oleic acid: Me = 1: 1: 1: 0.02 (mole), 20 ° C, 2 hours)

Fraction	Initial crude oil		Oxidized oil (Conditions 1)		Oxidized oil (Conditions 2)	
	Volume, ml	Sulfur content, ppm	Volume, ml	Sulfur content, ppm	Volume, ml	Sulfur content, ppm
Petrol (38°C – 180°C)	9	600	7.6	220	9	350
Diesel (180°C – 360°C)	16.5	6690	14.5	158	15	3200
Residue	24	19400	27	9800	25	12800
Oil	50	12400	50	4000	50	4500

The data obtained from table 4 indicate that the oxidation composition in an excess of hydrogen peroxide and formic acid changes the oil fractional composition. The decrease in the residual content of oil sulfur-containing compounds and in each of the fractions was also observed. When using a 10% solution of hydrogen peroxide, oleic acid and sodium molybdate, the residual sulfur content in the fractions is higher than when using an excess amount of hydrogen peroxide and formic acid.

Conclusion

The use of fatty acids in oxidizing systems allows to reduce the viscosity of oil by 10 – 15%, but not in all cases it allows to reduce the sulfur content to acceptable parameters specified when using the oxi-

dizing system with hydrogen peroxide (10%): formic acid (88%) 1: 1. The oxidative system with hydrogen peroxide (10%): oleic acid: sodium molybdate in a molar ratio of 1: 1: 0.02 able to transfer oil from medium-sulfur to low-sulfur and reduce kinematic viscosity by 12%.

Acknowledgments

The work was performed within the framework of implementation of and with financial support from the Federal Targeted Program for Research and Development in Priority Areas of Development of the Russian Scientific and Technological Complex for 2014–2020. Activity 1.3, Grant Agreement no. 14.607.21.0173. The unique identifier of applied research is RFMEFI60717X0173.

References

1. Javadli R., de Klerk A. // *Petrochem. Res.* 2012. N 1. P. 3-19.
2. Shang H., Zhang H. // *J. Industrial and Engineering Chem.* 2013. V. 19. P. 1426-1432.
3. Campos-Martin J.M., Capel-Sanchez M.C., Perez-Presas P., Fierro J.L. // *J. Chem. Technol. Biotechnol.* 2010. V. 85. P. 879-890.
4. Rana M.S., Samano V.A. // *Fuel.* 2007. V. 86. P. 1216-1231.
5. Akopyan A.V., Fedorov R.A., Anisimov A.V. et al. // *Petrol. Chemistry.* 2018. V. 58. №1. P. 13-17
6. Ismagilov Z., Yashnik S., Kerzhentsev M. et al. // *Catalysis Reviews.* 2011. V. 53. Is. 3. P. 199-255.
7. Akopyan A.V., Ivanov E.V., Polikarpova P.D. et al. // *Petrol. Chemistry.* 2015. V. 55. №7. P. 571-574
8. Jiang Z., Lu H., Zhang Y., Li C. // *Chin. J. Catal.* 2011. V. 32. Is. 5. P. 70-715.
9. Dehkordi A.M., Kiaei Z., Sobati M.A. // *Fuel Process. Technol.* 2009. V. 90. P. 435-445.
10. Akopyan A. V., Kardasheva Yu. S., Eseva E. A. et al. // *Petrol. Chemistry* 2016. V. 56. № 5. P. 1-3.
11. Sharipov A.Kh., Mukhametova R.R., Nigmatullin I.R., Nigmatullin V.R. et al. // *Petrol. Chemistry.* 2008. V. 48. № 6. P. 466-470.
12. Borisov I.M., Gazizova Z.Sh., Shayakhmetova G.V. et al. // *Petrol. Chemistry.* 2015. V. 55. №3. P. 224-228.
13. Gobara H.M., Nessim M.I., Zaky M.T. et al. // *Catal. Letters.* 2014. V.144. N 6. P. 1043-1052.
14. Pat. RU 2472841 C2 (2013). Sulfo-oxidation catalysts and methods and systems for their use.
15. Pat. RU 2235112 C1 (2012). Desulfurization of light oil distillates.
16. Husnutdinov I. Sh. // *Chemistry and chemical technology.* 2004. V. 47. № 4. P. 3-9.
17. Argillier J-F., Barré L., Brucy F. et al. // 2001 SPE International Thermal Operations and Heavy Oil Symposium held in Porlamar, Margarita Island, Venezuela, 12–14 March 2001.
18. Chavez-Miyauchi T. E., Zamudio-Rivera L.S., Barba-Lopez V. // *Energy & Fuels.* 2013. V. 27. P. 1994–2001.
19. Chia-Lu Chang, Scott Fogler H. // *Langmuir.* 1994. V. 10. P. 1749–1757.
20. Shkalikov N. V., Vasil'ev S. G., Skirda V.D. // *Colloid Journal.* 2010. V. 72. № 1. P. 133–140.
21. Zhang M., Zhu W., Hun S. et al. // *Chem. Eng. J.* 2013. V. 220. P. 328-336.
22. Rakhmanov E.V., Tarakanova A.V., Valieva T. et al. // *Petrol. Chemistry.* 2014. V. 54. №1. P. 48-50.